2002

DIPLÔME D'UNIVERSITÉ DE GEMMOLOGIE

Présenté

Devant l'Université de Nantes
U.F.R. des Sciences et des Techniques

Par

Jean-Marie DUROC-DANNER

A STUDY OF COLOMBIAN CORUNDUM

Soutenu publiquement le 23 septembre 2002
Au Département de Géologie
Devant la commission d'examen composée de :

M. B. LASNIER	**Professeur Université de Nantes.**	**Président**
M. E. FRITSCH	**Professeur "**	**Vice-Président**
M. S. LEFRANT	**Professeur "**	**Examinateur**
M. J. GIRARDEAU	**Professeur "**	**"**
M. J-P. GAUTHIER	**Professeur Université de Lyon 1.**	**"**
M. M. SPIESSER	**Maître de Conférences Université de Nantes.**	**"**
M. Ph. MAITRALLET	**Directeur du Laboratoire Français de gemmologie de la CCI de Paris.**	**"**
M. F. NOTARI	**Directeur du Laboratoire GemTechLab, Genève.**	**Membre invité**

A STUDY OF COLOMBIAN CORUNDUM

J.M. Duroc-Danner, Dip. I.U.E.D., F.G.A., G.G.
Geneva, Switzerland

Ruby, multicoloured sapphire and sapphire, studied in the following pages, recovered from the border of the departments of Cauca and Nariño, Colombia.

"Le mieux est l'ennemi du bien"
François Marie Voltaire

To Eliane, Myska, Monique, and my parents

CONTENTS

	Pages
A study of Colombian corundum	1
Abstract – introduction	5
References – Colombian corundum	6
Geography	10
Geology	13
Location and occurrence	19
Appearance	23
Refractive index, specific gravity, ultra-violet fluorescence	28
Pleochroism, spectroscopic examination	31
Microscopic examination	34
- Main inclusions observed in the rough corundums	34
- Main inclusions observed in the rubies	45
- Main inclusions observed in the sapphires	53
- Main inclusions observed in the heat-treated sapphires	68
Particle induced X-ray examination (PIXE)	74
- Qualitative characteristics for the rubies	74
- Quantitative analysis for the rubies	74
- Qualitative characteristics for the sapphires	77
- Quantitative analysis for the sapphires	77
Energy dispersive X-ray fluorescence (EDXRF)	85
- Chemical analysis of the rubies	85
- Chemical analysis of the sapphires	94
Ultra-violet spectrophotometry (UV-VIS)	124
- Spectroscopic analysis of the rough crystals	125
- Spectroscopic analysis of the rubies	151
- Spectroscopic analysis of the sapphires	157
- Spectroscopic analysis of the heat-treated sapphire	166
- Spectroscopic analysis of the multicoloured sapphires	168
- Spectroscopic analysis of the colour-change sapphire	176
- Spectroscopic analysis of the heat-treated colour-change sapphires	178
Infra-red spectrophotometry (FT-IR)	181
- Main peaks observed for the rubies	182
- Main peaks observed for the sapphires	192
Discussion	213
Conclusion	215
References	216

ACKNOWLEDGEMENTS

I hereby express my gratitude for the guidance patience and advice of **Professor Bernard LASNIER** and **Professor Emmanuel FRITSCH** (Université de Nantes, France), during the many months the elaboration of this Diploma took form, and without whose assistance this work would not have been possible.

I also would like to thank:

Professor Seung Mun TANG (National University of Singapore), for his help and advice dealing with PIXE analysis.

Professor Armando ESPINOSA (Universidad del Quindío, Armenia, Colombia), and **Professor Jairo MOJICA** (Universidad Nacional de Colombia, Bogotá), for their precious assistance locating some of the Colombian texts which I desperately needed, and also for their constant support, advice and comments.

I am also indebted towards:

Mr Frank NOTARI (Director Gemtechlab, Genève, Switzerland), for his help and talent dealing with EDXRF and UV-visible spectroscopic analysis.

Professor Henry HÄNNI (Director SSEF, Swiss Gemmological Institute, Basel), for kindly lending his rough and faceted corundums from Colombia *(Source HH),* and for the Raman spectra.

Dr Robert MORITZ (maître d'enseignement et de recherche, Section des Sciences de la Terre de l' Université de Genève), for kindly taking the Raman spectra of inclusions encountered in faceted corundums.

Mr Jaime ROTLEWICZ (C.I. Gemtec Ltda., Bogotá, Colombia), for the samples of Colombian corundum that were kindly offered for this study *(Source GT)*.

Mr Pierre VUILLET, who kindly furnished most of the rough corundum crystals and their accessory minerals from Colombia *(Source PV)*, various texts, maps, and his superb help translating passages from Colombian to French.

Dr Halil SARP (Curator Muséum de Genève, Switzerland), for the X-ray analysis of minute inclusions scraped from rough Colombian corundums.

Dr Norma BAKER (Director of Development, Library of Congress, Washington, U.S.A.), for generously supplying photocopies from almost all the Colombian authors which were impossible to obtain elsewhere.

Mrs Anne-Marie DEUS and **Miss Cristelle MOUGIN** (Bibliothèque du Muséum de Genève, Switzerland), for producing photocopies and loaning books of different authors.

Mrs Nancy RIHS (Bibliothèque des Sciences de la Terre, Faculté des Siences, Genève) for producing photocopies of articles by different authors.

ABSTRACT

Colombia has long been reputed for producing fine emeralds.
More recently, corundum has been recovered from streambeds and sands on both sides of the Rio Mayo, which forms part of the border between the departments of Cauca and Nariño.
Although this area is reported in the literature as a new source of gem sapphire, it is interesting to note that it was known and described as early as the 16th century (References – Colombian corundum).
The aim of this study is to analyse the gemmological properties, chemistry, and spectrometry, of these recently gathered Colombian corundums and demonstrate that if a basaltic origin dominates, non basaltic corundums coexist. Unfortunately, their characteristics being similar to corundums from other geographic origins, presently they cannot be separated.

RÉSUMÉ

La Colombie est depuis fort longtemps renommée pour ses émeraudes.
Plus récemment, des corindons ont été récoltés dans les sables denses de ruisseaux et de terrasses de petits affluents du Rio Mayo qui forme une partie de la frontière entre les départements de Cauca et de Nariño.
Bien que ces dépôts aient été relatés dans des articles comme de nouveaux gisements de saphirs, il est bon de noter que ces gîtes étaient connus et décrits dès le 16éme siècle (Références – Colombian corundum).
Le but de cette étude est de relever les propriétés gemmologiques, chimiques et spectrométriques de ces corindons récemment ramassés et de démontrer que si une origine basaltique domine largement, une origine non-basaltique coexiste. Malheureusement, comme leurs caractéristiques sont semblables à celles des corindons d'autres lieus géographiques, pour l'instant ils ne peuvent pas en être différenciés.

INTRODUCTION

In 1991, a parcel of thirty faceted corundums and twenty-two rough crystals recovered from Colombia were received for examination.
The parcel of thirty faceted corundums contained six rubies, fourteen sapphires, and ten multicoloured sapphires.
Their physical and gemmological properties were found to be so interesting that several years later, in 1997, a Diploma was undertaken at the University of Nantes, France.
Twelve of the faceted corundums examined earlier were re-examined to confirm their properties.
In addition, a new parcel of eleven faceted corundums (two rubies, two sapphires, a heat-treated sapphire, three multicoloured sapphire, a colour-change sapphire, and two heat treated colour-change sapphires), and two thousand seven hundred and ninety one rough Colombian corundums totalling over three thousand five hundred and fifty three carats were obtained from four different sources.
Results regarding the properties of the original 1991 specimens and the recently collected specimens of 1997 and 2000 are reported in the following pages.

REFERENCES – COLOMBIAN CORUNDUM

Anyjewel.com (2000). *Sapphire, Out Of The Blue! Who Knew?* http://www.anyjewel.com/info/news19.html. Pp. 1-2.

Arem J.E. (1997). *Color encyclopedia of Gemstones*, 2nd ed., Chapman & Hall, New York, NY, pp. 72-73.

Asselborn E., Chiappero P . J., and Galvier J. (1987). *Les minéraux.* Guide vert, Solar, imprimé en Espagne, Gráficias Estella, S.A. Navarra, p. 85.

Association des Experts en Diamant et Pierres Précieuses (2001). *Le Saphir.* http://www.gemmexpert.com/index.htm. Pp. 1-3.

Association Française de Gemmologie (1992). *"GEMMES"*. Recueil de fiches permettant une identification rapide des gemmes. 224 pages pour 108 pierres.

Bank H., Schmetzer K., and Maes J. (1978). *Durchsichtiger, blau-rot changierender Korund aus Kolumbien*. Zeitschrift der Deutschen Gemmologischen Gesellschaft, Vol. 27, No 2, pp. 102-103.

Bariand P. & Poirot J.-P. (1998). *Larousse des pierres précieuses.* Larousse Bordas. P. 235.

Barlow A.E. (1915). *Corundum, its Occurrence, Distribution, Exploitation, and Uses.* Geological Survey, Canada Department of Mines, No 50, Geological Series, Ottawa Government Printing Bureau. P. 228.

Buffon G.L. (1828). *Oeuvres complètes de Buffon, mises en ordre par M. le comte de Lacépède.* Nouvelle édition. Eymery, Fruger et Cie, Libraires, rue Mazarine, 30, Paris, France. Tome 8, minéraux, No 4, p. 244.

Chudoba K.F. & Gübelin E.J. (1974). *Edelsteinkundliches Handbuch*. 3. Auflage, Wilhelm Stollfuss Verlag, Bonn. P. 193.

Coenraads R.R. (1992). *Surface features on natural rubies and sapphires derived from volcanic provinces*. Journal of Gemmology, Vol. 23, No 3, pp. 151-160.

David C. & Fritsch E. (2001). *Identification du traitement thermique à haute température des corindons par spectrométrie infra-rouge.* Dossier central (suite). Revue de Gemmologie a.f.g., N°141/142, pp. 27-31.

Duda R. & Rejl L. (1999). *Les pierres précieuses.* Traduction Robert U. et Métais-Buhrendt C. Éditions Gründ, 60, rue Mazarine, 75006 Paris. P. 49.

Duroc-Danner J.M. (1999). *Une pierre revient d'actualité dans le jardin de la Colombie: le corindon.* Tribune des Arts, N° 269 Mars, Gemmes, Magasine de la "Tribune de Genève", p. 30.

Epstein D.S., Brennan W., and Mendes J.C. (1994). *The indaia sapphire deposits of Minas Gerais, Brazil*. Gems & Gemology, Vol. 30, No 1, pp. 24-32.

Gemtec Ltda. (1997). *Colombian corundum Ruby & Sapphire*. gemtec@impsat.net.co (last updated: March 15, 1997), pp. 1-7.

Grosse E. (1935). *Acerca de la geologia del Sur de Colombia, Patía y Nariño.* Compilación de los Estudios Geológicos Oficiales en Colombia – 1917 A 1933, Ministerio de Industrias, Comisión Científica Nacional. Biblioteca del Departamento de Minas y Petróleo, Bogotá, Imprenta Nacíonal, Tomo III, pp. 187-191.

Gübelin E.J. & Schmetzer K. (1982). *Gemstones with alexandrite effect.* Gems & Gemology, Vol. 18, No 4, pp. 197-203.

Gübelin E.J. & Koivula J.I. (1986). *Photoatlas of Inclusions in Gemstones*. ABC Edition, Zurich, p. 344.

Gübelin E.J. (1988). *World Map of Gem Deposits.* Swiss Gemmological Society, Lucerne, Switzerland.

Hall C. (1994). *Gemstones.* Eyewitness Handbooks, Dorling Kindersley Book, printed and bound by Kyodo Printing Co., Singapore. P. 95.

Hämmerle F. (1940). *Riqueza mineral de Nariño.* Anales Universidad de Nariño, Ep. 2, Nos 5-6, pp 569-580.

Herbert Smith G.F. (1972). *Gemstones* (revised by F.C. Phillips). Chapman and Hall Ltd, 11 New Fetter Lane, London EC4P 4EE, pp. 210, 301.

Hughes R.W. (1990). *Corundum.* Butterworth-Heinemann, London, p. 230.

Hughes R.W. (1997). *Ruby & sapphire*. RWH publishing, Boulder, Colorado, USA, pp. 273-274, and pp.354-355.

Johnson M.L., Koivula J.I., McClure S.F., and DeGhionno D., Eds. (2000). Gem news: *Rubies (and sapphires) from Colombia.* Gems & Gemology, Vol. 36, No 3, pp. 268-269.

Kane R.E. (1999). *Ruby and Sapphire Occurrences Around the World*. Gems & Gemology, Vol. 35, No 3, pp. 60-61.

Karsten L.G. (1886). *Géologie de l'ancienne Colombie bolivarienne, Vénézuela, Nouvelle-Grenade et Ecuador.* R. Friedländer & Sohn, Berlin. Pp. 33-34.

Keller P.C., Koivula J.I., and Jara G. (1985). *Sapphire from the Mercaderes-Rio Mayo area, Cauca, Colombia*. Gems & Gemology, Vol. 21, No 1, pp. 20-25.

Keller P.C. (1990). *Gemstones and their origins*. Van Nostrand Reinhold, 115 fith Avenue, New York, NY 10003, pp. 71-73.

Koivula J.I. & Kammerling R.C. (1990). Gem news: *New World sapphires.* Gems & Gemology, Vol. 26, No 1, p. 102.

Koivula J.I., Kammerling R.C., and Fritsch E. (1993). Gem News: *Tucson 1993*. Gems & Gemology, Vol. 29, No 1, p. 61.

Koivula J.I. (1998). Gem Trade Lab Notes: *Sapphire, internal diffusion revisited.* Gems & Gemology, Vol. 34, No 1, pp. 47-48.

Kunz G.F. (1908). *Precious Stones* [Colombian sapphires] in The Mineral Industry, Its Statistics, Technology and Trade, in the United States during 1907. New York, Hill Publishing Co, Vol. XVI, p. 796.

Levinson A.A. & Cook F.A. (1994). *Gem corundum in alkali basalt: origin and occurrence.* Gems & Gemology, Vol. 30, No 4, pp. 253-262.

Lleras Codazzi R. (1904). *Gemas y minerales litoides de la República de Colombia.* Trabajos de la Oficina de Historia Natural, Sección de Mineralogía y Geología, Imprenta Nacíonal, p. 5.

Lleras Codazzi R. (1925). *Notas mineralógicas y petrográficas.* Biblioteca del Museo Nacíonal. Imprenta Nacíonal, Bogotá, Colombia, pp. 15-16 & 39.

Lleras Codazzi R. (1926). *Notas geográficas y geológicas.* Biblioteca del Museo Nacional, Imprenta Nacíonal, Bogotá, p. 29.

Lleras Codazzi R. (1927). *Los minerales de Colombia*. Biblioteca del Museo Nacional, Imprenta Nacíonal, Bogotá, Colombia. Pp. 96-99.

Lleras Codazzi R. (1929a). *Las rocas andinas en Colombia.* Boletin de agricultura, ano II, numero 8, febrero de 1929. ministerio de industrias-sección de publicaciones. Pp. 9,10.

Lleras Codazzi R. (1929b). *Notas adicionales sobre los minerales y las rocas de Colombia.* Biblioteca del Museo Nacíonal, Imprenta Nacíonal, Bogotá, pp. 35-36.

Martín de Renata J.M. (1990). *El gran libro de la esmeralda* [otras gemas metales preciosos de Colombia]. Martín de Renata, editor y Federacion Nacional de Esmeraldas de Colombia, Gran Via, 8-5.°, Dpto. 8 (48001) Bilbao, Espana, pp. 102, 210-211, 363-372, 386, 431, 444-445, and 461.

Martinez S. & Garcia B. (1989). *Cartografia, Geología, Prospección de minerales semi preciosa en los municipios de Mercaderes (Cauca) y La Unión (Nariño).* Trabajo de Grado presentado como requisito parcial para optar al titulo de Geologo. Universidad Nacional de Colombia, Facultad de Ciencias, Dept. de Geociencias, Santa Fe de Bogotá. Pp. 1-169.

Montero M.A. (1992). *Estudio Mineralogico y Gemologico de los Corindones de Mercaderes - Cauca*. Trabajo de grado requisito parcial para optar al titulo de geologo. Universidad Nacional de Colombia, Facultad de Ciencias, Dept. de Geociencias, Santa Fe de Bogotá. Pp. 1-111.

Murcia L.A. & Cepeda V.H. (1991). *Mapa geologico de Colombia. Plancha 410 – La Union (departamento de Nariño). Escala 1:100.000. Memoria explicativa*. Ingeominas, Bogotá. Pp. 1-22.

Osario C.E. & Michelou J.C. (2000). *Nouvelles découvertes d'émeraudes et pierres de Colombie.* Revue de Gemmologie a.f.g. N° 140, pp. 14-15.

Pereira F. (1906). *Riqueza mineral de Colombia. Yacimientos de zafiro en el Río Mayo. Departamentos de Cauca y Nariño*. Análisis de Ingeniería, Vol. XIII, no. 159. Pp. 358-361.

Prévost d'Exiles (1757). *Histoire générale des voïages, ou nouvelle collection de toutes les relations de voïages par mer et par terre*, ..., Didot, Librairie, Quai des Augustins, à la bible d'or, Paris, France, Tome 14, p. 350.

Raleigh W. (1596). *The Discoverie of the large, rich, and bewtiful Empire of Guiana, with a relation of the great and Golden Citie of Manoa (which the Spanyards call El Dorado), And of the Provinces of Emeria, Arromaia, Amapaia and other Countries, with their rivers adioyning. Performed in the years 1595 etc.* Robert Robinson: London, 1596. 4°. P. 69.

Reiss W. & Stübel A. (1899). *Reisen in Süd-Amerika. Geologische studien in der Republik Colombia. II Petrogaphie. 2. Die älteren massengesteine, krystallinen, schiefer und sedimente.* Verlag von A. Asher & CO., Berlin. Pp. 152-153, 174.

Scheibe R. (1921). *Seccion Tecnica* [La Minería en Colombia] en Boletín de Minas y Petróleo, Organo del Departamento de Minas y Petróleo del Ministerio de Industrias, 1931, Tomo V, N^{os} 28 a 30, Bogotá,. Imprenta Nacíonal, P 85.

Schmetzer K. & Peretti (1999). *Some diagnostic features of russian hydrothermal synthetic rubies and sapphires.* Gems & Gemology, Vol. 35, No 1, pp. 20, 21.

Schubnel H.J. (1992). *La microsonde Raman en gemmologie [Une méthode d'identification et d'authentification des gemmes]*. Revue de Gemmologie a.f.g. numéro hors série, p. 7

Schwarz D. (1998). *Südamerika: Brasilien und Kolumbien*. extraLapis; No 15. Rubin, Saphir, Korund: schön, hart, selten, kostbar [Hrsg.: Christian Weisel]. – München : Weise. P. 69.

Shigley J.E., Dirlam D.M., Schmetzer K., and Jobbins A. (1990). *Gem localities of the 1980s*. Gems & Gemology, Vol. 26, No 1, pp. 12, 24.

Shigley J.E., Dirlam D.M., Laurs B.M., Boehm E.W., Bosshart G., and Larson W.F. (2000). *Gem localities of the 1990s*. Gems & Gemology, Vol. 36, No 4, p 316.

Shigley J.E., Dirlam D.M., Laurs B.M., Boehm E.W., Bosshart G., and Larson W.F. (2000). *Major World Gem Producing Regions*. G.I.A. chart with regional maps showing approximate locations of significant gem localities in the 1990s. Gems & Gemology, Vol. 36, No 4.

Simonet C. (1997). *Géologie des gisements de saphirs*. Mémoire de Diplôme d'Université de Gemmologie, Université de Nantes, Nantes, France, pp. 38, 51, 53.

Simonet C. (2000). *Géologie des gisements de saphir et de rubis. L'exemple de John Saul Ruby Mine, Mangare, Kenya.* Spécialité: géologie – géophysique. Thèse présentée à la Faculté des Sciences et des Techniques de l'Université de Nantes. P. 159

Stutzer O. (1927). *Beiträge zur Geologie un Mineralogie von Kolumbien. IX. Beiträge zur Geologie des Cauca–Patia – Grabens.* Neues Jahrbuch für Mineralogie, Geologie und Paläontologie, LVII. Beilage-Band Abteilung B. E Schweizerbart'sche Verlagsbuchhandlung (Erwin Nägele) G.m.b.H., Stuttgart. Pp. 152-154 & Taf. V.

Stutzer O. (1934). *Contribución a la geología del foso Cauca – Patía.* CEGOC, tomo II, Bogotá, pp. 120-123.

Stutzer O. & Scheibe E.A. (1934). *Compilacion de los estudios geologicos oficiales en Colombia 1917 a 1933.* Tomo II. Ministèrio de Industrias, biblioteca del departamento de minas y petroleo. Bogotá (Colombia) imprenta nacional. P. 122.

Tardy M. & Level D. (1980). *Les pierres précieuses*. 5éme édition, collection Tardy, imprimerie Lienhart et Cie à Aubenas (Ardèche), France, pp. 400, 415-416.

Themelis T. (1992). *The heat treatment of ruby and sapphire*. Gemlab Inc. U.S.A. Pp. 22, 33, 37, 45, 46, 55, 94, 140-142, and pp. 156-160.

The University of Texas at Austin (2000). *Corundum.* Updated 10/29/00, Department of Geological Sciences, http://www.geo.utexas.edu/courses/347k/redesign/gem-notes/corun…/corundum-main.ht , pp. 1-10.

VanLandingham S.L. (1985). *Geology of world gem deposits. Review of the Geology of World Gem Deposits* [Colombia]. Van Nostrand Reinhold company Inc. P. 227.

Webster R. (1979). *Gemmologists' compendium*. 6th ed/revised by E.A. Jobbins, N.A.G. Press Ltd., London, EC1V 7QA, p. 193.

Webster R. (1994). *Gems their sources, descriptions, and identification*. 5th ed/revised by Peter G. Read, Butterworth-Heinemann Ltd., Oxford, p. 102.

GEOGRAPHY

Corundum has been reported for several centuries, to occur in Colombia (References – Colombian corundum. Figure 1), situated in the North-western corner of South America between 12°30' and 4°13' N and 66°51' and 79°71' W. Total land area of 1,141,748 km^2 (Instituto Geográfico Augustin Codazzi). An area about the size of Spain, Portugal and France put together, making it the fourth-largest country in South America, after Brazil, Argentina and Peru.

Figure 1. Colombia's location in South America

Colombia is the sole country in South America with coastlines on both the Pacific Ocean and the Caribbean Sea.
Its neighbours are Venezuela to the Northeast, Brazil in the Southeast, Peru in the South, Ecuador in the Southwest and Panama in the Northwest (Ortiz, 1990-1991. Figure 2).

Colombia is formed of two major geographical divisions:

- The Llanos, or great plains, in the East
- The Cordillera Region in the West (Harrison, 1929).

Figure 2. Colombia and its neighbours

The corundum (ruby and sapphires) deposits are situated in the Colombian Andes, which forms part of the *Cordillera* ("The volcanoes boulevard" as Jean Mermoz used to name it), the great circum-Pacific orogenic belt, of Upper Cretaceous and Tertiary orogeny running from western southern South America to Alaska (see Box A).

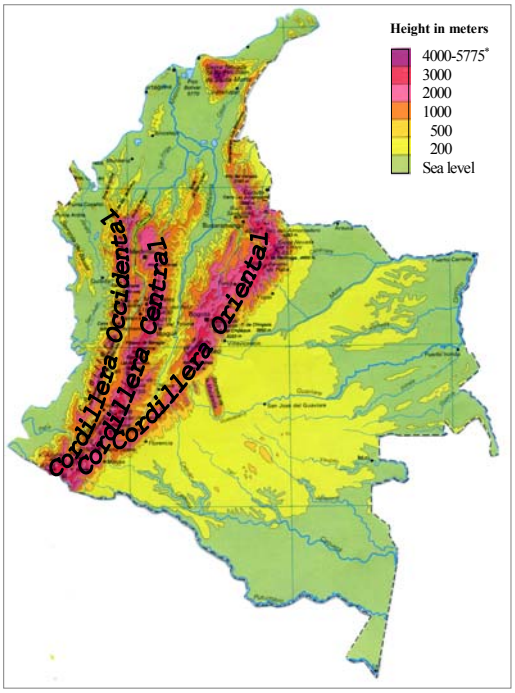

(Ortiz, 1990 – 1991)

Figure 3. The three Cordilleras.

* Twin peaks Simón Bolívar and Cristóbal Colón, both 5775 meters high, located 45 km from the Caribbean sea, in Sierra Nevada de Santa Marta, are Colombia's highest mountains (Dydiñsky, 1995).

When the 10000-Km Cordillera de los Andes (running from Tierra del Fuego to Curazao in the Caribbean Sea. Mojica, 1996), reaches Colombia (in Nariño), it divides into three elongated chains of mountains, respectively named, in the direction south-north, from east to west: Cordillera Oriental, Cordillera Central, and Cordillera Occidental (figure 3).

All three of the *Cordilleras* have peaks, mostly volcanic, and over 4,000 meters, which rise above the snow line. The Cordillera Central is the highest and most volcanic, with peaks over 5,000 meters, like the Nevado del Huila, its highest volcano, with 5,750 meters, and Los Nevados, a chain of volcanoes dominated by the Nevado del Ruiz at 5325 meters.

Twelve of the Colombian volcanoes are active (Azufral, Cerro Bravo, Chiles, Cumbral, Doña Juana, Galeras, Huila, Machín, Puracé, Ruiz, Sotará and Tolima) and have caused great destruction in the past, both with gas and ash explosions and by creating ice and mud slides (Brooks, 1977; Dydyñski, 1995; Espinosa, 1999; Pollard, 1998).

Two large valleys separate the three Cordilleras from one another: the Magdalena valley in the East, and the Cauca-Patía valley in the West.

It's in the high Patia valley (south of Patia valley), at the border between the Departments of Cauca and Nariño, south west of the village of Mercaderes (about 145 km SW of the city of Popayán), that the corundum deposits covering an area of some 60 km^2, are located (figure 4).

Unfortunately, due to political instability, the original (in situ) source as well as the parent rock of the Colombian corundum have not yet been determined.

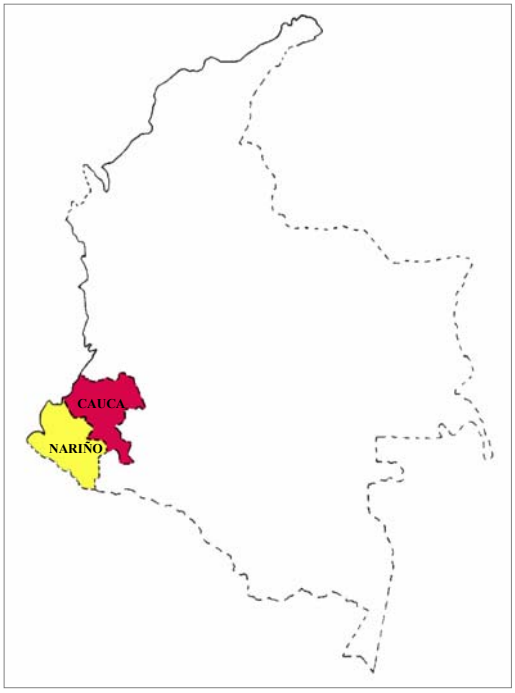

Figure 4. The corundum deposits located on the border between Cauca & Nariño.

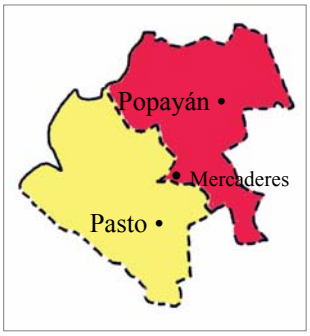

Department's Capital locality
CAUCA, Popayán
NARIÑO, Pasto

Box A: Colombian Cordilleran Orogeny

Most authors admit, that the Colombian Andes are the result of the superposition of different orogenies, produced by the interaction of two areas: the Pacific Oceanic area on the West, and the South American Continental area on the East.
They were formed by successive expansions of the continent from East to West, and their geologic sequences can be resumed in the following manner:

- During the Lower Palaeozoic, a Caledonian orogeny gives rise to the actual Cordillera Oriental.

- During the Upper Palaeozoic, a Hercyan orogeny forms the Cordillera Central.

- Finally, during the Upper Cretaceous and Tertiary, occurred the Andes orogeny, to which is attributed the formation of the Cordillera Occidental, an intense magmatic activity in the Cordillera Central, and the folding of Mesozoic and Tertiary sediments forming the burden of the Cordillera Oriental.

During the Upper Mesozoic, at the West of the Cordillera Central is located the Pacific Ocean area.
The limit between these two areas is a zone of subduction, the oceanic crust being generated in the Pacific ridge. This oceanic crust overlaps the continental crust during the Lower Cretaceous, and a new zone of subduction occurs at the West of the present Cordillera Occidental. During the remainder of the Cretaceous, the sediments of the Dagua Group, were deposited on the oceanic crust, then followed by the important submarine flows of the Diabasic Group. These last can be interpreted as the result of the volcanism attached to the new subduction zone, an “insular arc” type volcanism.
At the end of the Cretaceous, the Dagua Group and Diabasic Group are folded and form the Cordillera Occidental, and give rise between this one and the Cordillera Central to the small Cauca-Patia basin, in which the Tertiary sediments will be later deposited (Mosquera and Esmitta Formations).
(Espinosa, 1980).

GEOLOGY

The geology of the region (figure 5) consists of garnet-bearing tuffs extending on both sides of the central part of the Patía valley, ending in the south between the río Mayo and La Unión (La Caldera), and in the north between Mojarras and Dos Ríos.

The garnet-bearing tuffs usually are embedded in deep layers occupying the central part of the Patia valley, and can be seen only when they outcrop, in the south, in the region of Campamento and Mercaderes.
These outcrops are observed in the valley of Campamento (río Mayo), in the Honda valley (NW of Campamento), and also between Sombrerillo and Arboleda.
The maximum thickness registered for these tuffs, on the northern border of the río Mayo, does not exceed 200 meters. They generally consist of tuff agglomerates with volcanic bombs (geodes) which range in size from that of a human head (southern area), to that of an egg or a fist (western area), and to that of a small nut (northern area).
Amongst these volcanic bombs and lapillis, are found with andesite and basalt, other rocks from the deep algonkian (mica slates,

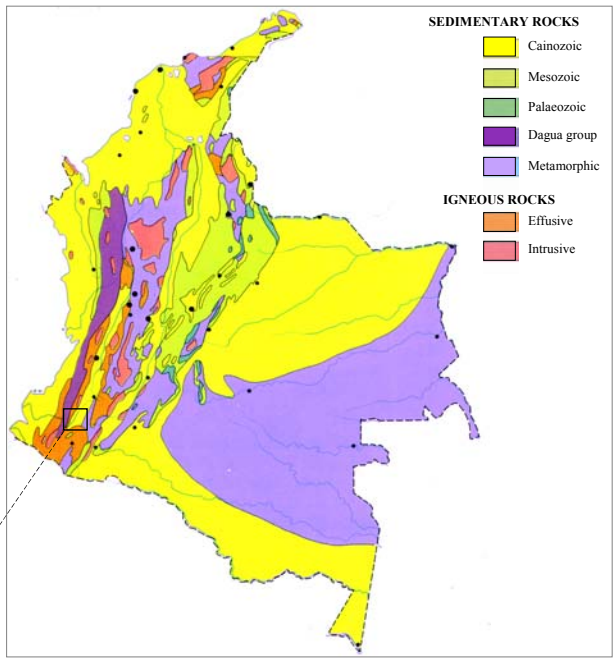

(Ortiz, 1990 – 1991)

Figure 5. Geological map of Colombia.

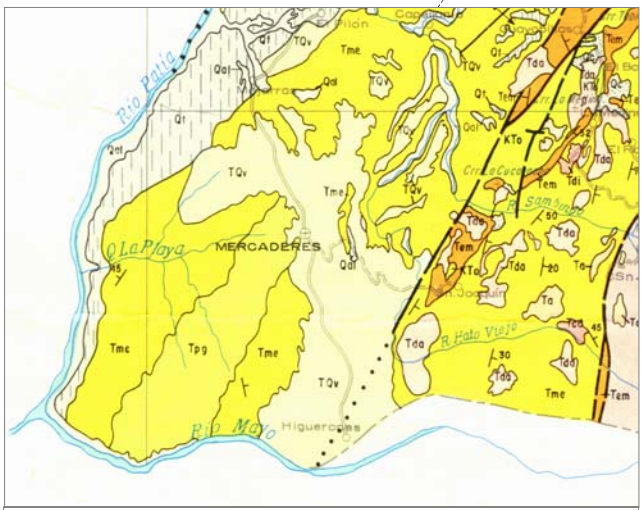

(Marin & Paris, 1979)

phyllites, and green shales, etc…) and archean bedrocks (eclogites, garnet-bearing amphibolites, shales, actinolite rocks, …). Volcanic bombs containing andine diorites, quartz and quartzites, are also encountered.
With the tuffs are found a lot of shale type and phyllitic rocks which are responsible for the characteristic dark grey colour of the tuff. Towards the West and North, amongst the agglomerated tuff, are found other rocks intercalated between the brownish grey tuff.
These rocks are observed between Sombrerillo and Arboleda, and in the slope of Mojarras.

In the region of Tapiales, NE of Rosario, are also found layers of white diatomaceous earth with gravels of quartz, quartzite, phyllite, ludite, porphyric and granitic rocks, andesite, porphyric tuff, silicitic shale, etc…

The fact that these garnet-bearing volcanic bombs (tuffites) not only diminish in size but also in quantity towards the West and the North, indicates that the eruption centre is located more East of Campamento.

The tuffs lie on cretaceous diabasic rocks between La Puertica and the Seca Valley, and on medio-*tertiary* purple clay in the slope of Campamento at río Mayo.
The garnet-bearing tuffs are without doubt caused by an andesic eruption as indicated by the frequency of the andesite volcanic bombs, while the basalt fragments are of a minor importance.
One of the most striking characteristics of the garnet-bearing tuffs lies in their very irregular position.
Most often they are inclined from 10 to 30 degrees and more, and even a vertical dip of heavy tuffs has been observed between Arboleda and Sombrerillo (figure 6).
In this case they are not the result of rising or folding as one would think at first sight, because the direction like the dip vary tremendously on very short distances.
The upper layers often lie in a discordant way on the inferior layers, in a concordant way between them and of the same lithological sequence. These conditions are identical to those observed in dunes and we therefore must consider the tuff formation as sub-aerial, deposited in a dry climate and under the action of very strong winds.
The best outcrops of the rocks are found between Sombrerillo and Arboleda. The agglomerated tuffs are not stratified to the contrary of dense tuffs interposition which frequently show a good stratification (Grosse, 1935).

It is of interest to note that Karsten (1886), Kunz (1908), Lleras Codazzi (1904; 1925; 1926; 1927), Scheibe (1921), Stutzer (1927, 1934), Stutzer & Scheibe (1934) observed corundum from these localities, while Grosse (1935) only noticed the presence of garnets.
Lleras Codazzi (1925; 1927; 1929a; 1929b), seems to be the only author to mention the occurrence of corundum in metamorphosed calcareous rocks, in the Northeastern Coast of Colombia, from the localities of la Sierra Nevada de Santa Marta (Department of Cesar), Ocaña, and near Pamplona, in the region between Cucutilla and Bochalema, and also near Chitagá, (Department of Norte de Santander, situated on the frontier with Venezuela).
It is interesting to note that Raleigh (1596) reported the existence of precious stones that look like sapphires (…"Captaine *Whiddon,* and our Chirurgion *Nich. Millechap* brought me a kinde of stones like *Saphires,* what they may proue I knowe not, I shewed them to some of the *Orenoqueponi,* and they promised to bring me to a montaine, that had of them very large peeces growing Diamond wise: whether it be Christall of the mountaine, *Bristoll Diamond,* or *Saphire* I doe not yet knowe, but I hope the best, sure I am that the place is as likely as those from whence all the rich stones are brought, and in the same height or very near."…), recovered from tributaries of the Río Caroní (one of the main tributary of the Orinoco, which forms part of the border between Colombia and Venezuela), in the vicinity of the Pacaraima mountains.

For the sapphires and rubies recovered presently (and for this study) solely from the río Mayo areas, from identical lithological sediments (figure 6), until the original source (*in situ*) as well as the parent rock is found, their origin can only be hypothesised:

- Maybe the sapphires and rubies crystallised in deep layers of the earth (ex. upper mantle), and were transported as xenocrysts to the earth's crust by alkali basalts?
- Or were formed in much older metamorphic rocks (probably palaeozoic) with other minerals (garnets, spinels, zircons, …) and were carried up by volcanic activity, and expelled to the earth's surface under the form of volcanic bombs?
- Or, maybe, both causes occurred, which means that, basaltic transported and metamorphic corundum can coexist?

These hypothesis seem possible due to the presence of basalt, metamorphic rocks, and to the numerous volcanoes in the region, like Los Coconucos volcanic Range, oriented N45W, composed of 9 aligned volcanoes of which the Pan de Azúcar 4670 m, and the Puracé 4650 m are the highest, the latter situated at the northern western extremity of the chain at almost the same latitude as Popayán, and distant of 27 km from this town, is the only active volcano in the park, with one of its most violent eruption taking place the 4th of November 1899 (see Box B), when rocks were thrown as far as Popayán, destroying it partially (Espinosa, 1999); or of the Doña Juana 4250 m (see Box C), situated some 20 km south of San Pablo, near the small town of San José, in the north east of Nariño, distant of 40 km from Mercaderes, with fully confirmed evidences that the volcano's rejections were transported to huge distances by the Río Mayo (Espinosa, 1999; Méndez, 1989); or of the Galeras 4250 m (again see Box C), distant of 8 km from its capital Pasto, and of 60 km from Mercaderes.
These hypothesis are in line with the accessory minerals found in most of the corundum placer deposits, which include:

- **Heavy minerals**

Black spinel (magnetite), ilmenite, olivine (peridot), garnet (almandite, pyrope and grossularite), kornerupine (green), hornblende, anthophyllite, sphene, augite, and hematite (Karsten, 1886; Keller *et al.,* 1985; Lleras Codazzi, 1927; Martinez and Garcia, 1989; Montero, 1992; Themelis, 1992).
All of these and, zircon* (colourless, transparent and doubly terminated with a very small inclusion of a metamict zircon), kyanite, actinolite, chromium pyroxene, ortho-pyroxene, and intergrown minerals garnet + peridot, were identified by the writer in gem concentrates from the Mercaderes area with the exception of anthophyllite and augite.

- **Light minerals**

Quartz, jasper, feldspar (plagioclase), apatite, man-made glass and sometimes volcanic glass.

---

* *Scheibe (1921) mentions colourless zircons encountered in the region of Tequendama, and Lleras Codazzi (1904, 1927) describes their occurrence as small crystals disseminated sporadically with volcanic tuffs, in many areas of Colombia, but particularly along the Cordillera Central, in the río Mayo, and other localities situated in the Southern part of Cauca department.*

REMPLACER CETTE PAGE PAR LA PAGE

Box B: Synthesis of Historic Activities of Volcano Puracé

Puracé volcano (2°22'N; 76°23'W; altitude 4650 meters) is the main active andesic stratovolcano of Los Coconucos volcanic range, located at the Cordillera Central of Colombia, in the Cauca department, 27 km from its capital city, Popayán.
It is interesting to note that between 1801 and 1977, the dormant period never exceeded 25 years (Espinosa, 1999; Méndez, 1989; Smithsonian Institution, 2000a).

Year	Description
1559-1560	Fumarole activities. Eruptions. Between 1540 and 1560, the cone's altitude diminishes.
1560-1583	Eruptions.
1789	Explosion?
1801	Fumarole activity.
1816	Small explosive activity.
1823	Fumaroles.
1835	Explosions.
1849	Important eruption, streams of mud and ashes. An explosion destroys the cone's summit.
1869	Violent explosions. Very thick rains of ashes which affected the Río Cauca and Popayán.
1871	Earthquake?
1875	Fumarole activity.
1878	Explosion and rain of ashes.
1899	Violent eruption with rocks thrown as far as Popayán, destroying partially the town, and streams of mud spreading towards the occidental part of Colombia.
1906	Explosions.
1907	Explosion.
1912	Eruption with lava flow?
1914	Eruption.
1919	Explosion and rain of ashes in Popayán.
1920	Explosion and rain of ashes over Popayán.
1925	Explosive eruptions.
1926	Eruption, rains of bombs and ashes.
1932	Explosion, rain of ashes over Popayán.
1933	Explosion, and stream of ashes.
1936	Explosion.
1939	Explosion with rain of ashes over Popayán.
1941	Explosion with rain of ashes over Popayán.
1946	Explosion with rain of ashes over Popayán.
1947	Explosion and fall of ashes and lapillis travelling a distance of 16 km.
1949	Explosions, with volcanic bombs and ashes.
1950	Explosions.
1954	Explosion.
1955	Explosions.
1956	Explosion and rain of ashes.
1958	Eruption.
1977	Explosion with ash emission.
1990	Sulfur-rich summit fumaroles and flank hot springs.
1993	Summit fumarole.
2000	Anomalous earthquakes and banded tremor.

Box C: Synthesis of Historic Activities of Volcanoes Doña Juana, Galeras and Azufral

Doña Juana volcano (1°31'N; 76°56'W; altitude 4250 meters) is an active stratovolcano, located at the Cordillera Central of Colombia, in the department of Nariño, distant of 40 km from Mercaderes and 20 km from San Pablo (Espinosa, 1999; Méndez, 1989).

Year	Description
1897-1898	Minor activity with eruptions in 1897.
1899	Explosions, with possible pyroclastic flows and flaming clouds.
1913	Eruption (no confirmation).
1922	Minor activity. Explosion.
1925	No fumarole activity (no confirmation).
1936	Minor activity. Explosion.

Galeras volcano (1°13'N; 77°22'W; altitude 4270 meters) is an active andesic stratovolcano, located at the Cordillera Central of Colombia, in the department of Nariño, distant of 8 km from its capital Pasto, and 60 km from Mercaderes. Bensusan (1934) mentions that the volcano is almost always emitting smoke, dense volumes at times rising up to some thousands of feet.
During the last 500 years, eruptions have been characterised by gas and ash emissions, small lava flows, and explosive eruptions producing pyroclastic flows that have travelled up to 15 km from the crater (Cepeda, 1989; Espinosa, 1999; Méndez, 1989; Smithsonian Institution, 2000b).

Year	Description
1535	Explosive eruption in the central crater.
1590	Explosive eruption in the central crater with lava flows.
1687	Explosive eruption in the central crater.
1690	Explosive eruption in the central crater.
1696	Explosive eruption in the central crater.
1717	Explosive eruption in the central crater.
1727	Explosive eruption in the central crater.
1736	Explosive eruption in the central crater.
1754-1756	Explosive eruption in the central crater.
1796-1801	Explosive eruption in the central crater with lava flows.
1831-1834	Explosive eruption in the central crater with lava flows.
1865-1870	Explosive eruption in the central crater with lava flows.
1924-1927	Explosive eruption in the central crater with dome extrusion.
1936	Explosive eruption in the central crater with lava flows.
1947	Explosive eruption in the central crater.
1973	Explosive eruption in the central crater.
1974-1977	Explosive eruption in the central crater.
1988	Fumarolic reactivation.
1989	Ash emission from secondary crater.
1992	Explosive eruption from the central crater with dome's destruction.
1993	Explosive eruptions from the central crater.
1994	Small eruption associated to gas emission.
2000	Small eruptions preceded by tornillo ("screw-type") seismic events.

Azufral volcano (1°05'N; 77°43'W; altitude 4070 meters) is an active stratovolcano-calderic, located at the Cordillera Central of Colombia, in the department of Nariño, distant some 45 Km from Pasto (Espinosa, 1999; Méndez, 1989; Smithsonian Institution, 2000c).

Year	Description
-	Historical activity unknown.
1990	Fumarolitic activity

LOCATION AND OCCURRENCE

Corundum is recovered from various stream beds, terraces, gravel, and numerous shallow creeks, situated on both sides of the Río Mayo, and from sands of the Río Platoyaco.

In the department of Cauca (figure 6)**:**

Near the village of Mercaderes: In Quebrada Senegetas, LaMaria ranch. Also in Río Sangandinga. (Themelis, 1992).
Close to the village of Sombrerillo and hamlet of Sombrerillos: In Quebrada del Rubi (Bergt, 1899; Karsten, 1886; Martinez and Garcia, 1989; Themelis, 1992), and Quebrada Limoncito.
In the region of the village of Arboleda: In Quebrada Las Cañadas (Themelis, 1992). In Quebrada Paloverde, Quebrada Honda, Quebrada Monserrate, Quebrada Monteoscuro (Martinez and Garcia, 1989; Stutzer, 1927, 1934,), and Alto La Cañada .

On the border between the departments of Cauca and Nariño (figure 7)**:**

Mixed with garnets and amethysts in the Río Mayo, which forms part of the border between Cauca and Nariño (Bergt, 1899; Montero, 1992; Karsten, 1886; Keller, Koivula *et al.*, 1985; Scheibe, 1921; Webster 1994).

In the department of Nariño (figure 8)**:**

At San Pablo, some 20 km from volcano Doña Juana.
In the immediate of Pasto, situated some 8 km from volcano Galeras, and 60 km from Mercaderes (Karsten, 1886; Lleras Codazzi, 1904, 1926, 1927).

In the department of Caquetá:

From sands of the Río Platoyaco, a tributary of the Río Caquetá (Scheibe, 1921; Webster 1994).

Figure 9. The village of Mercaderes.

Figure 10. Detail of Quebrada Limoncito.

The corundum crystals and the faceted stones studied in the following pages, were obtained from at least four different deposits, situated on the border between the departments of Cauca and Nariño.

In the department of Cauca:

- Near the village of Mercaderes (figure 9).
- Towards the North West of the village of Sombrerillo (Quebrada Limoncito. Figure 10).
- At the West of the village of Arboleda (Alto La Cañada).

In the department of Nariño:

- At San Pablo (Some 20 km SE from the village of Mercaderes).

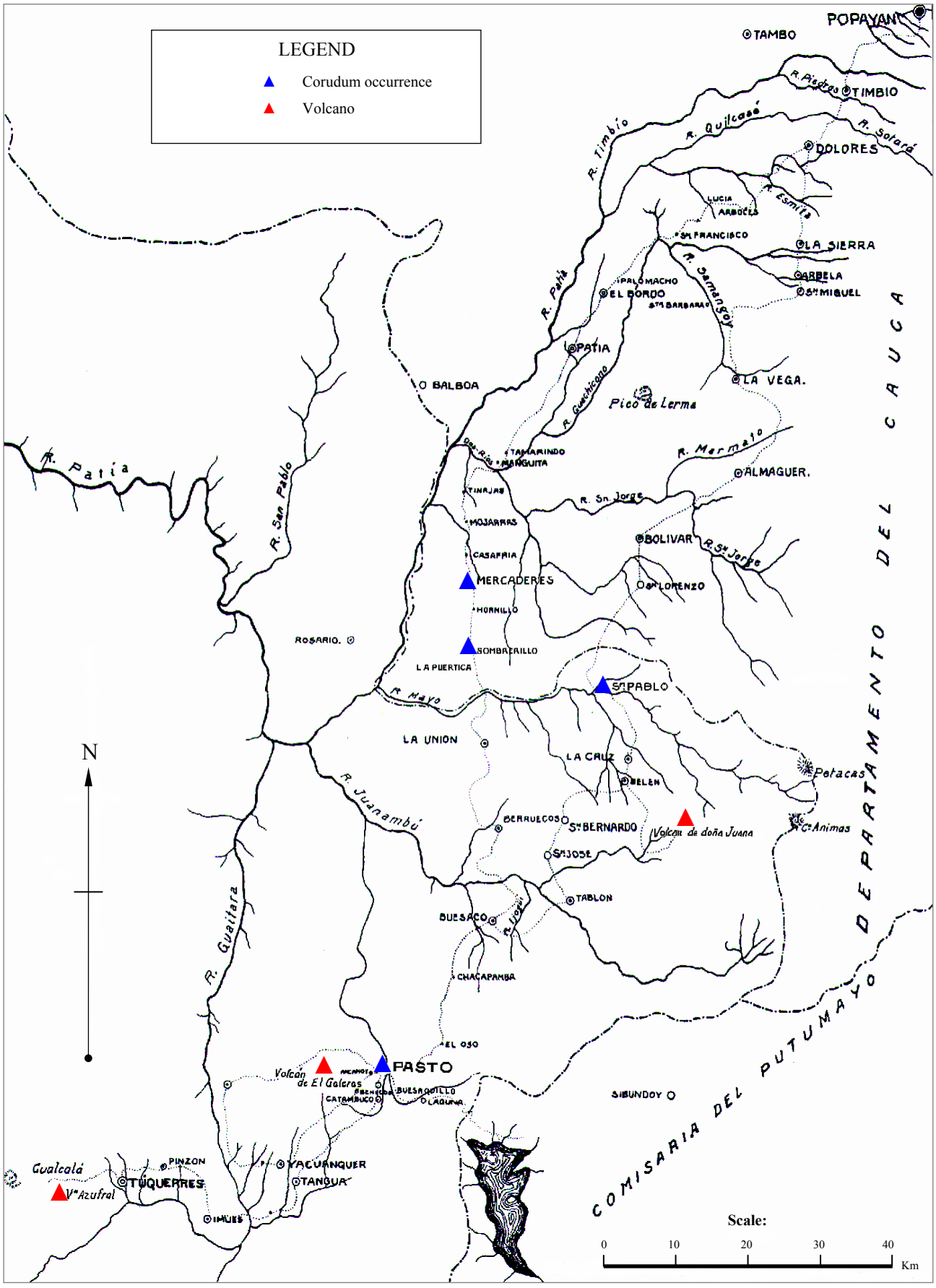

Figure 7. Geographic map showing corundum occurrence within the area of Popayan and Pasto.(Cauca and Nariño Departments).
(Stutzer, 1927)

REMPLACER CETTE PAGE PAR LA PAGE

REFERENCES

Brooks J. (1977). *South American Handbook*. Trade & Travel Publications Ltd., Bath BA1 1EN, England. P. 366.

Bensusan A.J. (1934). *Colombia revisited.* The Minig Magazine. Mining Publications, Ltd., at Salisbury House, London, E.C. 2., Vol. LI. No 4. Pp. 213-219;

Cepeda H (1986). *Investigaciones petrológicas en el ámbito de las planchas 429 Pasto y 410 La Unión, con especial énfasis en el Complejo Volcánico del Galeras.* Boletin geologica Ingeominas, Bogotá, Colombia, Vol. 30, No 1, pp. 43-113.

Dydyñski K. (1995). *Colombia.* Lonely Planet travel survival kit, Lonely Planet Publications, PO Box 617, Hawthorn, Vic 3122, Australia. Pp. 28-30, 455-456.

Espinosa A. (1980). *Sur les roches basiques et ultrabasiques du bassin du Patia (Cordillière Occidentale des Andes Colombiennes).* Etude géologique et pétrographique. Thèse présentée à la Faculté des Sciences de l'Université de Genève (dép. de minéralogie), N° 1970. Imprimerie Nationale, Genève. Pp 1-242.

Espinosa A. (1999). *Erupciones históricas de los volcanes colombianos* (en prensa). Academia Colombiana de Ciencias Exactas, Fisicas y Naturales / Universidad del Quindío.

Harding C. (1996). *Colombia*. In Focus, pub. By Latin America Bureau (Research and Action) Ltd, 1 Amwell Street, London EC1R 1UL. P. 71.

Harrison J.V. (1929). *The Magdalena Valley, Colombia, South America.* [Reprinted from Vol. II of the Compte Rendu, XV International Geological Congress, South Africa, 1929.] Pp. 400

Instituto Geográfico Augustín Codazzi (1996). *Mapa del departamento de Nariño. Escala 1:25.000.* República de Colombia, ministerio de hacienda y crédito público.

Martin P. & Paris G. (1979). *Mapa geologico generalizado del departamento del Cauca. Escala 1:350.000.* República de Colombia, ministerio de minas y energia, Instituto Nacional de investigaciones geologico-mineras, oficina regional Popayan.

Méndez R. (1989). *Católogo de los Volcanes Activos en Colombia*. Ingeominas, Boletín Geológico, Bogotá. Vol. 30, N°3, pp. 1-75.

Mojica J. (1996). *Generalidades acerca de la geología de Colombia*. Geología Colombiana No 20, pp. 157-162.

Ortiz F.G. (1990 – 1991). *Nuevo primer atlas de Colombia.* 6th ed., Editorial Voluntad S.A., Carrrera 7 No. 24 – 89 Piso 20, Bogotá – Colombia.

Ortiz F.G. (1991 – 1996). *Nuevo primer atlas de Colombia.* Editorial Voluntad S.A., Carrrera 7 No. 24 – 89 Piso 24, Santafé de Bogotá – Colombia.

Pollard P. (1998). *Colombia handbook.* Footprint Handbooks Ltd., 1st edn., Clays Ltd., Bungay, Suffolk, Great Britain. Pp. 33-35.

Smithsonian Institution (2000a). *Puracé Volcanic Activity Reports.* Global Volcanism Program, National Museum of Natural History, E-421, Washington DC 20560-0119. Pp. 1-4.

Smithsonian Institution (2000b). *Galeras Volcanic Activity Reports.* Global Volcanism Program, National Museum of Natural History, E-421, Washington DC 20560-0119. Pp. 1-14.

Smithsonian Institution (2000c). *Azufral Volcanic Activity Reports.* Global Volcanism Program, National Museum of Natural History, E-421, Washington DC 20560-0119. Pp. 1-2.

APPEARANCE

The first twenty-two rough crystals* (figure 11) and the recent two thousand seven hundred and ninety one rough corundum crystals were obtained from at least four different sources:

Year	*Rough corundum*	*Total weight*	*Sources*
1991	18*	No data	(A) San Pablo (Nariño)
1997	59	112.53 carats	(A) San Pablo (Nariño)
1997	10	45.57 carats	(HH) Mercaderes (Cauca)
1997	21	42.08 carats	(PV) Quebrada Limoncito (Cauca)
1997	5	20.75 carats	(GT) Alto La Cañada (Cauca)
1999	426	546.94 carats	(PV) Borders of the Río Mayo area (Cauca - Nariño)
1999	356	1268.70 carats	(PV) Borders of the Río Mayo area (Cauca - Nariño)
1999	1914	1516.51 carats	(PV) Borders of the Río Mayo area (Cauca - Nariño)
	2809	3553.08 carats	

**** Four rough crystals were proved to be garnets***

Figure 11. The twenty-two rough crystals from Colombia examined for this study in 1991. The four red crystals were positively identified as garnets by their absorption spectrum. (Size range: 3.30 x 3.30 x 2.50 mm to 6.80 x 6.30 x 16.20 mm)

These two thousand eight hundred and nine rough corundum crystals examined for this study showed a great variety of forms (figure 12):

Rolled crystals with or without discernible shape:

- Partly rolled crystals showing conchoidal fractures (66% of the rough crystals).
- Rolled pebbles without visible external crystal faces (20% of the rough crystals).

Crystals showing a geometric habitus:

(a) + (b) Columnar, first order hexagonal prism (100) or second order hexagonal prism (110), terminated by pinacoid basal planes (less than 9% of the rough crystals examined which often showed basal parting).

(c) Tabular hexagonal prism terminated by basal pinacoids (001) (less than 5% of the rough crystals examined).

(d) Pseudo hexagonal prism showing triangular striations on the basal plane (about ten rough crystals, figure 13).

(e) Columnar hexagonal truncated bipyramids with basal planes (about six rough crystals).

(f) Columnar half-hexagonal prism terminated by basal planes, showing a perfect parting plane parallel to a rhombohedral face (010) (less than five rough crystals).

(g) More or less columnar bipyramid (221) showing vague possible second order hexagonal bipyramids near the summit (223) (two rough crystals).

(h) Hexagonal prism showing interpenetrant twinning (one rough crystal, figure 14).

(i) Rolled tabular hexagonal sapphire with a yellow partly rolled columnar hexagonal sapphire breaking its surface (a rough crystal, figure 20 & 21).

Note Polysynthetic twinning is very common and apparent on most rough crystals, along the basal pinacoid faces {001}.

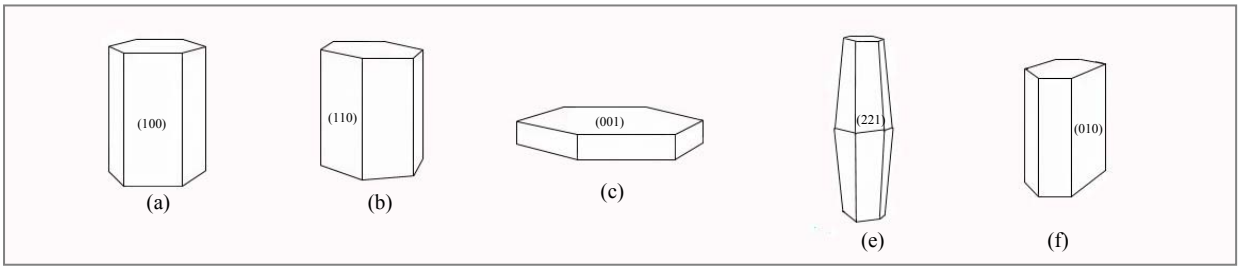

Figure 12. The main habitus exhibited by the Colombian rough corundums examined.

Only 384 rough crystals showed a more or less distinct hexagonal shape (less than 14% of the rough crystals examined), usually rounded and corroded, some with their crystal faces perforated, and many displaying surfaces due to fractures.

Surprisingly, twelve almost perfect hexagonal prisms were found to exhibit linear sharp edges (less than 0.5% of the rough crystals examined).

All the remainders of the rough crystals were so rounded or so fractured that no distinct shape could be recognised. Most had a frosted appearance, while others showed vermicules as a result of extensive stream wear due to their alluvial transportation.

The size of the rough crystals ranged from 2.40 x 2.20 x 1.70 mm (0.08 ct) to 8.90 x 6.40 x 7.90 mm (27.78 cts), for an average size of approx. 5.50 x 4.00 x 5.60 mm (1.10 ct).

It is interesting to note that pure (spectral) colours were virtually not encountered, but that variations of near colourless (less than five crystals), greenish-blue, greyish-blue, brownish-yellow, yellowish-green, brownish-red, and multicoloured predominated, with very often a more or less important yellow zone present.
Amongst these 2809 rough crystals, only a minute ruby crystal of 2.50 x 2.10 x 2.00 mm (0.07 ct) was encountered.
The multicoloured crystals had their colours sharply bounded from one another, and some crystals had their colour in layers parallel to the basal plane of the crystal, giving rise to a banded structure.
None of these rough crystals were truly of gem quality, but they permitted to obtain their physical and optical properties, absorption spectra, and to analyse the inclusions they contained.

Figure 13. A rough corundum crystal from Colombia, showing a hexagonal prism habitus with triangular growth planes along a basal plane.
(Dark field illumination 15x)

Figure 14. An hexagonal rough sapphire from Colombia, showing interpenetrant twinning very similar to those encountered in rough sapphires from Madagascar.
(Dark field illumination 30x)

Concerning the forty-one faceted corundums examined and described in the following pages, these were received at diverse times and lots, and from four sources:

Year	*VARIETY* *Reference*	*Specimen*	*Sources*
	RUBIES		
1991	A-01 to A-06	6	(A) San Pablo (Nariño)
1997	GT-01 & GT-02	2	(GT) Alto la Cañada (Cauca)
	Total	8	
	SAPPHIRES		
1991	A-07 to A-20	14	(A) San Pablo (Nariño)
1997	A-31	1	(A) San Pablo (Nariño)
1977	HH-01	1	(HH) Mercaderes area (Cauca)
	Total	16	
	HEAT-TREATED SAPPHIRE		
1997	TT-01	1	(TT) Borders of the Río Mayo (Cauca – Nariño)
	MULTICOLOURED SAPPHIRES		
1991	A-21 to A-30	10	(A) San Pablo (Nariño)
1997	A-32	1	(A) San Pablo (Nariño)
1997	HH-02	1	(HH) Mercaderes area (Cauca)
2000	A-34	1	(A) San Pablo (Nariño)
	Total	13	
	COLOUR-CHANGE SAPPHIRE		
1997	A-33	1	(A) San Pablo (Nariño)
	HEAT-TREATED COLOUR-CHANGE SAPPHIRES		
1997	TT-02 & TT-03	2	(TT) Borders of the Río Mayo (Cauca – Nariño)

As for the twelve corundums that were re-examined recently, they consisted in:

Reference	*VARIETY* *Cut or shape*	*Weight* *(carat)*	*Colour*
	RUIES		
A-01	Pear-shape	1.86	Deep pinkish-red
A-05	Cabochon	1.66	Pinkish-red
A-06	Cabochon	6.24	Violet-red
	SAPPHIRES		
A-07	Cabochon	3.01	Greyish-blue
A-08	Cabochon	2.66	Greenish-blue
A-11	Marquise	2.19	Greyish-blue
A-13	Oval-shape	3.42	Greenish-blue
A-14	Oval-shape	3.55	Light greenish-blue
A-17	Oval-shape	1.65	Slight greenish pale blue
	MULTICOLOURED SAPPHIRES		
A-25	Oval-shape	2.58	Violet-blue, pink, faint orange, pale yellow
A-28	Oval-shape	1.53	Violet-blue, violet-pink, yellow
A-30	Oval-shape	3.32	Red, yellow, blue, orange, purple

REFRACTIVE INDICES

The refractive index determinations obtained on some rough crystals but on all the faceted gems were carried out using a Rayner Dialdex refractometer and monochromatic sodium light. The refractive indices were found very constant and gave ω 1.768 to 1.772, ε 1.760 to 1.764, with a birefringence of .008, with optic sign (-) (Table 1).
A uniaxial interference figure was obtained readily, under the polariscope set to its dark position.

SPECIFIC GRAVITY

All the rough crystals sank rapidly in 3.32 methylene iodide heavy liquor. The specific gravity for the forty-one faceted crystals was obtained by hydrostatic weighing of the stones in distilled water using a Mettler electronic PL 300C carat scale, and the stones were found to have a specific gravity between 3.98 and 4.02 (Table 1).

ULTRA-VIOLET FLUORESCENCE

The stones were examined with a combined LW/SW Multispec Unit (Table 2).

- Under short-wave ultra-violet radiation, all but one remained inert: ruby (A-05), which fluoresced a weak red.
  Under long-wave ultra-violet radiation the same ruby (A-05), fluoresced a moderate red while all the others fluoresced a weak red.

- The sapphires showed no reaction under short-wave radiation.
  Under long-wave radiation, all remained inert except for two stones:
  A greyish-blue sapphire (A-12), which showed a light yellow colour zone in its centre, this zone, fluoresced weakly in yellow.
  An intense blue sapphire (A-18) glowed moderately in green colour.

- The heat-treated sapphire showed no reaction to both short-wave and long-wave radiations.

- The multicoloured sapphires showed no reaction under short-wave radiation, whereas under long-wave radiation, a stone (A-22) glowed in its centre in a strong yellow, while areas of orange fluorescence were observed in two other stones (A-25 and A-26).
  For stone A-25, the orange fluorescence came from the faint orange and pale yellow zone filling half of the stone.

- The only colour-change sapphire encountered, was found inert to short-wave and long-wave radiations.

- The heat-treated colour change sapphires remained inert to both short-wave and long-wave radiations.

TABLE 1 The physical properties of the forty-one faceted corundums from Mercaderes-Rio Mayo area, Cauca-Nariño, Colombia

Source	VARIETY Cut or shape	Weight (carat)	Colour	Refractive index	Double refraction	Specific gravity
	RUBIES					
A-01	Pear-shape	1.86	Deep pinkish-red	1.763-1.771	.008	4.000
A-02	Oval-shape	2.33	Pinkish-red	1.762-1.770	.008	4.020
A-03	Pear-shape	1.55	Purplish-red	1.762-1.770	.008	4.013
A-04	Pear-shape	1.42	Intense pink	1.762-1.770	.008	4.020
A-05	Cabochon	1.66	Pinkish-red	1.770 (spot)	No data	4.011
A-06	Cabochon	6.24	Violet-red	1.770 (spot)	No data	4.010
GT-01	Oval-shape	0.33	Pinkish-red	1.762-1.770	.008	4.000
GT-02	Pear-shape	0.19	Intense pink	1.762-1.770	.008	4.002
	SAPPHIRES					
A-07	Cabochon	3.01	Greyish-blue	1.770 (spot)	No data	3.996
A-08	Cabochon	2.66	Greenish-blue	1.770 (spot)	No data	3.998
A-09	Cabochon	3.24	Greyish-blue	1.770 (spot)	No data	3.998
A-10	Oval-shape	2.58	Violet-blue	1.762-1.770	.008	3.993
A-11	Marquise	2.19	Greyish-blue	1.762-1.770	.008	3.996
A-12	Oval-shape	6.89	Greyish-blue	1.762-1.770	.008	3.991
A-13	Oval-shape	3.42	Greenish-blue	1.762-1.770	.008	3.994
A-14	Oval-shape	3.55	Light greenish-blue	1.762-1.770	.008	3.993
A-15	Oval-shape	2.01	Light blue	1.762-1.770	.008	3.996
A-I6	Oval-shape	1.91	Lilac	1.762-1.770	.008	3.995
A-17	Oval-shape	1.65	Slight greenish pale blue	1.762-1.770	.008	3.997
A-18	Cabochon	3.22	Intense blue	1.770 (spot)	No data	No data
A-19	Cabochon	2.93	Intense blue	1.770 (spot)	No data	3.991
A-20	Cabochon	2.46	Intense blue	1.770 (spot)	No data	3.999
HH-01	Oval-shape	4.81	Greyish-blue	1.762-1.770	.008	4.011
A-31	Cabochon	0.71	Bluish-grey	1.770 (spot)	No data	4.005
	HEAT-TREATED SAPPHIRE					
TT-01	Oval-shape	2.14	Dark blue	1.764-1.772	.008	4.020
	MULTICOLOURED SAPPHIRES					
A-21	Oval-shape	2.36	Pink, blue, violet	1.762-1.770	.008	4.000
A-22	Oval-shape	2.80	Grey, blue, pink, orange	1.762-1.770	.008	3.992
A-23	Brilliant-cut	1.83	Grey-blue, pink	1.762-1.770	.008	4.001
A-24	Oval-shape	1.15	Lavender, grey, pink	1.760-1.768	.008	3.996
A-25	Oval-shape	2.58	Violet-blue, pink faint orange, pale yellow	1.762-1.770	.008	4.018
A-26	Oval-shape	2.58	Pale blue, grey, pink	1.762-1.770	.008	4.004
A-27	Oval-shape	2.96	Grey-blue, pale blue, pink	1.764-1.772	.008	4.000
A-28	Oval-shape	1.53	Violet-blue, violet-pink, yellow	1.762-1.770	.008	4.000
A-29	Brilliant-cu	1.90	Intense pink, lavender, light blue	1.762-1.770	.008	3.999
A-30	Oval-shape	3.32	Red, yellow, blue, orange, purple	1.762-1.770	.008	3.997
HH-02	Oval-shape	0.96	Parti-coloration: Blue; pink	1.762-1.770	.008	3.993
A-32	Cabochon	1.66	Blue, yellow, pink	1.770 (spot)	No data	3.990
A-34	Oval-shape	0.30	Dark blue, orangy-pink,	1.760-1.768	.008	3.991
	COLOUR-CHANGE SAPPHIRE					
A-33	Oval-shape	0.65	From blue to purple	1.762-1.770	.008	4.000
	HEAT-TREATED COLOUR-CHANGE SAPPHIRES					
TT-02	Oval-shape	0.96	From blue to purple	1.762-1.770	.008	4.000
TT-03	Oval-shape	0.95	From blue to purplish red	1.763-1.771	.008	3.987

Key to source: (A) San Pablo (Nariño). (HH) Collection H. Hänni. (GT) Alto La Cañada (Cauca). (TT) Heated by T. Themelis

TABLE 2 The ultra-violet fluorescence of the forty-one faceted corundums from Mercaderes-Rio Mayo area, Cauca-Nariño, Colombia

Source	VARIETY Cut or shape	Weight (carat)	Colour	UV 254 nm	UV 365 nm
	RUBIES				
A-01	Pear-shape	1.86	Deep pinkish-red	Nil	Weak, red
A-02	Oval-shape	2.33	Pinkish-red	Nil	Weak, red
A-03	Pear-shape	1.55	Purplish-red	Nil	Weak, red
A-04	Pear-shape	1.42	Intense pink	Nil	Weak, red
A-05	Cabochon	1.66	Pinkish-red	Weak, red	Moderate, red
A-06	Cabochon	6.24	Violet-red	Nil	Weak, red
GT-01	Oval-shape	0.33	Pinkish-red	Nil	Very weak, red
GT-02	Pear-shape	0.19	Intense pink		
	SAPPHIRES				
A-07	Cabochon	3.01	Greyish-blue	Nil	Nil
A-08	Cabochon	2.66	Greenish-blue	Nil	Nil
A-09	Cabochon	3.24	Greyish-blue	Nil	Nil
A-10	Oval-shape	2.58	Violet-blue	Nil	Nil
A-11	Marquise	2.19	Greyish-blue	Nil	Nil
A-12	Oval-shape	6.89	Greyish-blue	Nil	Weak, yellow centre
A-13	Oval-shape	3.42	Greenish-blue	Nil	Nil
A-14	Oval-shape	3.55	Light greenish-blue	Nil	Nil
A-15	Oval-shape	2.01	Light blue	Nil	Nil
A-I6	Oval-shape	1.91	Lilac	Nil	Nil
A-17	Oval-shape	1.65	Slight greenish pale blue	Nil	Nil
A-18	Cabochon	3.22	Intense blue	Nil	Moderate, green
A-19	Cabochon	2.93	Intense blue	Nil	Nil
A-20	Cabochon	2.46	Intense blue	Nil	Nil
HH-01	Oval-shape	4.81	Greyish-blue	Nil	Nil
A-31	Cabochon	0.71	Bluish-grey	Nil	Nil
	HEAT-TREATED SAPPHIRE				
TT-01	Oval-shape	2.14	Dark blue	Nil	Nil
	MULTICOLOURED SAPPHIRES				
A-21	Oval-shape	2.36	Pink, blue, violet	Nil	Nil
A-22	Oval-shape	2.80	Grey, blue, pink, orange	Nil	Strong, yellow centre
A-23	Brilliant-cut	1.83	Grey-blue, pink	Nil	Nil
A-24	Oval-shape	1.15	Lavender, grey, pink	Nil	Nil
A-25	Oval-shape	2.58	Violet-blue, pink faint orange, pale yellow	Nil	Moderate, half stone orange
A-26	Oval-shape	2.58	Pale blue, grey, pink	Nil	Moderate, half stone orange
A-27	Oval-shape	2.96	Grey-blue, pale blue, pink	Nil	Nil
A-28	Oval-shape	1.53	Violet-blue, violet-pink, yellow	Nil	Nil
A-29	Brilliant-cut	1.90	Intense pink, lavender, light blue	Nil	Nil
A-30	Oval-shape	3.32	Red, yellow, blue, orange, purple	Nil	Nil
HH-02	Oval-shape	0.96	Parti-coloration: Blue; pink	Nil	Nil
A-32	Cabochon	1.66	Blue, yellow, pink	Nil	Nil
A-34	Oval-shape	0.30	Dark blue, green, orangy-pink,	Nil	Nil
	COLOUR-CHANGE SAPPHIRE				
A-33	Oval-shape	0.65	From blue to purple	Nil	Nil
	HEAT-TREATED COLOUR-CHANGE SAPPHIRES				
TT-02	Oval-shape	0.96	From blue to purple	Nil	Nil
TT-03	Oval-shape	0.95	From blue to purplish red	Nil	Nil

Key to source: (A) San Pablo (Nariño). (HH) Collection H. Hänni. (GT) Alto La Cañada (Cauca). (TT) Heated by T. Themelis

PLEOCHROISM

Using a calcite dichroscope with fibre optic illumination, a distinct to strong dichroism was observed in all the corundums examined except for a bluish-grey sapphire (A-31), which exhibited a very weak dichroism (Table 3).

- All the rubies examined exposed purplish-red for the ω-ray (parallel to the c-axis), and orangy-red for the ε-ray (perpendicular to the c-axis).
- The sapphires examined, most often showed hues ranging from greyish-blue to greenish-blue or bluish-grey for the ω-ray, and either bluish-green, or greyish-green, or violetish-blue, or pinkish blue, or pinkish-grey, for the ε-ray.
- The heat-treated sapphire displayed dark blue for the ω-ray, and greenish-blue for the ε-ray.
- All the multicoloured sapphires examined exhibited violetish-red colours to pinkish-blue or light blue for the ω-ray, and either yellow-green, or greenish-yellow, or pink, or greyish-red, or yellowish-grey, for the ε-ray.
- The colour-change sapphire and the heat-treated colour-change sapphires displayed purple for the ω-ray and yellowish-grey to greyish-yellow for the ε-ray.

SPECTROSCOPIC EXAMINATION

The absorption spectrum seen through a Gem Beck Spectroscope Unit was observed in total darkness (Table 4).

- All the rough crystals were tested, and every sample of corundum displayed an absorption spectrum very similar to those recorded for the faceted stones.
- The rubies often showed a strong absorption 400-460 nm, very weak lines near 468, 474 and 478 nm, strong band 530-580 nm, distinct line 660 nm, and a fluorescent line near 690 nm.
- The sapphires generally showed a strong absorption 400-420 nm, a very strong band 450-460 nm, and a very strong band 620-700 nm.
- The heat-treated sapphire showed a strong absorption 400-420 nm, a strong band 450-460 nm, three lines centered at 600, 610, 620 nm, and a strong absorption 630-700 nm.
- The multicoloured sapphires showed a very strong absorption 400-420 nm, most often a strong band 450-460 nm, sometimes weak lines 472, 478 nm, weak band 530-560 nm, occasionally a line at 640 nm, and a very very strong absorption around 650-700 nm.
- The colour-change sapphire showed a very strong absorption 400-420 nm, a strong band 450-460 nm, and two lines centred respectively at 640 nm, and 670 nm.
- The heat-treated colour change sapphires showed a very strong absorption 400-440 nm, a strong band 450-460 nm, weak lines at 472, 478 nm, distinct band centred near 540-580 nm, and a strong absorption 660-700 nm.

TABLE 3 The pleochroism observed in the forty-one faceted corundums from Mercaderes-Rio Mayo area, Cauca-Nariño, Colombia

Source	VARIETY Cut or shape	Weight (carat)	Colour	Dichroic intensity	ω-ray colour	ε-ray colour
	RUBIES					
A-01	Pear-shape	1.86	Deep pinkish-red	Strong	Purplish-red	Orangy-red
A-02	Oval-shape	2.33	Pinkish-red	No data	No data	No data
A-03	Pear-shape	1.55	Purplish-red	No data	No data	No data
A-04	Pear-shape	1.42	Intense pink	No data	No data	No data
A-05	Cabochon	1.66	Pinkish-red	Strong	Purplish-red	Orangy-red
A-06	Cabochon	6.24	Violet-red	Strong	Purplish-red	Orangy-red
GT-01	Oval-shape	0.33	Pinkish-red	Distinct	Purplish-red	Orangy-red
GT-02	Pear-shape	0.19	Intense pink	Distinct	Purplish-red	Orangy-red
	SAPPHIRES					
A-07	Cabochon	3.01	Greyish-blue	Strong	Greyish-blue	Bluish-green
A-08	Cabochon	2.66	Greenish-blue	Strong	Greyish-blue	Bluish-green
A-09	Cabochon	3.24	Greyish-blue	No data	No data	No data
A-10	Oval-shape	2.58	Violet-blue	No data	No data	No data
A-11	Marquise	2.19	Greyish-blue	Strong	Greyish-blue	Greyish-green
A-12	Oval-shape	6.89	Greyish-blue	No data	No data	No data
A-13	Oval-shape	3.42	Greenish-blue	Distinct	Greenish-blue	Pale greyish-green
A-14	Oval-shape	3.55	Light greenish-blue	Distinct	Greenish-blue	Pale violetish-blue
A-15	Oval-shape	2.01	Light blue	No data	No data	No data
A-I6	Oval-shape	1.91	Lilac	No data	No data	No data
A-17	Oval-shape	1.65	Slight greenish pale blue	Distinct	Pale greyish-blue	Pale greyish-green
A-18	Cabochon	3.22	Intense blue	No data	No data	No data
A-19	Cabochon	2.93	Intense blue	No data	No data	No data
A-20	Cabochon	2.46	Intense blue	No data	No data	No data
HH-01	Oval-shape	4.81	Greyish-blue	Distinct	Greyish-blue	Pinkish-blue
A-31	Cabochon	0.71	Bluish-grey	V. weak	Pale bluish-grey	Pale pinkish-grey
	HEAT-TREATED SAPPHIRE					
TT-01	Oval-shape	2.14	Dark blue	Strong	Dark blue	Greenish-blue
	MULTICOLOURED SAPPHIRES					
A-21	Oval-shape	2.36	Pink, blue, violet	No data	No data	No data
A-22	Oval-shape	2.80	Grey, blue, pink, orange	No data	No data	No data
A-23	Brilliant-cut	1.83	Grey-blue, pink	No data	No data	No data
A-24	Oval-shape	1.15	Lavender, grey, pink	No data	No data	No data
A-25	Oval-shape	2.58	Violet-blue, pink faint orange, pale yellow	Strong	Pink	Pale yellow-green
A-26	Oval-shape	2.58	Pale blue, grey, pink	No data	No data	No data
A-27	Oval-shape	2.96	Grey-blue, pale blue, pink	No data	No data	No data
A-28	Oval-shape	1.53	Violet-blue, violet-pink, yellow	Strong	Violetish-pink	Greenish-yellow
A-29	Brilliant-cu	1.90	Intense pink, lavender, light blue	No data	No data	No data
A-30	Oval-shape	3.32	Red, yellow, blue, orange, purple	Strong	Violetish-pink	Pink
HH-02	Oval-shape	0.96	Parti-coloration: Blue; pink	Strong	Violetish-red	Greyish-red
A-32	Cabochon	1.66	Blue, yellow, pink	Strong	Pinkish-blue	Yellowish-grey
A-34	Oval-shape	0.30	Dark blue, orangy-pink,	Strong	Light blue	Yellowish-green
	COLOUR-CHANGE SAPPHIRE					
A-33	Oval-shape	0.65	From blue to purple	Strong	Purple	Yellowish-grey
	HEAT-TREATED COLOUR-CHANGE SAPPHIRES					
TT-02	Oval-shape	0.96	From blue to purple	Strong	Purple	Yellowish-grey
TT-03	Oval-shape	0.95	From blue to purplish red	Strong	Purple	Greyish-yellow

Key to source: (A) San Pablo (Nariño). (HH) Collection H. Hänni. (GT) Alto La Cañada (Cauca). (TT) Heated by T. Themelis

TABLE 4 The absorption spectrum of the forty-one faceted corundums from Mercaderes-Rio Mayo area, Cauca-Nariño, Colombia

Source	VARIETY Cut or shape	Weight (carat)	Colour	Spectrum bands and lines (nm)
	RUBIES			
A-01	Pear-shape	1.86	Deep pinkish-red	**400-460**, 474, 480, **530-580**, **660**, **690**
A-02	Oval-shape	2.33	Pinkish-red	**400-460**, 468, 474, **530-560**, **660**, **690**
A-03	Pear-shape	1.55	Purplish-red	**400-460**, 468, 472, **530-580**, **660**, **690**
A-04	Pear-shape	1.42	Intense pink	**400-440**, 468, 474, **530-580**, **640**, **690**
A-05	Cabochon	1.66	Pinkish-red	**400-450**, 460, 468, 472, **520-580**, **690**
A-06	Cabochon	6.24	Violet-red	**400-460**, 474, 478, **540-580**, **660**, **685**
GT-01	Oval-shape	0.33	Pinkish-red	**400-450**, 460, 468, 474, **530-580**, **660**, **685**
GT-02	Pear-shape	0.19	Intense pink	**400-440**, 450-460, 468, **540-580**, **660**, **690**
	SAPPHIRES			
A-07	Cabochon	3.01	Greyish-blue	**400-420**, **450-460**, 510, 524, **610-700**
A-08	Cabochon	2.66	Greenish-blue	**400-420**, **450-460**, 470, **630-700**
A-09	Cabochon	3.24	Greyish-blue	**400-420**, **450-460**, **600-700**
A-10	Oval-shape	2.58	Violet-blue	**400-420**, **450-460**, **600-700**
A-11	Marquise	2.19	Greyish-blue	**400-420**, **450-460**, **620-700**
A-12	Oval-shape	6.89	Greyish-blue	**400-420**, **450-460**, **610-700**
A-13	Oval-shape	3.42	Greenish-blue	**400-420**, **450-460**, 650, **660-700**
A-14	Oval-shape	3.55	Light greenish-blue	**400-420**, **450**, 630, 650, **660-700**
A-15	Oval-shape	2.01	Light blue	**400-430**, **450-460**, 630, 650, **660-700**
A-I6	Oval-shape	1.91	Lilac	**400-430**, **450-460**, 540-560, 620, **630-700**
A-17	Oval-shape	1.65	Slight greenish pale blue	**400-420**, **450**, 620, **630-700**
A-18	Cabochon	3.22	Intense blue	**400-430**, **450-460**, **610-700**
A-19	Cabochon	2.93	Intense blue	**400-420**, **450**, **600-700**
A-20	Cabochon	2.46	Intense blue	**400-420**, **450-460**, **600-700**
HH-01	Oval-shape	4.81	Greyish-blue	**400-420**, **455-460**, 640, **660-700**
A-31	Cabochon	0.71	Bluish-grey	**400-420**, **450-460**, 640, 660
	HEAT-TREATED SAPPHIRE			
TT-01	Oval-shape	2.14	Dark blue	**400-420**, **450-460**, 600, 610, 620, **630-700**
	MULTICOLOURED SAPPHIRES			
A-21	Oval-shape	2.36	Pink, blue, violet	**400-420**, **450-460**, 468, 472, 530-560, 640, **650-700**
A-22	Oval-shape	2.80	Grey, blue, pink, orange	**400-440**, **450-460**, 472, 620, **630-700**
A-23	Brilliant-cut	1.83	Grey-blue, pink	**400-420**, **450-460**, 472, 478, 540-570, 640, **650-700**
A-24	Oval-shape	1.15	Lavender, grey, pink	**400-410**, **450-460**, 478, 620, **630-700**
A-25	Oval-shape	2.58	Violet-blue, pink faint orange, pale yellow	**400-430**, **450-460**, 472, 478, 628, **650-700**
A-26	Oval-shape	2.58	Pale blue, grey, pink	**400-420**, **450-460**, 640, 660, **670-700**
A-27	Oval-shape	2.96	Grey-blue, pale blue, pink	**400-420**, **450-460**, 470, 478, 640, 670, **680-700**
A-28	Oval-shape	1.53	Violet-blue, violet-pink, yellow	**400-410**, **450-460**, 630, **640-670**
A-29	Brilliant-cu	1.90	Intense pink, lavender, light blue	**400-410**, 530-580, **640-700**
A-30	Oval-shape	3.32	Red, yellow, blue, orange, purple	**400-440**, **450-460**, 468, 472, **540-570**, **660**, **690**
HH-02	Oval-shape	0.96	Parti-coloration: Blue; pink	**400-420**, **445-465**, 640, 660, 670
A-32	Cabochon	1.66	Blue, yellow, pink	**400-420**, **455-460**, 640, 660, **670-700**
A-34	Oval-shape	0.30	Dark blue, green, orangy-pink,	**400-420**, **450-470**, **630-700**
	COLOUR-CHANGE SAPPHIRE			
A-33	Oval-shape	0.65	From blue to purple	**400-420**, **450-460**, 640, 670
	HEAT-TREATED COLOUR-CHANGE SAPPHIRES			
TT-02	Oval-shape	0.96	From blue to purple	**400-440**, **450-460**, 478, **540-570**, 640, 660, **680-700**
TT-03	Oval-shape	0.95	From blue to purplish red	**400-440**, **450-460**, 468, 472, 478, **540-590**, **650-700**

Key to source: (A) San Pablo (Nariño). (HH) Collection H. Hänni. (GT) Alto La Cañada (Cauca). (TT) Heated by T. Themelis

MICROSCOPIC EXAMINATION

Main inclusions observed in the rough corundums

The rough corundums were examined under a Bausch & Lomb Mark V Gemolite binocular microscope using dark field illumination or overhead lighting depending on whether internal or external features were to be examined.

The most characteristic inclusions, nearly always present, consisted of columnar doubly terminated crystals.
These crystals are most often found in great number, usually they occur as terminated single prisms, colourless and transparent (see caption figure 15).
Less frequently, some appear dark to red, opaque to semitransparent, and can show a geniculate twinning {011} (figure 16).

- Dark opaque crystals similar to the one described above were found lying at the surface of a multicoloured rough corundum (figure 17).
  When these were scraped to be analysed, they proved to be red, and one which was polished accidentally in order to reach a group of transparent pale yellow crystals with low relief, showed an adamantine-metallic lustre (figure 18 & 19).
  A minute scraping from these red inclusions, taken from three apparently different minerals and locations (surface and interior), were submitted to a beam of monochromatic X-ray (Cu/Ni) in a cylindrical Gandolfi Camera of diameter 114.6 mm.
  After an exposure time of approximately seven hours, under working conditions of 40 KV, 20 mA, the most important lines observed could be matched in the Powder File (J.C.P.D.S. 21-1276) to those diagnostic for rutile.

- The small transparent pale yellow crystals analysed by the X-ray powder technique described above, revealed under the same working conditions, an X-ray spectrum that matched the Powder File (J.C.P.D.S. 9-432) characteristic for apatite.

  For all the other inclusions which were found well beneath the surface of a stone, and proved too difficult to reach for identification, a more sophisticated technique was needed, i.e., a Raman-laser probe.
  A monochromatic laser beam is focused on an inclusion. The laser beam undergoes a frequency change characteristic of the material excited, through interaction with vibrating molecules. The spectra recorded in the infrared region are compared with reference spectra for known solid, liquid, and gaseous phases (Hänni, 1987; Hänni *et al.,* 1997; Pinet *et al.,* 1992; Schubnel, 1992).

  The Raman spectroscopy analysis were carried in three different locations:

  <u>In France:</u>

  At the Institut des matériaux Jean Rouxel, in the laboratory of crystalline physics of professor Lefrant, Université de Nantes.
  The Raman spectra were recorded at room temperature with a T64000 spectrometer triple monochromator in a single channel mode, by JOBIN-YVON S.A. The Raman spectra were excited by the green 514,53 nm line (19435 $^{cm-1}$) of an Ar^{+} laser. The beam power was approximately 700 mW, for a time of 60 seconds with two accumulations. The laser light was focused on the sample and the scattering collected by a Leitz microscope equipped with UTK50 objectives. The spectra are reported with a spectral resolution of ± 4 $^{cm-1}$, and a wavenumber accuracy of about ± 1 $^{cm-1}$. A computer with LabSpe software was used to collect and store the Raman spectra.

In Switzerland:

At the Swiss Foundation for the Research of Gemstones (SSEF), Basel.
The Raman spectra were performed using a RENISHAW RAMAN SYSTEM 1000 equiped with a Peltier cooled CCD detector, together with a 25 mW air-cooled argon ion laser (Omnichrome) lasing at 514 nm. The laser light was focused on to the sample and the scattering collected with an Olympus BH series microscope equipped with 10x, 20x and 50x MSPlan objectives. The spectra are reported with a spectral resolution of ± 2 $^{cm-1}$ and a wavenumber accuracy of about ± 1 $^{cm-1}$. A standard PC computer with GRAMS/386^{TM} software was used to collect and store the Raman spectra.

At the Sciences de la Terre, Université de Genève.
The sample was investigated at room temperature using a Raman LABRAM spectrometer. The Raman spectra were excited either by the green 532 nm line of a Nd-YAG laser, or the red 632,8 nm line of a He-Ne laser. The time varied from 7 to 20 seconds for a single accumulation. Either green or red laser light (as convenient) was focused on the sample and the scattering collected by an Olympus microscope equipped with 10x, 50x, 100x MSPlan objectives. The spectra are reported with a spectral resolution of ± 4 $^{cm-1}$ and a wavenumber accuracy of about ± 1 $^{cm-1}$. A computer with Dilor software was used to collect and store the Raman spectra.

- The colourless and transparent crystals with high relief observed in many rough corundums proved to be zircon, characterised by their Raman spectrum showing the strongest peak at ± 1011 $^{cm-1}$, and by other peaks of lower intensities found at 978, 440, 360, and 217 $^{cm-1}$.

  It must be remembered here that zircon incorporates, among a number of other trace elements, U and Th, which can substitute for Zr^{4+}.
  With time, the zircon structure can break down from “high type” zircon to the metamict state “low type” zircon. Metamictization results from radiation damage to the latice caused by α particles originating from the decay of uranium and thorium.
  In addition to physical and structural changes, metamict zircons show:
  - An increase in unit-cell dimensions, and a broadening of x-ray diffraction patterns.
  - A decrease in infra-red and Raman intensities, and dramatic band broadening.
  - Decreases in refractive index and birefringence.
  - An increase in fracture toughness.
  - A decrease in hardness and bulk modulus.

  The final totally metamict state of zircon, is a structure that appears to be amorphous when analyzed by X-ray and electron techniques (Nasdala *et al.,* 1995; Wopenka *et al.,* 1996; Zhang *et al.,* 2000; Nasdala *et al.,* 2001)

  Since most of the zircon crystals encountered in the host Colombian corundums, do not show any stress cracks, and are highly transparent, they must be uranium and thorium poor, and be of the “high type” zircon (similar to those observed in Kashmir sapphires).
  Less frequently, a few of these colourless zircon crystals were seen with tension fissures (similar to those encountered in corundums from Sri Lanka), or surrounded by a halo and tension fissures, and must therefore be “low-type” metamict zircons, resulting from an inner radioactive breakdown due to thorium or uranium atoms which they contain.

- Occasionally, the zircons were short to large, semi-translucent, dark reddish-brown, and sometimes displayed important stress fractures.

- Very small near to colourless rounded crystallites of feldspar plagioclase were irregularly observed.

- A small light blue rounded and corroded hexagonal rough corundum with a frosted appearance, full of doubly terminated zircon inclusions, was found to contain on a glassy-like fracture plane showing conchoidal fractures, partly inside and partly outside in open air, a very small yellow transparent slightly waterworned crystal displaying a columnar flattened hexagonal prism terminated by a pinacoid.
  Raman spectroscopy analysis performed on both the rough crystal and the yellow inclusion proved corundum sapphire, which suggest at least two generations of corundum (figure 20). The yellow colour of the included sapphire is due most probably to "iron oxide".
  It is of interest to note that under high magnification a zircon inclusion containing two pinpoint solid inclusions was observed in this yellowish sapphire crystal (figure 21).

- “Fingerprints” produced by the healing of fractures by a complex pattern of liquid filled small channels (very similar to those seen in corundum from Sri Lanka. Figure 22 & 23), were sporadically encountered. Occasionally these fingerprints instead of the liquid filled channels, showed dendritic inclusions of various oxides (unidentified).

- Straight parallel narrow to broadly spaced planes of polysynthetic twinning were observed in most rough corundums, either under the microscope, or when immersed in methylene iodide between crossed polaroids (figure 24 & 25).
  A corroded columnar truncated hexagonal bipyramidal corundum crystal, showed strong polysynthetic twinning in two directions on the rhombohedron faces and one parallel to the basal pinacoid (figure 26).
  The combination of these three sets of polysynthetic twinning or boehmite lamellae?, encountered in two different planes, when the crystal was viewed along the C-axis, immersed in methylene iodide and between crossed polaroids, formed a lozenge-shaped striation pattern (figure 27).
  This lozenge-shaped striation pattern which could be followed deep inside the crystal, showed three sets of white "needles" (presumably boehmite) lying at the junctions of intersecting twinning planes, while the crystal was examined in methylene iodide with dark field illumination (figure 28).

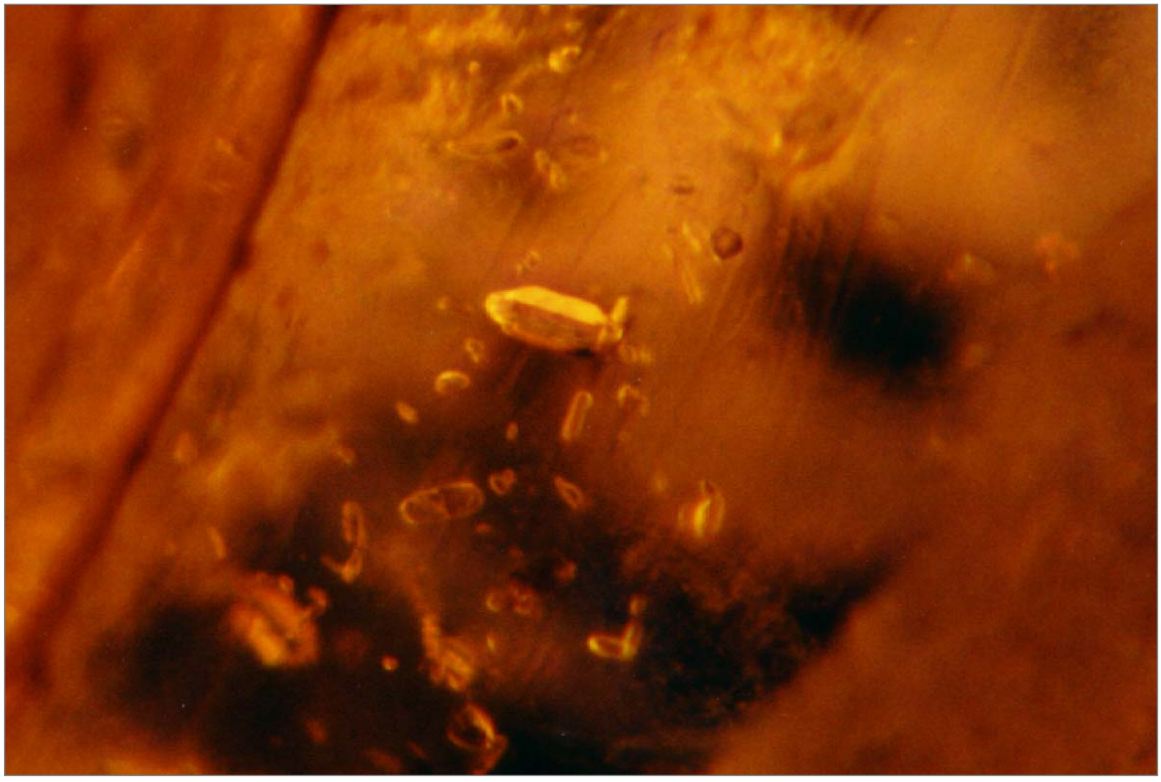

Figure 15. A doubly terminated crystal of zircon observed in a rough multicoloured sapphire from Colombia. Note the absence of stress cracks. (Dark field illumination 80x)

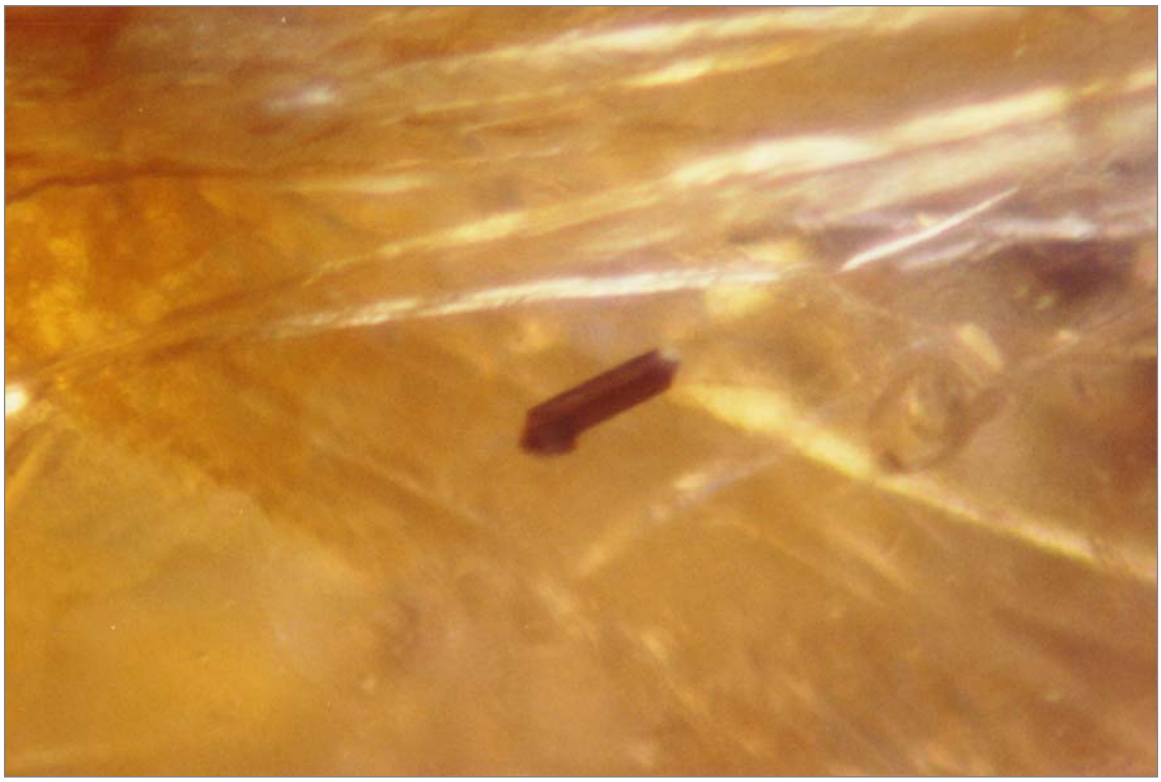

Figure 16. An elongated crystal of rutile observed in a multicoloured rough sapphire crystal from Colombia. Note the geniculate twinning on (011). (Dark field illumination 90x)

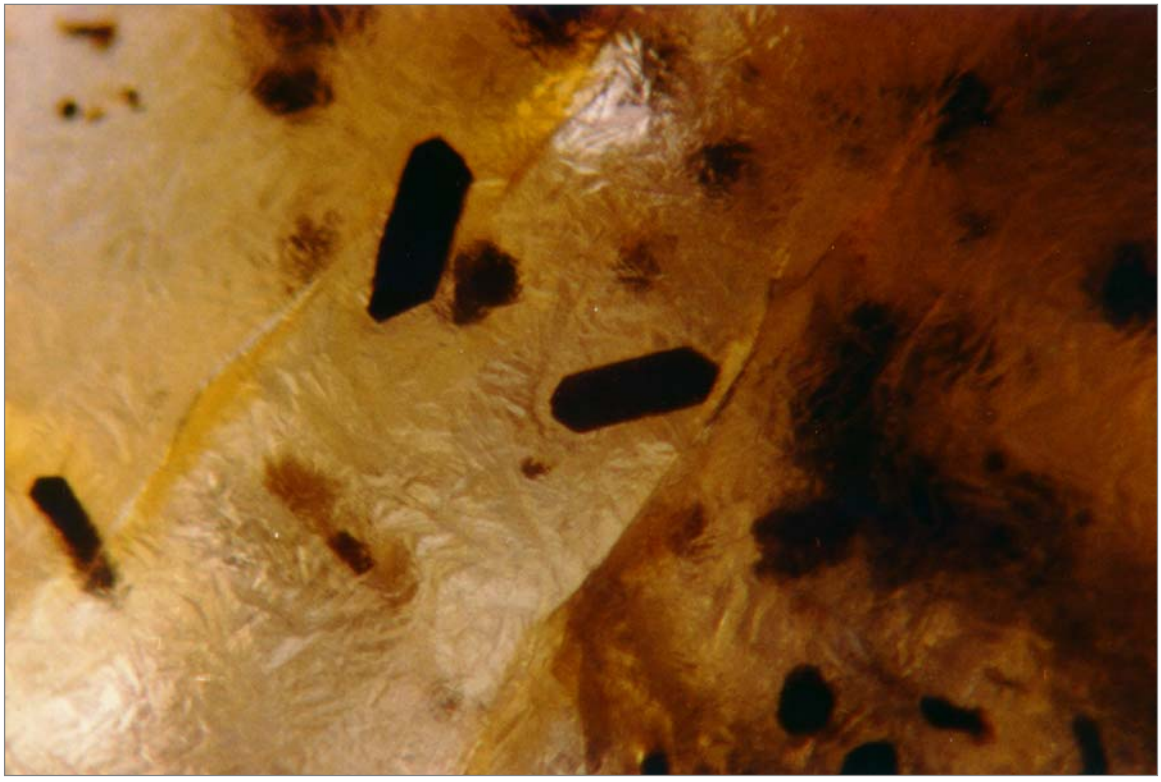

Figure 17. Similar inclusions of rutile observed at the surface of a multicoloured rough corundum crystal from Colombia. Note the frosted appearance of the corundum, and the opaque, black to dark brown colour of the rutile crystals (overhead and dark field illumination 40x).

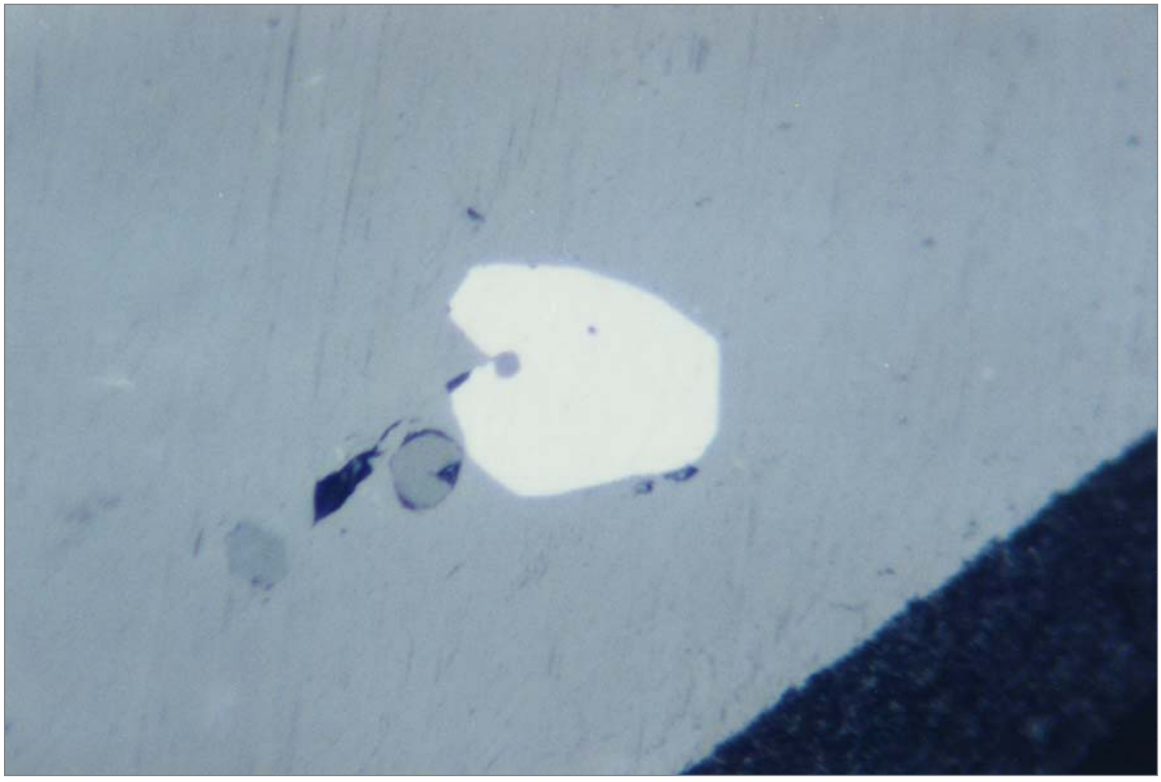

Figure 18. A group of rutile crystals breaking the surface of a Colombian rough crystal. Note the metallic lustre, which appeared silvery and opaque with overhead lighting, and how different is the one shown by the apatite crystals found lying next to them.

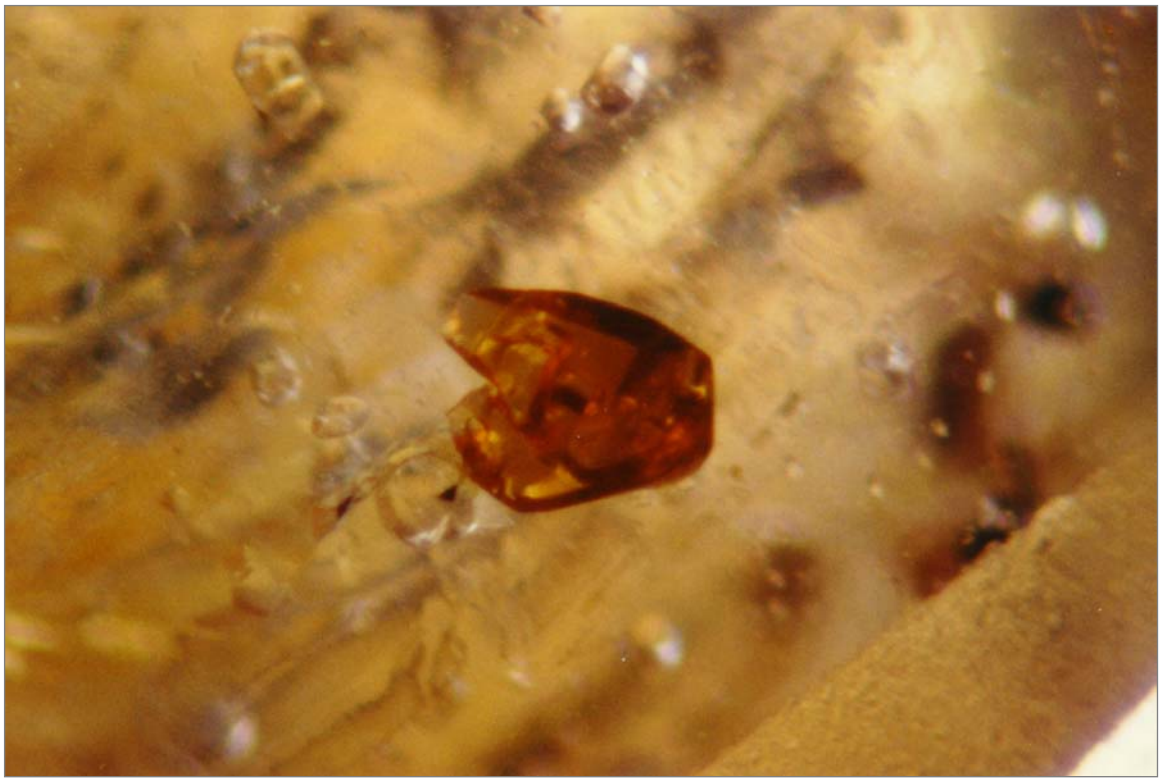

Figure 19. The same group of rutile inclusions showing the adamantine-metallic lustre. (Dark field illumination 95x).

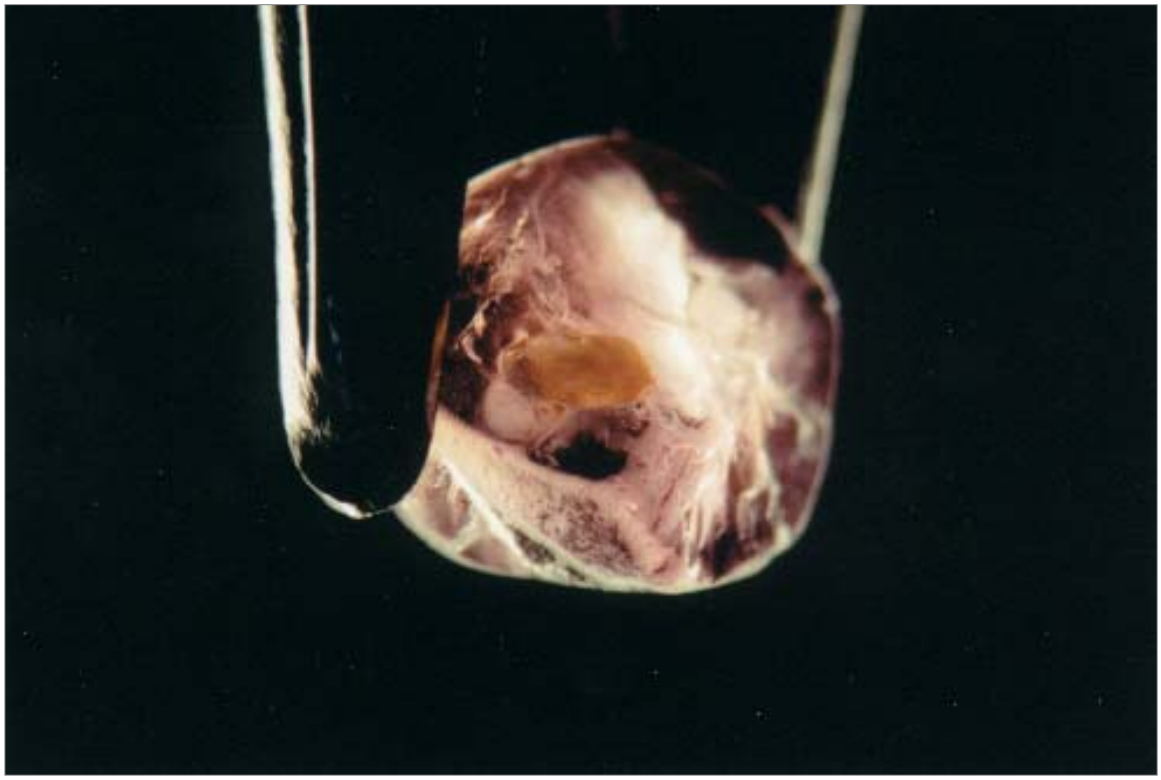

Figure 20. A very small yellow transparent slightly waterworned corundum crystal, partly inside and partly outside in open air, included in a small rounded tabular hexagonal rough sapphire from Colombia. (Dark field illumination 20x)

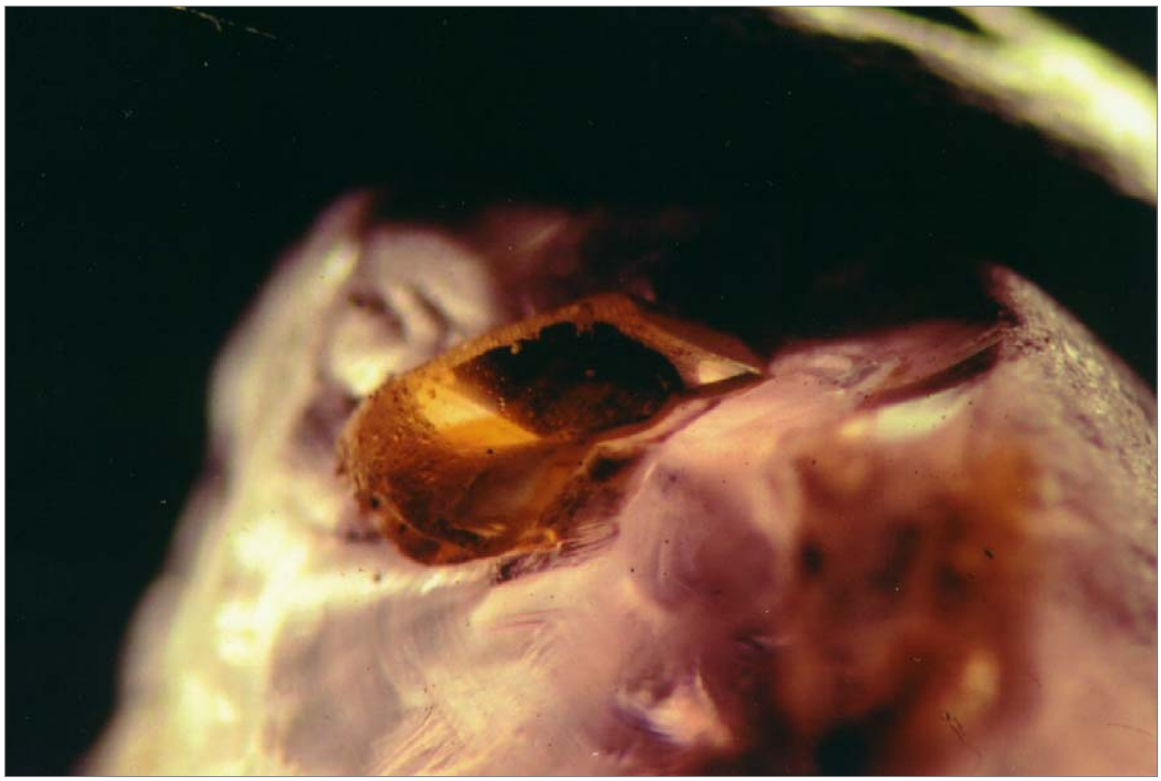

Figure 21. The same transparent yellow corundum crystal, displaying a slightly waterworned columnar habit. The rough yellow corundum revealed a doubly terminated zircon crystal containing two pinpoint inclusions (not shown on the picture). (Dark field illumination 40x)

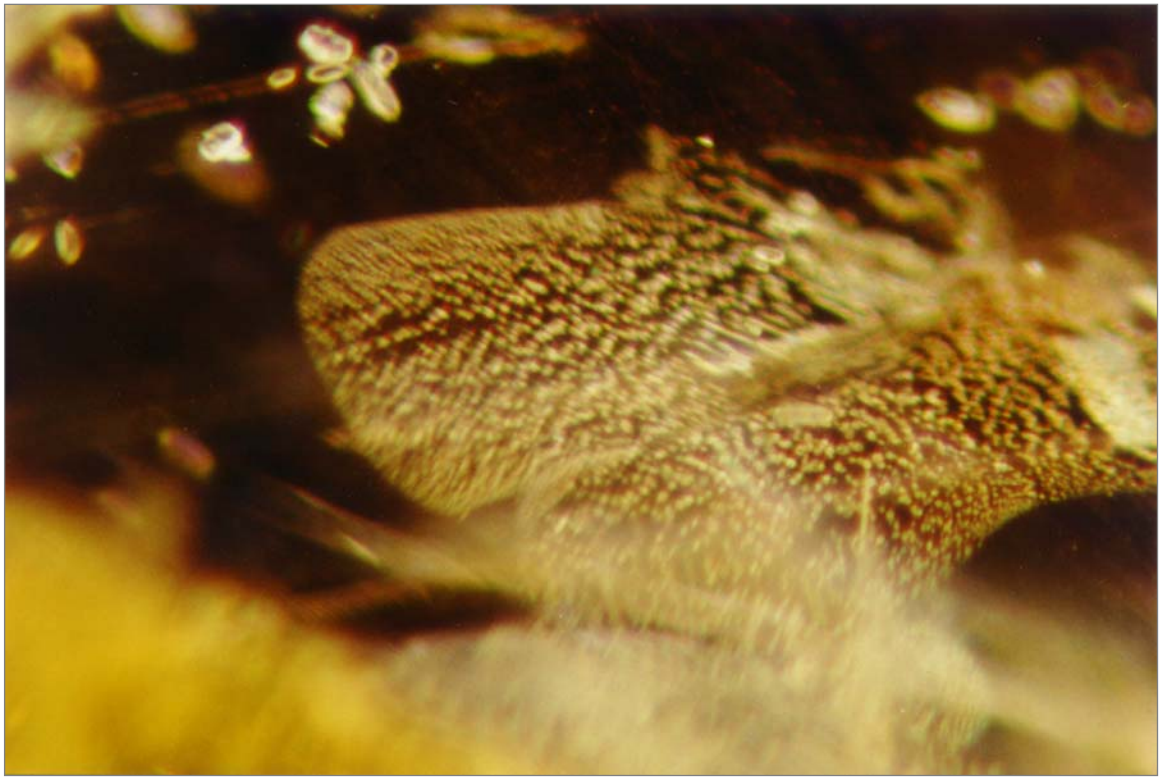

Figure 22. A fingerprint filled with liquid channels (similar to those observed in sapphires from Sri Lanka), encountered here in a rough multicoloured sapphire from Colombia. Note in top left corner, a group of zircon crystals. (Dark field illumination 40x)

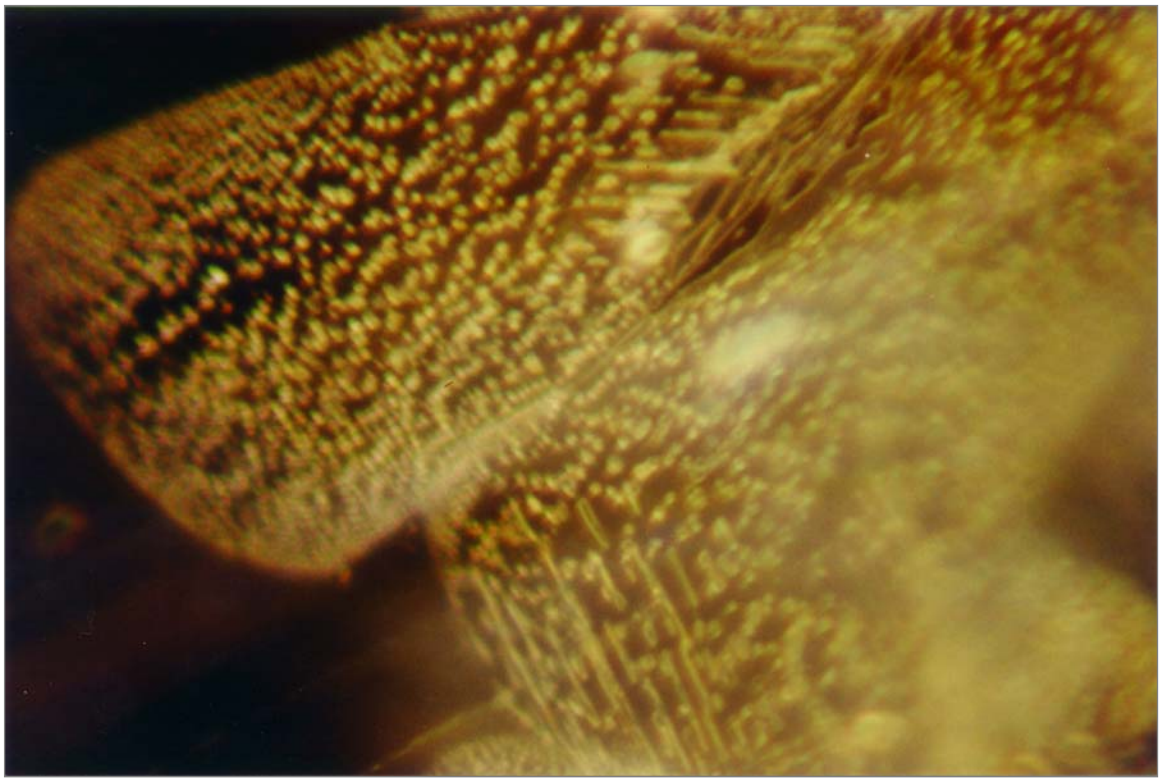

Figure 23. The same inclusion showing the liquid filled channels. (Dark field illumination 60x)

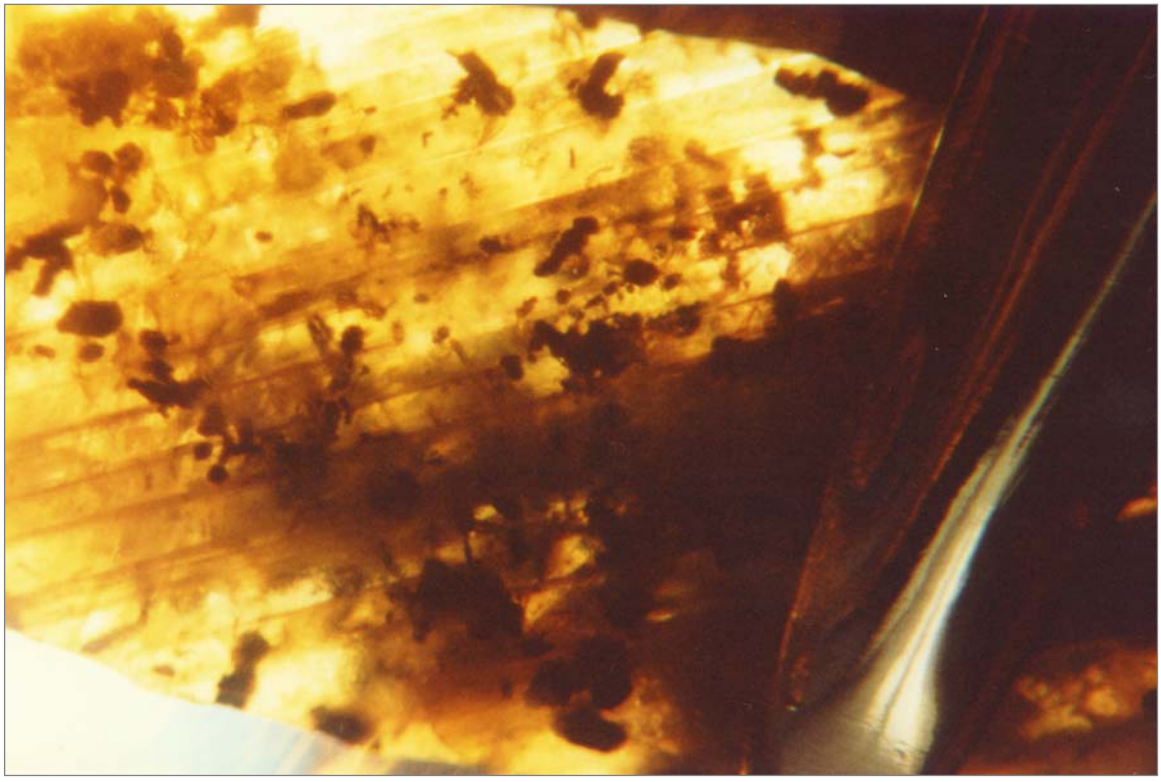

Figure 24. Straight parallel narrow lines of polysynthetic twinning observed in a Colombian rough corundum crystal. Note the numerous dark coloured rutile crystals. (Immersed in methylene iodide between crossed polaroids 30x)

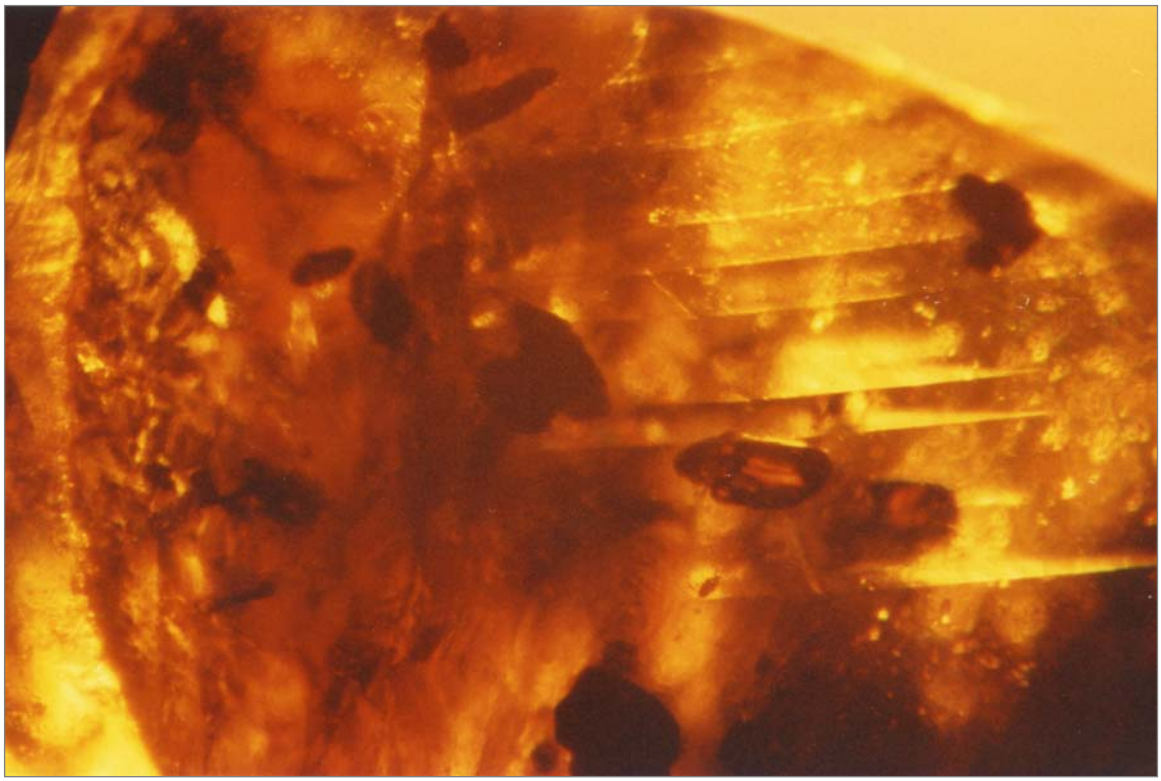

Figure 25. Similar polysynthetic twinning observed in another rough corundum crystal from Colombia. Note the numerous thick rutile crystals. (Immersed in methylene iodide between crossed polaroids 30x)

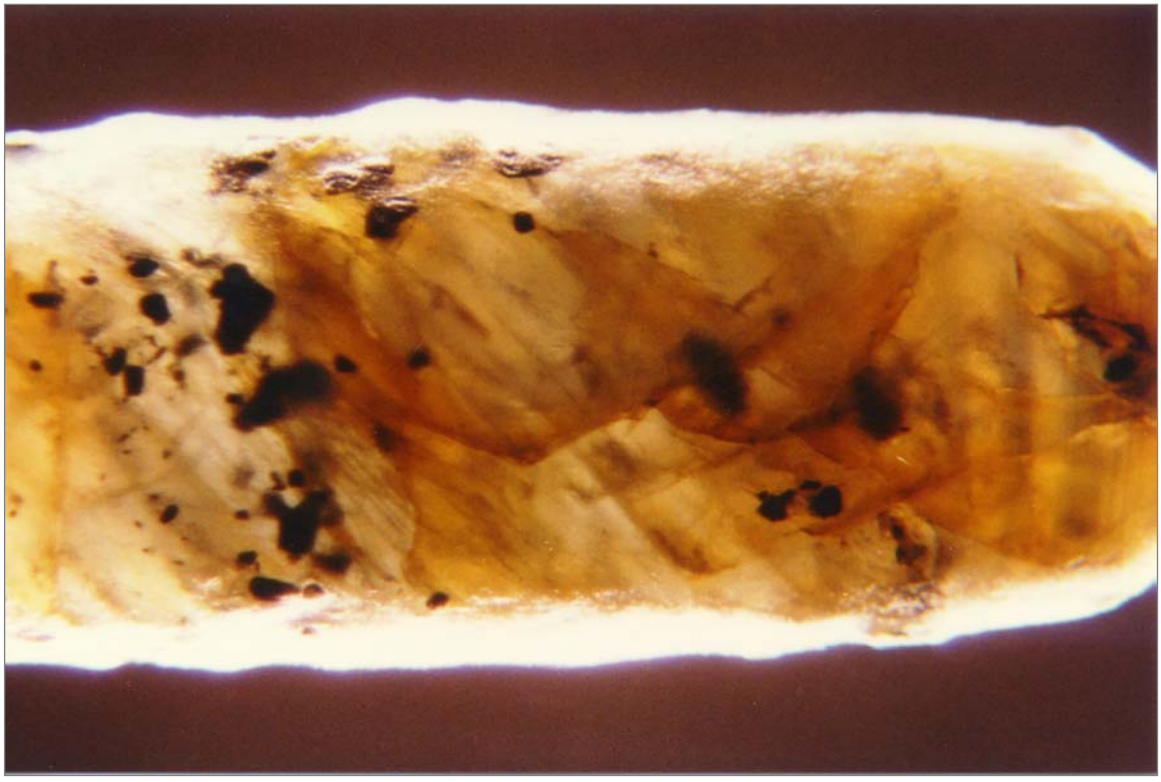

Figure 26. A Colombian columnar hexagonal bipyramidal corroded corundum crystal showing polysynthetic twinning or boehmite lamellae? in three directions (two on the rhombohedron faces and one parallel to the basal pinacoid). (Dark field illumination 25x)

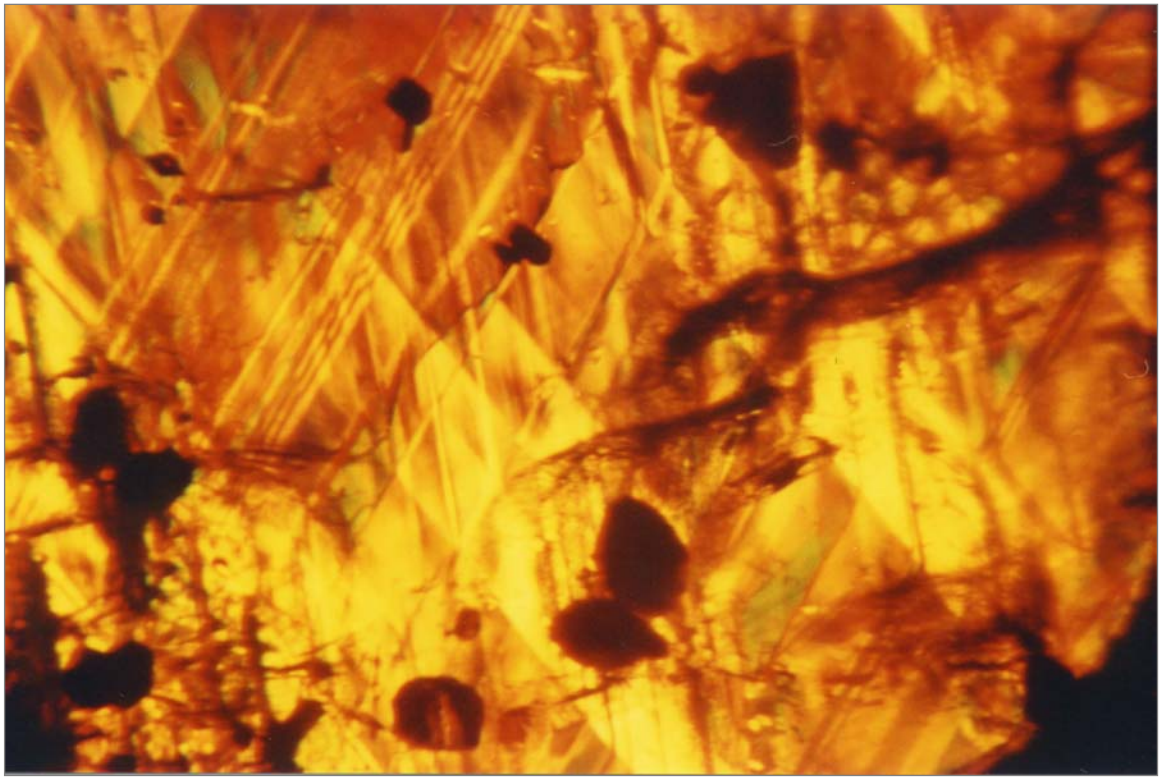

Figure 27. *Three sets of polysynthetic twinning or boehmite lamellae? observed along the C-axis direction, forming a lozenge-shaped striation pattern. (Same rough Colombian crystal as described previously, immersed in methylene iodide, between crossed polaroids 40x).*

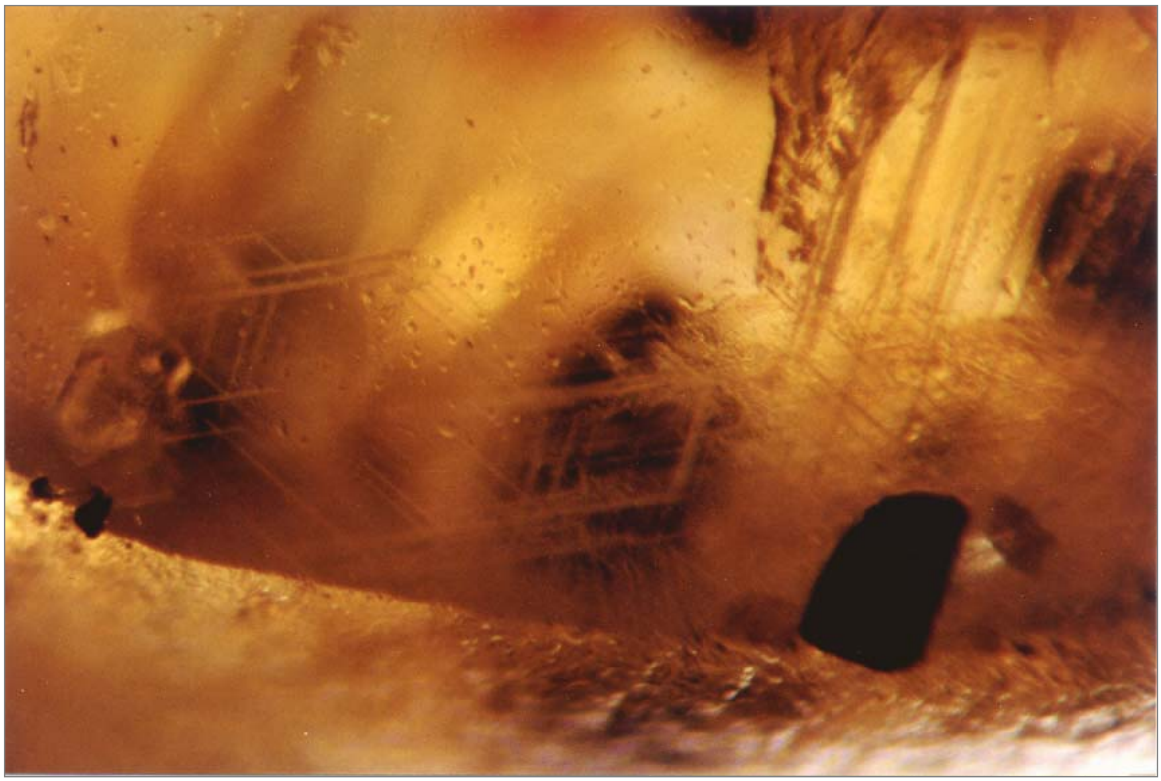

Figure 28. *The same rough corundum crystal showing three sets of white needles (presumably boehmite) lying at the junctions of intersecting twinning planes. (Immersed in methylene iodide with dark field illumination 40x).*

Main inclusions observed in the rubies (Table 5)

- Numerous colourless, transparent doubly terminated zircon crystals. Occasionally the zircon crystals were encountered with tension fractures. Raman spectroscopy analysis revealed an absence of broadening Raman peaks (width of the bands increasing with the degree of metamictization), and changes in frequency from about 1007 $^{cm-1}$ for well-crystallised zircon (well-ordered), to 955 $^{cm-1}$ for metamict zircons (Nasdala *et al., 1995;* Nasdala *et al., 2001;* Wopenka *et al., 1996;* Zhang *et al.,* 2000). Therefore these zircons must have suffered a weak degree of metamictisation, and to the most show only a little disordered Raman spectra compared to the well-crystallised zircons (for comparison purposes, all the Raman spectra were put to the same intensity 0 to 30000, with wavenumber from 100 $^{cm-1}$ to 1200 $^{cm-1}$). Less frequently, some zircon crystals were found showing pinpoint inclusions (figure 29-32). These pinpoint inclusions, also identified by Raman spectroscopy, proved to be sometimes rutile, and occasionally zircon.

- Some dark red doubly terminated opaque rutile crystals (very similar to those seen in rubies from Tanzania).

- An important pseudo-hexagonal sapphire core (crystalline zoning) was observed in the centre of a ruby (figure 33-34).

- Straight parallel narrow to broadly spaced planes of polysynthetic twinning were observed in many rubies (figure 35).
  Some, which showed polysynthetic twinning, showed white "needles" lying in three directions at the junction of intersecting twinning planes.
  Three different types of white "needles" were encountered:

  (a) Fine white "needles" forming a scaffold of stringers (similar to those observed in East African rubies. Figure 36).
  (b) Coarse "needles" intersecting in three directions, forming a more rigid structure (similar to those found in Thai rubies. Figure 37).
  (c) Alignment of long and thick "needles" (similar to those present in Kenyan rubies. Figure 38).

  All these acicular crystals proved too difficult to be analysed by Raman-laser, but are most probably boehmite.

- Small dense nests composed of very short "needles" (most probably rutile), densely woven to form a "silk" (similar to those found in rubies from Myanmar), were observed in some rubies (figure 36), and in particular in a cabochon (figure 39). With a single pinpoint overhead light source, a six-rayed star could be obtained (figure 40).

- Some "fingerprints" were observed, and these most often showed a dentritic-like pattern instead of the usual liquid filled channels.

- Hexagonal growth colour zoning were observed in many rubies (figure 41).

- Healing fractures were found occasionally.

- "Bleeding of colour" was also observed in some rubies (figure 39).

- Some rubies were found to have a pronounced yellow colour zone (Fe-oxide? Figure 42).

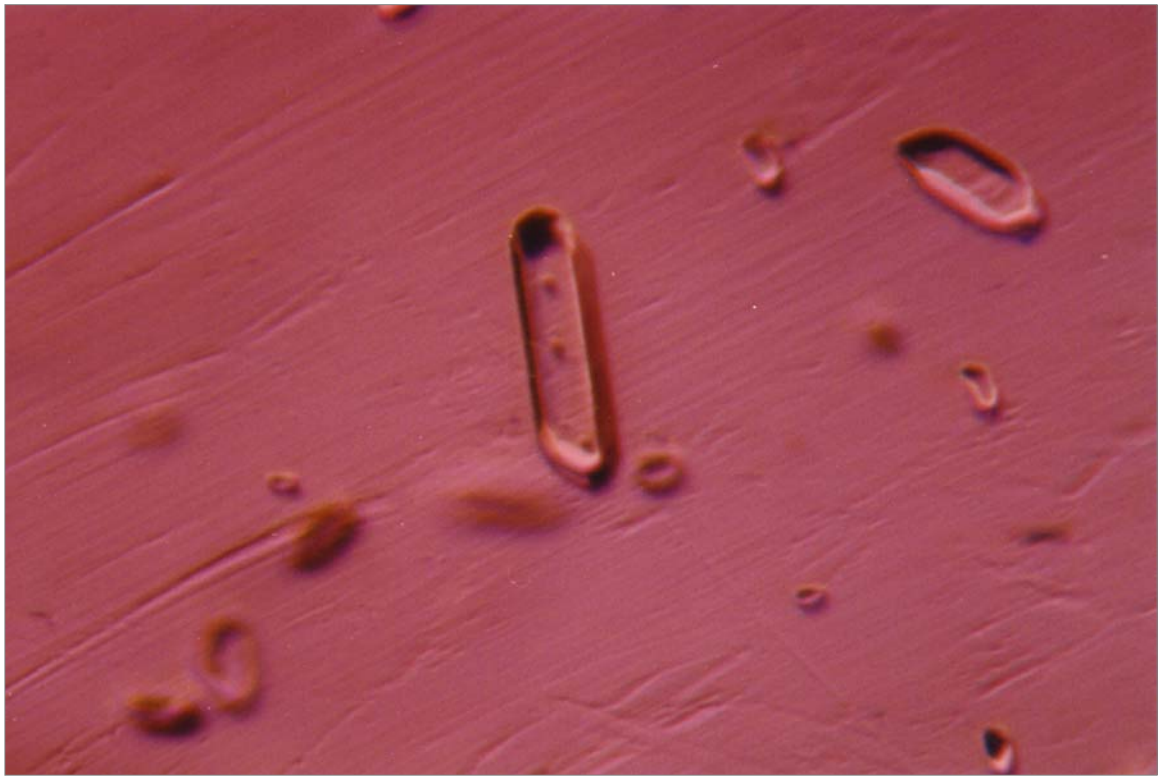

Figure 29. *Group of colourless zircon crystals, some doubly terminated showing voids (or cavities) filled with pinpoint inclusions, observed in (A-01), a pear-shaped ruby of 1.86 ct, from Colombia. (Dark field illumination 95x)*

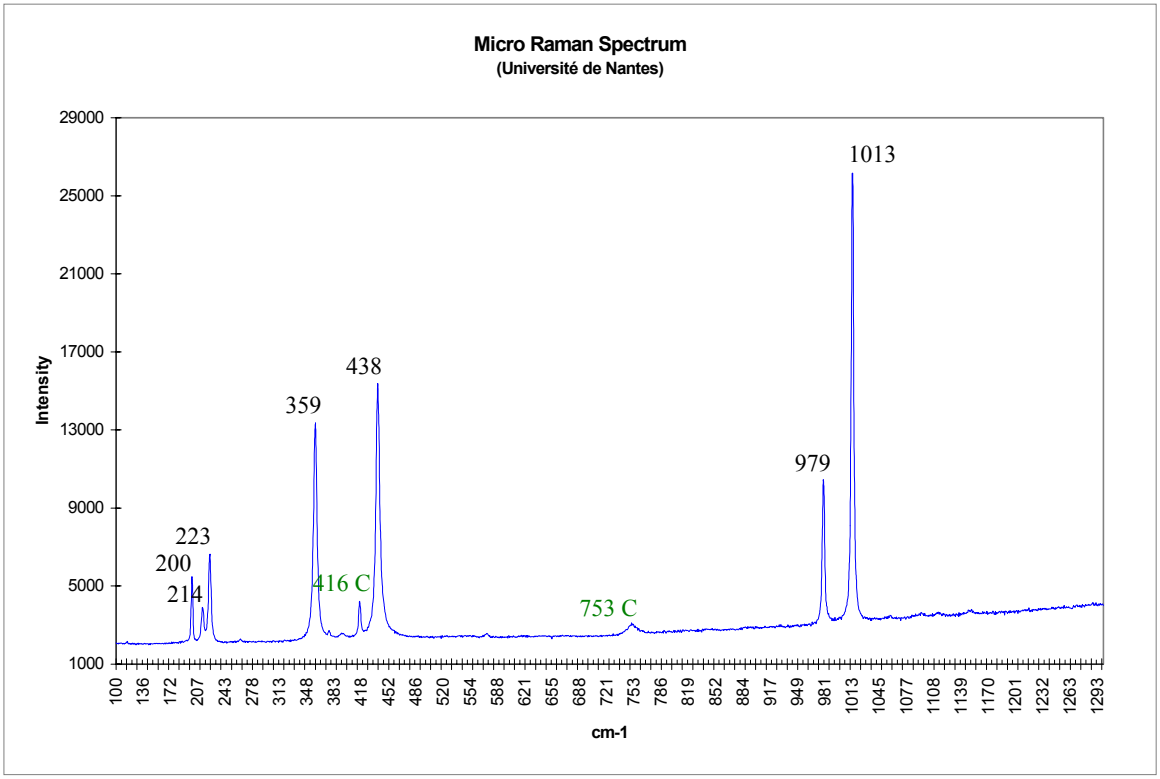

Figure 30. *The Raman spectrum of the main doubly terminated colourless zircon crystal poor in rare earth elements (Wopenka, et al., 1996), observed in the above ruby (A-01), is characterised by the strong peaks at 359, 438, 979, and 1013 $^{cm-1}$. Other peaks of lower intensity are found at 200, 214, and 223 $^{cm-1}$. The peaks 416, and 753 $^{cm-1}$, correspond to the host corundum ruby (C).*

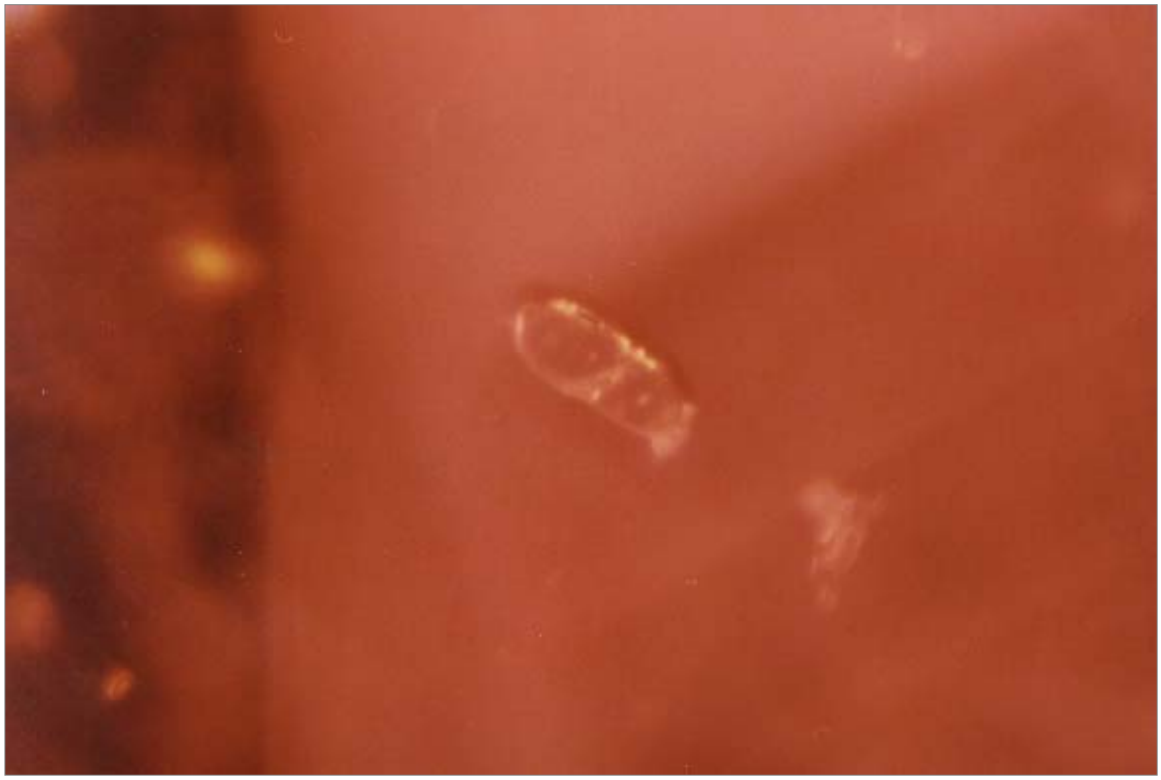

Figure 31. *A doubly terminated colourless zircon crystal filled with pinpoint inclusions, observed in (A-06), a cabochon ruby of 6.24 ct, from Colombia. (Dark field illumination 95x)*

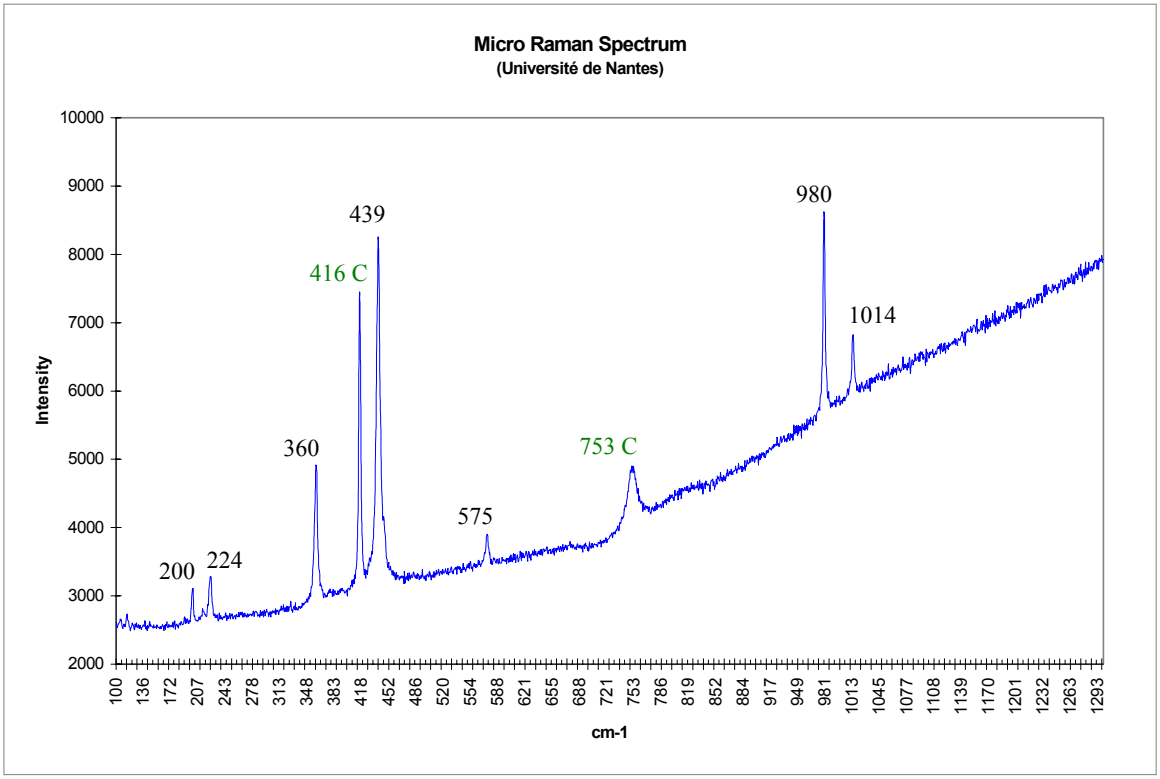

Figure 32. *The Raman spectrum of the zircon crystal rich in rare earth elements (Wopenka, et al., 1996), observed in the above ruby (A-06), is characterised by the peaks at 360, and 1014 $^{cm-1}$.*
The less diagnostic peaks are found at 200, 224, 439, and 980 $^{cm-1}$. The peaks 416, and 753 $^{cm-1}$, correspond to the host ruby (C).

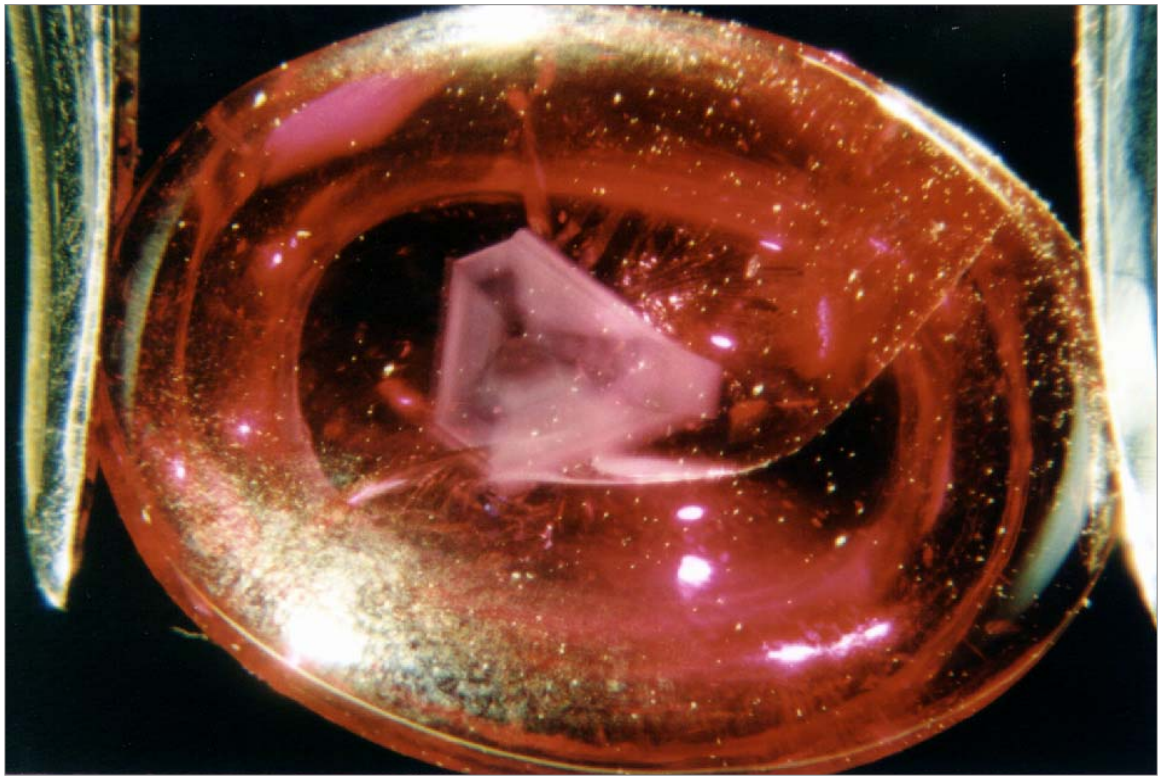

Figure 33. *A large sapphire "core" observed parallel to the C-axis in (A-06), a cabochon ruby of 6.24 ct, from Colombia. Note the stress fissures around the "core" (similar "cores" have been observed in rubies from Mong Hsu, Myanmar). (Dark field & oblique fibre optic illumination 12x).*

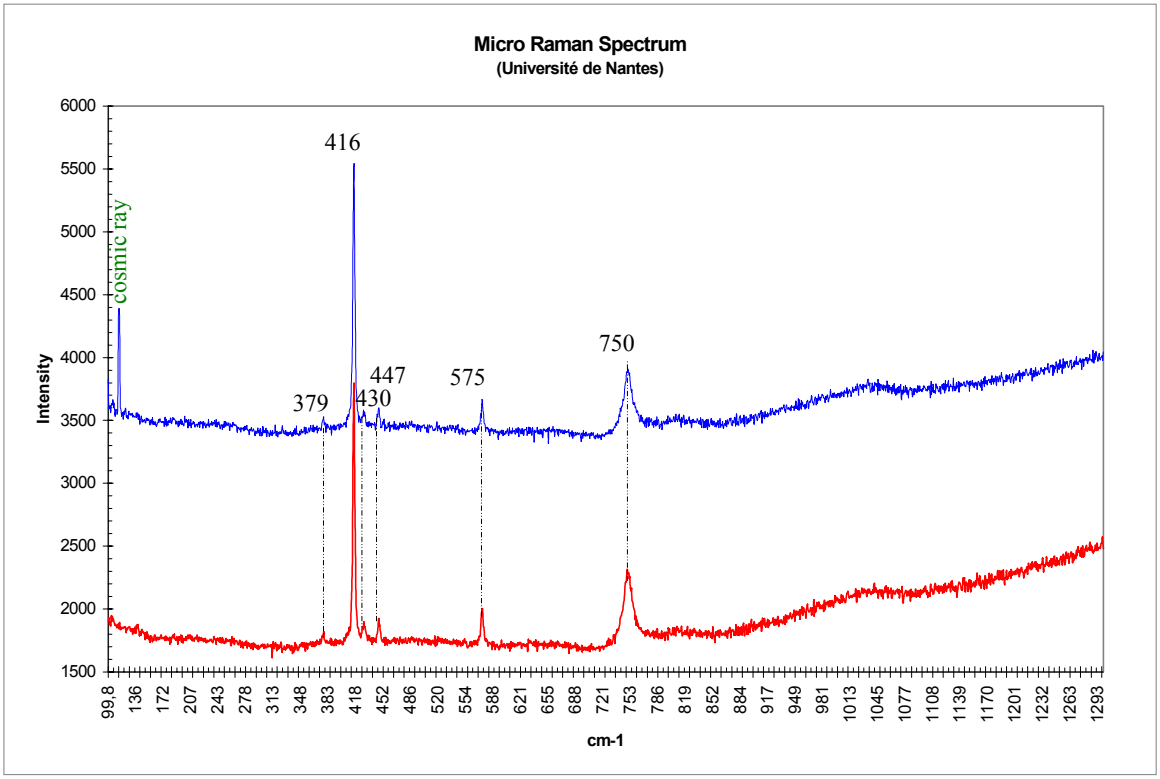

Figure 34. *The Raman spectrum of the sapphire "core" (in blue) and the hosting ruby (in red), observed in the ruby (A-06), are characterised by the strongest peaks at 416, and 750 $^{cm-1}$. Less diagnostic peaks, and of lower intensities are found at 379, and 430 $^{cm-1}$.*

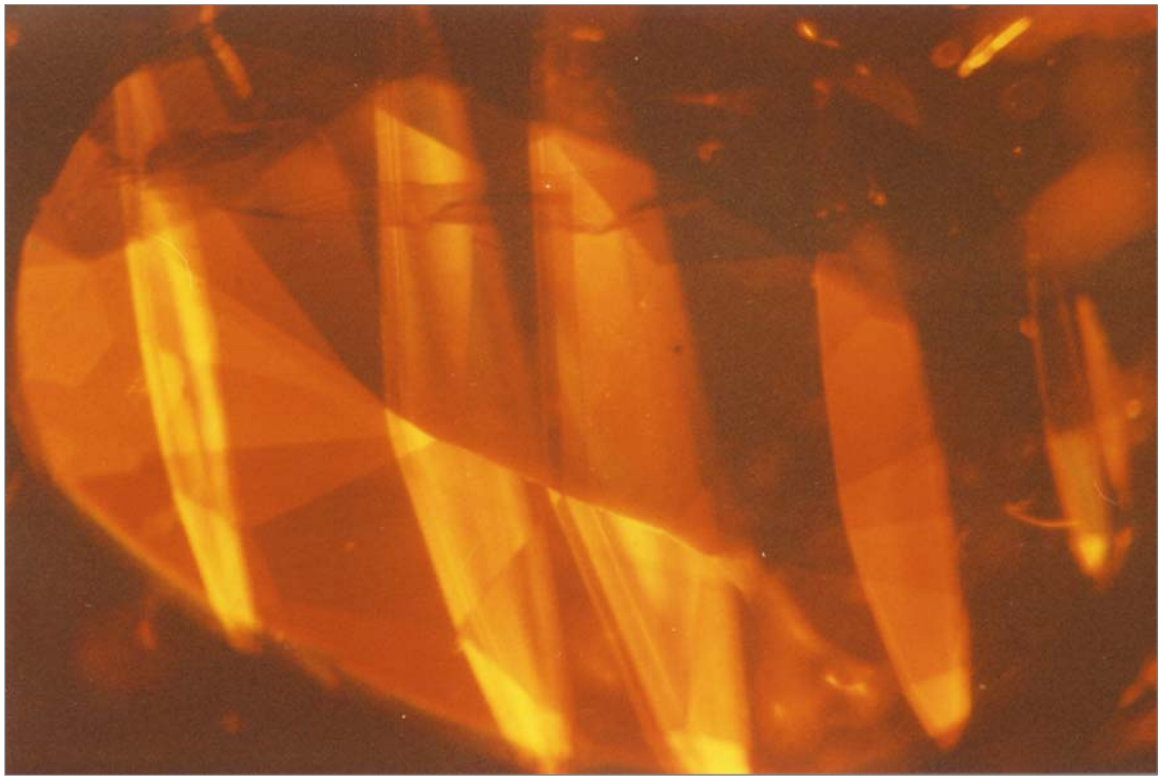

Figure 35. *Straight parallel broadly spaced lines of polysynthetic twinning observed in (A-02), an oval-shaped ruby of 2.33 ct, from Colombia.*
(Immersed in methylene iodide between crossed polaroids 30x)

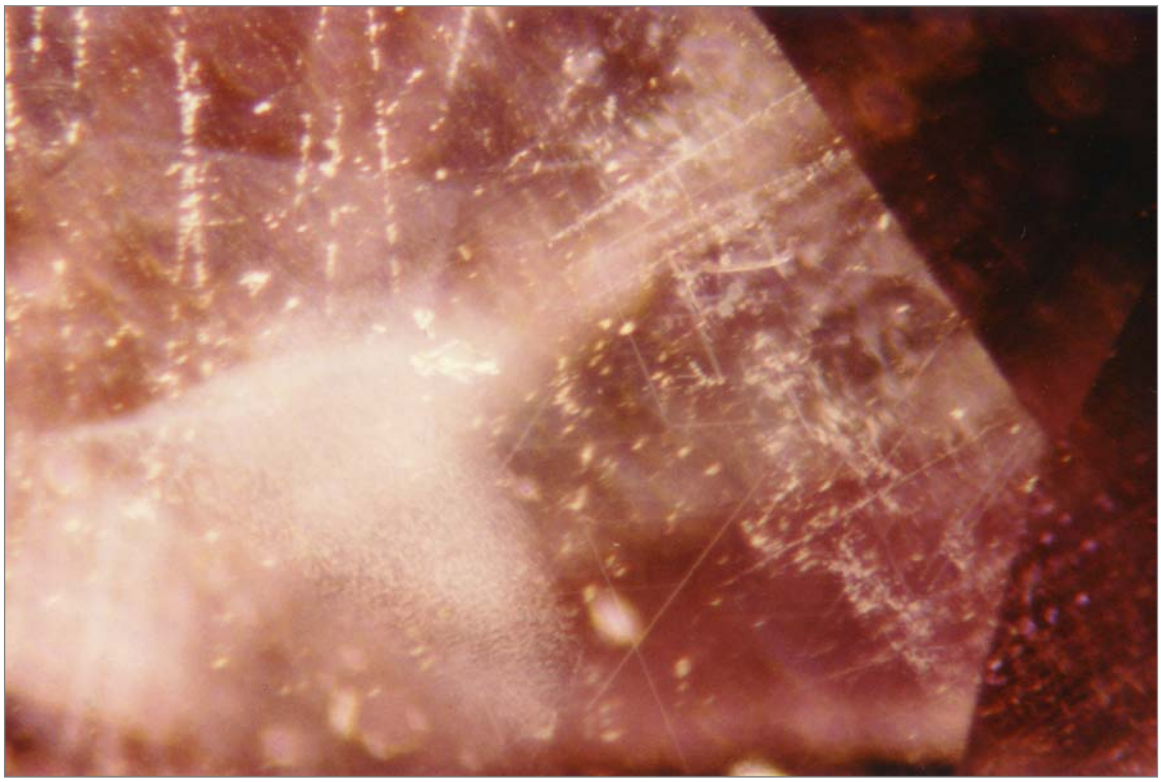

Figure 36. *Scaffold of stringers (similar to those found in East African rubies), here observed in (A-03), a pear-shaped ruby of 1.55 ct, from Colombia. Note the dense nest of minute inclusions (unidentified).*
(Dark field illumination 40x)

Figure 37. *Scaffold of coarse needles of presumably boehmite intersecting in three directions (similar to those encountered in Thai rubies), here observed in (A-04), a pear-shaped ruby of 1.42 ct, from Colombia. Note the dense nest of minute inclusions (unidentified, but presumably rutile).*
(Dark field illumination 40x)

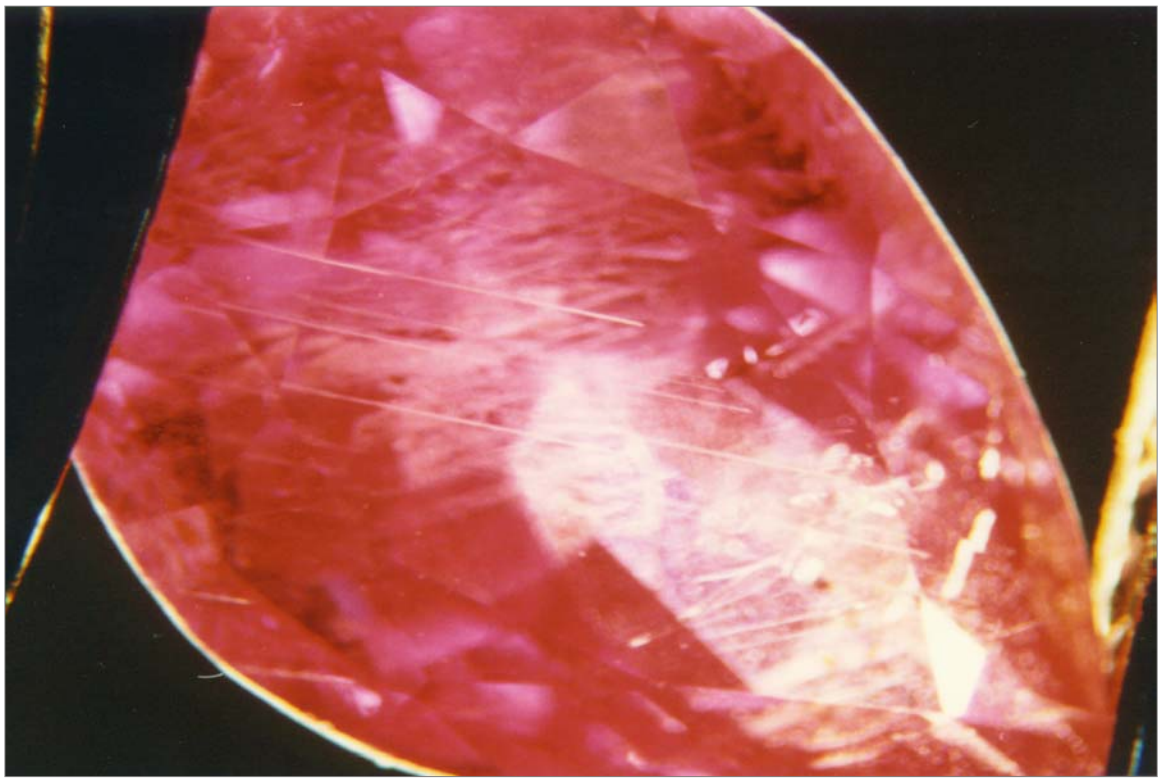

Figure 38. *Alignment of long and thick needles of presumably boehmite (similar to those seen in kenyan rubies), observed in the same (A-04), pear-shaped ruby of 1.42 ct, from Colombia.*
(Dark field illumination 20x)

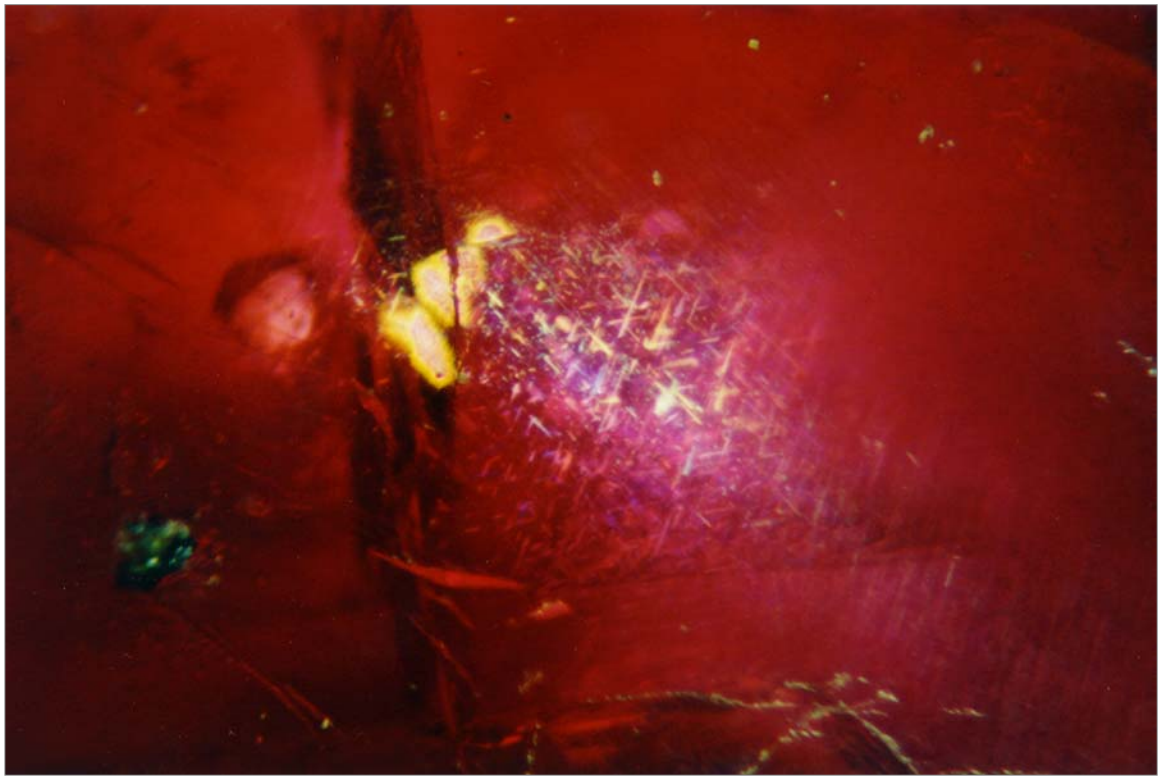

Figure 39. *A small dense nest of very short exsolved rutile needles, viewed along the C-axis (similar inclusions are encountered in Myanmar rubies), here observed in (A-06), a cabochon ruby of 1.66 ct, from Colombia. This stone also showed pronounced "bleeding of colour" which is frequently seen in rubies from Myanmar. (Overhead and dark field illumination 45x)*

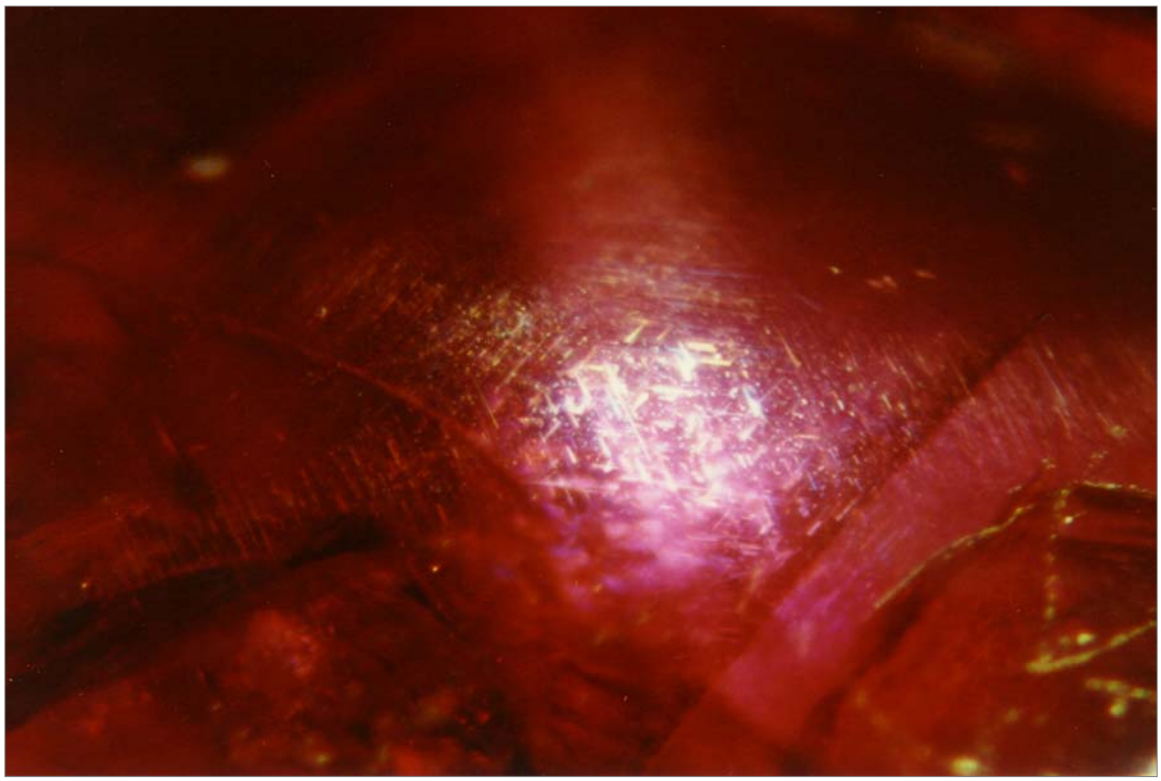

Figure 40. *The same small dense nest of very short rutile needles, showing a six-rayed star viewed by light reflected from a single pinpoint overhead light.*

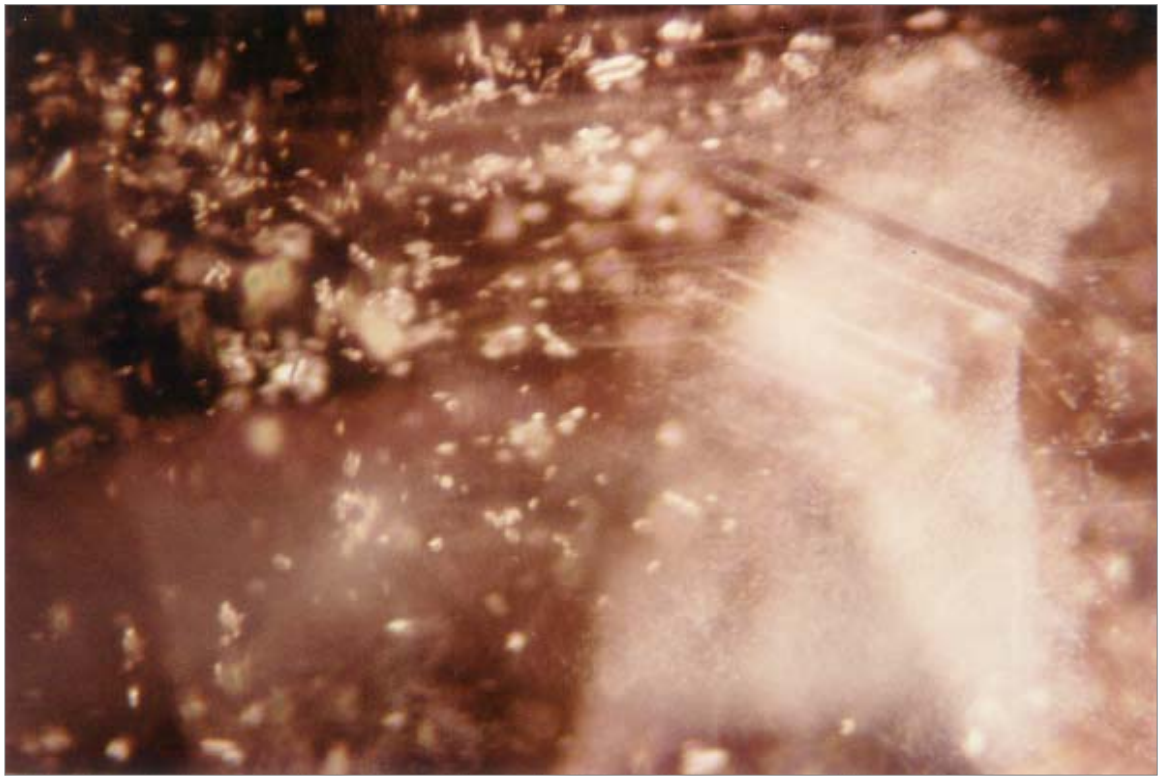

Figure 41. *Hexagonal colour and growth zoning observed parallel to the C-axis in (A-03), a pear-shaped ruby of 1.53 ct, from Colombia. Note the numerous zircon crystals. (Dark field illumination 40x)*

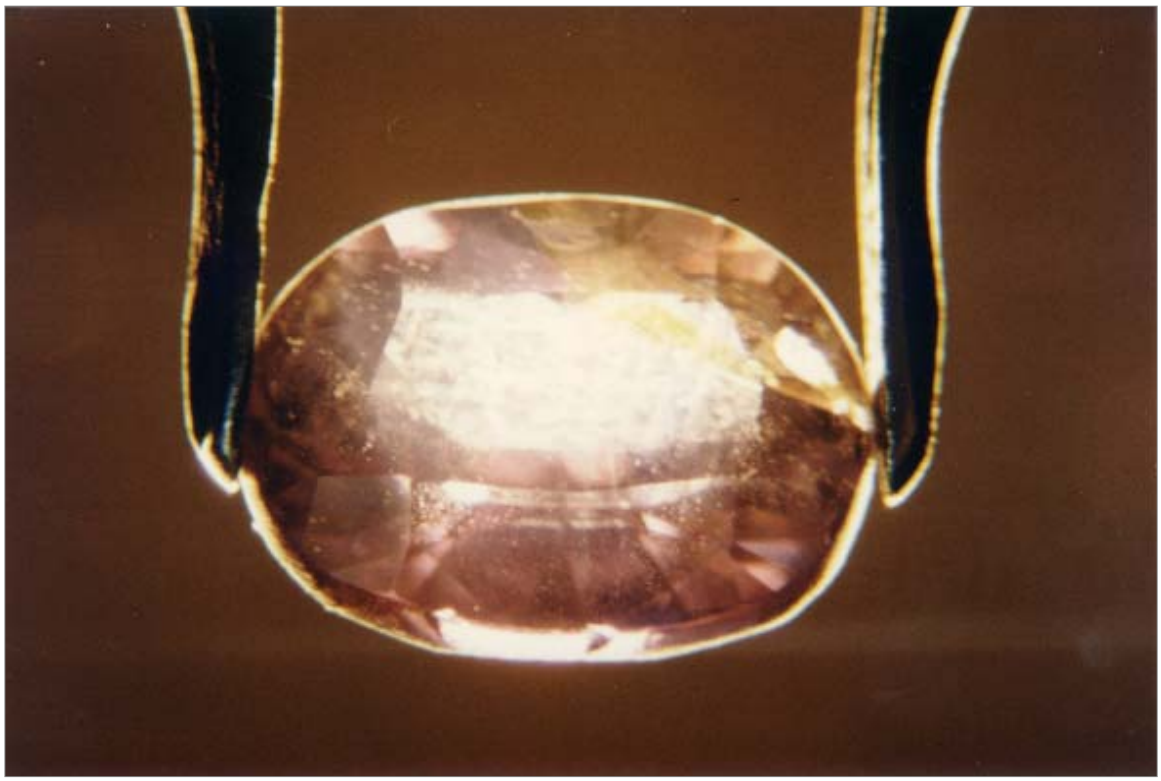

Figure 42. *Yellow colour zone observed in (A-02), an oval-shaped ruby of 2.33 ct, from Colombia. (Dark field illumination 10x)*

Main inclusions observed in the sapphires (Table 5)

- Numerous colourless, transparent doubly terminated zircon (similar to those reported for sapphires from Kashmir. Figure 43-46, and 53-54), or less often rounded zircon crystals, were frequently encountered. Some of these zircon crystals contained pinpoint inclusions, which analysed by Raman-laser proved to be either zircon, rutile (figure 47 & 48) or apatite (observed by Schubnel, 1992). Very occasionally, some of the doubly terminated zircon crystals were found with a halo and tension fissures (figure 47 to 50). Sometimes these zircon were very similar to those observed in sapphires from Sri Lanka (figure 49).

- Some brownish lamellar plagioclase feldspar crystals were noticed in a sapphire, often lying next to zircons (figure 55-56).

- Some dark to red, semitransparent to opaque, doubly terminated rutile crystals (figure 57-58), or exhibiting pseudo-triangular sections, were very often observed (figure 59-60). In one occasion, a dark rutile crystal showed interpenetrant twinning (figure 61-62).

- Boehmite needles or threads were seen in many sapphires, but scaffolds of boehmite needles, or V-shaped polycrystalline boehmite, were only sporadically observed (figure 59).

- Occasionally, some pale yellow, transparent rounded crystals showing low relief, of apatite, were encountered.

- An important pseudo-hexagonal core (crystalline zoning) was observed in the centre of some sapphires (figure 63).

- Straight parallel narrow to broadly spaced planes of polysynthetic twinning have been observed in most of the sapphires.

- Distinct pseudo-hexagonal and straight colour zoning was apparent in many sapphires (figure 64 and 66). A sapphire even exhibited a succession of pseudo-hexagonal growth steps reminiscent of a *"ziggurat"* or *terraced farmlands*, very similar to those observed in sapphires from Yogo Gulch, Montana (N. America). (Figure 65).

- Most sapphires were found to have a pronounced yellow colour zone most probably due to Fe-oxide? (Figure 64, 66 & 67).

- Healed fractures (figure 67), and internal stress fractures, were occasionally observed. In a sapphire, the internal stress fractures were found similar in appearance to those due to "quench-crackling" with a notable difference, that they seldom if ever reach or break the surface, and seem to follow crystalline orientations (Duroc-Danner, 1992. Figure 68).

- Few "fingerprints" were encountered. In some stones, tension fractures seemed to be filled by dendritic-like patterns instead of the usual liquid filled channels (figure 69). In other stones, healing fissures were found to be similar to those encountered in sapphires from Sri Lanka (figure 70).

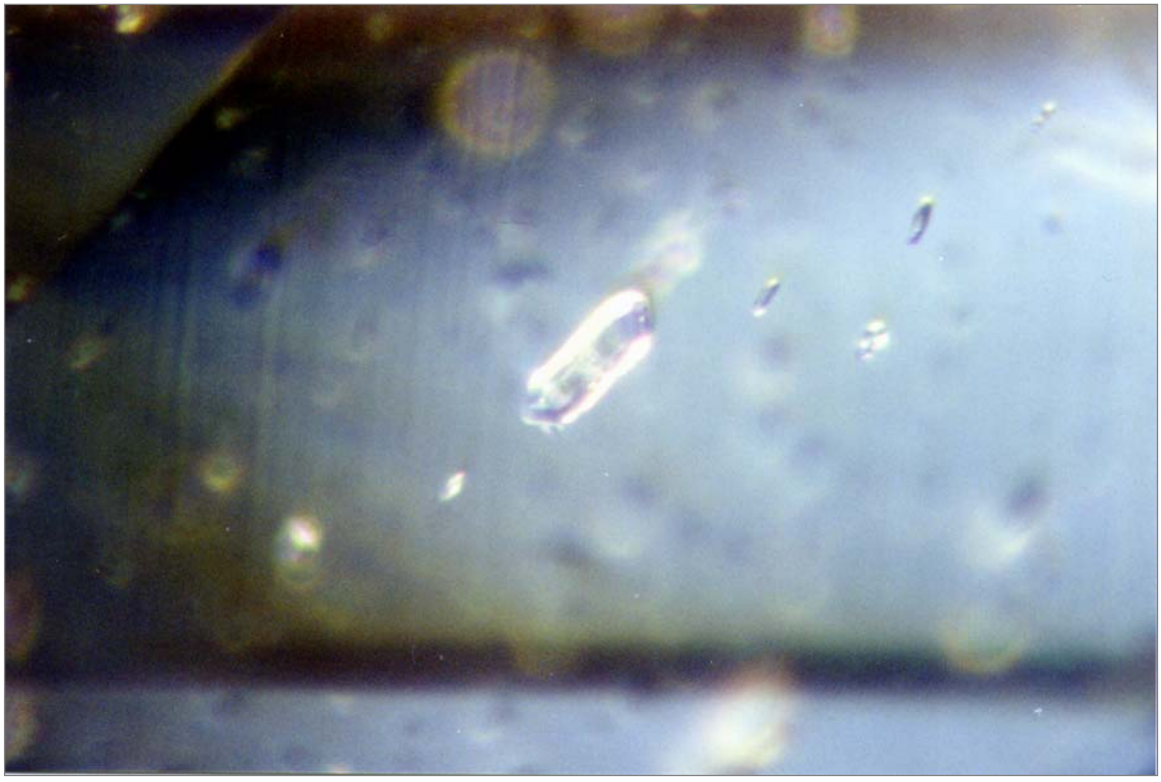

Figure 43. *A doubly terminated colourless crystal of zircon observed in (A-11), a marquise sapphire of 2.19 ct, from Colombia. Note the transparency and the absence of stress cracks (similar inclusions have been observed in Kashmir sapphires).*
(Dark field illumination 80x)

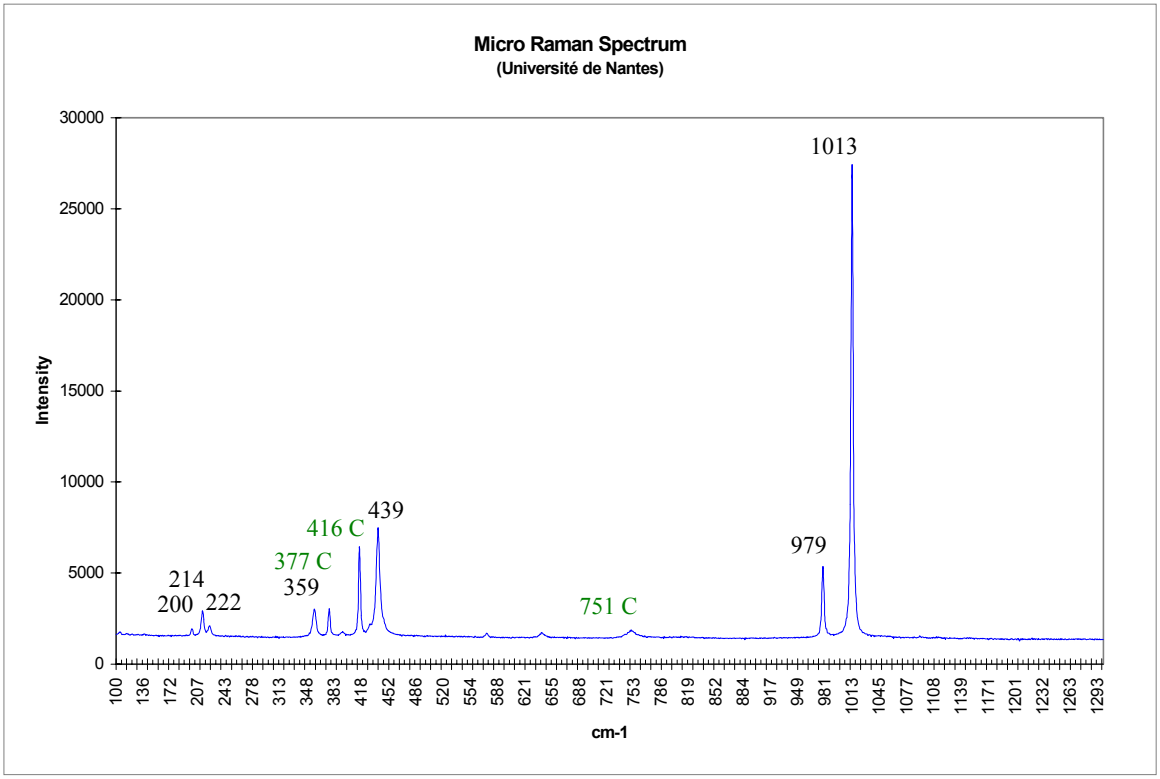

Figure 44. *The Raman spectrum of the doubly terminated colourless zircon crystal poor in rare earth elements (Wopenka, et al., 1996), observed in the above sapphire (A-11), is characterised by the strongest peaks at 439, 979, and 1013 $^{cm-1}$. The other peaks of lower intensity are found at: 200, 214, 222, and 359 $^{cm-1}$. The peaks 377, 416, and 751 $^{cm-1}$, correspond to the host corundum sapphire (C).*

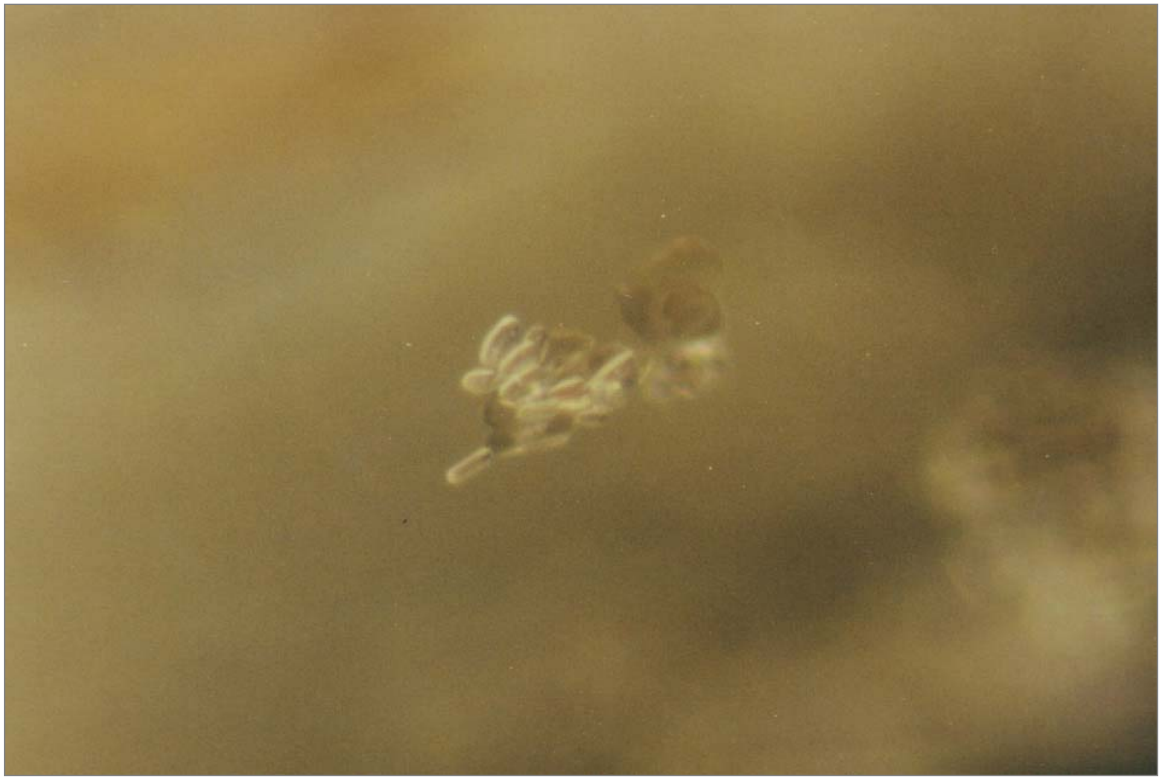

Figure 45. *A group of doubly terminated colourless zircon crystals, observed in (A-07), a greyish-blue cabochon sapphire of 3.01 ct, from Colombia. (Dark field illumination 70x).*

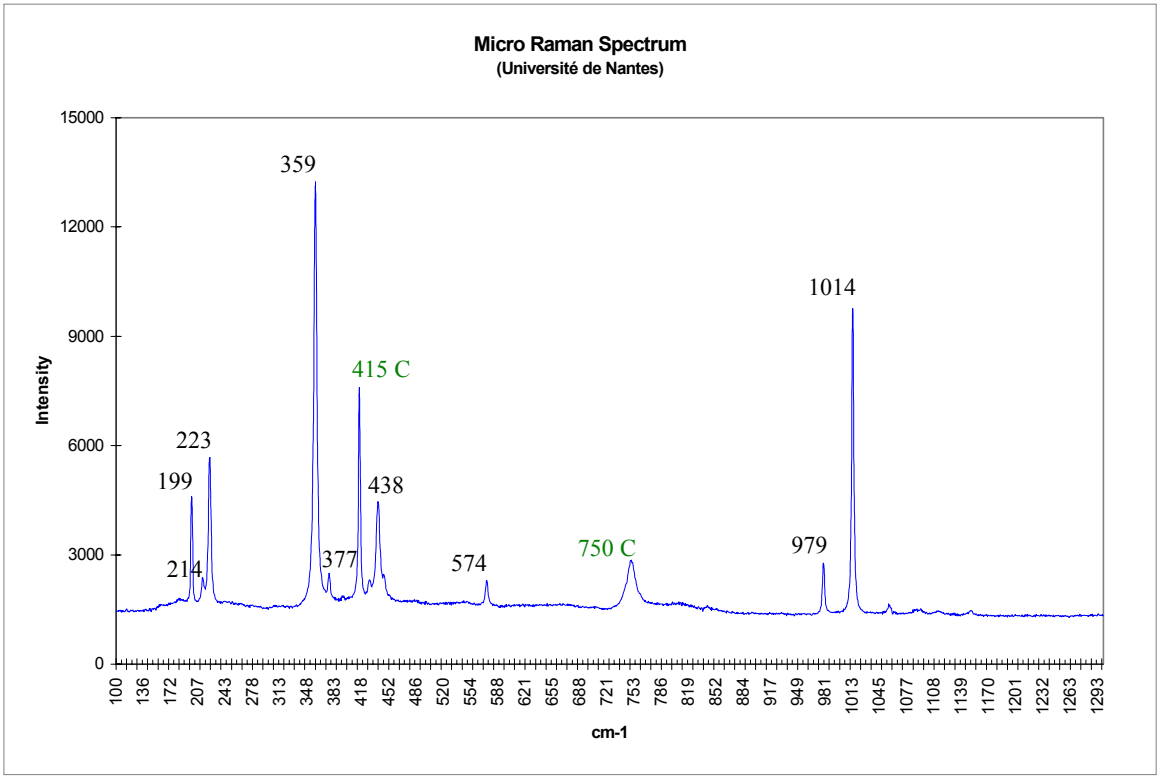

Figure 46. *The Raman spectrum of one of the doubly terminated colourless zircon crystal poor in rare earth elements (Wopenka, et al., 1996), observed in the above sapphire (A-07), is characterised by the strongest peaks at 359, and 1014 $^{cm-1}$. The less diagnostic peaks and of lower intensity are found at: 199, 214, 223, 438, and 979 $^{cm-1}$. The peaks 415, and 750 $^{cm-1}$, correspond to the host corundum sapphire (C).*

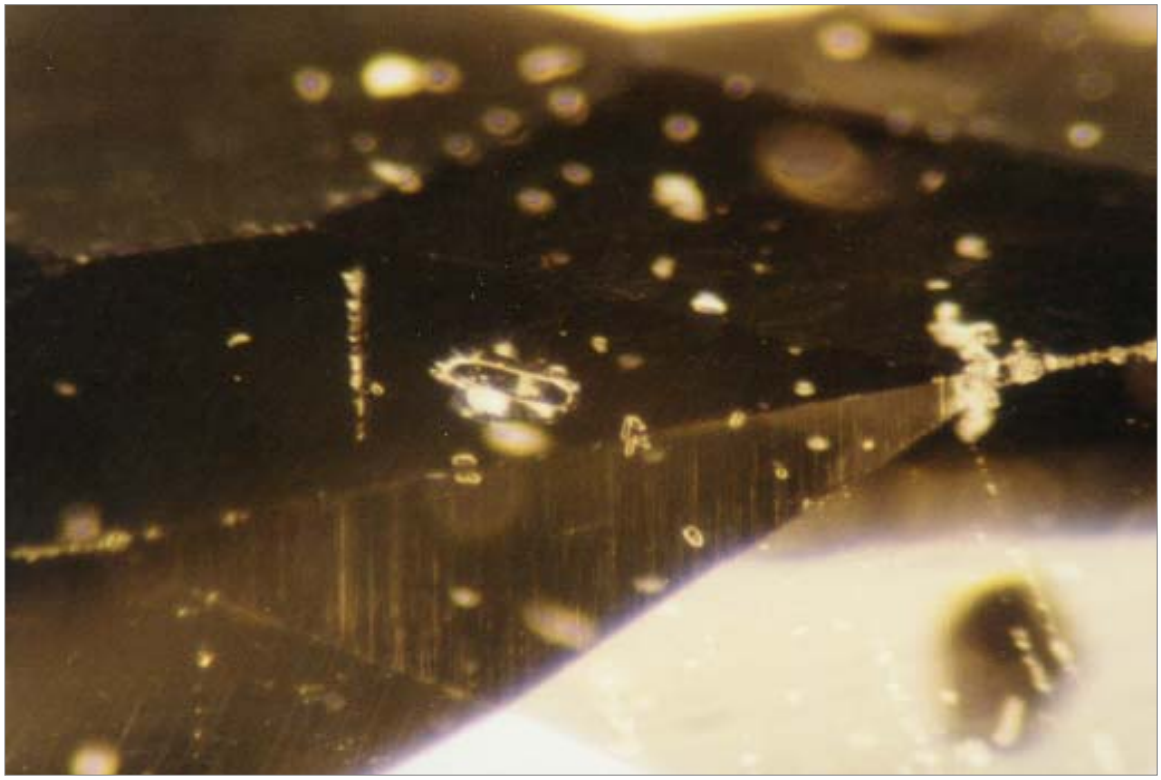

Figure 47. *Zircon inclusion with pinpoints of rutile, observed in (HH-02), a multicoloured oval-shaped sapphire of 0.96 ct, from Colombia. (Dark field illumination 40x)*

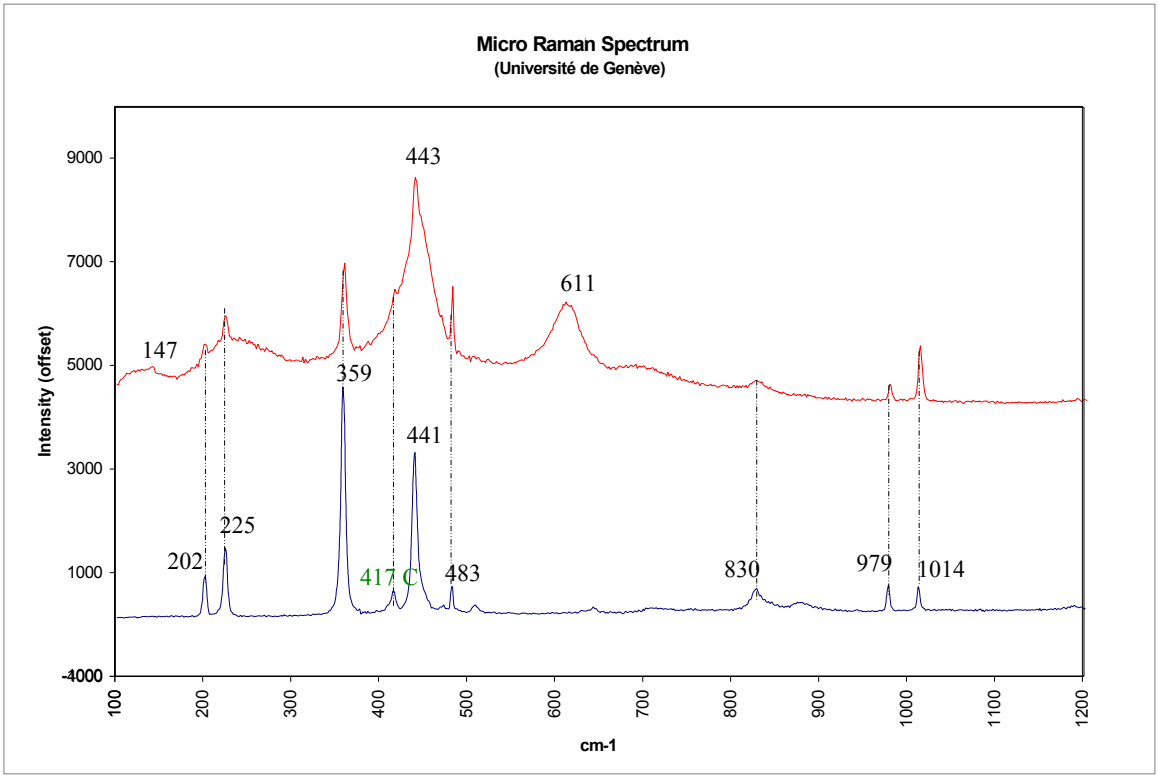

Figure 48. *The Raman spectrum of the trace element poor zircon inclusion (in blue) with its pinpoint inclusion of rutile (in red), observed in the above sapphire (HH-02), is characterised for zircon, by the strongest peaks at 359, and 441 $^{cm-1}$. Other peaks of lower intensity are seen at: 202, 225, 979, and 1014 $^{cm-1}$. The rutile is characterised by the peaks at 611, 147, and 443 $^{cm-1}$. The peak 417 $^{cm-1}$ corresponds to the host corundum sapphire (C).*

Figure 49. *A pair of colourless zircon crystals surrounded by tension fissures (similar to those encountered in sapphires from Sri Lanka), observed in (A-25), a multicoloured oval-shape sapphire of 2.58 ct, from Colombia.*
(Dark field illumination 80x)

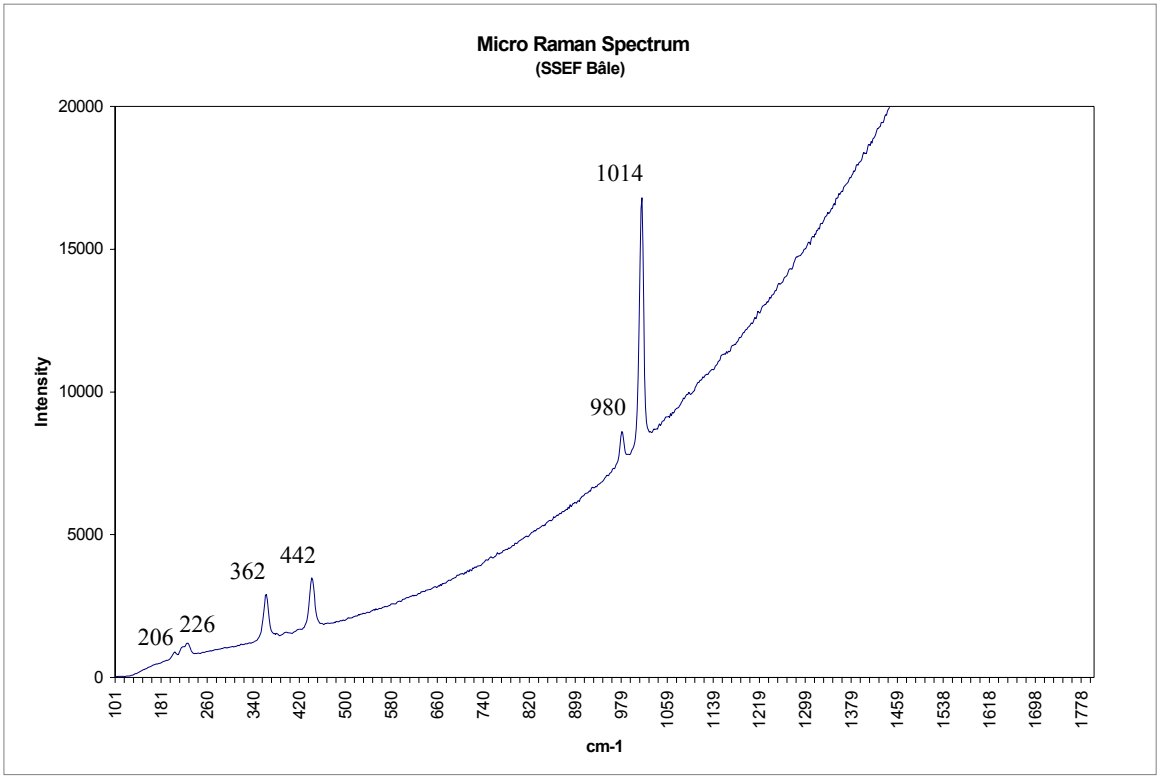

Figure 50. *The Raman spectrum of one of the zircon inclusions rich in rare earth elements (Wopenka, et al., 1996), observed in the above multicoloured sapphire (A-25), is characterised by an absence of peaks in the region of 450 to 950 $^{cm-1}$, by the strongest peak at 1014 $^{cm-1}$, and by the other peaks of lower intensity found at, 206, 226, 362, 442, and 980 $^{cm-1}$. The peaks are ± 6 $^{cm-1}$ off (1014 instead of 1008, 980 instead of 974 $^{cm-1}$, etc.)*

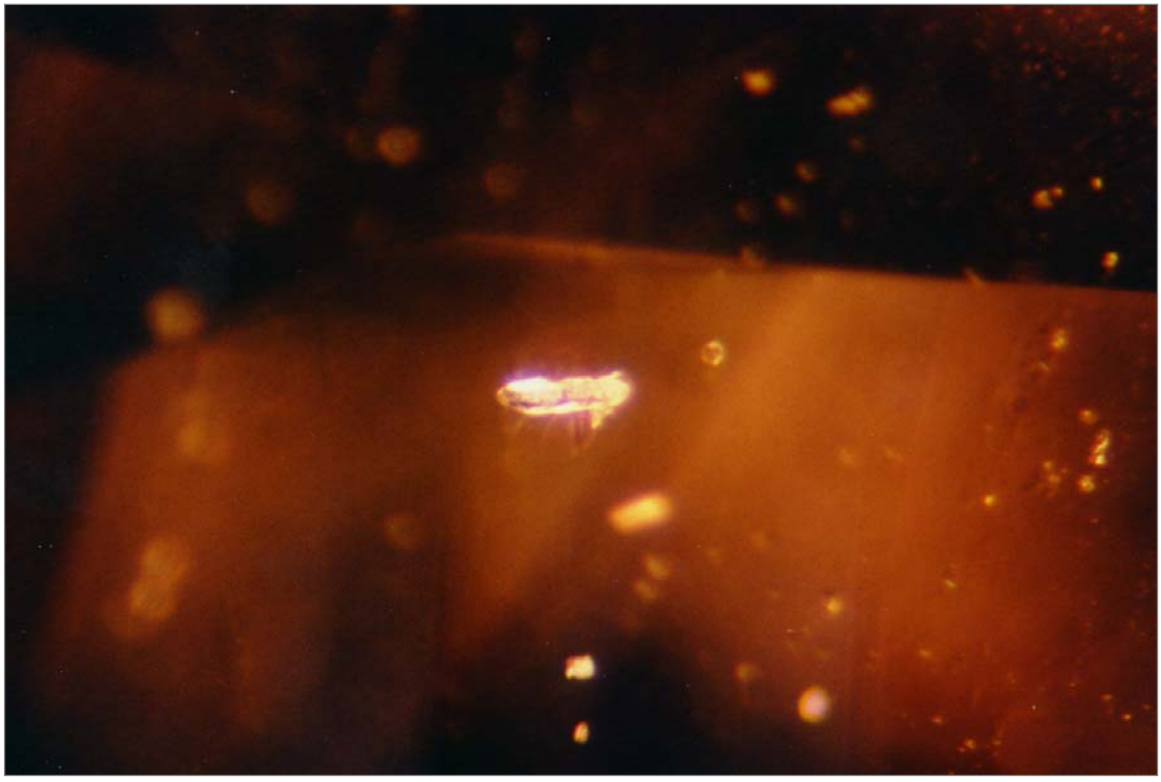

Figure 51. *A large doubly terminated colourless zircon crystal surrounded by numerous sets of halos and tension fissures. Observed in the same multicoloured oval-shaped sapphire of 2.58 ct (A-25), from Colombia. (Dark field illumination 80x)*

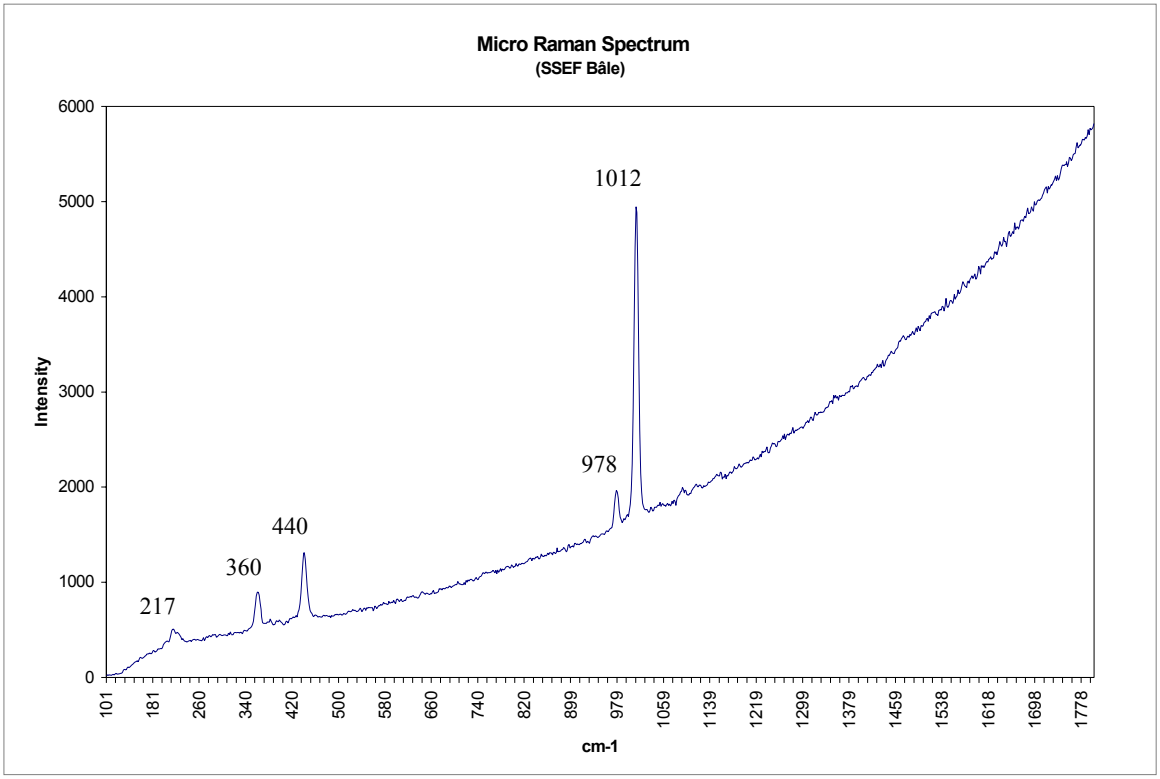

Figure 52. *The Raman spectrum of the large colourless zircon crystal rich in rare earth elements (Wopenka, et al., 1996), observed in the multicoloured sapphire (A-25), is characterised by the strongest peak at 1012 $^{cm-1}$, and by the other peaks of lower intensity found at 217, 360, 440, and 978 $^{cm-1}$.*

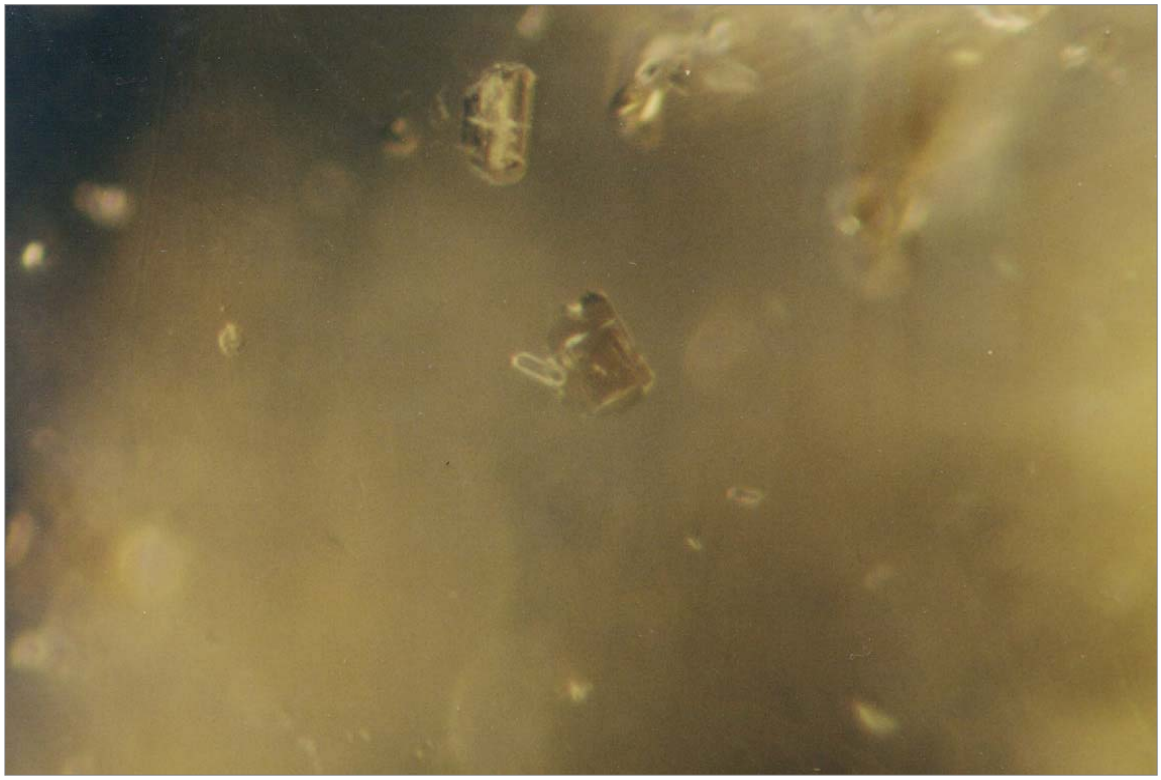

Figure 53. *A doubly terminated colourless zircon crystal encountered next to a plagioclase feldspar crystal, observed in (A-07), a greyish-blue cabochon sapphire of 3.01 ct, from Colombia. (Dark field illumination 70x).*

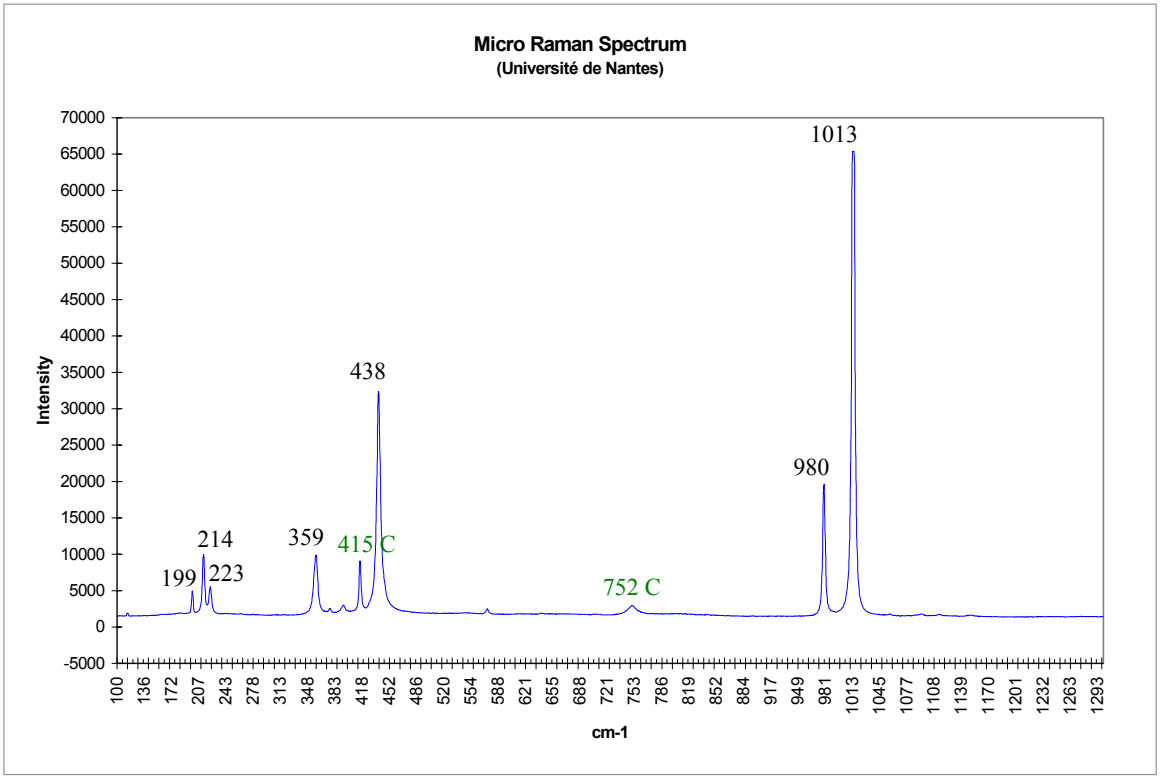

Figure 54. *The Raman spectrum of a doubly terminated colourless zircon crystal poor in rare earth elements (Wopenka, et al., 1996), observed in the above sapphire (A-07), is characterised by the strongest peak at 1013 $^{cm-1}$, and also by peaks of lower intensity found at: 199, 214, 223, 438, and 980 $^{cm-1}$. The peaks 415, and 752 $^{cm-1}$, correspond to the host corundum sapphire (C).*

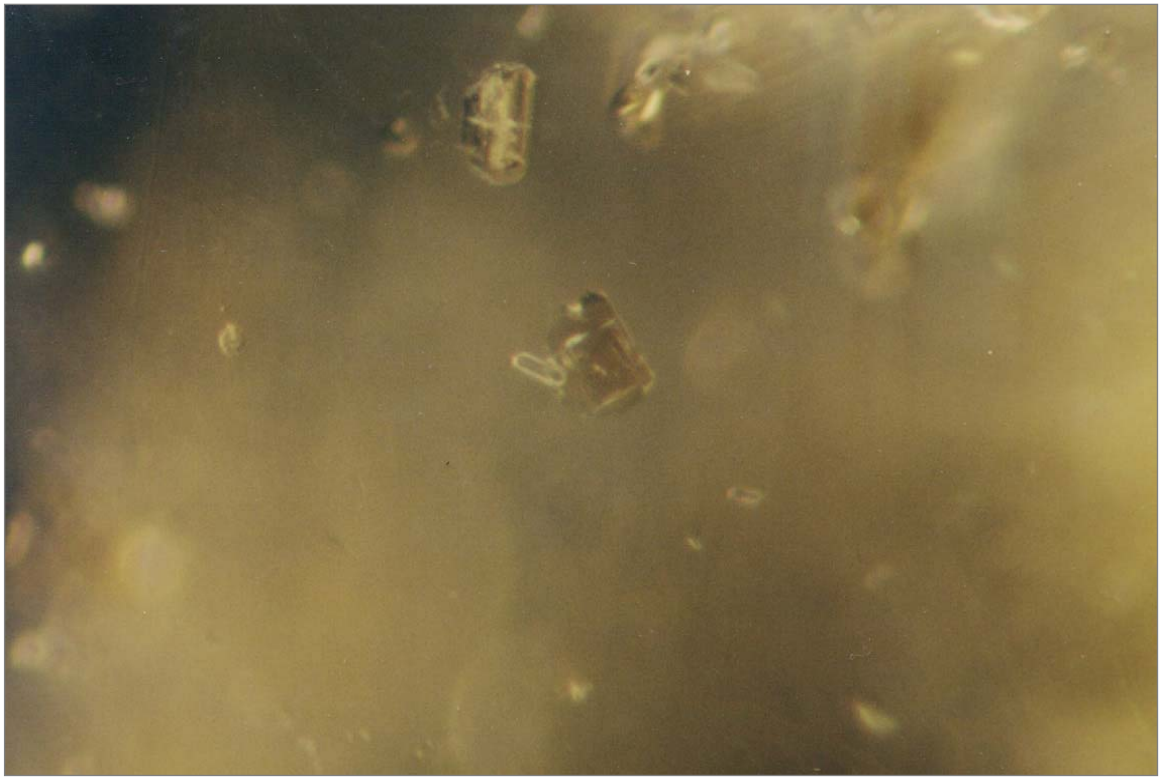

Figure 55. *A plagioclase feldspar crystal, encountered next to a colourless doubly terminated zircon poor in rare earth elements, observed in (A-07), a greyish-blue cabochon sapphire of 3.01 ct, from Colombia. (Dark field illumination 70x)*

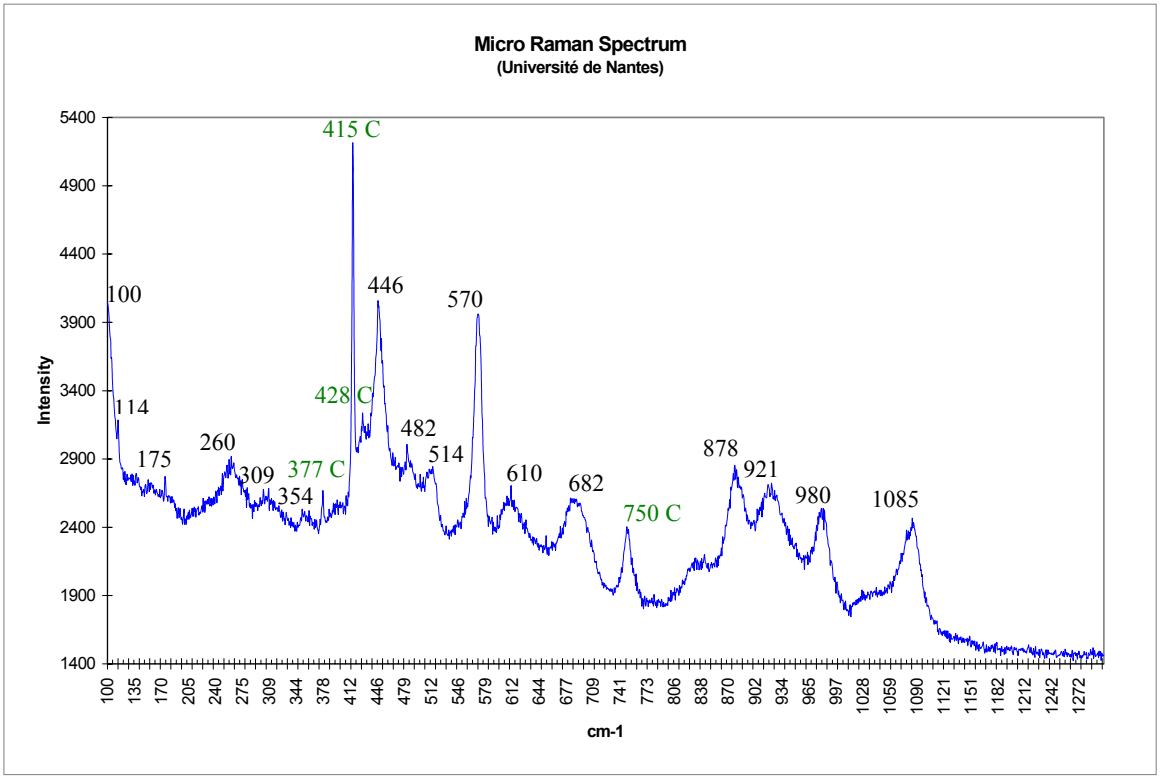

Figure 56. *The Raman spectrum of a plagioclase feldspar crystal, observed in the above sapphire (A-07), is characterised by the peaks at 114, 175, 482, 514, and 980 $^{cm-1}$. The peaks at 377, 415, 428, and 750 $^{cm-1}$, correspond to the host corundum sapphire (C).*

Figure 57. *A group of rounded colourless zircon crystals, with a few colourless doubly terminated zircon crystals, observed near a doubly terminated red rutile crystal, observed in a cabochon sapphire (A-31) of 0.71 ct, from Colombia. Note also the intersecting boehmite needles, oriented in two directions. (Dark field illumination 95x)*

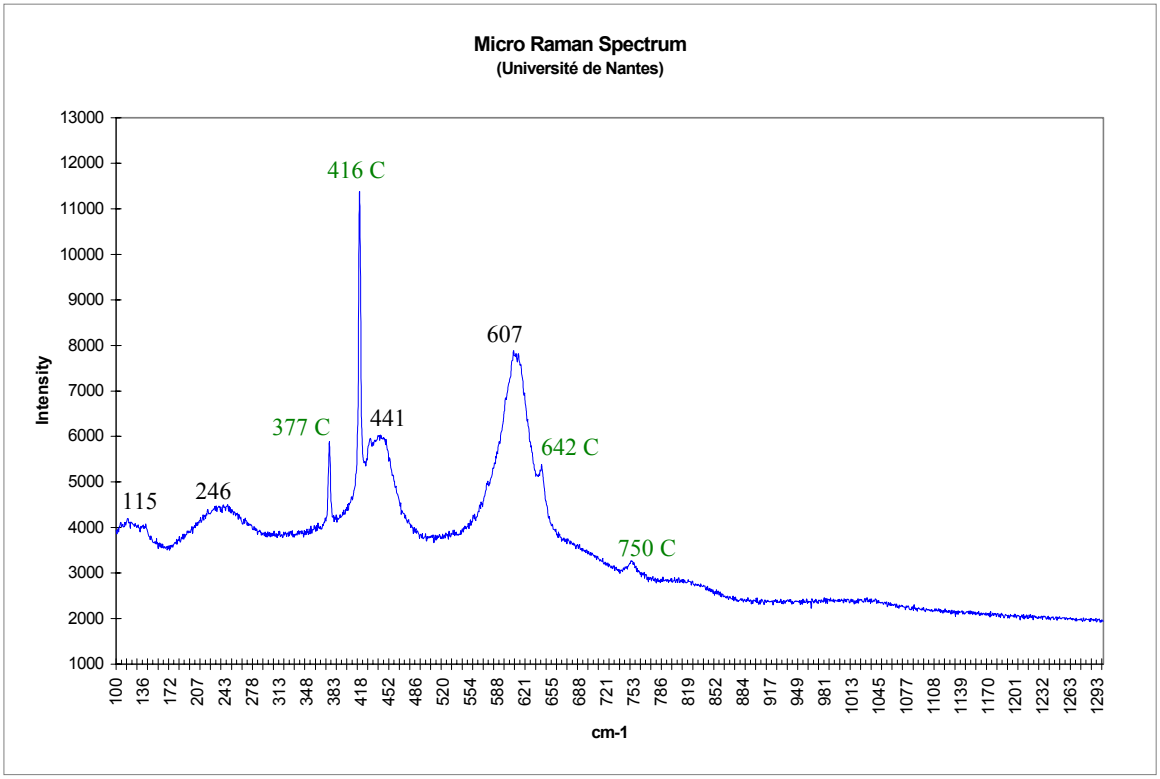

Figure 58. *The Raman spectrum of the doubly terminated red rutile crystal observed in the above cabochon sapphire (A-31), is characterised by the strongest peak at 607 $^{cm-1}$, and by the lower intensity peaks found at: 246, and 441 $^{cm-1}$. The peaks 377, 416, 642, and 750 $^{cm-1}$, correspond to the host corundum sapphire (C).*

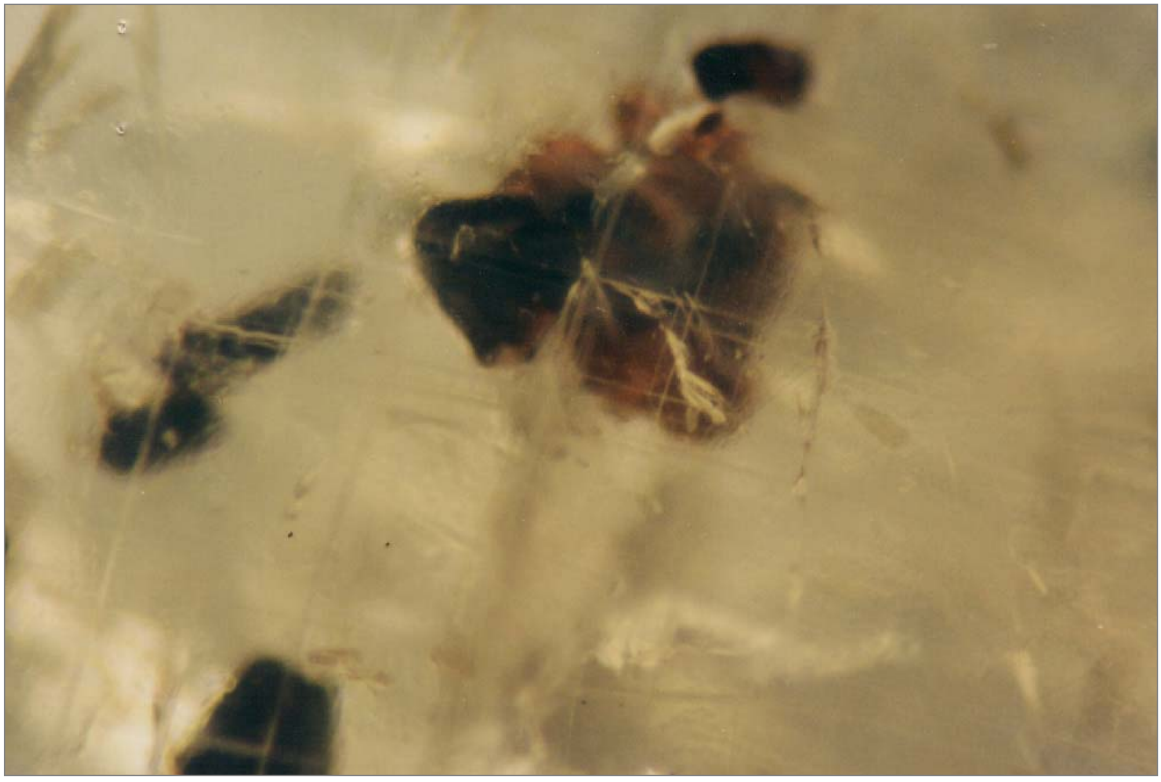

Figure 59. *A group of large rutile crystals (some showing pseudo-triangular sections), breaking the surface of a cabochon sapphire (A-31) of 0.71 ct, from Colombia. Note also the scaffolds of boehmite needles, oriented in two directions, forming angles of almost 90°, which often follow the juncture of intersecting twin-lamellae. (Dark field illumination 30x)*

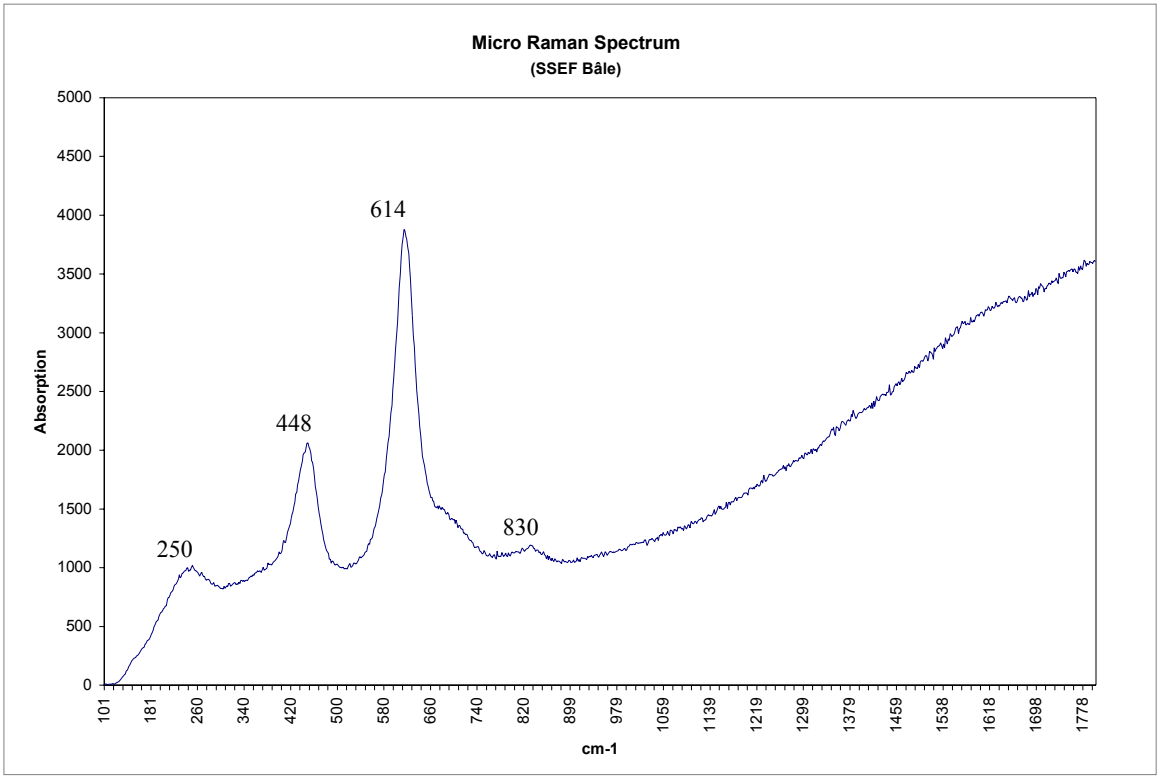

Figure 60. *The Raman spectrum of the large pseudo-triangular section rutile inclusion breaking the surface of the above cabochon sapphire (A-31), is characterised by the strongest peak at 614 $^{cm-1}$, and by the lower intensity peaks found at: 250, and 448 $^{cm-1}$.*

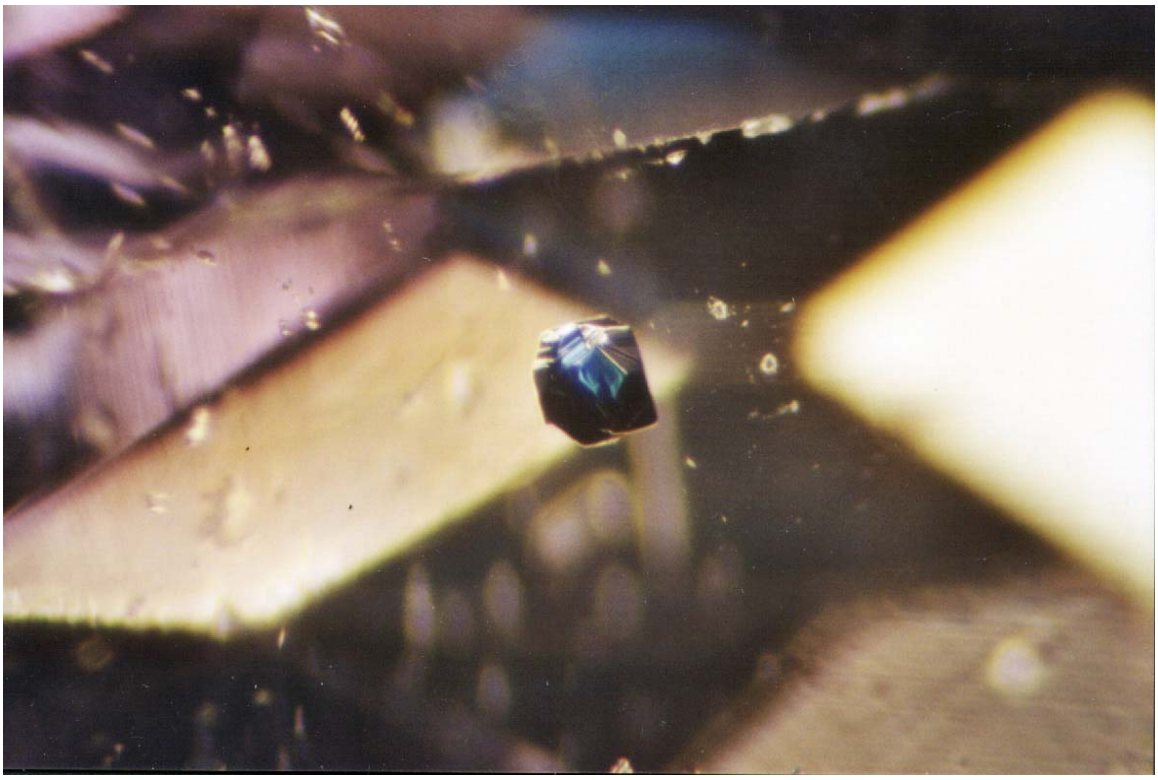

Figure 61. *A rutile crystal exhibiting a random interpenetration, observed in (HH-02), an oval-shape multicoloured sapphire of 0.96 ct, from Colombia. Note also the numerous colourless zircon crystals surrounding the large rutile crystal. (Dark field illumination 40x)*

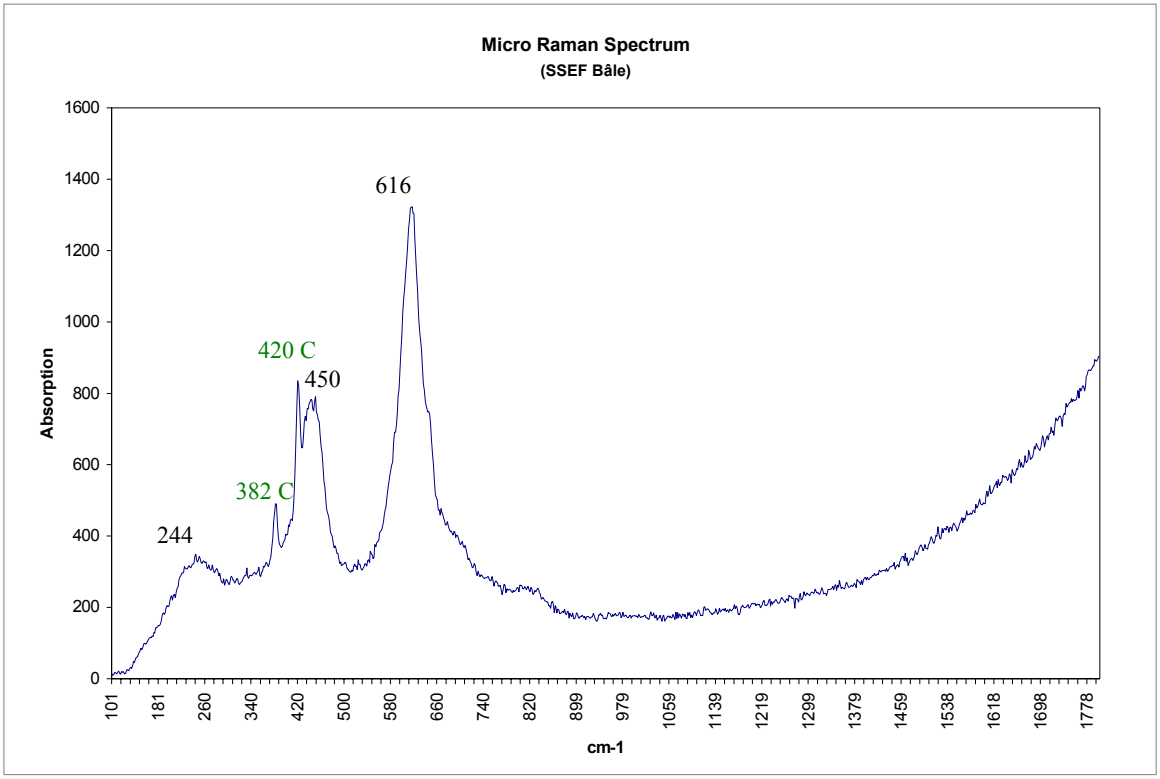

Figure 62. *The Raman spectrum of the rutile crystal exhibiting interpenetrant twin observed in the above multicoloured sapphire (HH-02), is characterised by its strongest peak at 616 $^{cm-1}$, and by other peaks of lower intensity at 244, and 450 $^{cm-1}$. The peaks 382 $^{cm-1}$, and 420 $^{cm-1}$, correspond to the host corundum sapphire (C).*

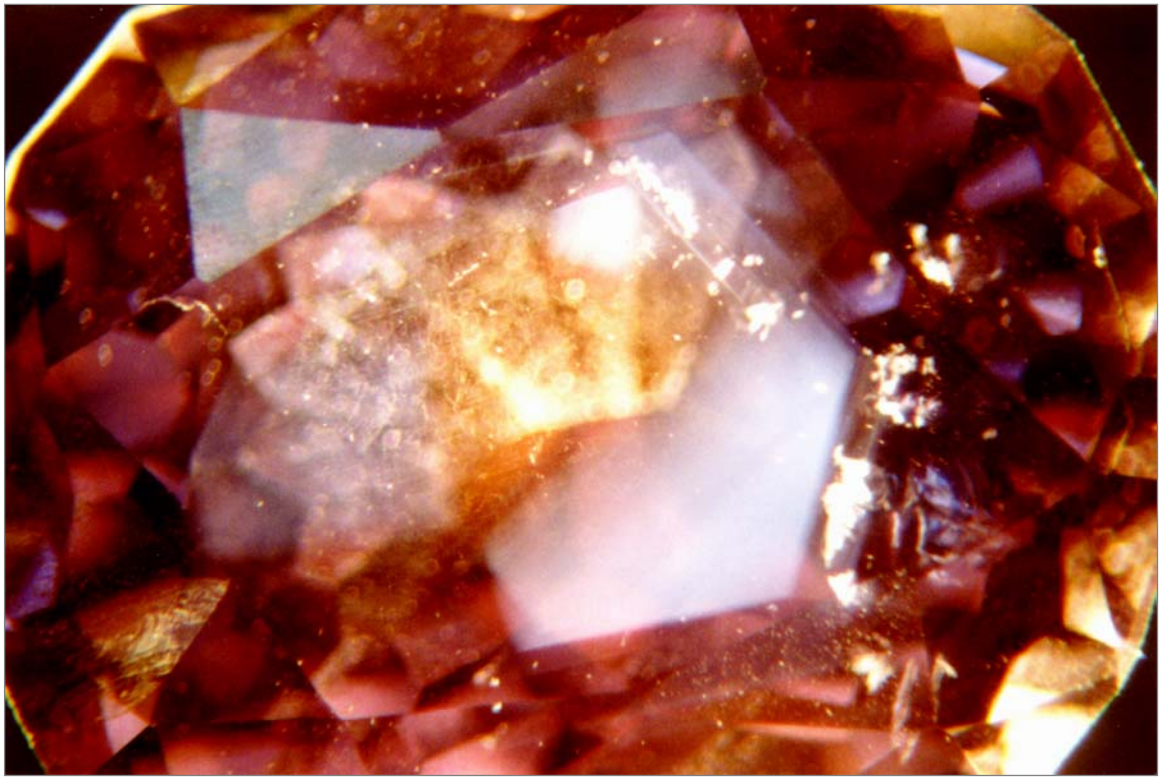

Figure 63. *A pseudo-hexagonal core of presumably sapphire, observed in the centre of (A-29), a multicoloured brilliant-cut sapphire of 1.90 ct, from Colombia. (Dark field illumination 30x)*

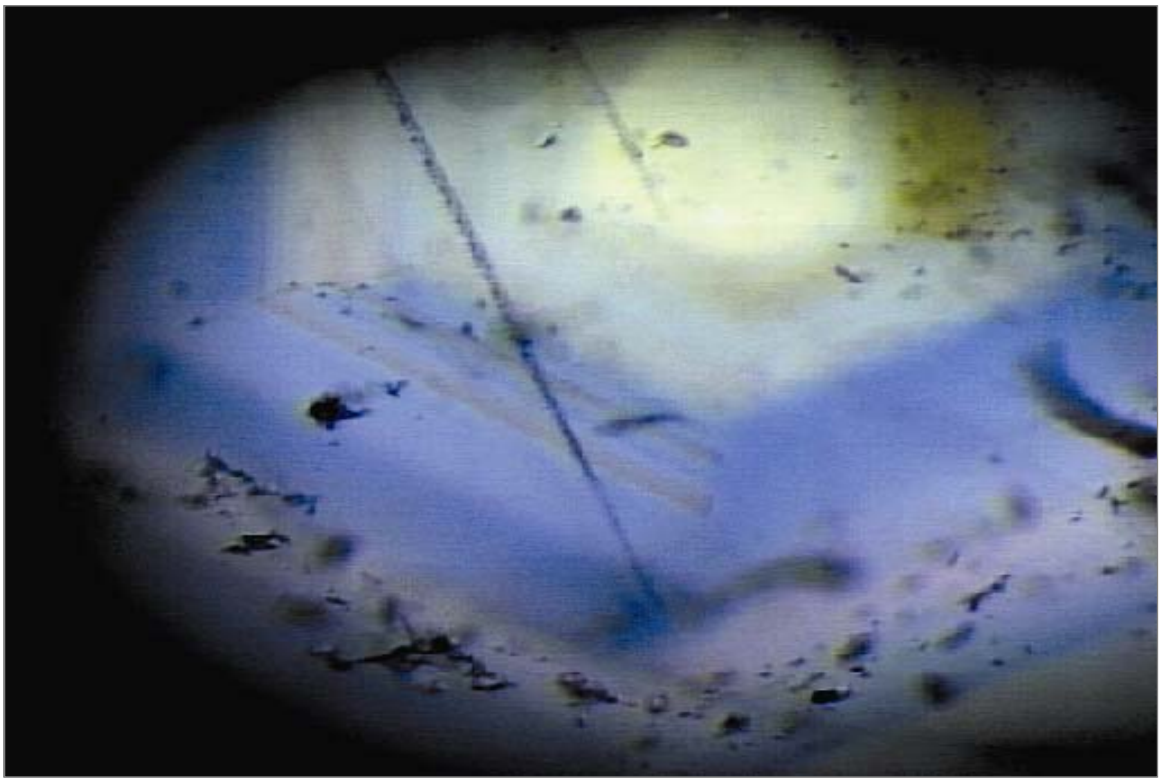

Figure 64. *Strong hexagonal growth zones with a yellow colour centre observed in (A-32), a cabochon multicoloured sapphire of 1.66 ct, from Colombia. Note the two long boehmite needles showing fringed tension-fissures, and the orientation of the zircon crystals, which form phantoms in the hexagonal zonings. (Dark field illumination 25x)*

Figure 65. *Distinct hexagonal growth steps reminiscent of terraced farmlands (similar to those seen in sapphires from Montana, N. America), observed perpendicular to the C-axis in (A-12), an oval-shape sapphire of 6.89 ct, from Colombia. (Dark field illumination 15 x)*

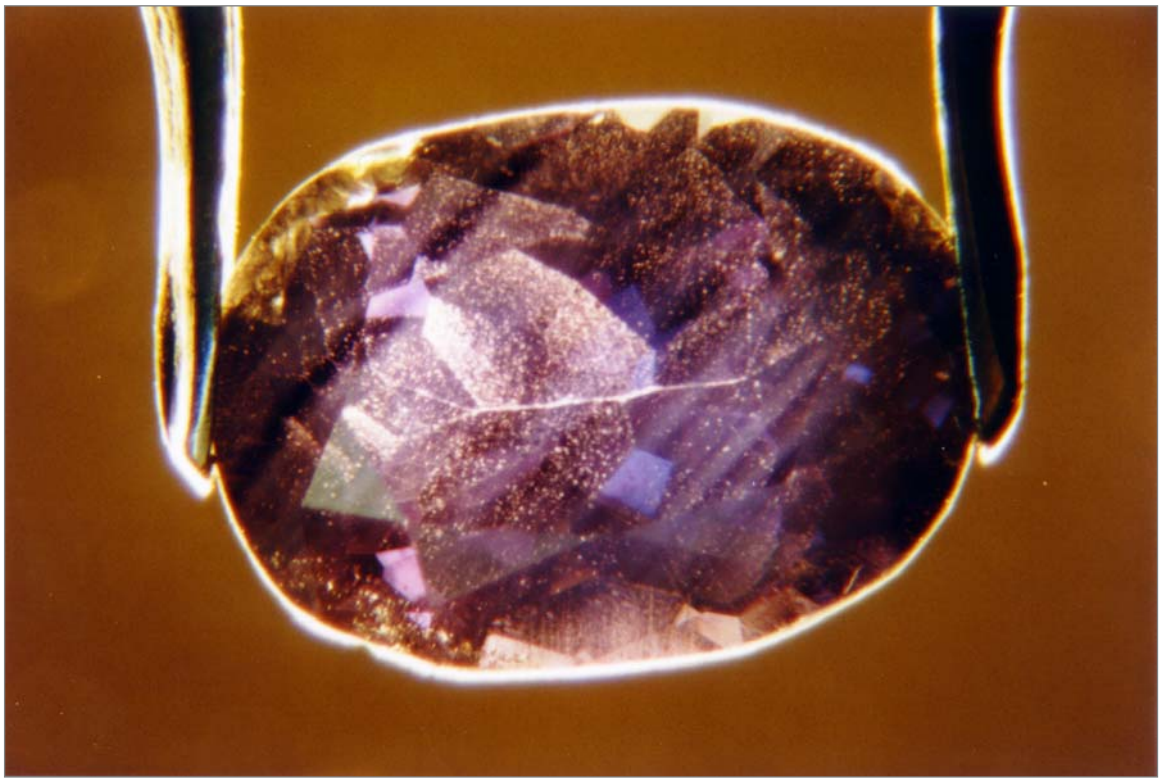

Figure 66. *Distinct straight colour bands and yellow colour zone, observed in (A-28), an oval-shape multicoloured sapphire of 1.53 ct, from Colombia. (Dark field illumination 25x)*

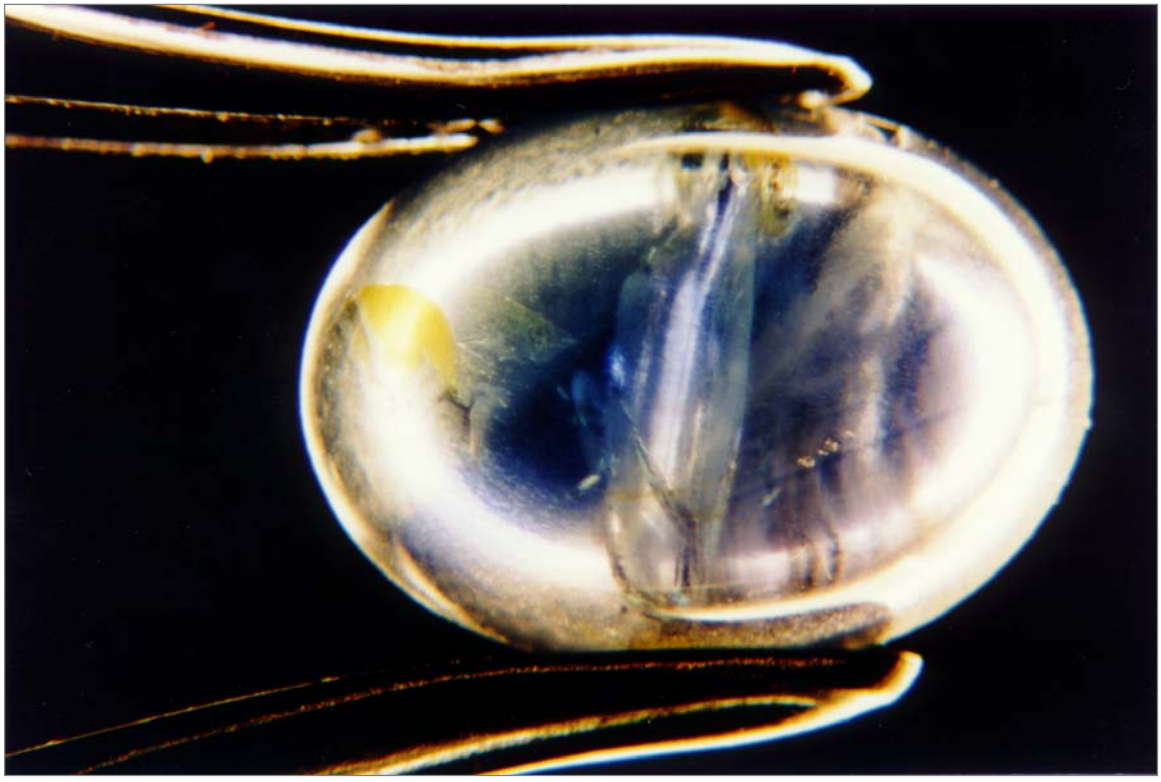

Figure 67. *Important healed fracture, and a yellow colour zone, observed in (A-08), a cabochon sapphire of 2.66 ct, from Colombia. (Dark field illumination 20x)*

Figure 68. *Numerous internal stress fractures, similar in appearance to those caused by "quench-crackling", were observed in (HH-01), a greyish-blue sapphire of 4.81 ct, from Colombia. (Dark field illumination 20x)*

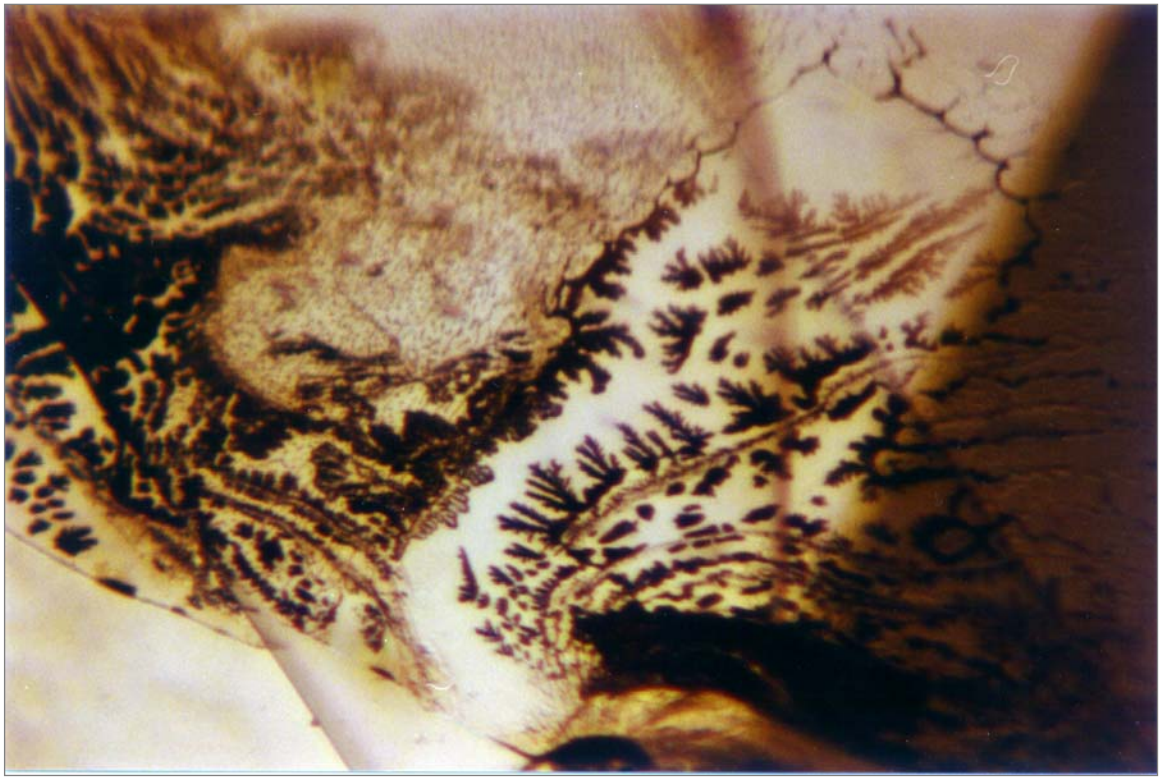

Figure 69. *A fingerprint filled with dendritic-like patterns, observed in (A-28), an oval-shape multicoloured sapphire of 1.53 ct, from Colombia. (Dark field illumination 50x)*

Figure 70. *A "fingerprint" filled with two-phase inclusions observed in (A-33), an oval-shape colour-change sapphire of 0.65 ct, from Colombia. (Dark field illumination 40x)*

Main inclusions observed in the heat-treated sapphires (Table 5)

- "Fingerprints" filled with two-phase inclusions, or discoid-like without any filling, and thus showing a glassy appearance.

- Intense heating (near the melting point of rutile 1830-1850°C), corrodes (begins to melt) the solid rutile inclusions, that interact with the iron present in the sapphire (or in the rutile itself) causing "internal diffusion" which results in an intense colour halo (blue in sapphires. Blue in daylight or purplish red in incandescent light, for colour-change sapphires), found sometimes containing pinpoint inclusions (presumably rutile? Unidentified. Figure 71, and 73-75).

- "Fingerprints". Some observed next to corroded rutile crystals, gathered their blue colour from internal diffusion (figure 72).

- Very short doted needles of presumably rutile (not confirmed).

- Small to large dark reddish brown often doubly terminated zircon crystals, sometimes showing stress fissures (figure 76).

- Doubly terminated colourless transparent zircon crystals, occasionally containing pinpoint inclusions (rutile, apatite, zircon?).

- Hexagonal growth zoning.

- Polysynthetic twinning.

- Yellow colour zone (Fe oxide?).

Rarely if ever, only one of these inclusions was solely encountered in either rubies or sapphires from Colombia (again see Table 5).
Nevertheless, and as has been observed, the inclusions are similar to those found in corundums from other sources.
Since their Colombian identification cannot rely on the morphology of their inclusions, it was decided to search for other characteristics by which these corundums could be distinguished.

Figure 71. *Corroded rutile crystals due to intense heating, diffusing intense blue patches, responsible for the internal dark blue colour of the sapphire. Observed in (TT-01), an oval-shape heat-treated sapphire of 2.14 ct, from Colombia. (Dark field illumination 10x)*

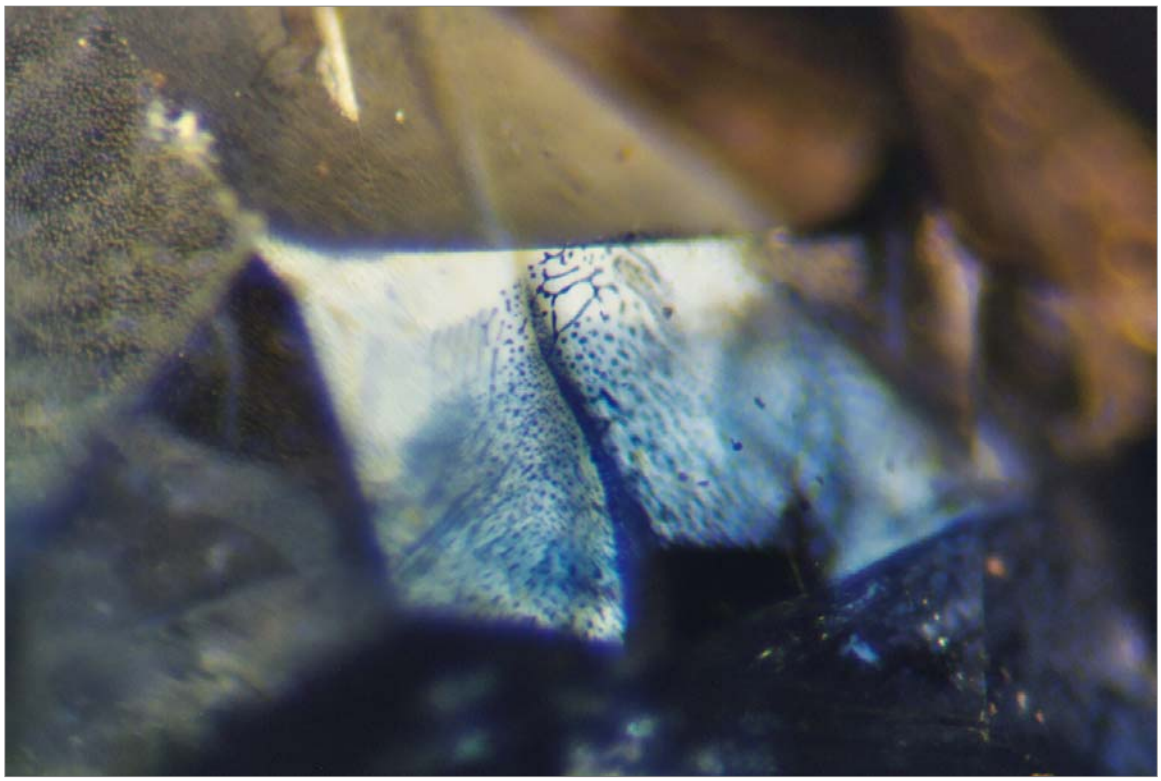

Figure 72. *A "fingerprint" showing blue diffusion, observed in the same (TT-01), oval shape heat-treated sapphire of 2.14 ct, from Colombia. (Dark field illumination 40 x)*

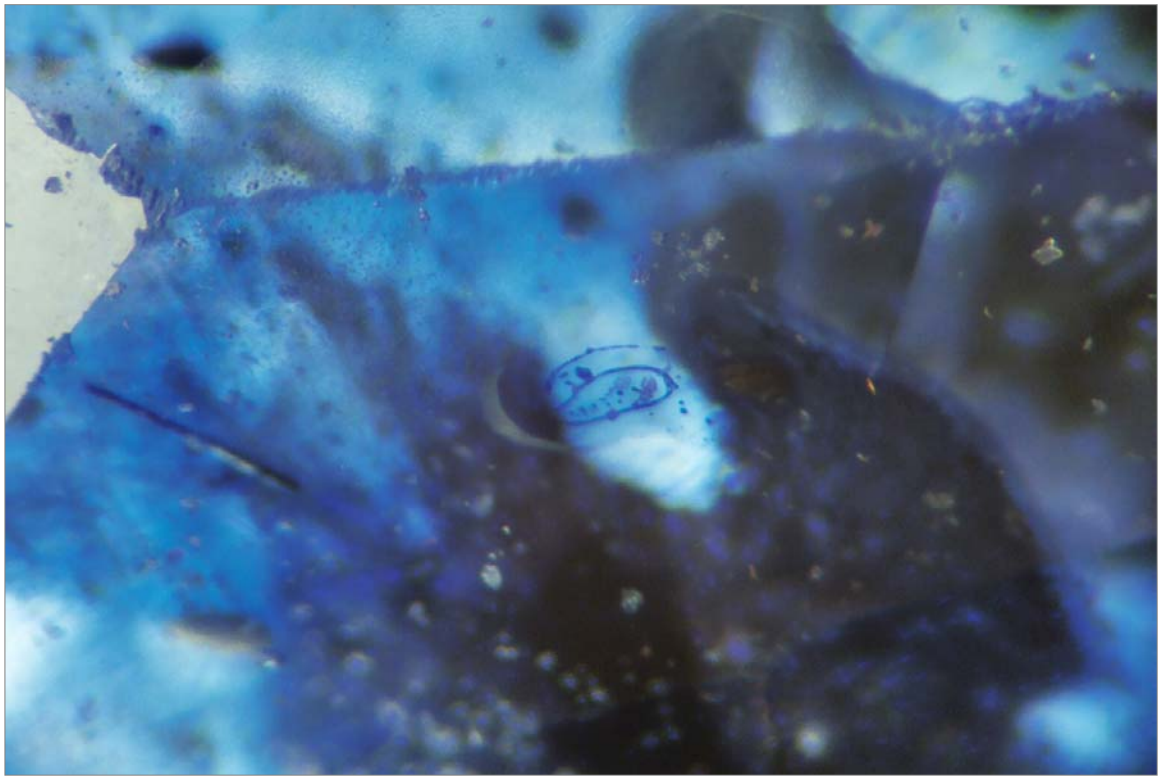

Figure 73. *Dark blue rim circling an atoll-like inclusion, filled with oriented dark pinpoint inclusions (also diffusing a dark blue colour, due to intense heating). Observed in (TT-01), an oval-shape heat-treated sapphire of 2.14 ct, from Colombia. (Dark field illumination 40x)*

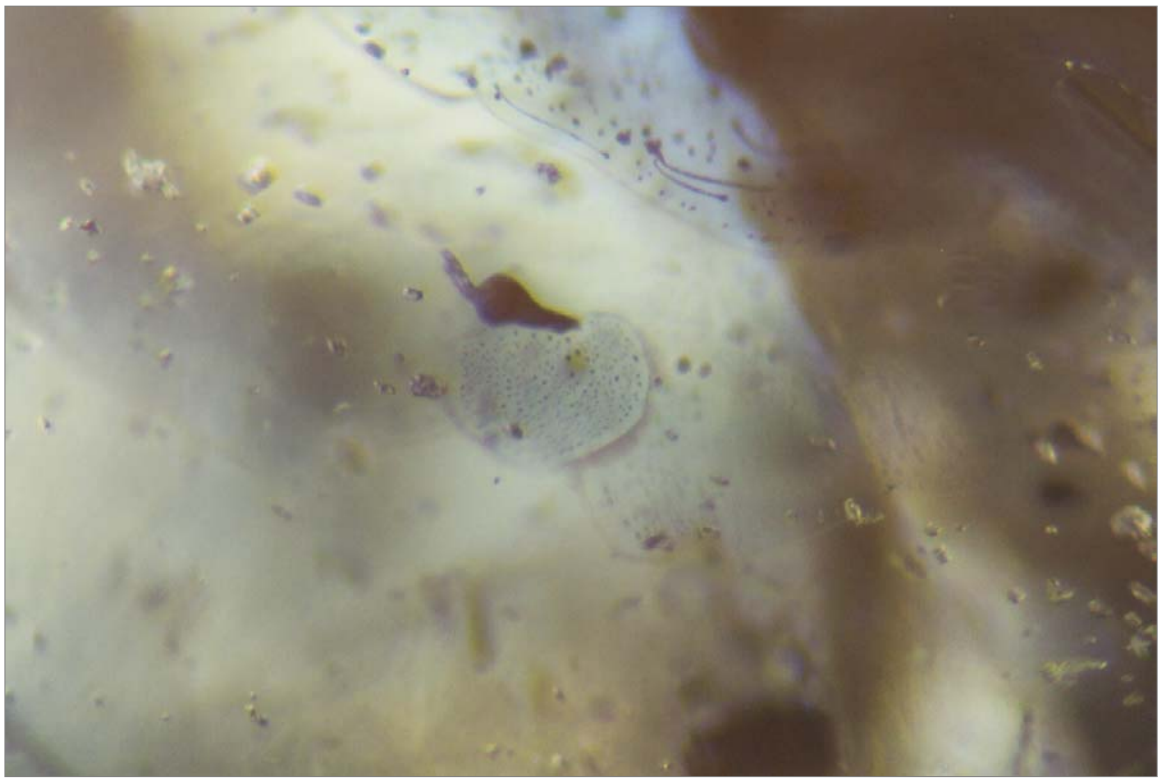

Figure 74. *An "atoll-like" "fingerprint" filled with numerous circling dark pinpoints (presumably rutile), diffusing blue colour from a corroded rutile crystal also diffusing blue colour. Observed in the same (TT-01), oval shape heat-treated sapphire of 2.14 ct, from Colombia. (Dark field illumination 40 x)*

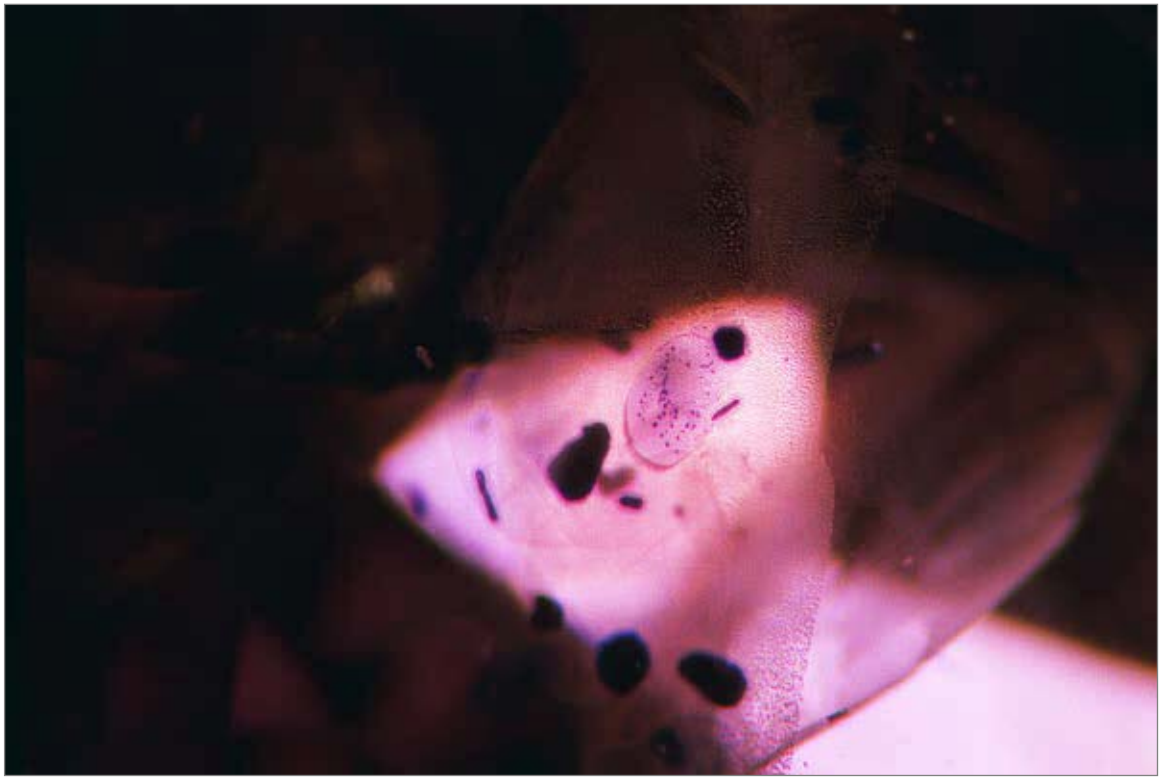

Figure 75. *Corroded rutile crystals surrounded by a violetish red halo (incandescent light) containing pinpoint inclusions, observed in (TT-02), an oval-shape heat-treated colour-change sapphire of 0.96 ct, from Colombia. (Dark field and incandescent illumination 40x)*

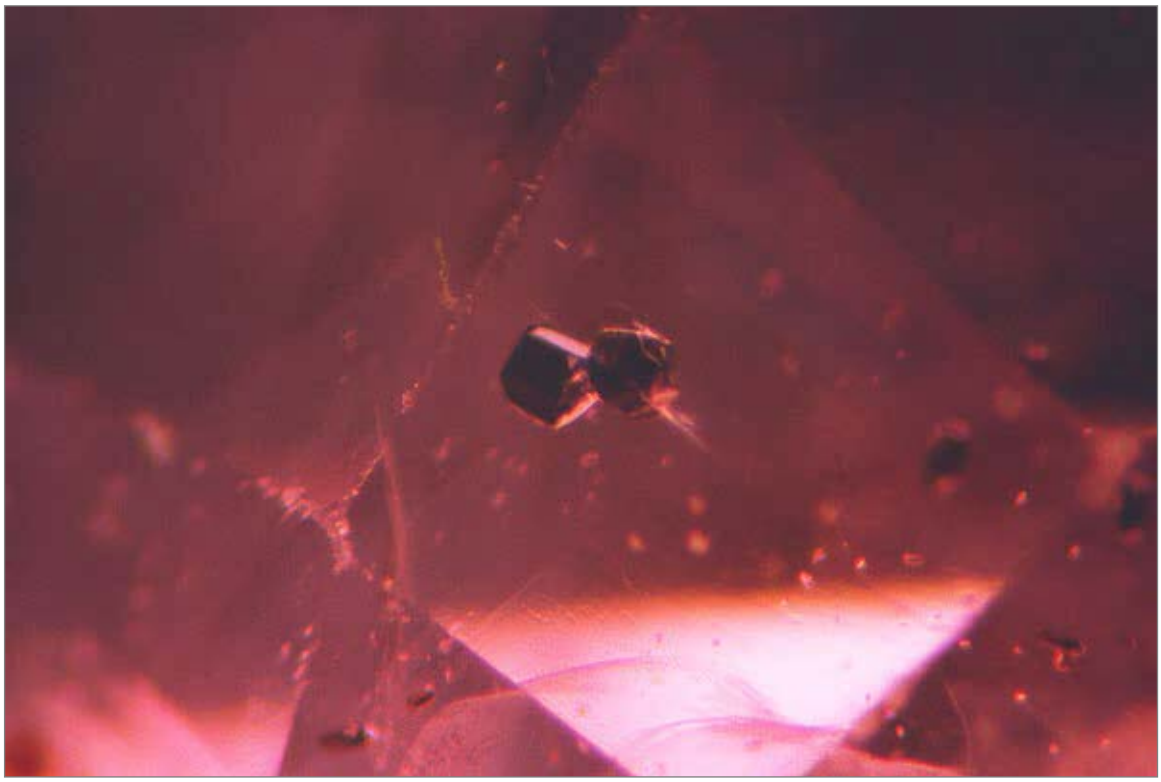

Figure 76. *A dark reddish brown zircon crystal showing stress fissures observed in (TT-03), an oval shape heat-treated colour change sapphire of 0.95 ct, from Colombia. (Dark field illumination 60 x)*

TABLE 5 The internal characteristics observed in the forty-one faceted corundums from Mercaderes-Rio Mayo area, Cauca-Nariño, Colombia

Source	VARIETY Cut or shape	Weight (carat)	Colour	Characteristics
	RUBIES			
A-01	Pear-shape	1.86	Deep pinkish-red	Numerous colourless, transparent doubly terminated zircon crystals (some containing one or more pinpoints), sometimes showing stress fractures. Polysynthetic twinning, and fine lashes of boehmite.
A-02	Oval-shape	2.33	Pinkish-red	Polysynthetic twinning, boehmite needles, and a yellow colour zone (iron oxide?).
A-03	Pear-shape	1.55	Purplish-red	Some minute, colourless, transparent doubly terminated zircon crystals, polysynthetic twinning, threads of boehmite, dense nest of exsolution of presumably rutile needles (?), hexagonal colour and growth zoning, and dentritic-like “fingerprints”.
A-04	Pear-shape	1.42	Intense pink	Some minute, colourless, transparent doubly terminated zircon crystals, very narrow spaced polysynthetic twinning lines, alignment of thick boehmite needles (in one area forming a scaffold). Also present, some dentritic-like “fingerprints”, and healing fractures.
A-05	Cabochon	1.66	Pinkish-red	Many healed fractures, some dark red opaque rutile crystals, few very small colourless doubly terminated zircon crystals, a rather large pink transparent hexagonal crystal (unidentified, but presumably corundum), polysynthetic twinning, “bleeding” of colour, and a dense nest of very short rutile needles forming a "silk".
A-06	Cabochon	6.24	Violet-red	Many colourless, transparent doubly terminated zircon crystals with few showing stress fractures (some with pinpoint inclusions. Identified by Raman to be zircon), Also present, a very thick and large hexagonal sapphire core, colour zoning and “bleeding” of colour.
GT-01	Oval-shape	0.33	Pinkish-red	Strong narrow spaced polysynthetic twinning, exsolution of presumably rutile needles (?), some healed fractures, a large dentritic-like “fingerprint”, and a yellow colour zone (iron oxide?).
GT-02	Pear-shape	0.19	Intense pink	Some minute, colourless, transparent doubly terminated zircon crystals, a large healed fracture, and some very small flat elongated “fingerprints” filled with two-phase inclusions.
	SAPPHIRES			
A-07	Cabochon	3.01	Greyish-blue	Numerous colourless, transparent doubly terminated zircon crystals (some with pinpoint inclusions). Few transparent pale yellow apatite crystals, some brownish lamellar plagioclase feldspar, polysynthetic twinning, hexagonal growth zonings, and healing fractures.
A-08	Cabochon	2.66	Greenish-blue	Polysynthetic twinning, cloud of dissolved inclusions (unidentified), yellow colour zone (iron oxide?), and “fingerprints” in healed fractures.
A-09	Cabochon	3.24	Greyish-blue	Numerous colourless, transparent doubly terminated zircon crystals, dark opaque rutile crystals, pale yellow transparent apatite crystals, a yellow colour zone (iron oxide?), and healed fractures.
A-10	Oval-shape	2.58	Violet-blue	Some dark, semi-transparent doubly terminated rutile crystals, and polysynthetic twinning.
A-11	Marquise	2.19	Greyish-blue	Numerous colourless, transparent doubly terminated zircon crystals (some with pinpoint inclusions), and a colour zoning.
A-12	Oval-shape	6.89	Greyish-blue	Dark red, opaque doubly terminated rutile crystals, polysynthetic twinning, strong hexagonal growth and colour zoning, and a light yellow colour zone (iron oxide?).
A-13	Oval-shape	3.42	Greenish-blue	Numerous colourless, transparent doubly terminated zircon crystals, polysynthetic twinning, and hexagonal growth zoning.
A-14	Oval-shape	3.55	Light greenish-blue	Numerous colourless, transparent doubly terminated zircon crystals (some with a halo and tension fissures), polysynthetic twinning, healing fractures, and a yellow colour zone (iron oxide?).
A-15	Oval-shape	2.01	Light blue	Weak polysynthetic twinning, and faint hexagonal zoning.
A-16	Oval-shape	1.91	Lilac	A large red, transparent doubly terminated rutile crystal.
A-17	Oval-shape	1.65	Slightly greenish pale blue	Some very small colourless, transparent doubly terminated zircon crystals, polysynthetic twinning, threads of boehmite, and “fingerprints”.
A-18	Cabochon	3.22	Intense blue	Polysynthetic twinning, boehmite needles, and “fingerprints”.
A-19	Cabochon	2.93	Intense blue	Two dark opaque doubly terminated rutile crystals, polysynthetic twinning, boehmite needles, and hexagonal zoning.
A-20	Cabochon	2.46	Intense blue	Some dark red, semi-transparent arrow-shaped rutile crystals, polysynthetic twinning, and boehmite needles.
HH-01	Oval-shape	4.81	Greyish-blue	Hexagonal growth and colour zoning, polysynthetic twinning, scaffold of boehmite needles, V-shaped polycrystalline boehmite, numerous internal stress fractures, clusters of very small colourless and transparent doubly terminated zircon crystals, sometimes seen with a rutile crystal, or as a solitary zircon crystal (some showing stress fractures), and few “fingerprints”.
A-31	Cabochon	0.71	Bluish-grey	Numerous and large opaque rutile crystals, scaffolds of boehmite needles, colourless and transparent doubly terminated zircons (some showing stress fractures), while others shorter also colourless, were found rounded.

Source	VARIETY Cut or shape	Weight (carat)	Colour	Characteristics
	HEAT-TREATED SAPPHIRE			
TT-01	Oval-shape	2.14	Dark blue	Numerous zircons (some very small, colourless, contain pinpoint inclusions), numerous discoid-like "fingerprints" and rutile crystals both surrounded by a blue halo. Also observed, a yellow colour zone (iron oxide).
	MULTICOLOURED SAPPHIRES			
A-21	Oval-shape	2.36	Pink, blue, violet	Polysynthetic twinning, clouds of exsolution of presumably rutile needles (?), and faint hexagonal zoning.
A-22	Oval-shape	2.80	Grey, blue, pink, orange	Some colourless, transparent doubly terminated zircon crystals, polysynthetic twinning, and faint hexagonal zoning.
A-23	Brilliant-cut	1.83	Grey-blue, pink	Some colourless, transparent doubly terminated zircon crystals, weak polysynthetic twinning, numerous boehmite needles, hexagonal core (most probably corundum), and faint hexagonal growth zoning.
A-24	Oval-shape	1.15	Lavender, grey, pink	Numerous colourless, transparent doubly terminated zircon crystals, some boehmite needles, weak hexagonal zoning, but distinct growth and colour zoning, and a very small "fingerprint".
A-25	Oval-shape	2.58	Violet-blue, pink faint orange, pale yellow	Colourless, transparent doubly terminated zircon crystals (one containing a pinpoint, others surrounded by a halo and tension fissures), polysynthetic twinning, threads of boehmite, exsolution of presumably rutile needles (unidentified), "fingerprints", a healed fracture with a yellow colour zone (iron oxide?), and hexagonal growth zoning.
A-26	Oval-shape	2.58	Pale blue, grey, pink	Colourless, transparent doubly terminated zircon crystals, polysynthetic twinning, threads of boehmite, "fingerprints", a yellow colour zone (iron oxide?), and healed fractures.
A-27	Oval-shape	2.96	Grey-blue, pale blue, pink	No data available.
A-28	Oval-shape	1.53	Violet-blue, violet-pink, yellow	Polysynthetic twinning, threads of boehmite, strong hexagonal and straight growth and colour zoning, and a yellow colour zone (iron oxide?).
A-29	Brilliant-cut	1.90	Intense pink, lavender, light blue	Dark opaque doubly terminated rutile crystals, a very large hexagonal core (most probably corundum), polysynthetic twinning, hexagonal growth zoning, "fingerprints", and a yellow colour zone (iron oxide?).
A-30	Oval-shape	3.32	Red, yellow, blue, orange, purple	Numerous colourless, transparent doubly terminated zircon crystals, polysynthetic twinning, boehmite needles, dentritic-like "fingerprints", and a yellow colour zone (iron oxide?),
HH-02	Oval-shape	0.96	Parti-coloration: Blue; pink	Hexagonal growth zoning, three dark opaque rutile crystals, two of triangular section, one of prismatic habit exhibiting interpenetrant twin, and numerous colourless doubly terminated zircon crystals (many showing pinpoint inclusions, identified in a specimen as rutile), few larger, surrounded by a halo and tension fissures.
A-32	Cabochon	1.66	Blue, yellow, pink	Numerous colourless and transparent doubly terminated zircon crystals (some with pinpoint inclusions of zircon, few showing stress fissures) with epitaxial orientation following the strong hexagonal zonings initiated by a yellow colour centre. Polysynthetic twinning, boehmite needles, "fingerprints" filled with two-phase inclusions, and healed fractures.
A-34	Oval-shape	0.30	Dark blue, green, orangy-pink	Very short rutile needles forming a silk and strong polysynthetic twinning.
	COLOUR-CHANGE SAPPHIRE			
A-33	Oval-shape	0.65	From blue to purple	Strong straight colour zoning, "fingerprints" filled with two-phase inclusions, and a few colourless doubly terminated zircon crystals.
	HEAT-TREATED COLOUR-CHANGE SAPPHIRES			
TT-02	Oval-shape	0.96	From blue to purple	Numerous blotty-like rutile crystals surrounded by a halo (blue in daylight or purplish red in incandescent light) containing pinpoint inclusions of zircon, few "fingerprints" (one without negative crystals shows a glassy appearance), and polysynthetic twinning.
TT-03	Oval-shape	0.95	From blue to purplish red	Hexagonal growth zoning, polysynthetic twinning, numerous rutile crystals, small to large dark reddish brown often doubly terminated zircon crystals (sometimes showing stress fissures), doubly terminated colourless transparent zircon crystals, and a zone of very short doted needles of presumably rutile.

Key to source: (A) San Pablo (Nariño). (HH) Collection H. Hänni. (GT) Alto La Cañada (Cauca). (TT) Heated by T. Themelis

PARTICLE INDUCED X-RAY EMISSION (PIXE)

PIXE is basically a technique for quantitative elemental analysis which uses nuclear particles (usually protons or alpha particles at a few MeV) from an accelerator to knock off K- or L-shell electrons from atoms in the target, causing them to emit X-rays at energies which are characteristic of the atoms present in the target. By measuring this X-ray spectrum concentrations in ppm level can easily be measured for many elements (Johansson, *et al.,* 1988; Tang, 1992).
The measurements were made with the use of 1.8 MeV protons produced from a 2,5 mV Van de Graaff accelerator at the National University of Singapore.
Six corundums selected for their diversity of colours and inclusions were studied:

- Ref. A-04 Pear-shape ruby 1.42 carat
- Ref. A-05 Cabochon ruby 1.66 carat

- Ref. A-09 Cabochon sapphire 3.24 carats
- Ref. A-17 Oval-shape sapphire 1.65 carat

- Ref. A-24 Oval-shape multicoloured sapphire 1.15 carat
- Ref. A-28 Oval-shape multicoloured sapphire 1.53 carat

Qualitative characteristics for the rubies (Table 6)

From seven to ten trace elements were observed in varying concentrations in the two samples studied (Ref. A-04 & Ref. A05).
The more prominent trace elements for the rubies were found to be: Silicon* (Si), chromium (Cr), and iron (Fe).
Those present in less abundance were: Calcium (Ca), titanium (Ti), vanadium (V), and gallium (Ga).
The ones encountered sometimes were: Phosphorus (P), cobalt (Co), and zirconium (Zr).

Quantitative analysis for the rubies

Vanadium and iron (as well as other trace elements), can be useful indicators for origin attribution to corundum which can be classified into two different groups:

- Those which were carried as xenocrysts in alkali basalts (although they did not crystallise from the magma itself), are named "basaltic", and show a high iron concentration.
- Those, which were not transported by basalts, are referred to as "non basaltic", and show weak iron concentrations.

Thai rubies have high contents of iron and very low concentrations of vanadium, while Myanmar rubies on the reverse contain significant amounts of vanadium, but their iron contents, generally show four times lower than those present in Thai rubies (Tang *et al.*, 1991a).
Table 6 gives the concentrations expressed in weight % in respect to Al_2O_3, and figure 77, the X-ray spectra.
One of the rubies with low concentrations of vanadium, but high concentrations of chromium and iron, seems to correspond to a Thai ruby (figure 77. Ref. A-04 pear-shape ruby of 1.42

carat, while the other, with a higher content of vanadium, and low iron, seems to correspond to a Myanmar type ruby (figure 77. Ref. A-05 cabochon ruby of 1.66 carat).
It is of interest to note that this seems to follow the inclusions observed for these two rubies, which were said to be similar to a Thai ruby for the pear-shape of 1.42 carat, and to a Myanmar ruby for the cabochon of 1.66 carat.
The main difference for these two rubies (in comparison to the origin to which they seem to correspond: Thailand for A-04 ruby, and Myanmar for A-05 ruby), lies in the fact that:

- Ref. A-04 pear-shaped 1.42 carat ruby shows a rather high concentration of Ga (detected at levels > 0.01 wt.%) and Zr (not seen in Thai rubies), to be from Thailand.
- Ref. A-05 cabochon 1.66 carat ruby shows a too high concentration of Ga (detected at levels > 0.06 wt.%) to be from Myanmar (Tang *et al.*, 1991a; Tang *et al.,* 1991b).

In order to understand more clearly the difference observed both in the inclusions, and trace elements content of the two rubies, Table 7 gives the major world occurrences of rubies and their type of origin (non basaltic or basaltic).
It appears here, that according to the concentrations of the trace elements recovered, that the rubies from Colombia could be from two different origins:

- Ref. A-04 Pear-shaped ruby of 1.42 carat, is of Basaltic origin.
- Ref. A-05 Cabochon ruby of 1.66 carat shows Non basaltic type.

This fact is in line with the geology of the area (mentioned earlier), and seems to confirm that the rubies of basaltic and metamorphic origin coexist.

---

* *The silicon concentrations observed, are most probably due either to an experimental artefact, or confused with the foot of the aluminium peak.*

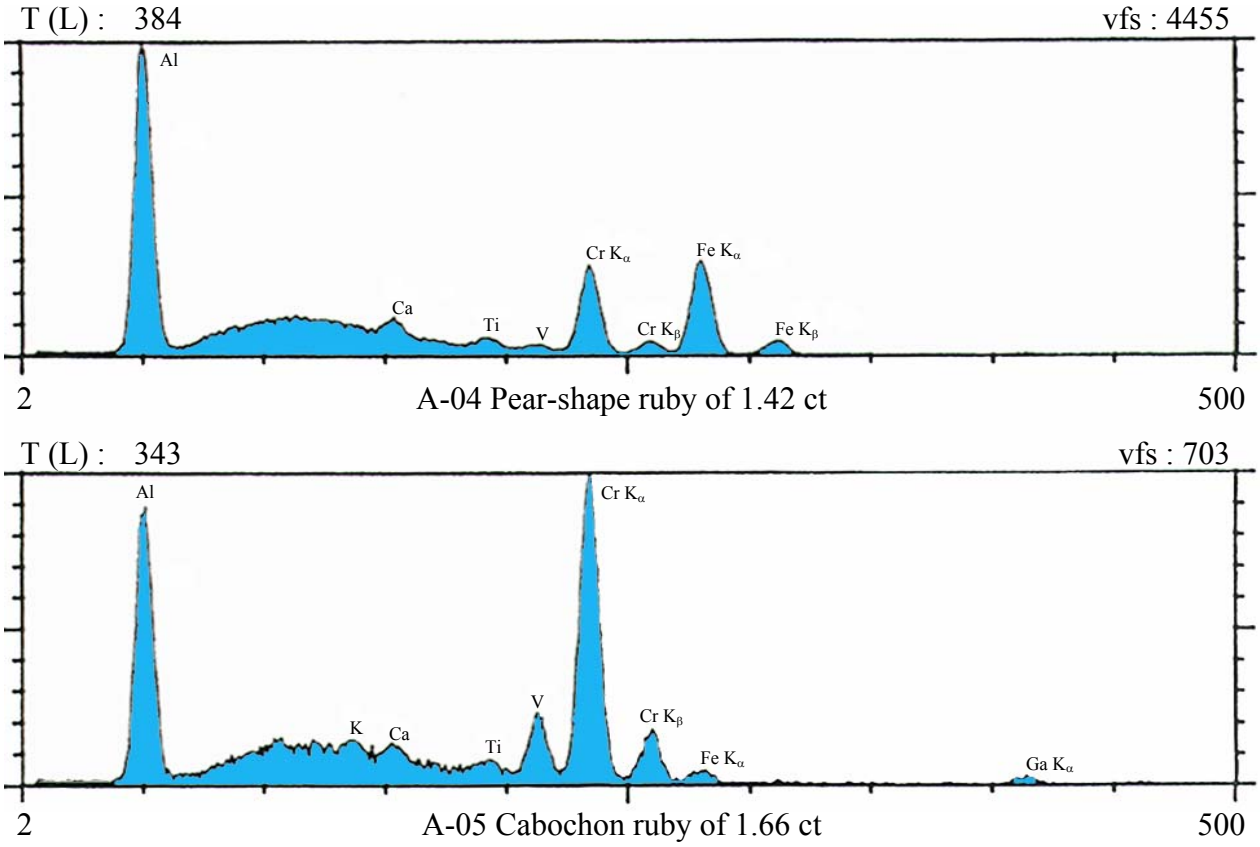

Figure 77. X-ray energy spectra for the two rubies.

Qualitative characteristics for the sapphires (Table 6)

From ten to eleven trace elements were observed in varying concentrations in each of the four samples studied (Ref. A-09, Ref. A-17, Ref. A-24 & Ref. A-28).
The most abundant trace elements present were found to be: Iron (Fe) and silicon (Si).
Those present in less abundance were: Calcium (Ca), titanium (Ti), zirconium (Zr), chromium (Cr), sulfur (S), gallium (Ga), vanadium (V), cobalt (Co), phosphorus (P), copper (Cu), and scandium (Sc).
For the less abundant trace elements, except for chromium (Cr), vanadium (V), and gallium (Ga), the other elements observed sporadically (i.e., zirconium, calcium, sulfur, and phosphorus), could be due to rays emitted by inclusions very near the surface or breaking the surface of the zone examined? Or maybe correspond to trace elements present in the corundum itself?
For the elements observed only very occasionally, and at levels < 0.002 wt.% (i.e., copper, cobalt, and scandium), these could be due to rays emitted from polishing residues trapped in open fissures of the polished gem? Or maybe due to experimental artefacts?

Quantitative analysis for the sapphires

Table 6 gives the concentrations expressed in weight % in respect to Al_2O_3, and figure 78, the X-ray spectra.
The two sapphires (Ref. A-09 and A-17), and the two multicoloured sapphires (A-24 and A-28), show a high concentration of iron and silicon.
The high iron content (detected at levels from > 0.26 to > 0.52 wt.% for the two sapphires, and at levels from > 0.29 to > 0.33 wt.% for the two multicoloured sapphires), points towards a basaltic origin for these four sapphires.
In order to help in the differentiation of these Colombian sapphires from those of other sources, with which they could be confused, table 8 gives the major world occurrences of sapphires and their different geologic origin (non basaltic or basaltic).

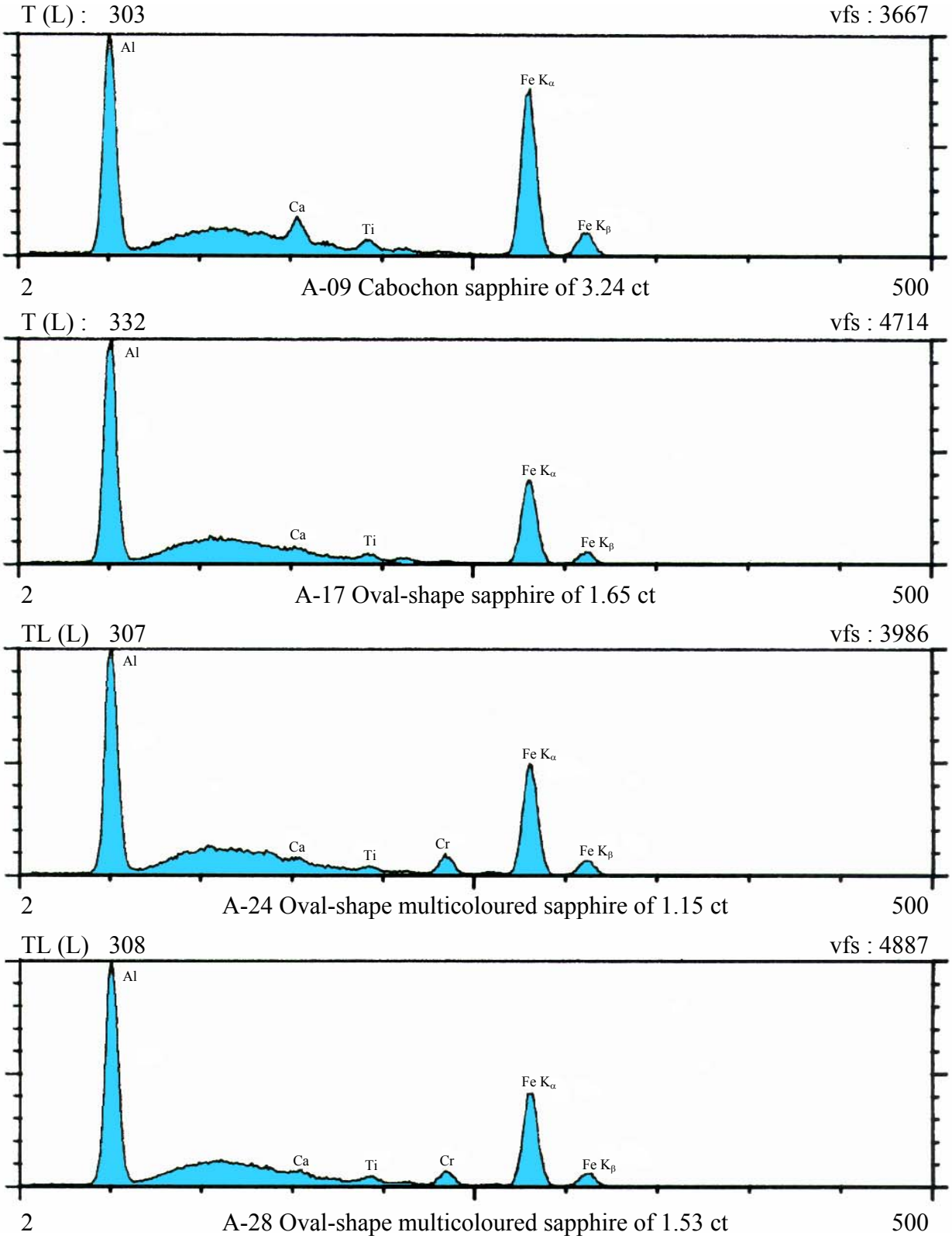

Figure 78. X-ray energy spectra for the four sapphires.

REMPLACER CETTE PAGE PAR LA PAGE

TABLE 7 Major world occurrences of rubies and their type of origin

Non basaltic origin	Basaltic origin*
AFRICA	**AMERICA**
Kenya (East Africa). Ref. 1 (Amboseli & Mangari districts). *Metasomatic*	Colombia (South America, N-W). Ref.15 (Mercaderes district).
Malawi (East Africa). Ref. 2 (Lake Nyasa district). *Metasomatic*	**ASIA**
Tanzania. Ref. 3 (Lake Manyara district; Longido district; Ngorongoro district & Umba Valley district). *Metasomatic*	Kampuchea (formerly Cambodia). Ref. 16 (Pailin district). Thailand (South-eastern). Ref. 17 (Chanthaburi-Trat Provinces: Nong Bon-Khong Phaya-Bo Rai & Welu Klang-Bo Nbawong districts). Vietnam (Southern). Ref. 18 (Di Linh District ; Phan Thiet District ; Gia Kjiem District).
AMERICA	**AUSTRALIA**
North Carolina(North America, USA). Ref. 4 (Macon, Jackson, Clay, Yancey & Alexander Counties *Metasomatic*	Eastern seaboard. Ref. 19 (Barrington).
ASIA	
Afghanistan. Ref. 5 (Sorobi district, Jegdalek district). *Marble-hosted* China. Ref. 6 (Yunnan Province, Ailao Mountains). *Marble-hosted* India. Ref. 7 (Channa-Patna, and Orissa districts). *Metasomatic* Myanmar (formerly Burma). (Mogok district. Ref. 8 & Mong Hsu). Ref. 9 *Marble-hosted* Nepal. Ref. 10 (Taplejung district, Dhankuta zone of eastern Nepal). *Marble-hosted* Pakistan. (Hunza Valley district, Ref. 11 & Kashmir, Ref. 12). *Marble-hosted* Sri Lanka. Ref. 13 (Sabaragamuwa Province; Ratnapura district). *Metasomatic* Vietnam (Northern). Ref. 14 Luc Yen district; Xuan Le district: Bu Xang district; Bien Ho district). *Marble-hosted*	

* The sapphires and rubies were transported to the surface by the alkali basalts, sometimes with other stones like zircons, or olivines (peridots, in volcanic bombs), supposingly from broken fragments of the Earth's upper mantle from approximately 15 km depth and at a temperature around 1100°C.

REFERENCES for rubies

1. **Key R.M. & Ochieng J.O**. (1991). *The growth of rubies in south-east Kenya.* Journal of Gemmology, Vol. 22, N°8, pp. 484-496.

2. **Henn U., Bank H., and Bank F.H.** (1990). *Red and orange corundum (ruby and padparadscha) from Malawi.* Journal of Gemmology, Vol. 22, N°2, pp. 83-89.

3. **Hänni H.A.** (1987). *On corundums from Umba Valley, Tanzania.* Journal of Gemmology, Vol. 20, N°5, pp. 278-284.

4. **Hughes R.W.** (1977). *Ruby and sapphire.* RWH Publishing Boulder, Colorado USA. Pp. 454, 472-473.

5. **Bowersox G.W.** (1985). *A status report on gemstones from Afghanistan.* Gems & Gemology, Vol. 21, No 4, pp. 192-204.

6. **Hughes R.W.** (1997). *Ruby and sapphire.* RWH Publishing Boulder, Colorado USA. P. 352.

7. **Hughes R.W.** (1997). *Ruby and sapphire.* RWH Publishing Boulder, Colorado USA. Pp. 368-374.

8. **Keller P.C.** (1983). *The rubies of Burma: a review of the Mogok stone tract.* Gems & Gemology, Vol. 20, No 4, pp. 209-219.

9. **Peretti A., Schmetzer K., Bernhardt H-J., and Mouawad F.** (1995). *Rubies from Mong Hsu.* Gems & Gemology, Vol. 31, No 1, pp. 2-25.

10. **Smith C.P., Gübelin E.J., Basset A.M., and Manandhar M.N.** (1997). *Rubies and fancy-color sapphires from Nepal.* Gems & Gemology, Vol. 33, No 1, pp. 24-41.

11. **Gübelin E.G.** (1982). *Gemstones of Pakistan: emerald, ruby, and spinel.* Gems & Gemology, Vol. 18, No 3, pp. 123-139.

12. **Kane, R.E.,** (1998). *Kashmir: die neuen Rubine.* Extra-Lapis. Rubin, Saphir, Korund: schön, hart, selten, kostbar [Hrsg.: Christian Weisel]. – München : Weise. Pp. 40-43.

13. **Zwaan P.C.** (1982). *Sri Lanka the gem Island.* Gems & Gemology, Vol. 18, No 2, pp. 62-71.

14. **Kane R.E., McClure S.F., Kammerling R.C., Khoa N.D., Mora C., Repetto S., Khai N.D., and Koivula J.I.** (1991). *Rubies and fancy sapphires from Vietnam.* Gems & Gemology, Vol. 27, No 3, pp. 136-155.

15. **Keller P.C., Koivula J.I., and Jara G.** (1985). *Sapphires from the Mercaderes-Río Mayo area, Cauca, Colombia.* Gems & Gemology, Vol. 21, No 1, pp. 20-25.

16. **Jobbins E.A. & Berrangé J.P.** (1981). *The Pailin ruby and sapphire gemfield, Cambodia.* Journal of Gemmology, Vol. 17, N°8, pp. 555-567.

17. **Keller P.C.** (1982). *The Chanthaburi-Trat gem field, Thailand.* Gems & Gemology, Vol. 8, No 4, pp. 186-196.

18. **Kane R.E., McClure S.F., Kammerling R.C., Khoa N.D., Mora C., Repetto S., Khai N.D., and Koivula J.I.** (1991). *Rubies and Fancy Sapphires From Vietnam.* Gems & Gemology, Vol. 27, No 3, pp 136-155.

19. **Sutherland F.L., Schwarz D., Jobbins E.A., Coenraads R.R., and Webb G.** (1988). *Distinctive gem corundum suites from discrete basalt fields: a comparative study of Barrington, Australia, and West Pailin, Cambodia, gemfields*. Journal of Gemmology, Vol. 26, No 2, pp. 65-85.

TABLE 8 Major world occurrences of sapphires and their type of origin

Non basaltic origin	Basaltic origin*
AFRICA	**AFRICA**
Madagascar (S.E). Ref. 20 (Toliara Province: Andranondambo area). *Metasomatic*	Burundi (East Central Africa). Ref. 30 (Near Rwanda border).
Malawi (East Africa). Ref. 21 (Lake Nyasa district). *Metamorphic*	Kenya (East Africa). Ref. 31 (Northern Rift Valley Province: Turkan district).
Tanzania (East Africa). Ref. 22 (Umba Valley district). *Metasomatic*	Madagascar (Northern) (Ambondromifehy, Antsiranana Province. Ref. 32 & 33).
AMERICA	Nigeria (West Africa, N-W). Ref. 34 (Kaduna Province: Jos plateau).
Brazil (South America). Ref. 23 (Minas Gerais district). *Metamorphic*	Rwanda (East Central Africa). Ref. 35 (Cyangugu district).
Montana (North America, USA). Ref. 24 (Missouri River & Rock Creek districts, and Yogo Gulch districts). *Metamorphic*	**AMERICA**
ASIA	Colombia (South America, N-W). Ref. 36 (Mercaderes district).
Afghanistan. Ref. 25 (Jegdalek district) *Marble-hosted*	**ASIA**
India (Kashmir). Ref. 26 (Soomjam, Paddar district). *Metamorphic*	China (North-eastern). Ref. 37 (Central Shandong Province, near Wutu, Changle County). (South West). Ref. 38 (Fujian Province: Lindi mine, Mingxi district). (Southern). Ref. 39 (Hainan Island: Penglai & Wenchang districts).
Myanmar (formerly Burma). Ref. 27 (Kyankpyatthat & Mogok district). *Metasomatic and skarn*	Kampuchea (formerly Cambodia). Ref. 40 (Chamnop, Khum Samlot, Pailin & Phnum Chnom districts).
Sri Lanka. Ref. 28 (Central Province: Elahera district & Sabaragamuwa Province: Ratnapura district). *Metasomatic and skarn*	Thailand (Western). Ref. 41 (Kanchanaburi Province: Bo Ploi district). (South-eastern). Ref. 42 (Chanthaburi-Trat Provinces: Khao Ploi Waen & Bang Kha Cha. Bo Rai, Bo Waen, Nong Bon districts).
Vietnam (Northern). Ref. 29 (Luc Yen district; Xuan Le district: Bu Xang district; Bien Ho district). *Metamorphic*	Vietnam (Southern). Ref. 43 (Binh Thuan, Lam Dong, Dong Nai, and Dac Lac provinces).
	AUSTRALIA
	Eastern seaboard. Ref. 44 (Central Queensland: Anakie district, & northern New South Wales: New England district).

* The sapphires and rubies were transported to the surface by the alkali basalts, sometimes with other stones like zircons, or olivines (peridots, in volcanic bombs), supposingly from broken fragments of the Earth's upper mantle from approximately 15 km depth and at a temperature around 1100°C.

REFERENCES for sapphires

20. **Gübelin E.J. & Peretti A.** (1997). *Sapphires from the Andranondambo mine in SE Madagascar: evidence for metasomatic skarn formation*. Journal of Gemmology, Vol. 25, N°7, pp. 453-470.

21. **Rutland E.H.** (1969). *Corundum from Malawi.* Journal of Gemmology, Vol. 11, N°8, pp. 320-323.

22. **Bridges C.R.** (1982). *Gemstones of East Africa.* International Gemological symposium. GIA, Santa Mnonica, New York, pp. 263-275.

23. **Epstein D.S., Brennan W., and Mendes J.C.** (1994). *The Indaia sapphire deposits of Minas Gerais, Brazil*. Gems & Gemology, Vol. 30, No 1, pp. 24-32.

24. **Baron A.A.** (1982). *The Yogo Sapphire.* International Gemological symposium. GIA, Santa Monica, New York. Pp. 341-347.

25. **Bowersox G.W., Foord E.E., Laurs B.M., Shigley J.E., and Smith C.P.** (2000). *Ruby and sapphire from Jegdalek, Afghanistan.* Gems & Gemology, Vol. 36, No 2, pp. 110-126.

26. **Atkinson D., and Kothavala R.Z.** (1983). *Kashmir sapphires.* Gems & Gemology, Vol. 19, No 2, pp. 64-76.

27. **Hughes W.** (1997). *Ruby & sapphire.* RWH Publishing Boulder, Colorado, USA. Pp. 300-348.

28. **Gunawardene M. & Rupasinghe M.S.** (1986). *The Elahera gem fields in Central Sri-Lanka.* Gems & Gemology, Vol. 22, No 2, pp. 80-95.

29. **Kane R.E., McClure S.F., Kammerling R.C., Khoa N.D., Mora C., Repetto S., Khai N.D., and Koivula J.I.** (1991). *Rubies and fancy sapphires from Vietnam.* Gems & Gemology, Vol. 27, No 3, pp. 136-155.

30. **Koivula J.I. & Kammerling R.C.** (1989). Gem News: *Sapphires found in Burundi*. Gems & Gemology, Vol. 25, No 4, p. 247.

31. **Barot N.R., Flamini A., Graziani G., and Gübelin E.J.** (1989*). Star sapphire from Kenya.* Journal of Gemmology, Vol. 21, N°8, pp. 467-473.

32. **Johnson M.L. & Koivula J.I.** (1997). Gem News: *Sapphires from northern Madagascar.* Gems & Gemology, Vol. 33, No 4, p. 305.

33. **Johnson M.L. & Koivula J.I.** (1998). Gem News: *Star sapphire from Madagascar.* Gems & Gemology, Vol. 34, No 2, p. 140.

34. **Kiefert L. & Schmetzer K.** (1987). *Blue and yellow sapphire from Kaduna Province, Nigeria.* Journal of Gemmology, Vol. 20, N°7/8, pp. 427-442.

35. **Krzemnicki M.S. & Hänni H.A., Guggenheim R., and Nmathys D.** (1996). *Investigations on sapphires from an alkali basalt, South West Rwanda.* Journal of Gemmology, Vol. 25, N°2, pp. 90-106.

36. **Keller P.C., Koivula J.I., and Jara G.** (1985). *Sapphire from the Mercaderes-Río Mayo area, Cauca, Colombia.* Gems & Gemology, Vol. 21, No 1, pp. 20-25.

37. **Guo J., Wang F., and Yakoumelos G.** (1992). *Sapphires from Changle in Shandong Province, China.* Gems & Gemology, Vol. 28, No 4, pp.255-260.

38. **Keller A.S. & Keller P.C.,** (1986). *The sapphires of Mingxi, Fujian Province, China.* Gems & Gemology, Vol. 22, No 1, pp. 41-45.

39. **Galibert O. & Hughes W.** (1995). *Chinese ruby and sapphire – a brief history.* Journal of Gemmology, Vol. 24, N°7, pp. 467-473.

40. **Jobbins E.A. & Berrangé J.P.** (1981). *The Pailin ruby and sapphire gemfield, Cambodia.* Journal of Gemmology, Vol. 17, N°8, pp. 555-567.

41. **Gunawardene M. & Chawla S.S.** (1984). *Sapphires from Kanchanaburi Province, Thailand.* Journal of Gemmology, Vol. 19, N°3, pp. 228-239.

42. **Keller P.C.** (1982). *The Chanthaburi-Trat gem field, Thailand.* Gems & Gemology, Vol. 18, No 4, pp. 186-196.

43. **Smith C.P., Kammerling R.C., Keller A.S., Peretti A., Scarratt K.V., Khoa N.D., and Repetto S.** (1995). *Sapphires from Southern Vietnam*. Gems & Gemology, Vol. 31, No 3, pp. 168-185.

44. **Coldham T.** (1985). *Sapphires from Australia.* Gems & Gemology, Vol. 21, No 3, pp. 130-146.

ENERGY DISPERSIVE X-RAY FLUORESCENCE (EDXRF)

EDXRF works as follows: A relatively low voltage is used to heat the filament wire so that it will thermally emit electrons (or X-rays). A potential is applied between the filament (cathode) and a target of a pure element (anode) which accelerates the electrons to the anode. The deceleration of the electrons interacting with orbital electrons of the anode element, give rise to the production of continuous and characteristic X-rays emitted from the anode. Because the tube is under high vacuum, X-rays must pass through a window, usually made of beryllium (Leyden, 19??).
The X-ray beam directed at a sample (without any particular orientation, simply placed in a holder above the beam), causes the individual chemical elements present in the sample to emit X-rays of a characteristic energy. The instrument's solid-state detector and multichannel analyzer sort the X-rays, making it possible to detect which elements are present. When the instrument is carefully calibrated, the intensity of a given peak can be quantified to indicate the concentration of the corresponding element (Fritsch *et al.,* 1990).
The measurements were made with the use of an X-ray tube voltage of 25 KV and a current of 200 mA, produced from a Philips PV 9500 spectrometer.

Twenty-three faceted corundums were studied, and their EDXRF results described below.

Five rubies

- Ref. A-01 Pear-shape 1.86 carat
- Ref. A-05 Cabochon 1.66 carat
- Ref. A-06 Cabochon 6.24 carats
- Ref. GT-01 Oval-shape 0.33 carat
- Ref. GT-02 Pear-shape 0.19 carat

Chemical analysis of these rubies

For four of the rubies: A-01, A-06, GT-01, and GT-02, The most significant trace element variations recorded were in the iron (Fe) concentrations, followed by chromium (Cr), which showed a concentration from three to six times less than iron, correlated directly to the depth of red to pink colour of the ruby examined. The sole other trace element recorded in little quantity was gallium (Ga).
The high iron (Fe), little gallium (Ga) without detectable vanadium (V), contained in these four rubies, associated with their mineral inclusions, proves their basalt-hosted origin (Muhlmeister *et al.,* 1998).
As for the ruby A-05, the more prominent trace elements were found to be chromium (Cr), which showed a concentration of approximately three times more than iron, followed by iron (Fe) and gallium (Ga) of roughly the same amount, and a little vanadium (V). This points towards a non-basaltic origin for this ruby, which is confirmed by its mineral inclusions, and the trace element concentrations recovered by PIXE.
The chemical spectrums obtained for each of these rubies can be viewed in the following pages.

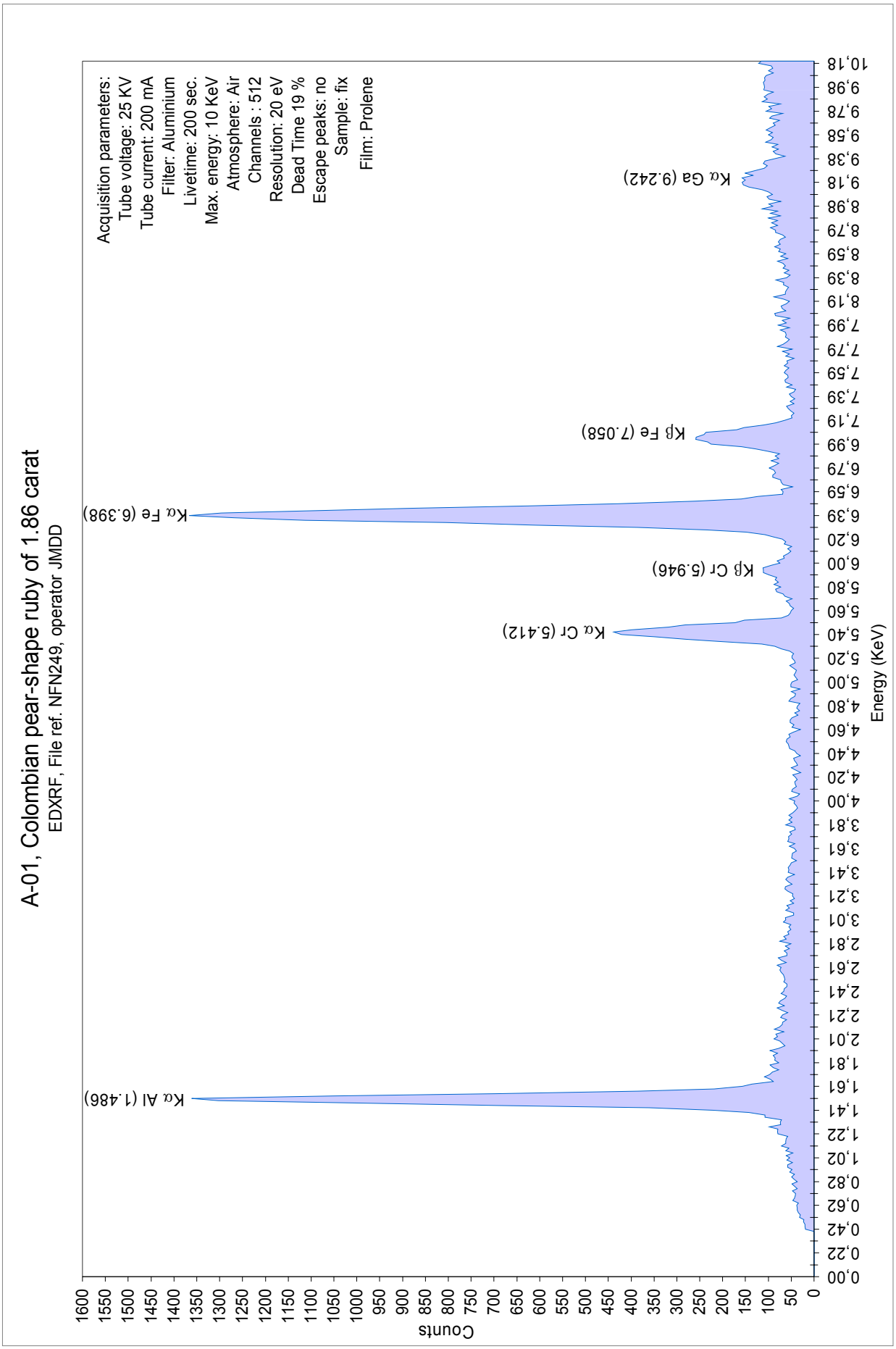
A-01, Colombian pear-shape ruby of 1.86 carat
EDXRF, File ref. NFN249, operator JMDD
Acquisition parameters:
Tube voltage: 25 KV
Tube current: 200 mA
Filter: Aluminium
Livetime: 200 sec.
Max. energy: 10 KeV
Atmosphere: Air
Channels : 512
Resolution: 20 eV
Dead Time 19 %
Escape peaks: no
Sample: fix
Film: Prolene
Kα Al (1.486)
Kα Fe (6.398)
Kβ Fe (7.058)
Kα Cr (5.412)
Kβ Cr (5.946)
Kα Ga (9.242)
Counts
Energy (KeV)

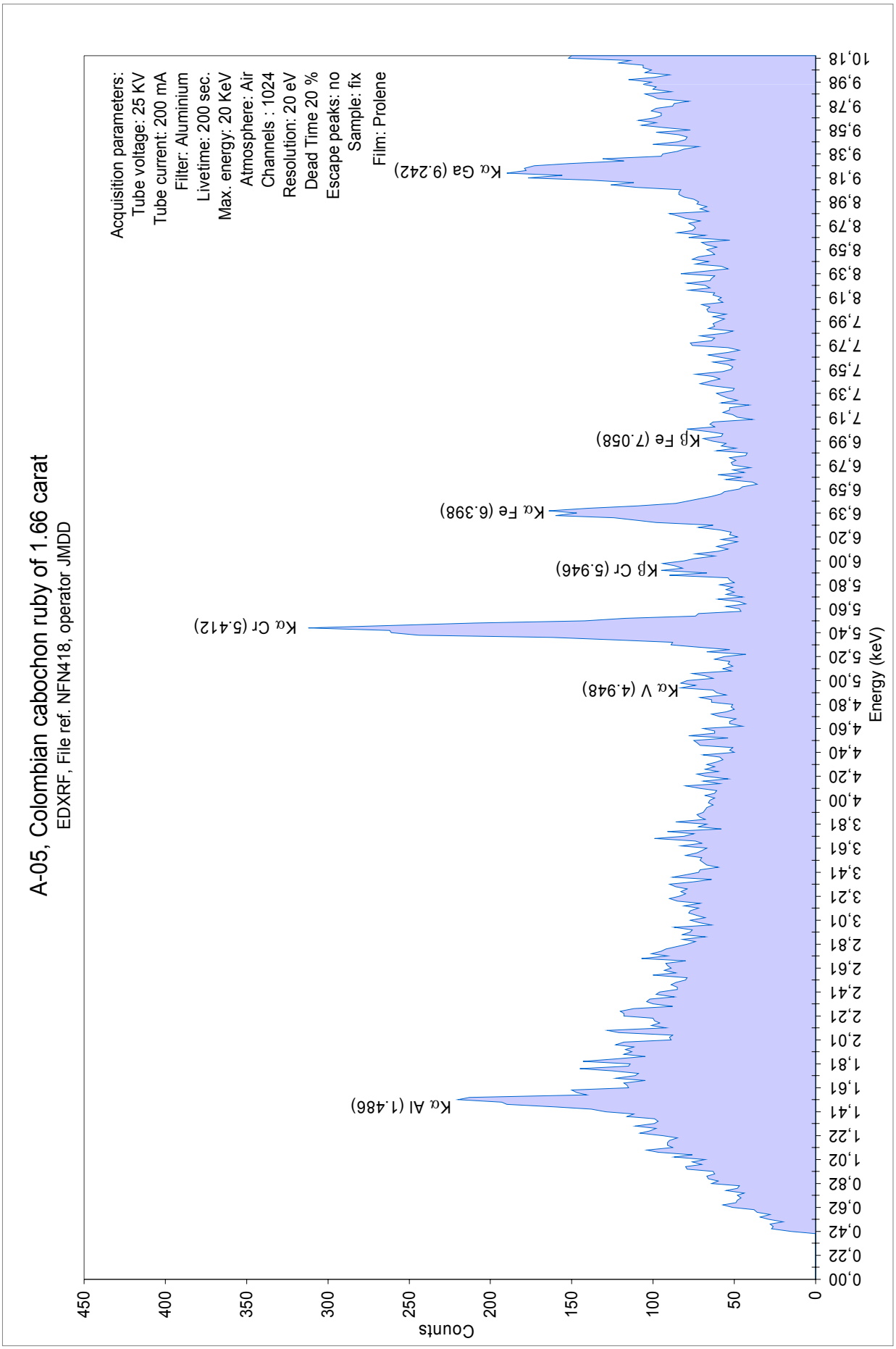
A-05, Colombian cabochon ruby of 1.66 carat
EDXRF, File ref. NFN418, operator JMDD
Acquisition parameters:
Tube voltage: 25 KV
Tube current: 200 mA
Filter: Aluminium
Livetime: 200 sec.
Max. energy: 20 KeV
Atmosphere: Air
Channels : 1024
Resolution: 20 eV
Dead Time 20 %
Escape peaks: no
Sample: fix
Film: Prolene
Kα Al (1.486)
Kα V (4.948)
Kα Cr (5.412)
Kβ Cr (5.946)
Kα Fe (6.398)
Kβ Fe (7.058)
Kα Ga (9.242)
Counts
Energy (keV)

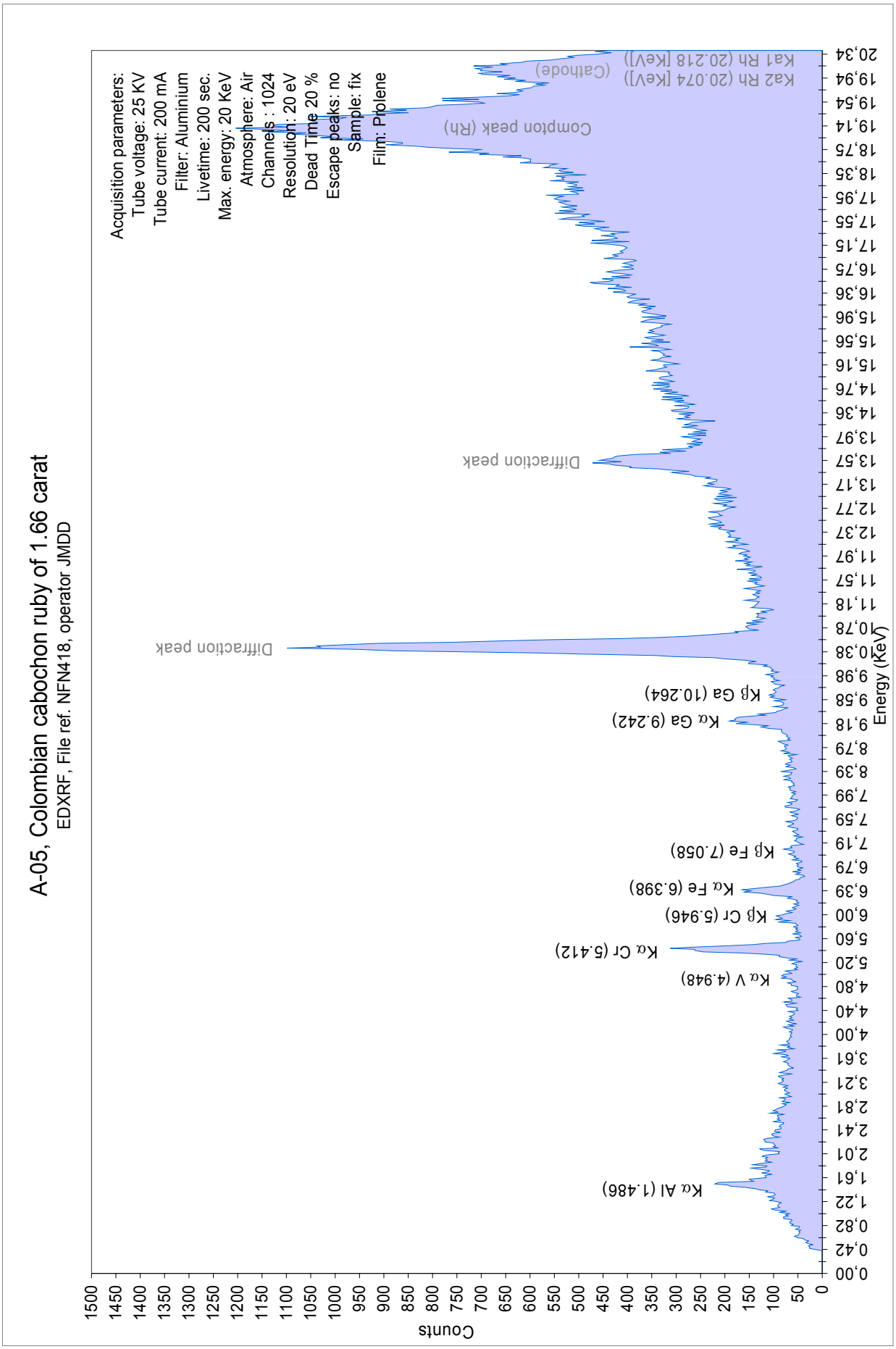
A-05, Colombian cabochon ruby of 1.66 carat
EDXRF, File ref. NFN418, operator JMDD
Acquisition parameters:
Tube voltage: 25 KV
Tube current: 200 mA
Filter: Aluminium
Livetime: 200 sec.
Max. energy: 20 KeV
Atmosphere: Air
Channels : 1024
Resolution: 20 eV
Dead Time 20 %
Escape peaks: no
Sample: fix
Film: Prolene
Kα Al (1.486)
Kα V (4.948)
Kα Cr (5.412)
Kβ Cr (5.946)
Kα Fe (6.398)
Kβ Fe (7.058)
Kα Ga (9.242)
Kβ Ga (10.264)
Diffraction peak
Diffraction peak
Compton peak (Rh)
(Cathode)
Kα2 Rh (20.074 [KeV])
Kα1 Rh (20.218 [KeV])
Counts
Energy (KeV)

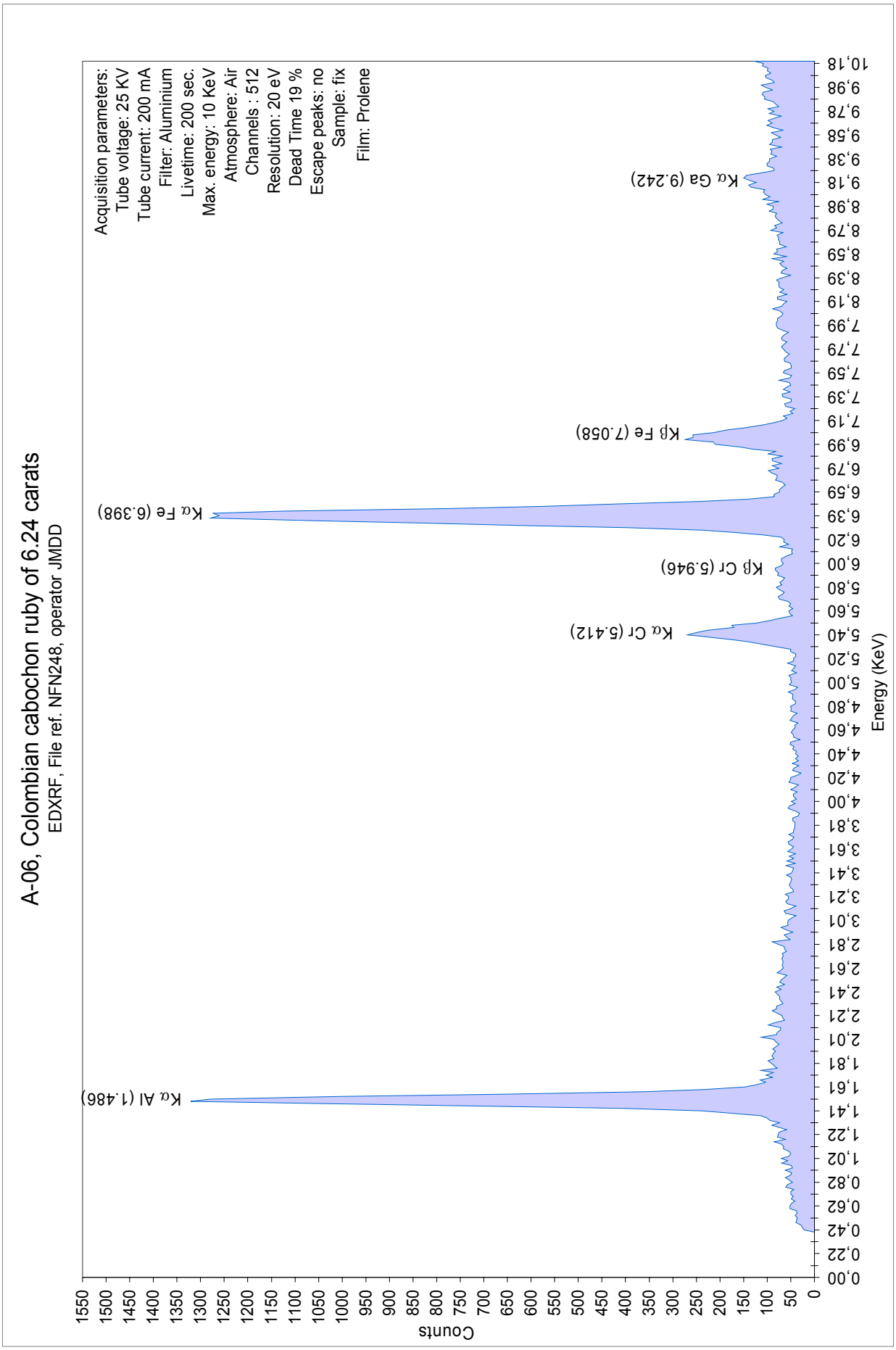
A-06, Colombian cabochon ruby of 6.24 carats
EDXRF, File ref. NFN248, operator JMDD
Acquisition parameters:
Tube voltage: 25 KV
Tube current: 200 mA
Filter: Aluminium
Livetime: 200 sec.
Max. energy: 10 KeV
Atmosphere: Air
Channels : 512
Resolution: 20 eV
Dead Time 19 %
Escape peaks: no
Sample: fix
Film: Prolene
Kα Al (1.486)
Kα Fe (6.398)
Kβ Cr (5.946)
Kα Cr (5.412)
Kβ Fe (7.058)
Kα Ga (9.242)
Counts
Energy (KeV)

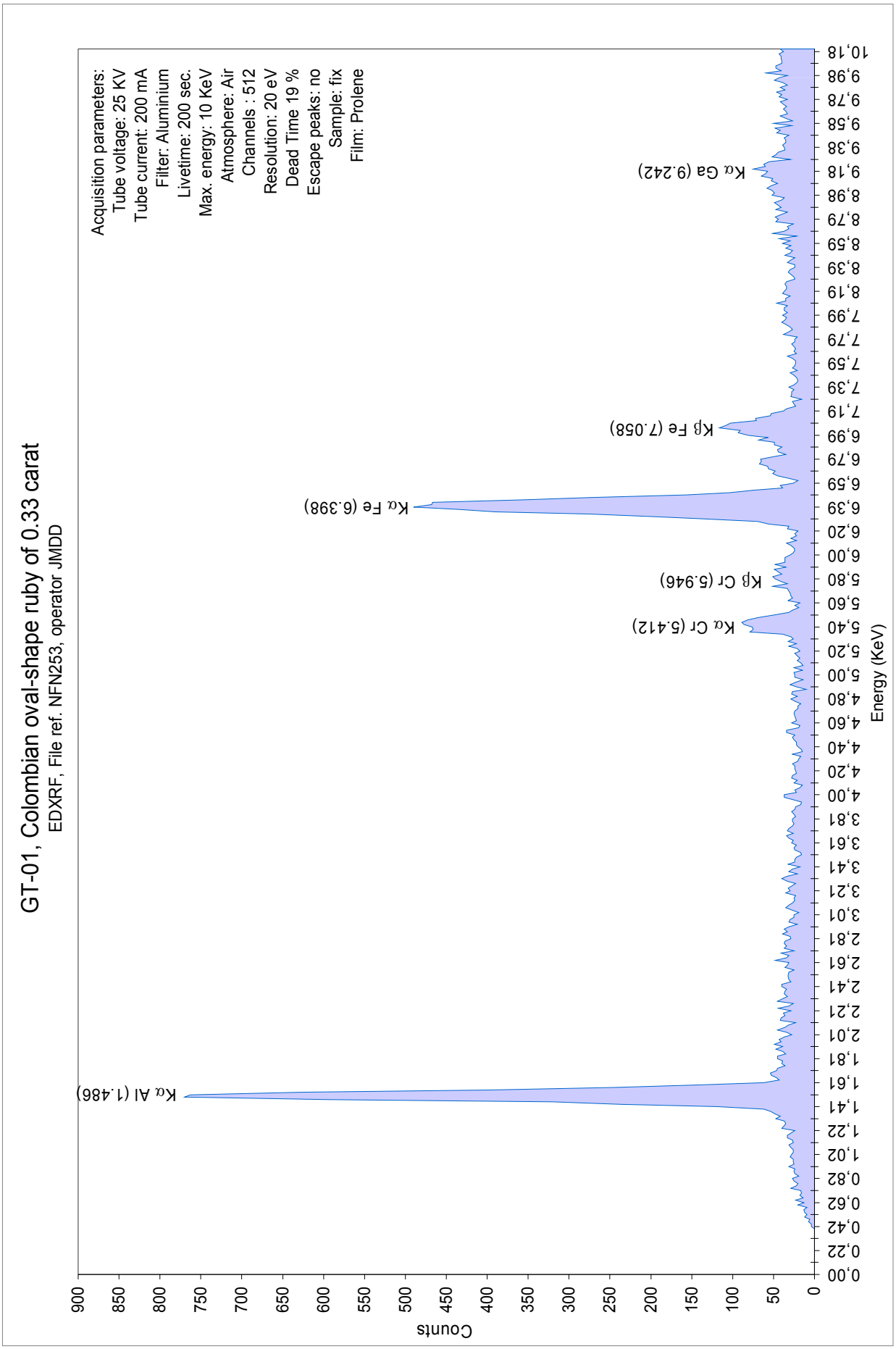
GT-01, Colombian oval-shape ruby of 0.33 carat
EDXRF, File ref. NFN253, operator JMDD
Acquisition parameters:
Tube voltage: 25 KV
Tube current: 200 mA
Filter: Aluminium
Livetime: 200 sec.
Max. energy: 10 KeV
Atmosphere: Air
Channels : 512
Resolution: 20 eV
Dead Time 19 %
Escape peaks: no
Sample: fix
Film: Prolene
Kα Al (1.486)
Kα Fe (6.398)
Kβ Fe (7.058)
Kα Ga (9.242)
Kα Cr (5.412)
Kβ Cr (5.946)
Counts
Energy (KeV)

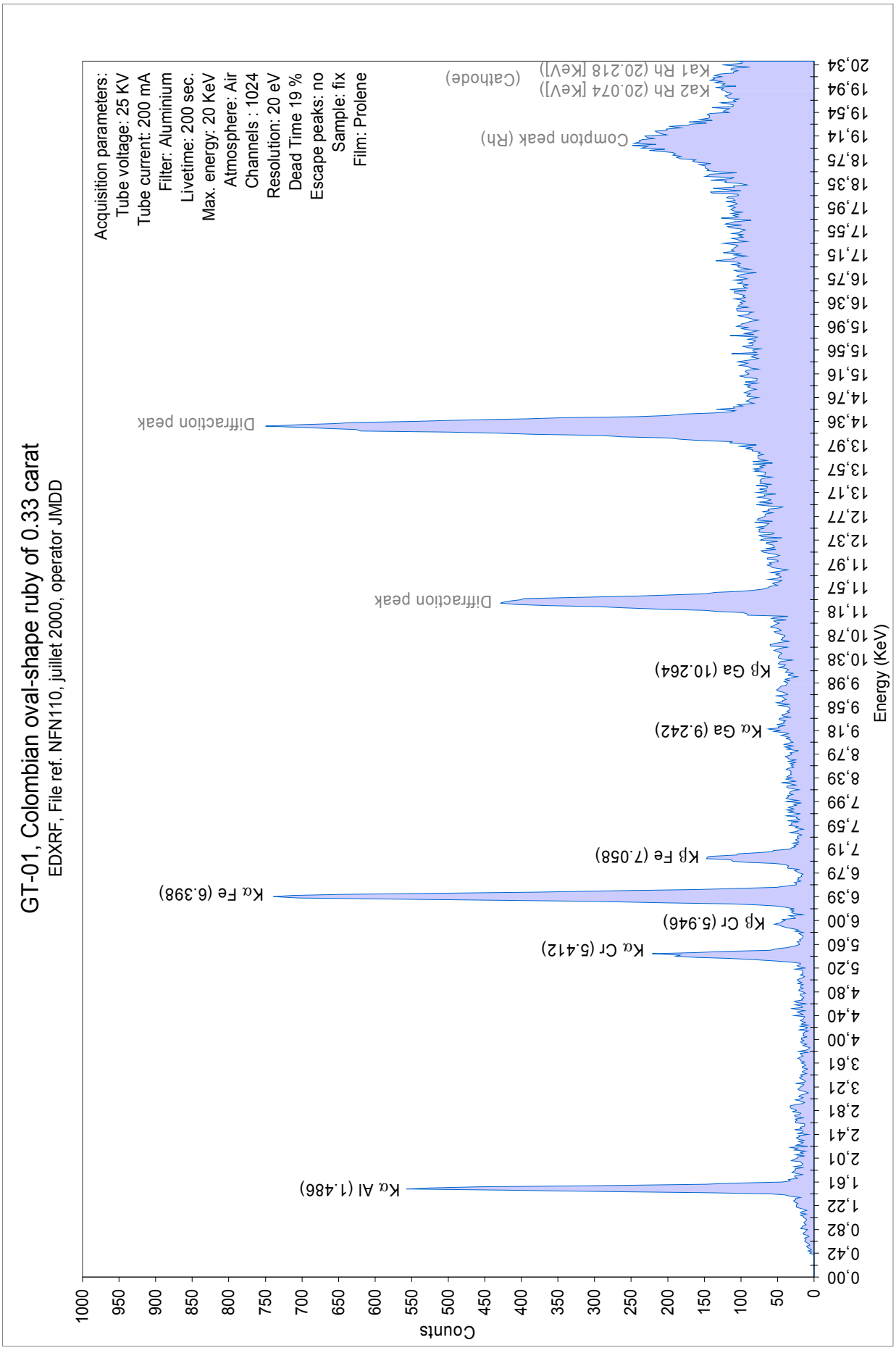
GT-01, Colombian oval-shape ruby of 0.33 carat
EDXRF, File ref. NFN110, juillet 2000, operator JMDD
Acquisition parameters:
Tube voltage: 25 KV
Tube current: 200 mA
Filter: Aluminium
Livetime: 200 sec.
Max. energy: 20 KeV
Atmosphere: Air
Channels : 1024
Resolution: 20 eV
Dead Time 19 %
Escape peaks: no
Sample: fix
Film: Prolene
Counts
Energy (KeV)
Kα Al (1.486)
Kα Cr (5.412)
Kβ Cr (5.946)
Kα Fe (6.398)
Kβ Fe (7.058)
Kα Ga (9.242)
Kβ Ga (10.264)
Diffraction peak
Diffraction peak
Compton peak (Rh)
Ka2 Rh (20.074 [KeV])
Ka1 Rh (20.218 [KeV])
(Cathode)

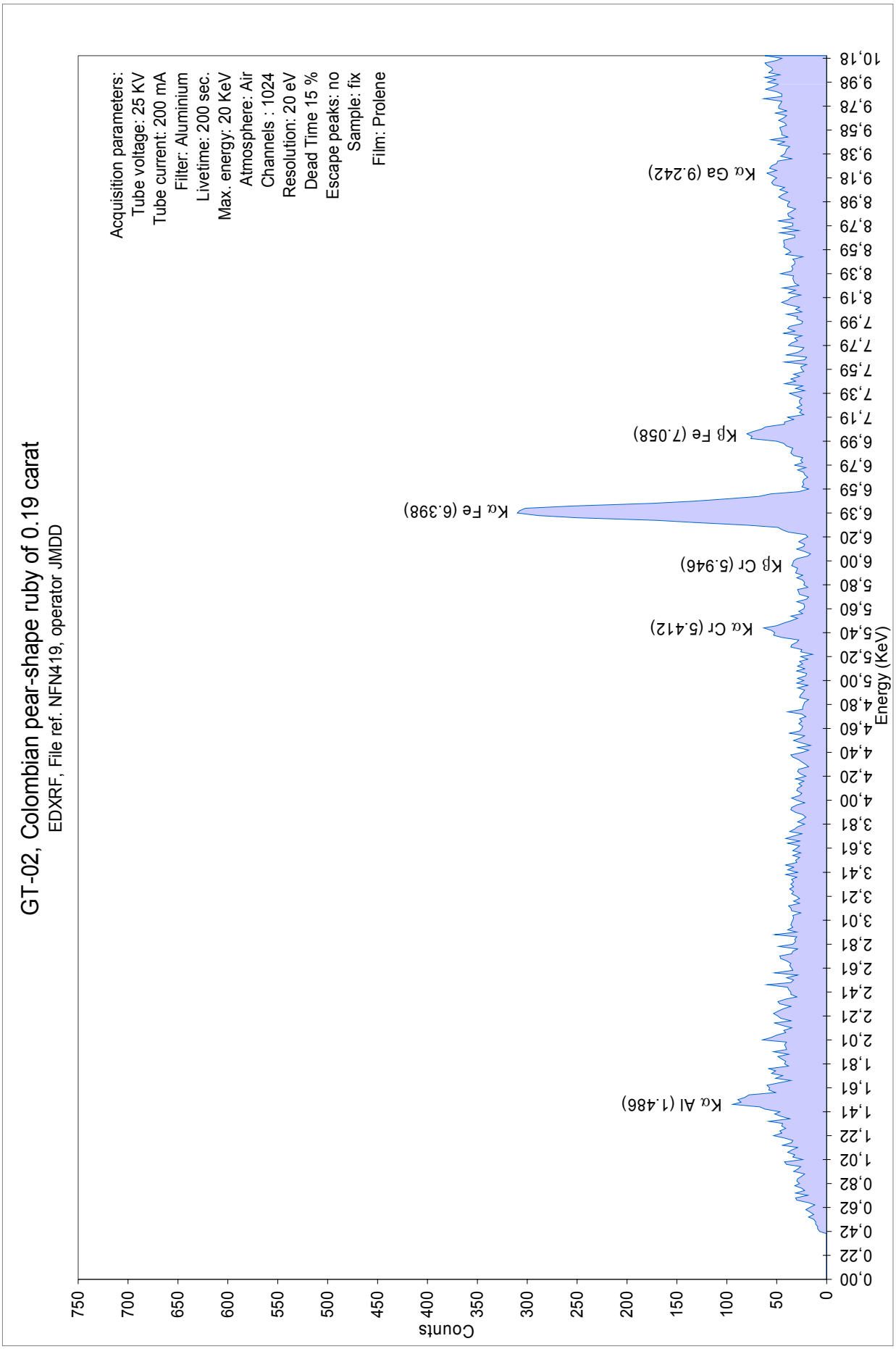
GT-02, Colombian pear-shape ruby of 0.19 carat
EDXRF, File ref. NFN419, operator JMDD
Acquisition parameters:
Tube voltage: 25 KV
Tube current: 200 mA
Filter: Aluminium
Livetime: 200 sec.
Max. energy: 20 KeV
Atmosphere: Air
Channels : 1024
Resolution: 20 eV
Dead Time 15 %
Escape peaks: no
Sample: fix
Film: Prolene
Kα Al (1.486)
Kα Cr (5.412)
Kβ Cr (5.946)
Kα Fe (6.398)
Kβ Fe (7.058)
Kα Ga (9.242)
Counts
Energy (KeV)

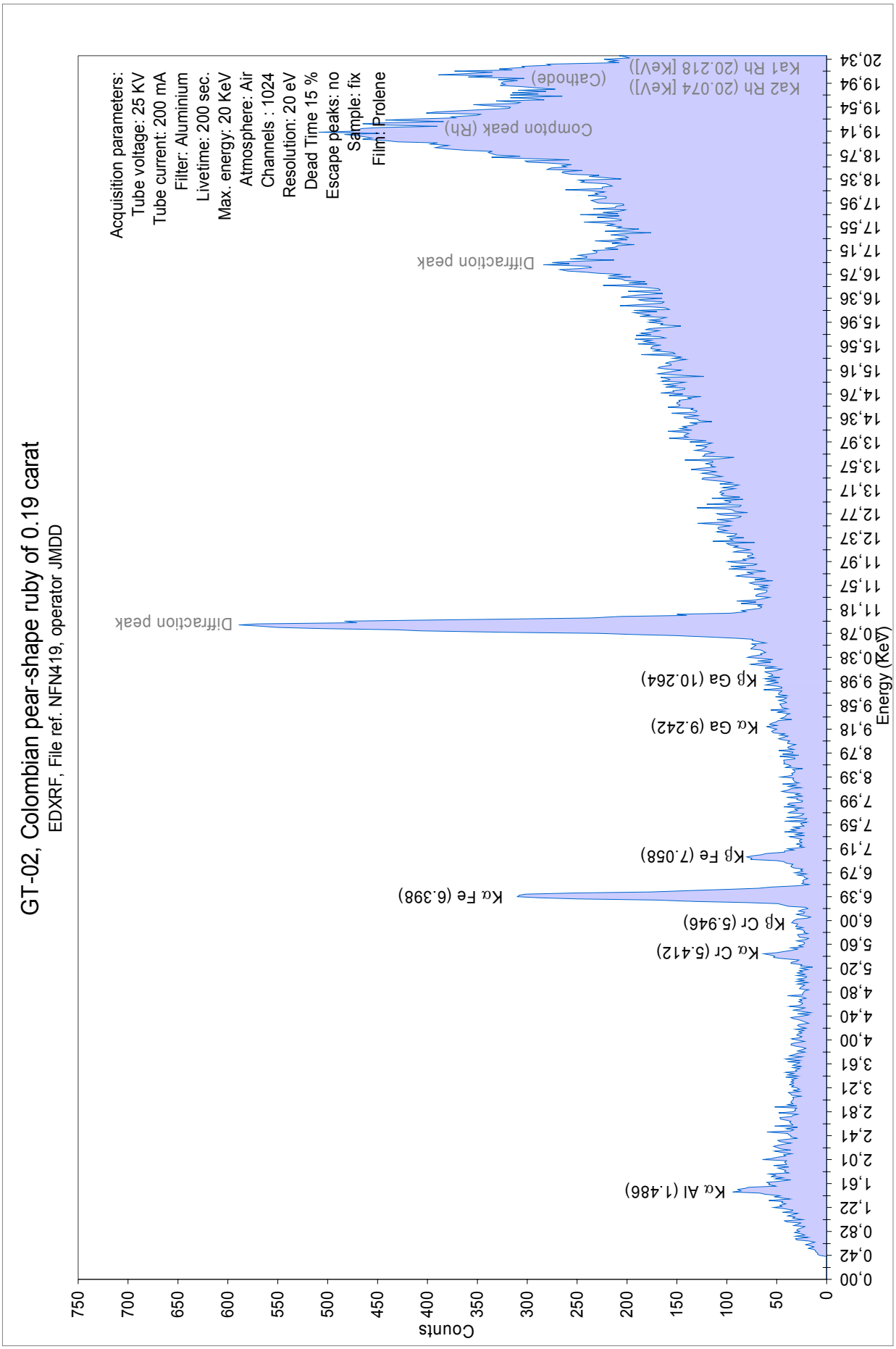
GT-02, Colombian pear-shape ruby of 0.19 carat
EDXRF, File ref. NFN419, operator JMDD
Acquisition parameters:
Tube voltage: 25 KV
Tube current: 200 mA
Filter: Aluminium
Livetime: 200 sec.
Max. energy: 20 KeV
Atmosphere: Air
Channels : 1024
Resolution: 20 eV
Dead Time 15 %
Escape peaks: no
Sample: fix
Film: Prolene
Counts
Energy (KeV)
Kα Al (1.486)
Kα Cr (5.412)
Kβ Cr (5.946)
Kα Fe (6.398)
Kβ Fe (7.058)
Kα Ga (9.242)
Kβ Ga (10.264)
Diffraction peak
Compton peak (Rh)
(Cathode)
Kα2 Rh (20.074 [keV])
Kα1 Rh (20.218 [keV])

Eight sapphires

- Ref. A-07 Cabochon 3.01 carats
- Ref. A-08 Oval-shape 2.66 carats
- Ref. A-11 Marquise 2.19 carats
- Ref. A-13 Oval-shape 3.42 carats
- Ref. A-14 Oval-shape 3.55 carats
- Ref. A-17 Oval-shape 1.65 carat
- Ref. HH-01 Oval-shape 4.81 carats
- Ref. A-31 Cabochon 0.71 carat

A heat-treated sapphire

- Ref. TT-01 Oval-shape 2.14 carats

Six multicoloured sapphires

- Ref. A-25 Oval-shape 2.58 carats
- Ref. A-28 Oval-shape 1.53 carat
- Ref. A-30 Oval-shape 3.32 carats
- Ref. HH-02 Oval-shape 0.96 carat
- Ref. A-32 Cabochon 1.66 carat
- Ref. A-34 Oval-shape 0.30 carat

A colour-change sapphire

- Ref. A-33 Oval-shape 0.65 carat

Two heat-treated colour-change sapphires

- Ref. TT-02 Oval-shape 0.96 carat
- Ref. TT-03 Oval-shape 0.95 carat

Chemical analysis of these sapphires

EDXRF analysis revealed aluminium (Al) as the sole major element, which is consistent with the chemical formula of corundum (Al_2O_3). Oxygen (O), with an atomic number of 8 (too low to be detected by this method), is assumed to be stoichiometric.
Typical of basaltic sapphires, iron (Fe) was the most significant minor element, present as an impurity.
If gallium (Ga) was always detected, titanium (Ti), was measured in six sapphires (33.33% of the above sapphires tested. Its presence is necessary to the colour-causing mechanism in blue sapphires $Fe^{2+} \rightarrow Ti^{4+}$). When in measurable amount, titanium (Ti), was found to be in either weaker concentration (for sapphires A-08, A-25, A-30, TT-02), or in superior concentration to gallium (Ga) (for sapphires A-31 and TT-01).
Other trace elements were occasionally seen in various amounts such as chromium (Cr): mainly in the multicoloured and heat-treated colour-change sapphires, or zirconium (Zr): probably due to inclusions near the surface. Copper (Cu), was measured in a two sapphires, and in negligible amount (probably due to polishing residues).
The chemical spectrums obtained for each of these sapphires can be viewed in the following pages.

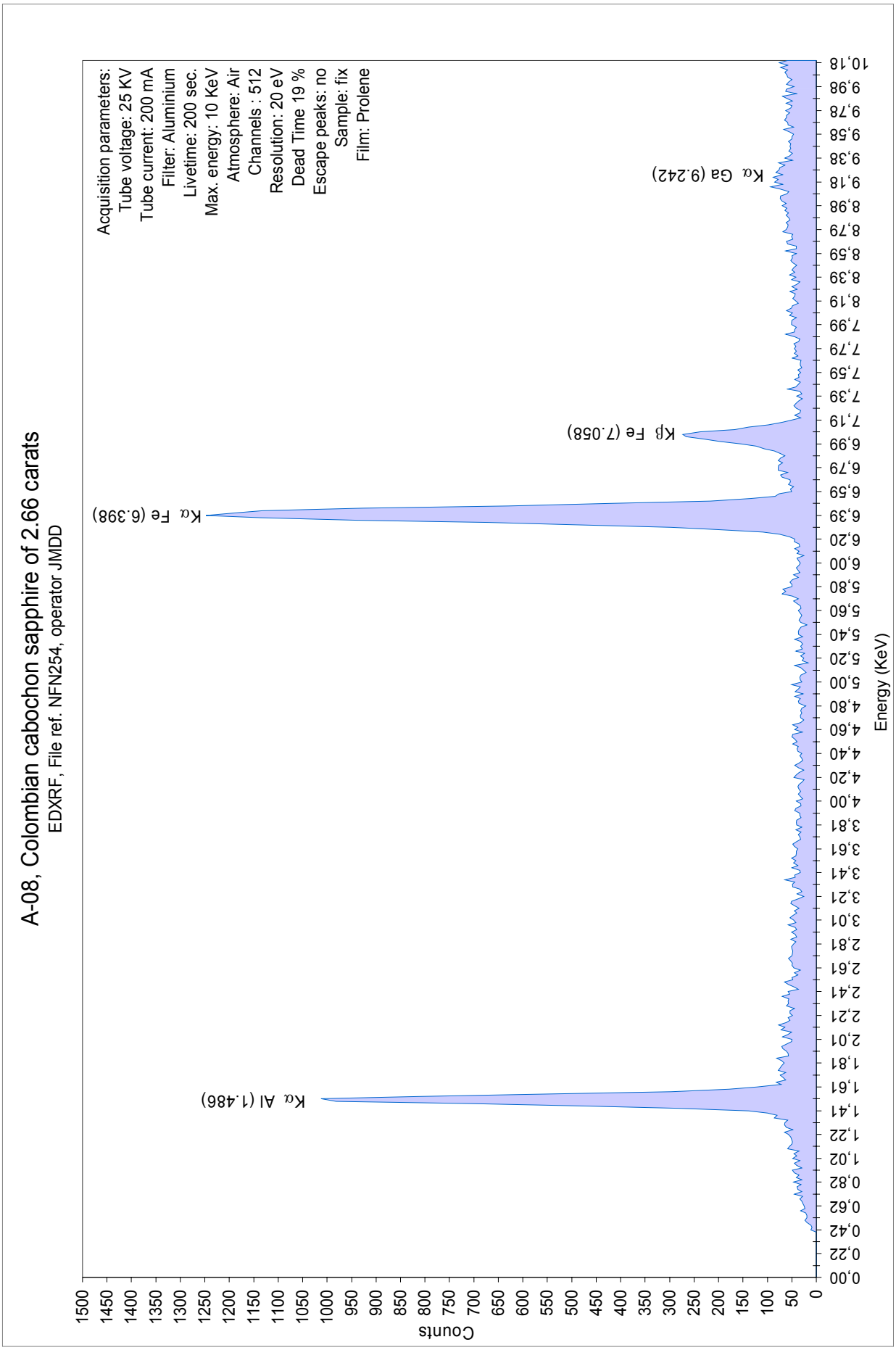
A-08, Colombian cabochon sapphire of 2.66 carats
EDXRF, File ref. NFN254, operator JMDD
Acquisition parameters:
Tube voltage: 25 KV
Tube current: 200 mA
Filter: Aluminium
Livetime: 200 sec.
Max. energy: 10 KeV
Atmosphere: Air
Channels : 512
Resolution: 20 eV
Dead Time 19 %
Escape peaks: no
Sample: fix
Film: Prolene
Kα Al (1.486)
Kα Fe (6.398)
Kβ Fe (7.058)
Kα Ga (9.242)
Counts
Energy (KeV)

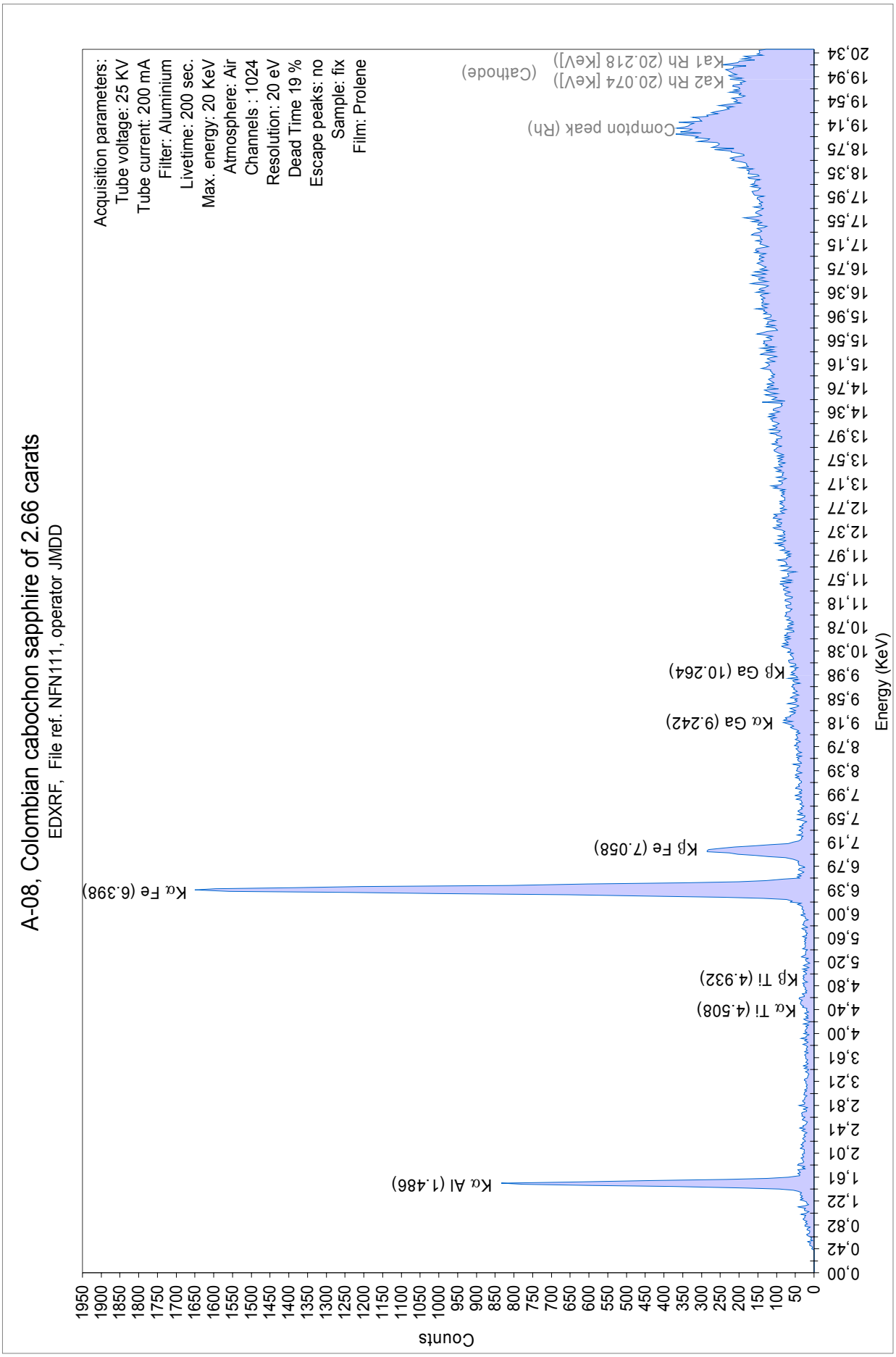
A-08, Colombian cabochon sapphire of 2.66 carats
EDXRF, File ref. NFN111, operator JMDD
Acquisition parameters:
Tube voltage: 25 KV
Tube current: 200 mA
Filter: Aluminium
Livetime: 200 sec.
Max. energy: 20 KeV
Atmosphere: Air
Channels : 1024
Resolution: 20 eV
Dead Time 19 %
Escape peaks: no
Sample: fix
Film: Prolene
Counts
Energy (KeV)
Kα Al (1.486)
Kα Ti (4.508)
Kβ Ti (4.932)
Kα Fe (6.398)
Kβ Fe (7.058)
Kα Ga (9.242)
Kβ Ga (10.264)
Compton peak (Rh)
Ka2 Rh (20.074 [KeV])
Ka1 Rh (20.218 [KeV])
(Cathode)

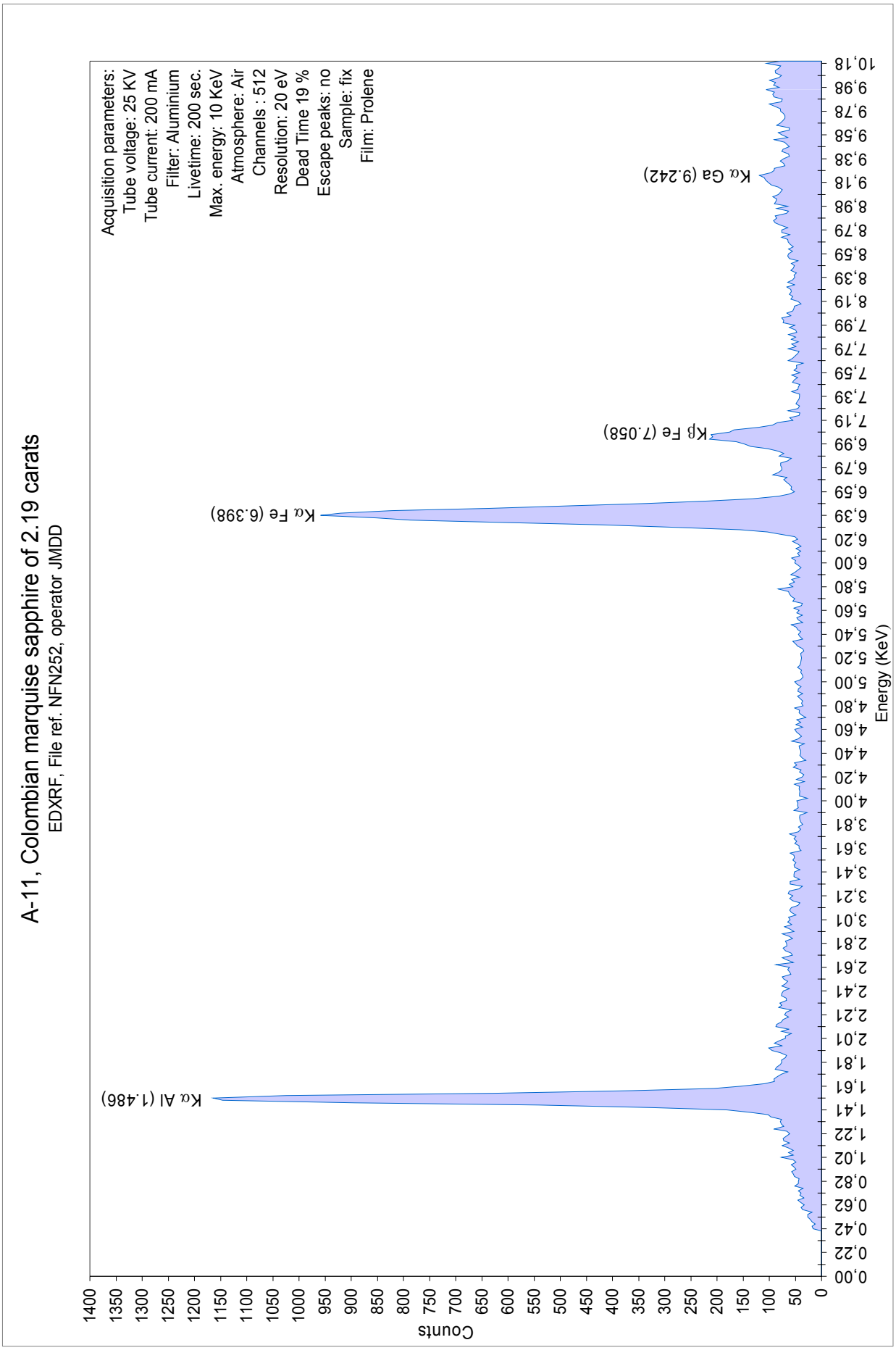
A-11, Colombian marquise sapphire of 2.19 carats
EDXRF, File ref. NFN252, operator JMDD
Acquisition parameters:
Tube voltage: 25 KV
Tube current: 200 mA
Filter: Aluminium
Livetime: 200 sec.
Max. energy: 10 KeV
Atmosphere: Air
Channels : 512
Resolution: 20 eV
Dead Time 19 %
Escape peaks: no
Sample: fix
Film: Prolene
Kα Al (1.486)
Kα Fe (6.398)
Kβ Fe (7.058)
Kα Ga (9.242)
Counts
Energy (KeV)

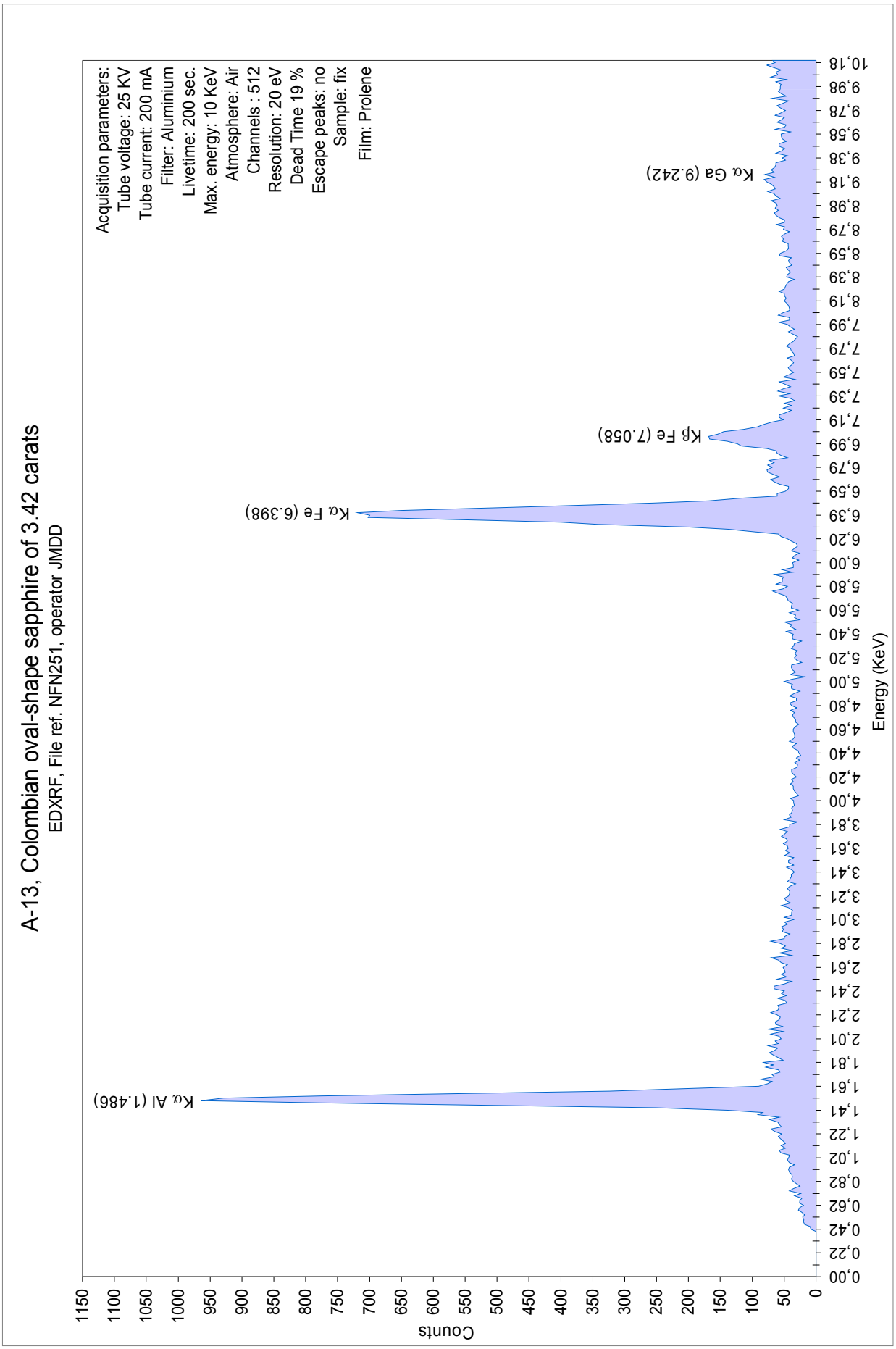
A-13, Colombian oval-shape sapphire of 3.42 carats
EDXRF, File ref. NFN251, operator JMDD
Acquisition parameters:
Tube voltage: 25 KV
Tube current: 200 mA
Filter: Aluminium
Livetime: 200 sec.
Max. energy: 10 KeV
Atmosphere: Air
Channels : 512
Resolution: 20 eV
Dead Time 19 %
Escape peaks: no
Sample: fix
Film: Prolene
Kα Al (1.486)
Kα Fe (6.398)
Kβ Fe (7.058)
Kα Ga (9.242)
Counts
Energy (KeV)

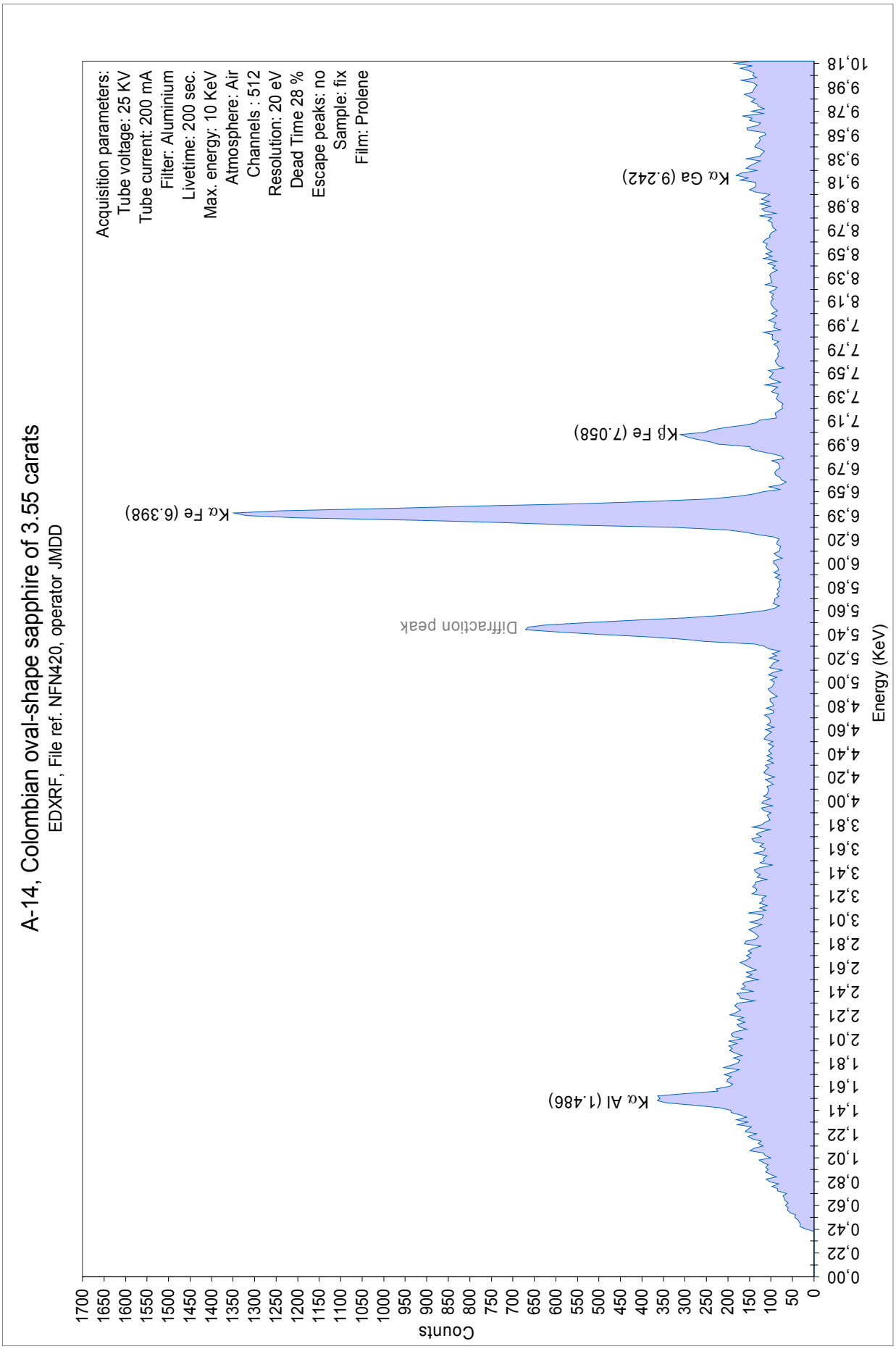
A-14, Colombian oval-shape sapphire of 3.55 carats
EDXRF, File ref. NFN420, operator JMDD
Acquisition parameters:
Tube voltage: 25 KV
Tube current: 200 mA
Filter: Aluminium
Livetime: 200 sec.
Max. energy: 10 KeV
Atmosphere: Air
Channels : 512
Resolution: 20 eV
Dead Time 28 %
Escape peaks: no
Sample: fix
Film: Prolene
Kα Al (1.486)
Diffraction peak
Kα Fe (6.398)
Kβ Fe (7.058)
Kα Ga (9.242)
Counts
Energy (KeV)

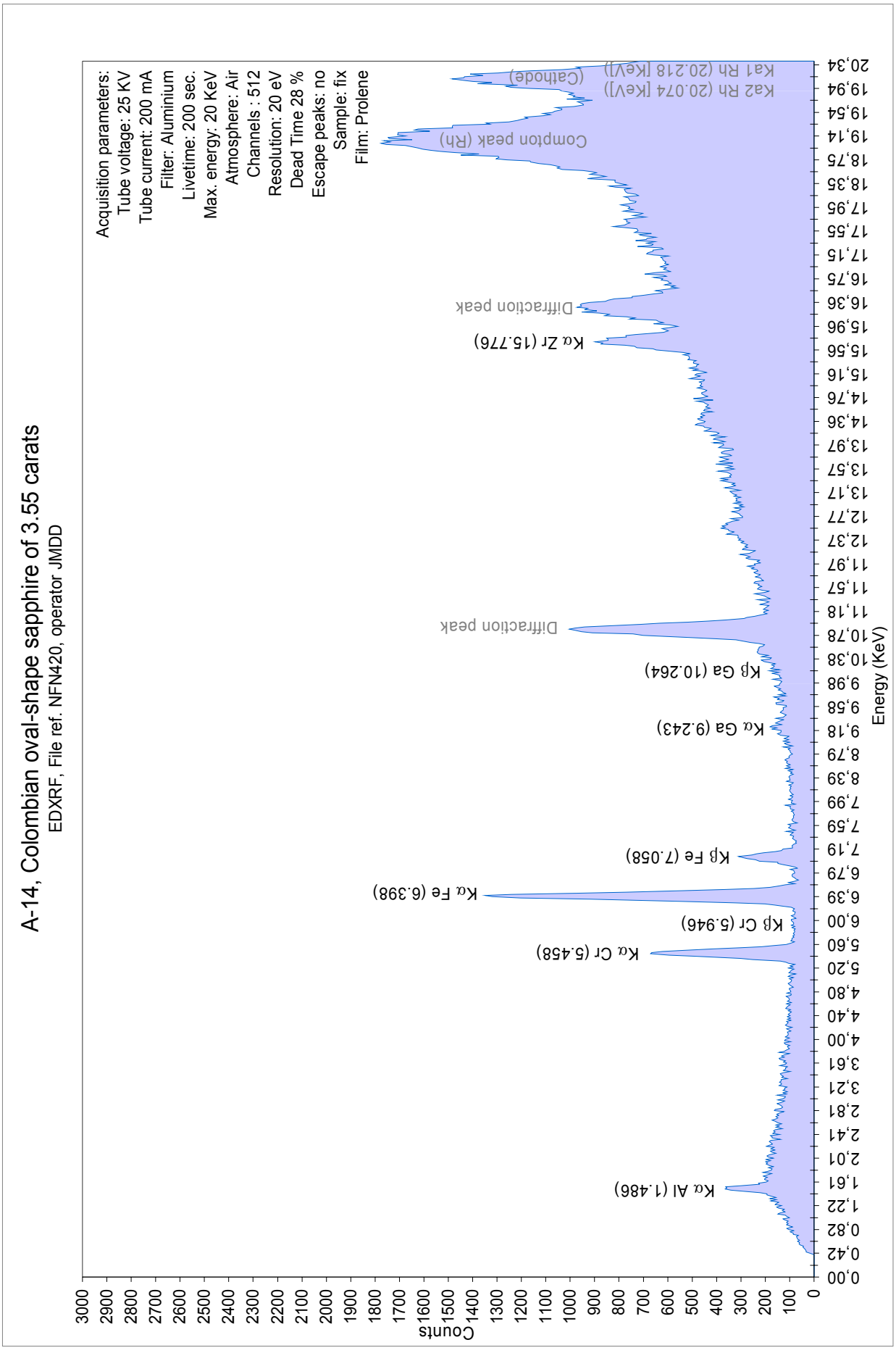
A-14, Colombian oval-shape sapphire of 3.55 carats
EDXRF, File ref. NFN420, operator JMDD
Acquisition parameters:
Tube voltage: 25 KV
Tube current: 200 mA
Filter: Aluminium
Livetime: 200 sec.
Max. energy: 20 KeV
Atmosphere: Air
Channels : 512
Resolution: 20 eV
Dead Time 28 %
Escape peaks: no
Sample: fix
Film: Prolene
Counts
Energy (KeV)
Kα Al (1.486)
Kβ Cr (5.946)
Kα Cr (5.458)
Kβ Fe (7.058)
Kα Fe (6.398)
Kα Ga (9.243)
Kβ Ga (10.264)
Diffraction peak
Kα Zr (15.776)
Diffraction peak
Compton peak (Rh)
Kα2 Rh (20.074 [KeV])
Kα1 Rh (20.218 [KeV])
(Cathode)

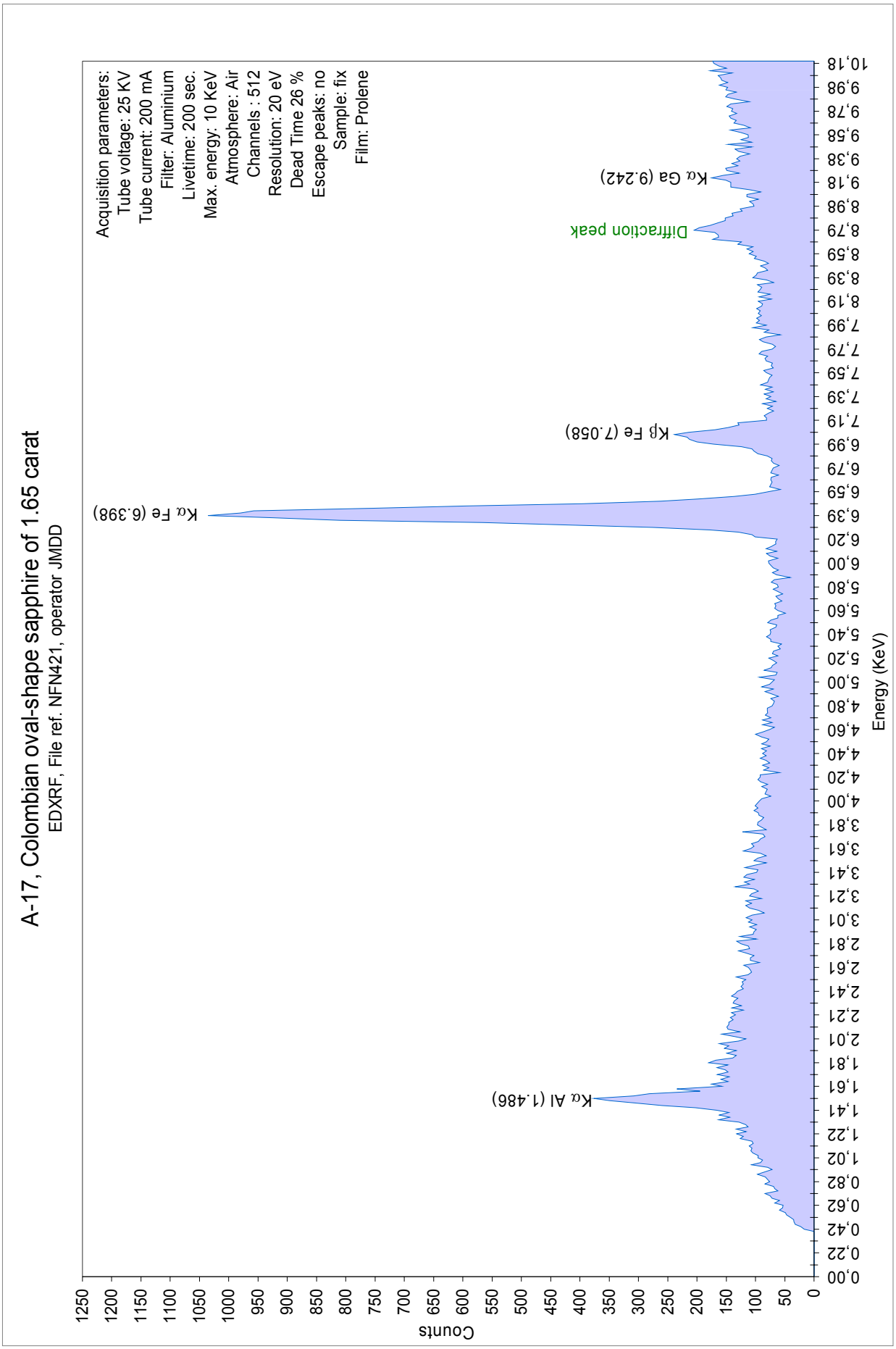
A-17, Colombian oval-shape sapphire of 1.65 carat
EDXRF, File ref. NFN421, operator JMDD
Acquisition parameters:
Tube voltage: 25 KV
Tube current: 200 mA
Filter: Aluminium
Livetime: 200 sec.
Max. energy: 10 KeV
Atmosphere: Air
Channels : 512
Resolution: 20 eV
Dead Time 26 %
Escape peaks: no
Sample: fix
Film: Prolene
Kα Al (1.486)
Kα Fe (6.398)
Kβ Fe (7.058)
Diffraction peak
Kα Ga (9.242)
Counts
Energy (KeV)

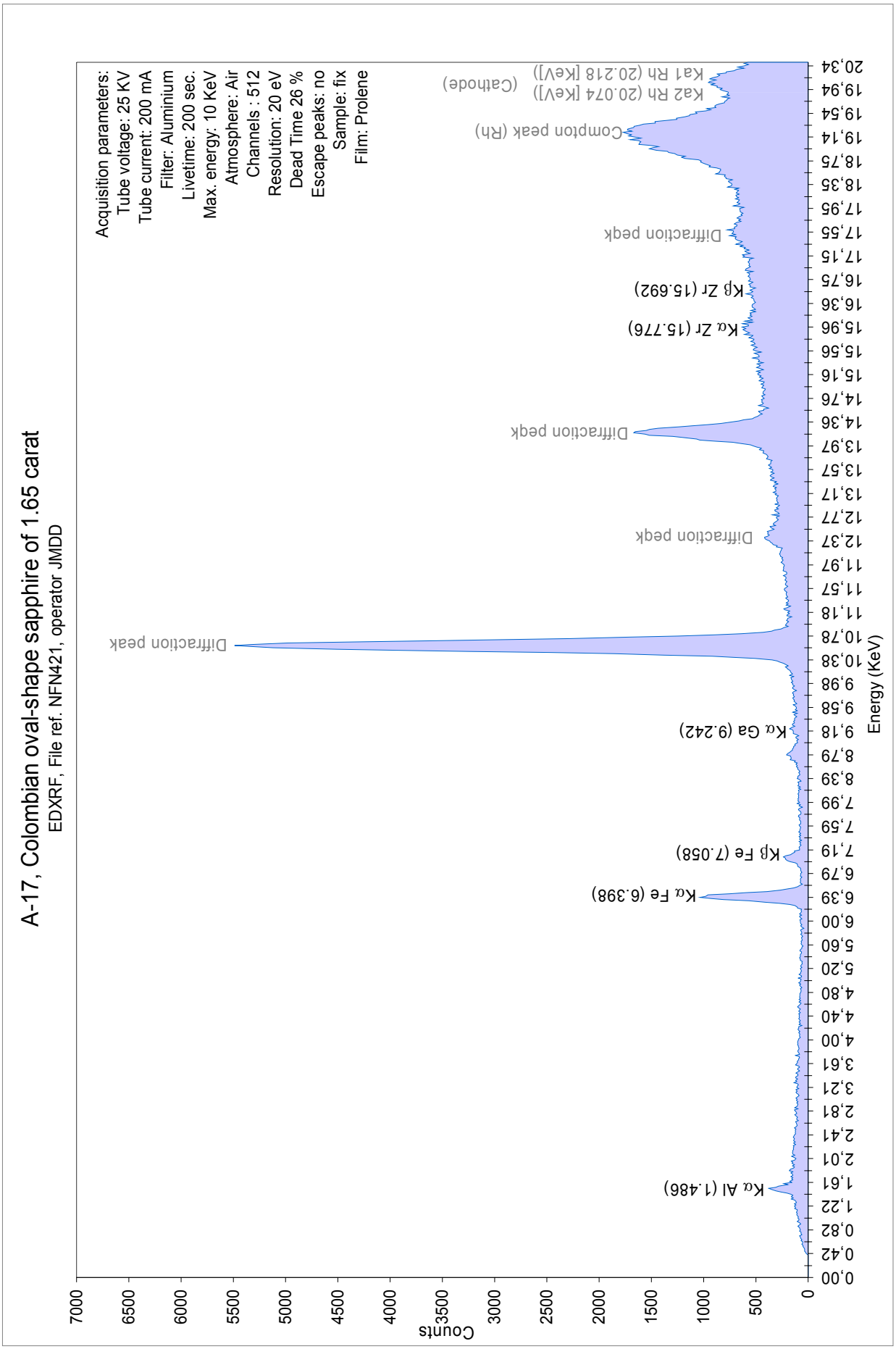
A-17, Colombian oval-shape sapphire of 1.65 carat
EDXRF, File ref. NFN421, operator JMDD
Acquisition parameters:
Tube voltage: 25 KV
Tube current: 200 mA
Filter: Aluminium
Livetime: 200 sec.
Max. energy: 10 KeV
Atmosphere: Air
Channels : 512
Resolution: 20 eV
Dead Time 26 %
Escape peaks: no
Sample: fix
Film: Prolene
Counts
Energy (KeV)
Kα Al (1.486)
Kα Fe (6.398)
Kβ Fe (7.058)
Kα Ga (9.242)
Diffraction peak
Diffraction peak
Diffraction peak
Kα Zr (15.776)
Kβ Zr (15.692)
Diffraction peak
Compton peak (Rh)
Ka2 Rh (20.074 [KeV])
Ka1 Rh (20.218 [KeV])
(Cathode)

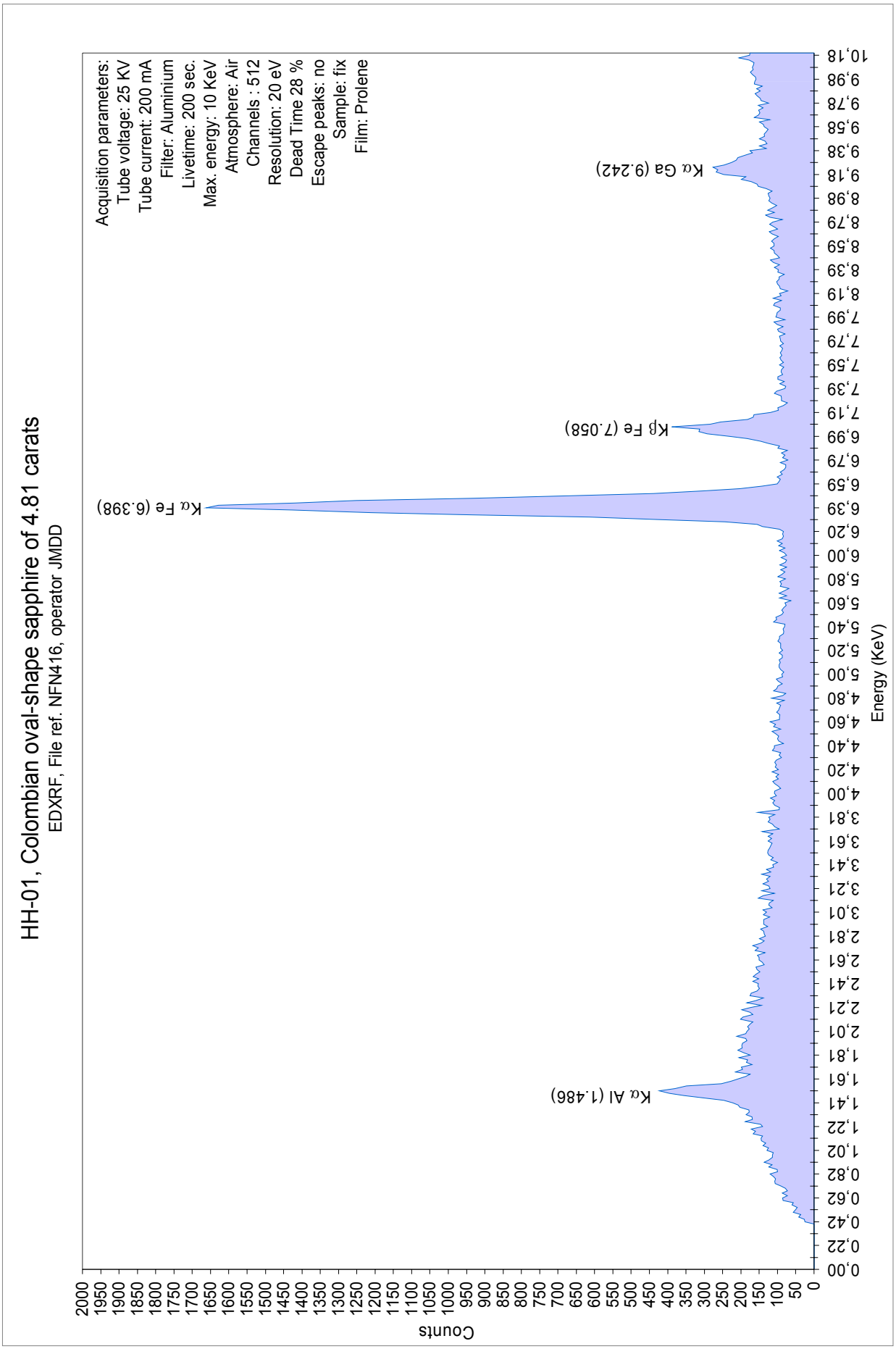
HH-01, Colombian oval-shape sapphire of 4.81 carats
EDXRF, File ref. NFN416, operator JMDD
Acquisition parameters:
Tube voltage: 25 KV
Tube current: 200 mA
Filter: Aluminium
Livetime: 200 sec.
Max. energy: 10 KeV
Atmosphere: Air
Channels : 512
Resolution: 20 eV
Dead Time 28 %
Escape peaks: no
Sample: fix
Film: Prolene
Kα Al (1.486)
Kα Fe (6.398)
Kβ Fe (7.058)
Kα Ga (9.242)
Counts
Energy (KeV)

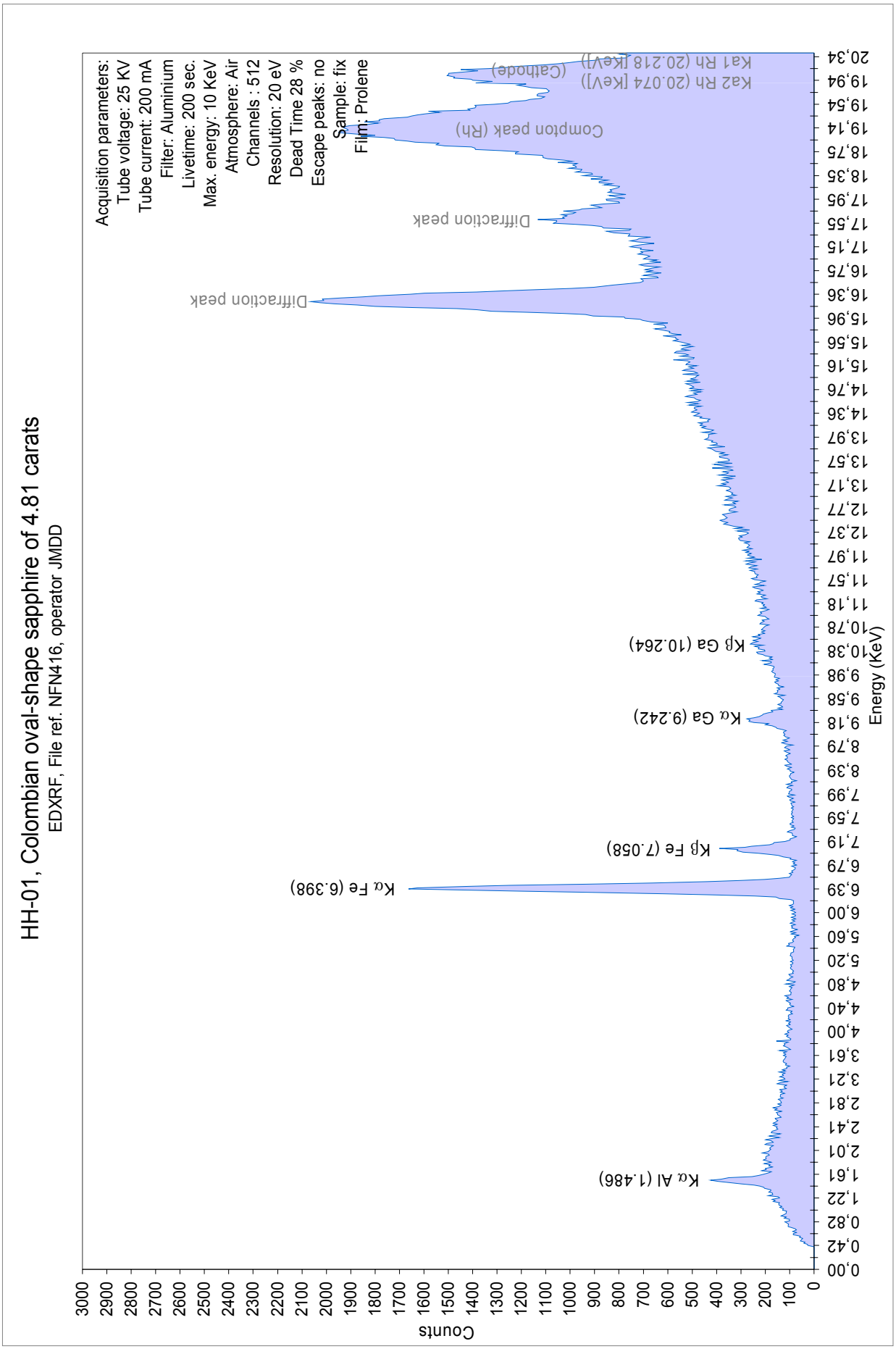
HH-01, Colombian oval-shape sapphire of 4.81 carats
EDXRF, File ref. NFN416, operator JMDD
Acquisition parameters:
Tube voltage: 25 KV
Tube current: 200 mA
Filter: Aluminium
Livetime: 200 sec.
Max. energy: 10 KeV
Atmosphere: Air
Channels : 512
Resolution: 20 eV
Dead Time 28 %
Escape peaks: no
Sample: fix
Film: Prolene
Kα Al (1.486)
Kα Fe (6.398)
Kβ Fe (7.058)
Kα Ga (9.242)
Kβ Ga (10.264)
Diffraction peak
Diffraction peak
Compton peak (Rh)
Kα2 Rh (20.074 [KeV])
Kα1 Rh (20.218 [KeV])
(Cathode)
Counts
Energy (KeV)

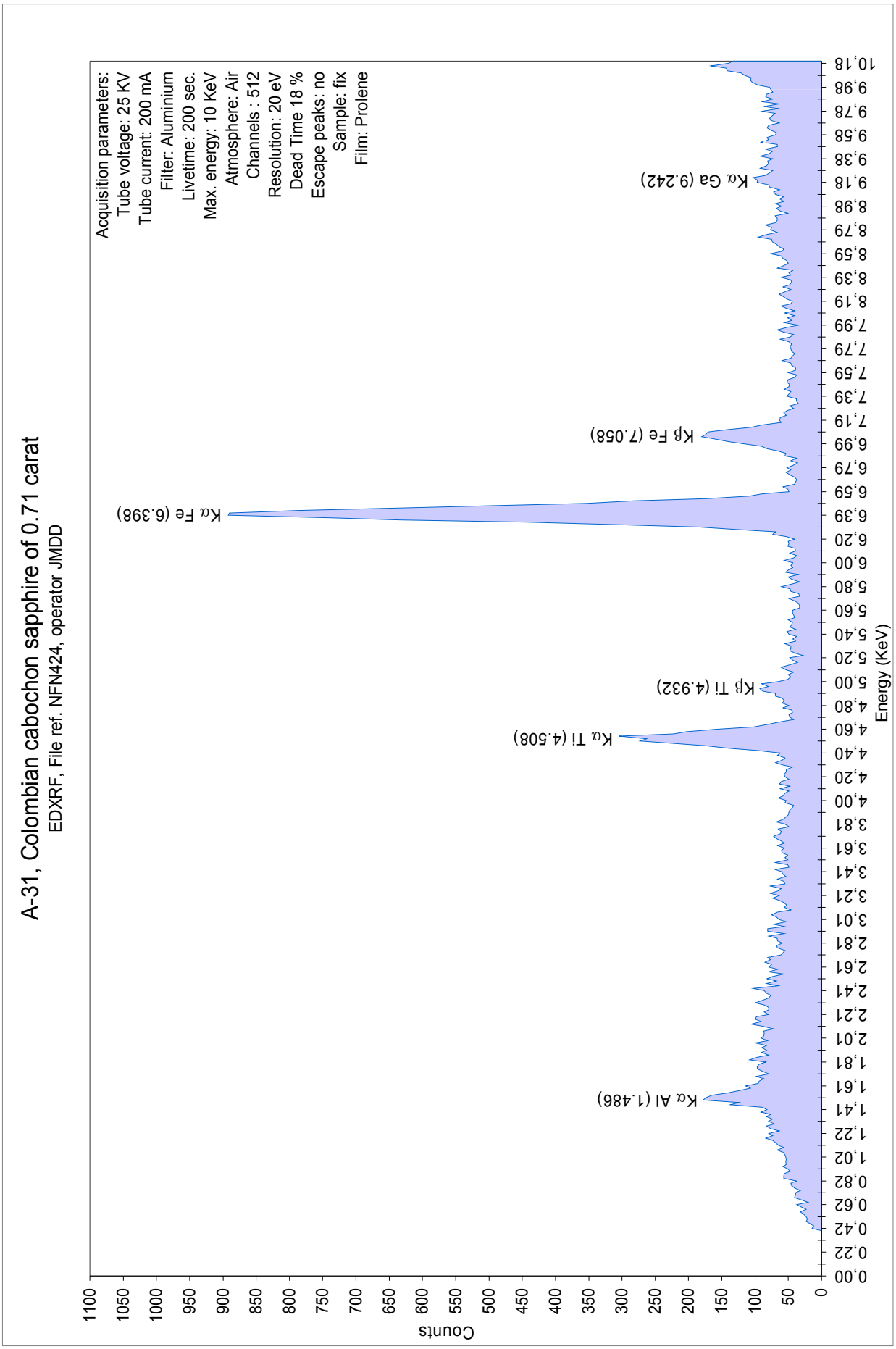
A-31, Colombian cabochon sapphire of 0.71 carat
EDXRF, File ref. NFN424, operator JMDD
Acquisition parameters:
Tube voltage: 25 KV
Tube current: 200 mA
Filter: Aluminium
Livetime: 200 sec.
Max. energy: 10 KeV
Atmosphere: Air
Channels : 512
Resolution: 20 eV
Dead Time 18 %
Escape peaks: no
Sample: fix
Film: Prolene
Kα Al (1.486)
Kα Ti (4.508)
Kβ Ti (4.932)
Kα Fe (6.398)
Kβ Fe (7.058)
Kα Ga (9.242)
Counts
Energy (KeV)

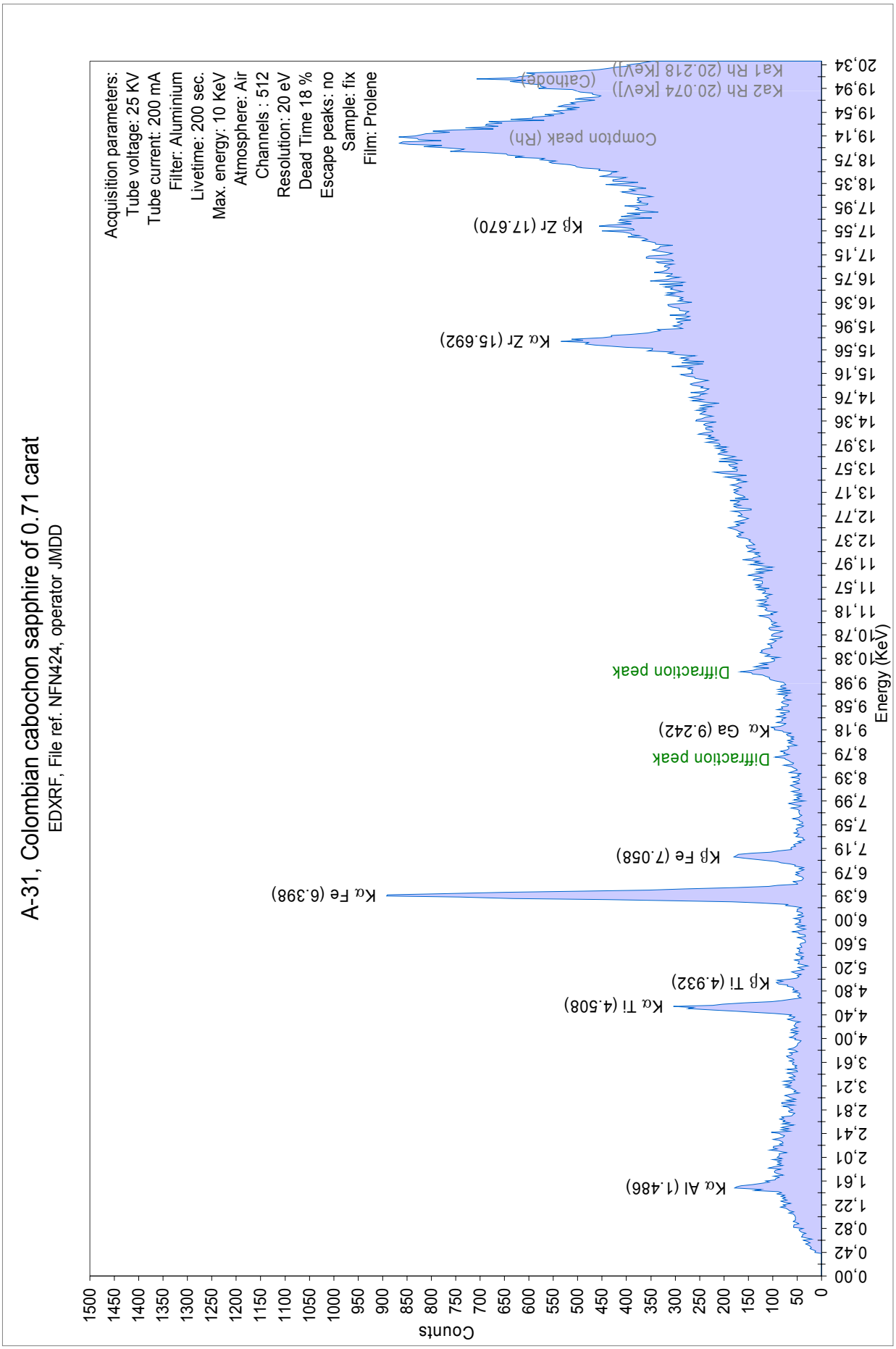
A-31, Colombian cabochon sapphire of 0.71 carat
EDXRF, File ref. NFN424, operator JMDD
Acquisition parameters:
Tube voltage: 25 KV
Tube current: 200 mA
Filter: Aluminium
Livetime: 200 sec.
Max. energy: 10 KeV
Atmosphere: Air
Channels : 512
Resolution: 20 eV
Dead Time 18 %
Escape peaks: no
Sample: fix
Film: Prolene
Counts
Energy (KeV)
Kα Al (1.486)
Kα Ti (4.508)
Kβ Ti (4.932)
Kα Fe (6.398)
Kβ Fe (7.058)
Diffraction peak
Kα Ga (9.242)
Diffraction peak
Kβ Zr (17.670)
Kα Zr (15.692)
Compton peak (Rh)
Kα2 Rh (20.074 [KeV])
Kα1 Rh (20.218 [KeV])
(Cathode)

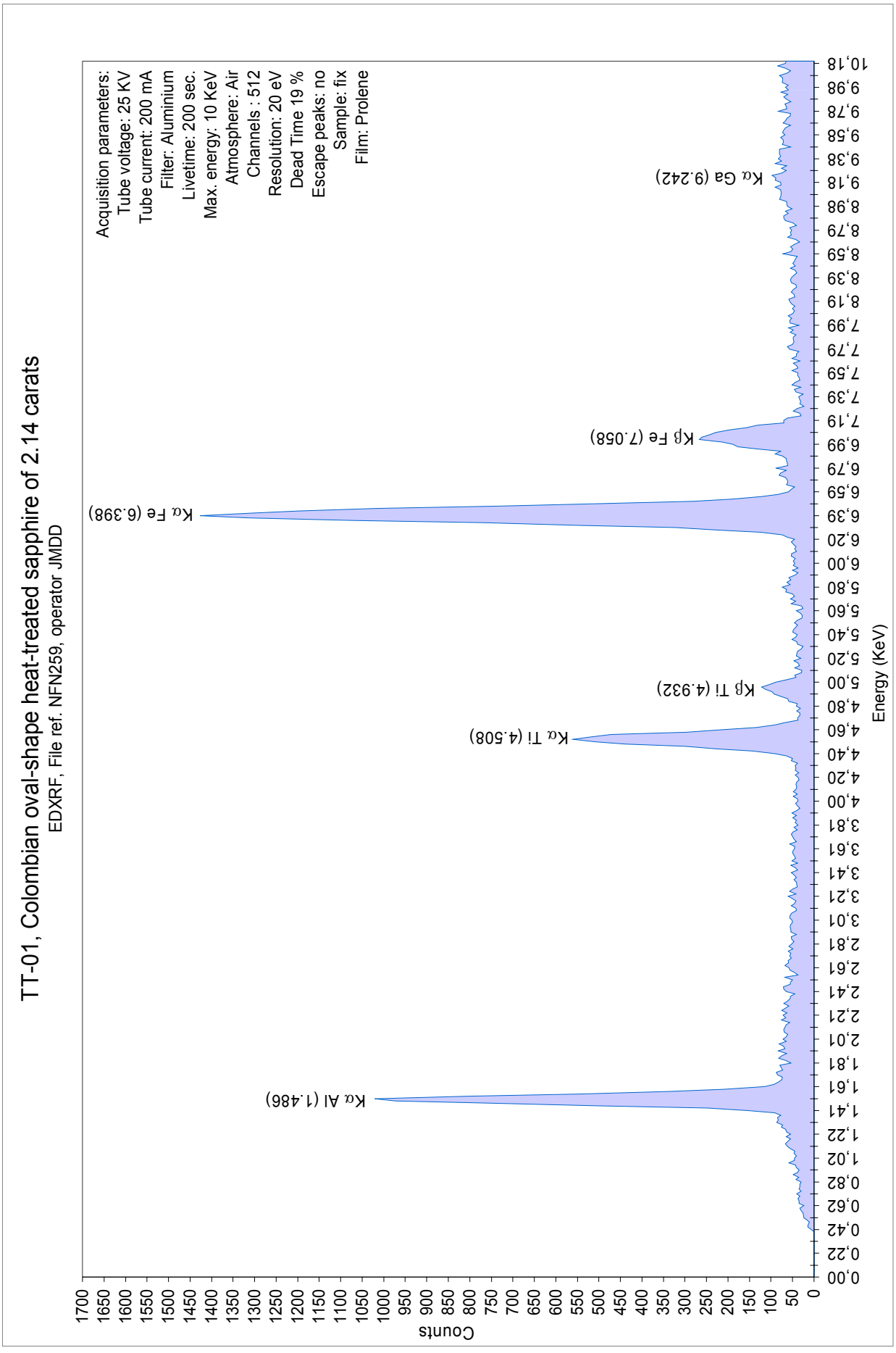
TT-01, Colombian oval-shape heat-treated sapphire of 2.14 carats
EDXRF, File ref. NFN259, operator JMDD
Acquisition parameters:
Tube voltage: 25 KV
Tube current: 200 mA
Filter: Aluminium
Livetime: 200 sec.
Max. energy: 10 KeV
Atmosphere: Air
Channels : 512
Resolution: 20 eV
Dead Time 19 %
Escape peaks: no
Sample: fix
Film: Prolene
Kα Al (1.486)
Kα Ti (4.508)
Kβ Ti (4.932)
Kα Fe (6.398)
Kβ Fe (7.058)
Kα Ga (9.242)
Counts
Energy (KeV)

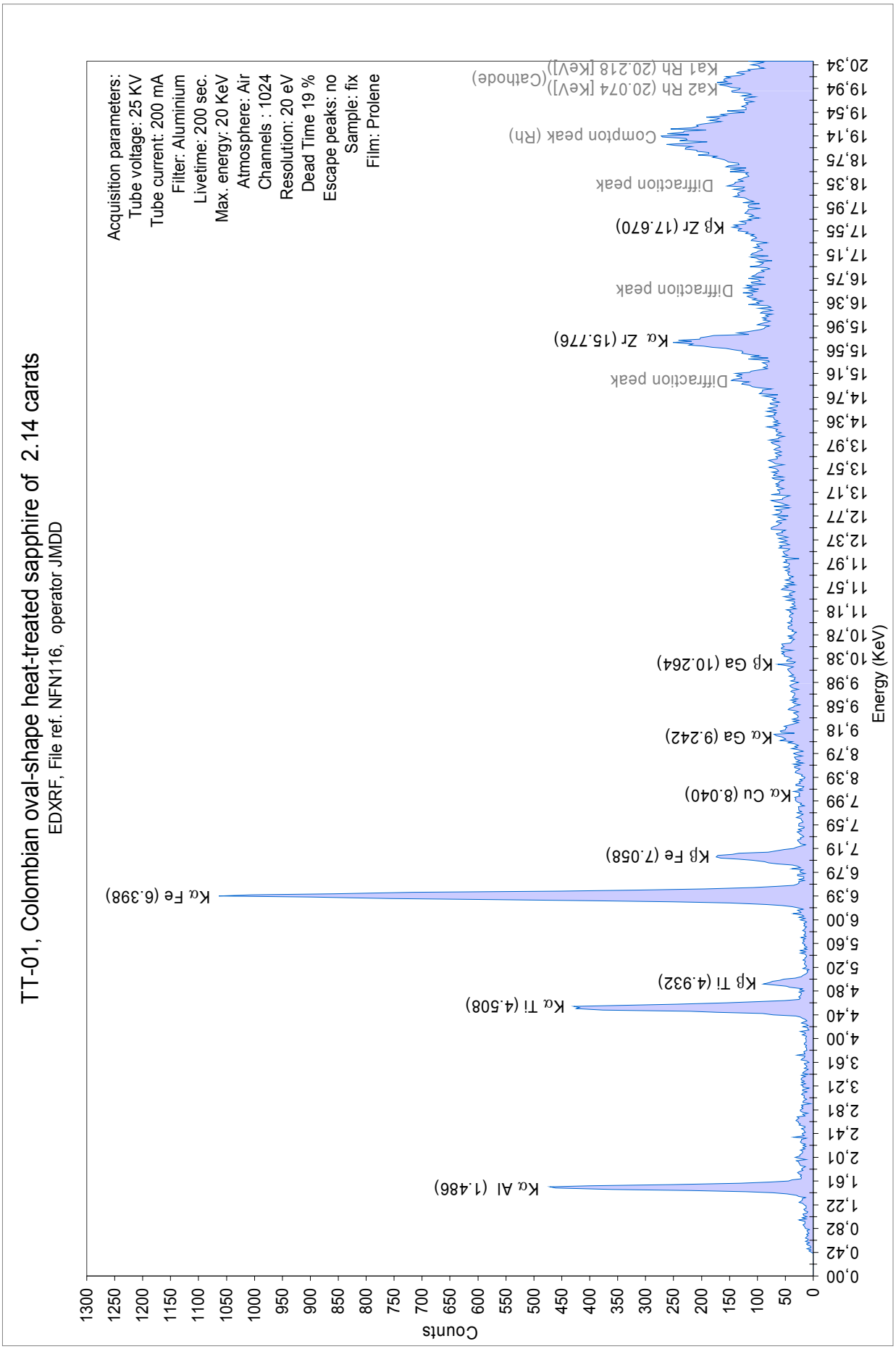
TT-01, Colombian oval-shape heat-treated sapphire of 2.14 carats
EDXRF, File ref. NFN116, operator JMDD
Acquisition parameters:
Tube voltage: 25 KV
Tube current: 200 mA
Filter: Aluminium
Livetime: 200 sec.
Max. energy: 20 KeV
Atmosphere: Air
Channels : 1024
Resolution: 20 eV
Dead Time 19 %
Escape peaks: no
Sample: fix
Film: Prolene
Counts
Energy (KeV)
Kα Al (1.486)
Kα Ti (4.508)
Kβ Ti (4.932)
Kα Fe (6.398)
Kβ Fe (7.058)
Kα Cu (8.040)
Kα Ga (9.242)
Kβ Ga (10.264)
Kα Zr (15.776)
Kβ Zr (17.670)
Diffraction peak
Compton peak (Rh)
Ka2 Rh (20.074 [keV])
Ka1 Rh (20.218 [keV])
(Cathode)

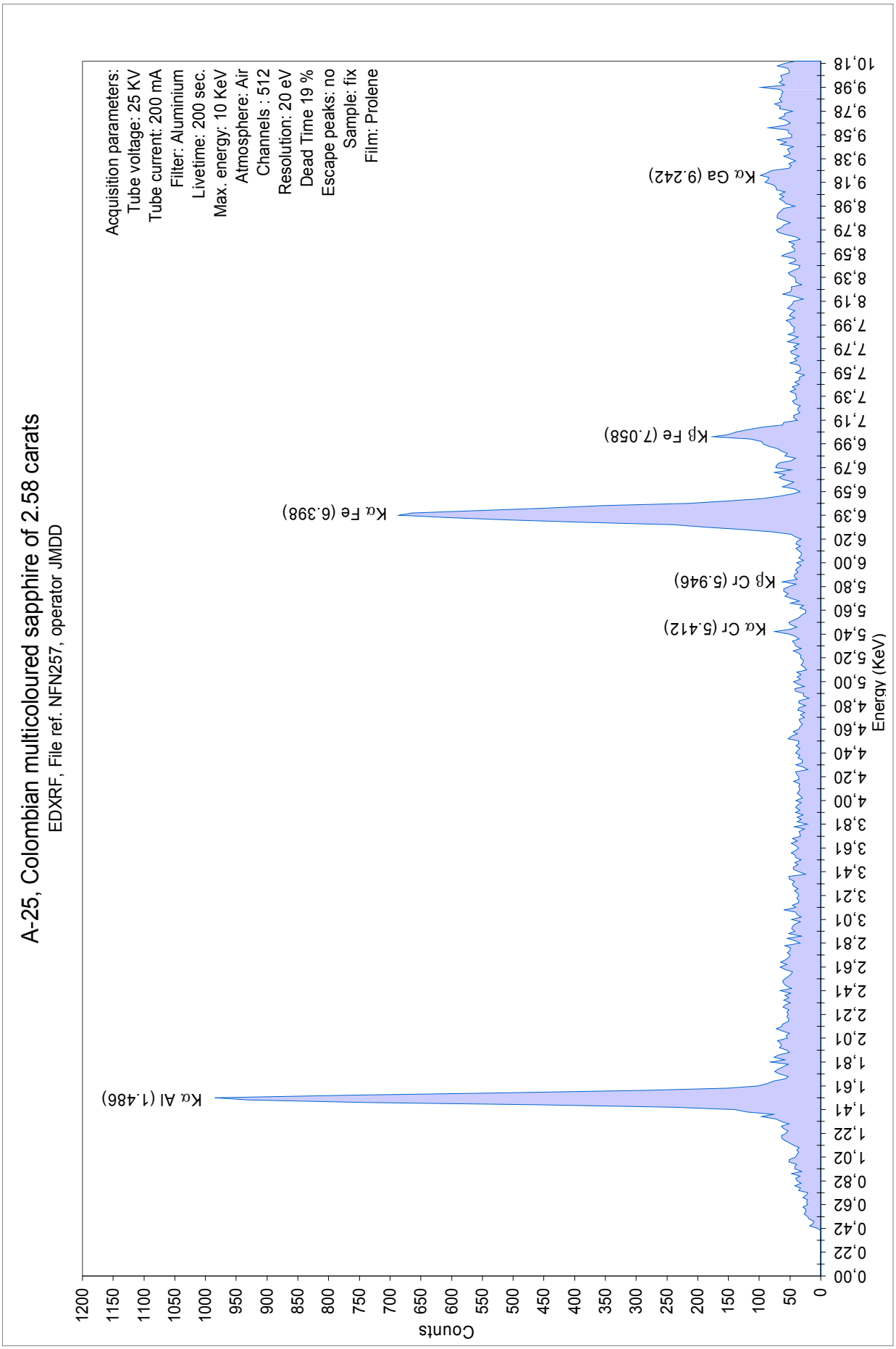
A-25, Colombian multicoloured sapphire of 2.58 carats
EDXRF, File ref. NFN257, operator JMDD
Acquisition parameters:
Tube voltage: 25 KV
Tube current: 200 mA
Filter: Aluminium
Livetime: 200 sec.
Max. energy: 10 KeV
Atmosphere: Air
Channels : 512
Resolution: 20 eV
Dead Time 19 %
Escape peaks: no
Sample: fix
Film: Prolene
Kα Al (1.486)
Kα Cr (5.412)
Kβ Cr (5.946)
Kα Fe (6.398)
Kβ Fe (7.058)
Kα Ga (9.242)
Counts
Energy (KeV)

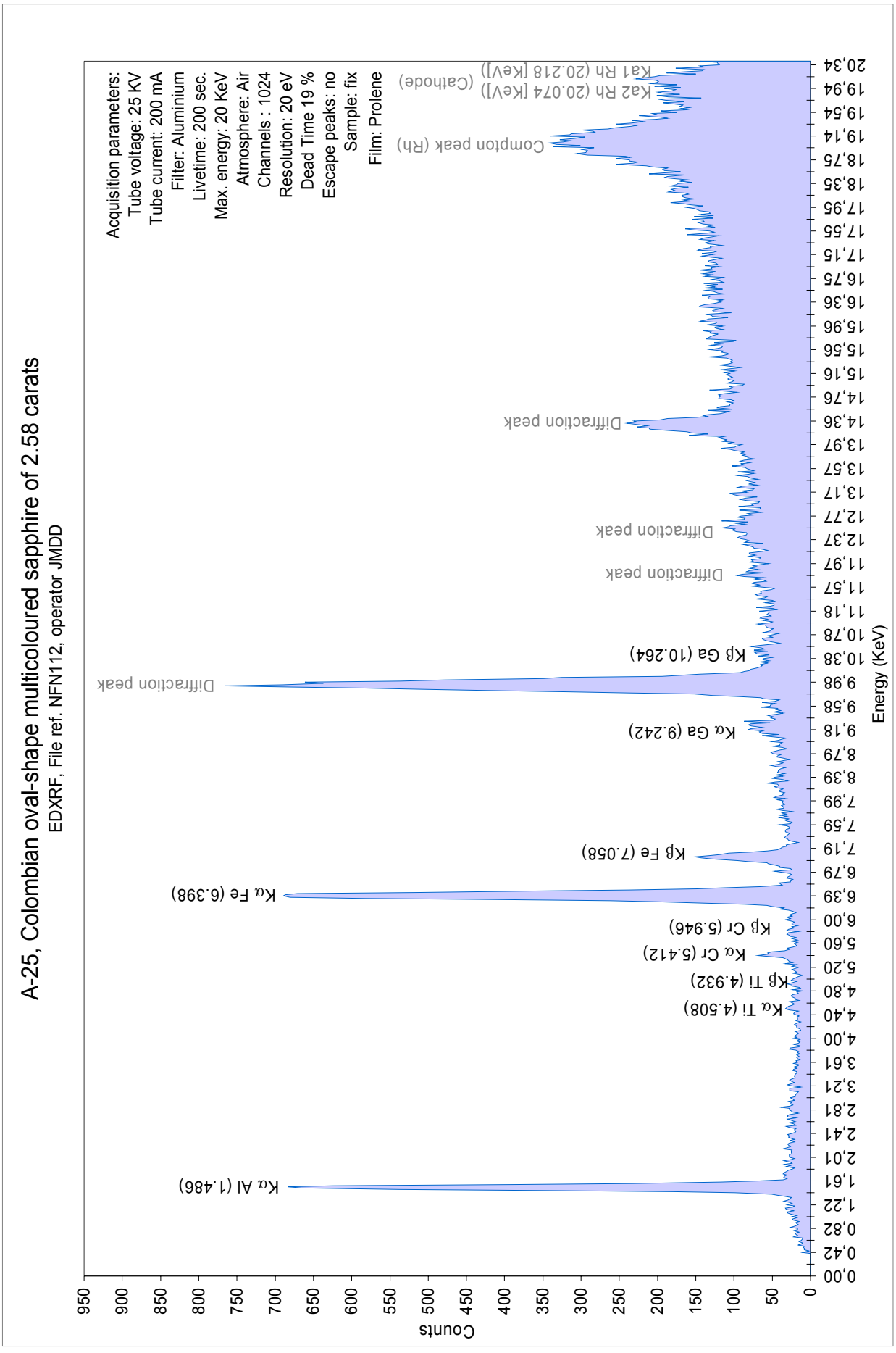
A-25, Colombian oval-shape multicoloured sapphire of 2.58 carats
EDXRF, File ref. NFN112, operator JMDD
Acquisition parameters:
Tube voltage: 25 KV
Tube current: 200 mA
Filter: Aluminium
Livetime: 200 sec.
Max. energy: 20 KeV
Atmosphere: Air
Channels : 1024
Resolution: 20 eV
Dead Time 19 %
Escape peaks: no
Sample: fix
Film: Prolene
Counts
Energy (KeV)
Kα Al (1.486)
Kα Ti (4.508)
Kβ Ti (4.932)
Kα Cr (5.412)
Kβ Cr (5.946)
Kα Fe (6.398)
Kβ Fe (7.058)
Kα Ga (9.242)
Kβ Ga (10.264)
Diffraction peak
Diffraction peak
Diffraction peak
Diffraction peak
Compton peak (Rh)
Kα2 Rh (20.074 [KeV])
Kα1 Rh (20.218 [KeV]) (Cathode)

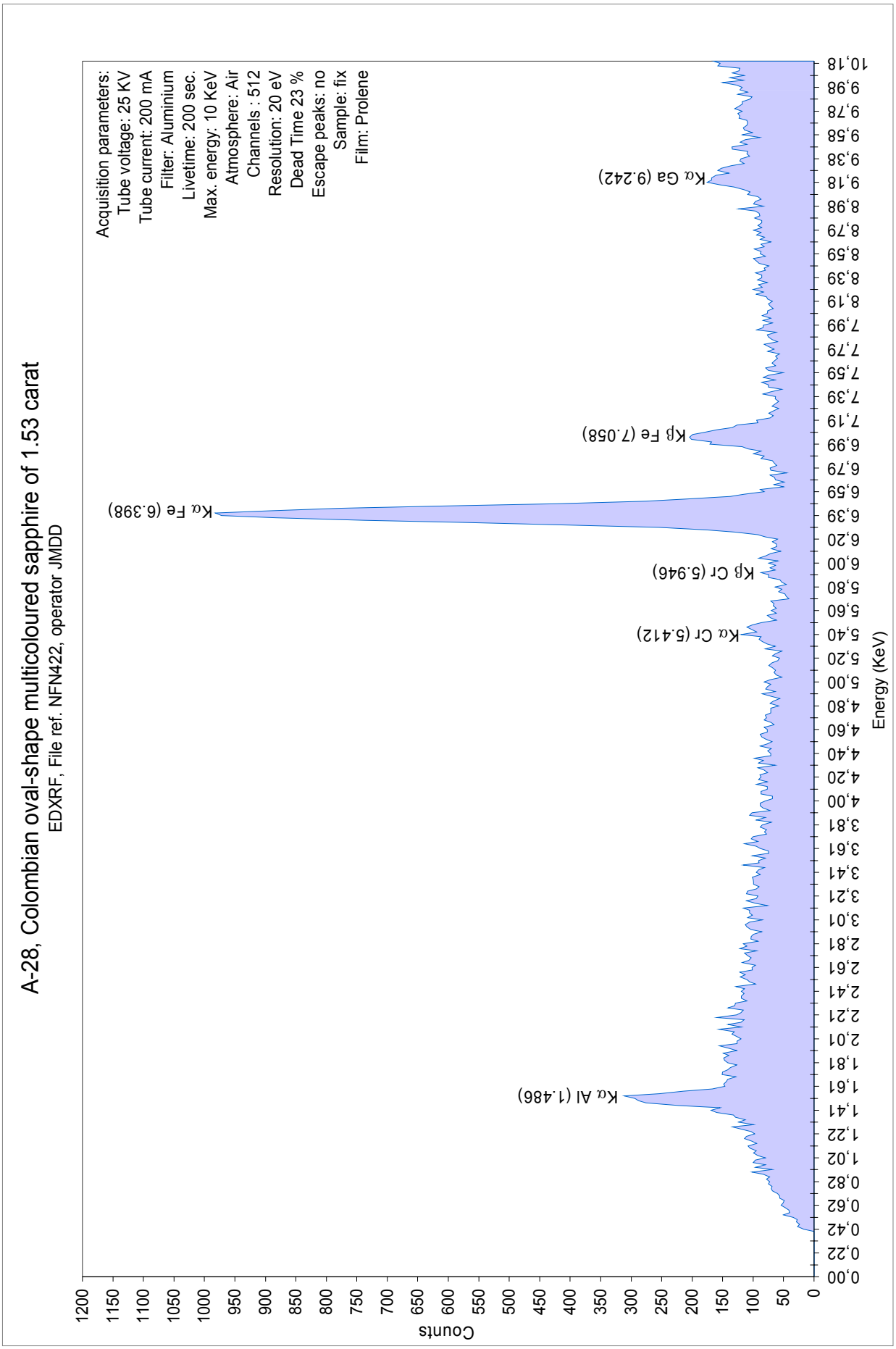
A-28, Colombian oval-shape multicoloured sapphire of 1.53 carat
EDXRF, File ref. NFN422, operator JMDD
Acquisition parameters:
Tube voltage: 25 KV
Tube current: 200 mA
Filter: Aluminium
Livetime: 200 sec.
Max. energy: 10 KeV
Atmosphere: Air
Channels : 512
Resolution: 20 eV
Dead Time 23 %
Escape peaks: no
Sample: fix
Film: Prolene
Kα Al (1.486)
Kα Cr (5.412)
Kβ Cr (5.946)
Kα Fe (6.398)
Kβ Fe (7.058)
Kα Ga (9.242)
Counts
Energy (KeV)

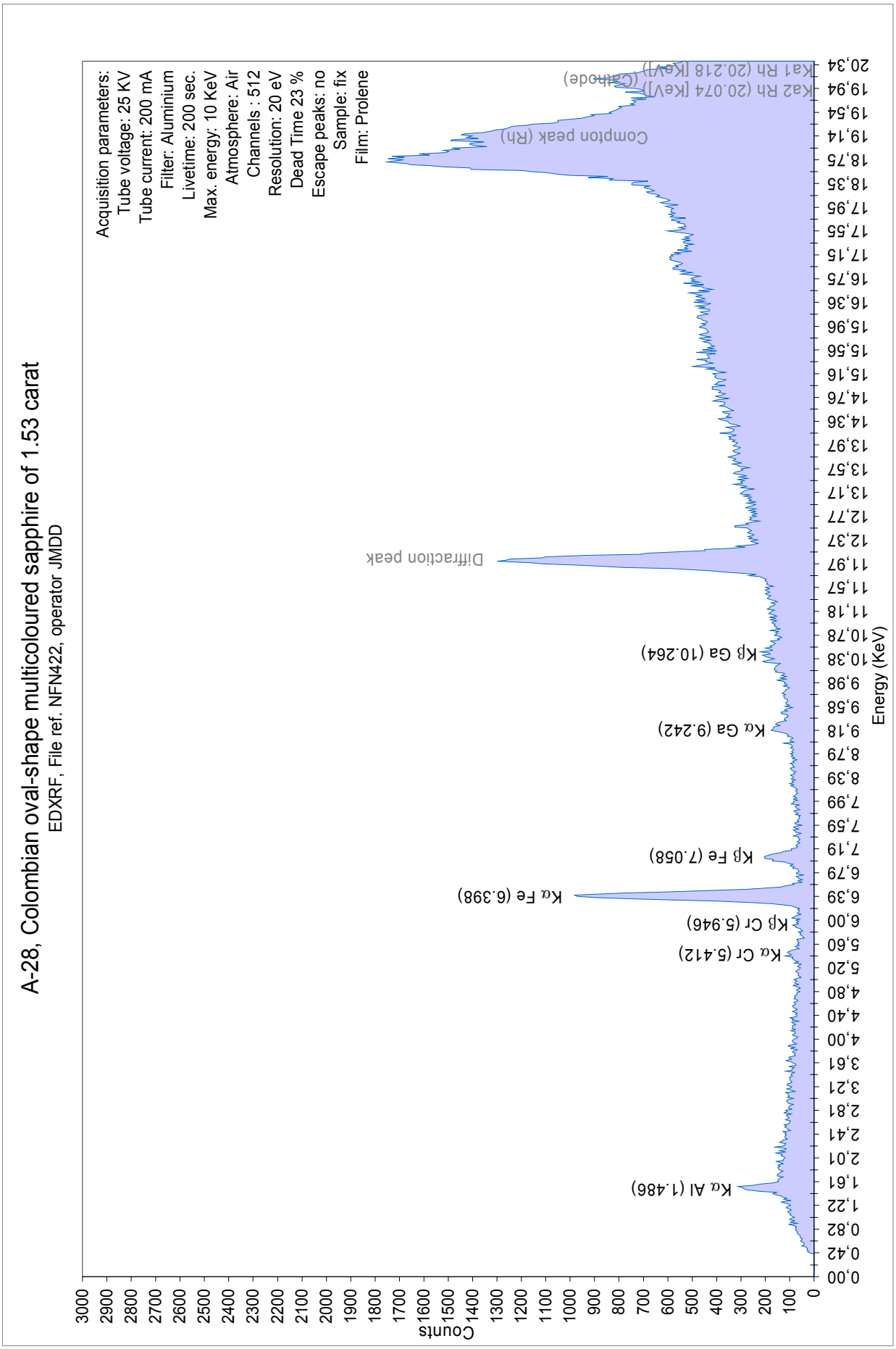
A-28, Colombian oval-shape multicoloured sapphire of 1.53 carat
EDXRF, File ref. NFN422, operator JMDD
Acquisition parameters:
Tube voltage: 25 KV
Tube current: 200 mA
Filter: Aluminium
Livetime: 200 sec.
Max. energy: 10 KeV
Atmosphere: Air
Channels : 512
Resolution: 20 eV
Dead Time 23 %
Escape peaks: no
Sample: fix
Film: Prolene
Counts
Energy (KeV)
Kα Al (1.486)
Kα Cr (5.412)
Kβ Cr (5.946)
Kα Fe (6.398)
Kβ Fe (7.058)
Kα Ga (9.242)
Kβ Ga (10.264)
Diffraction peak
Compton peak (Rh)
Kα2 Rh (20.074 [KeV])
Kα1 Rh (20.218 [KeV])
(Cathode)

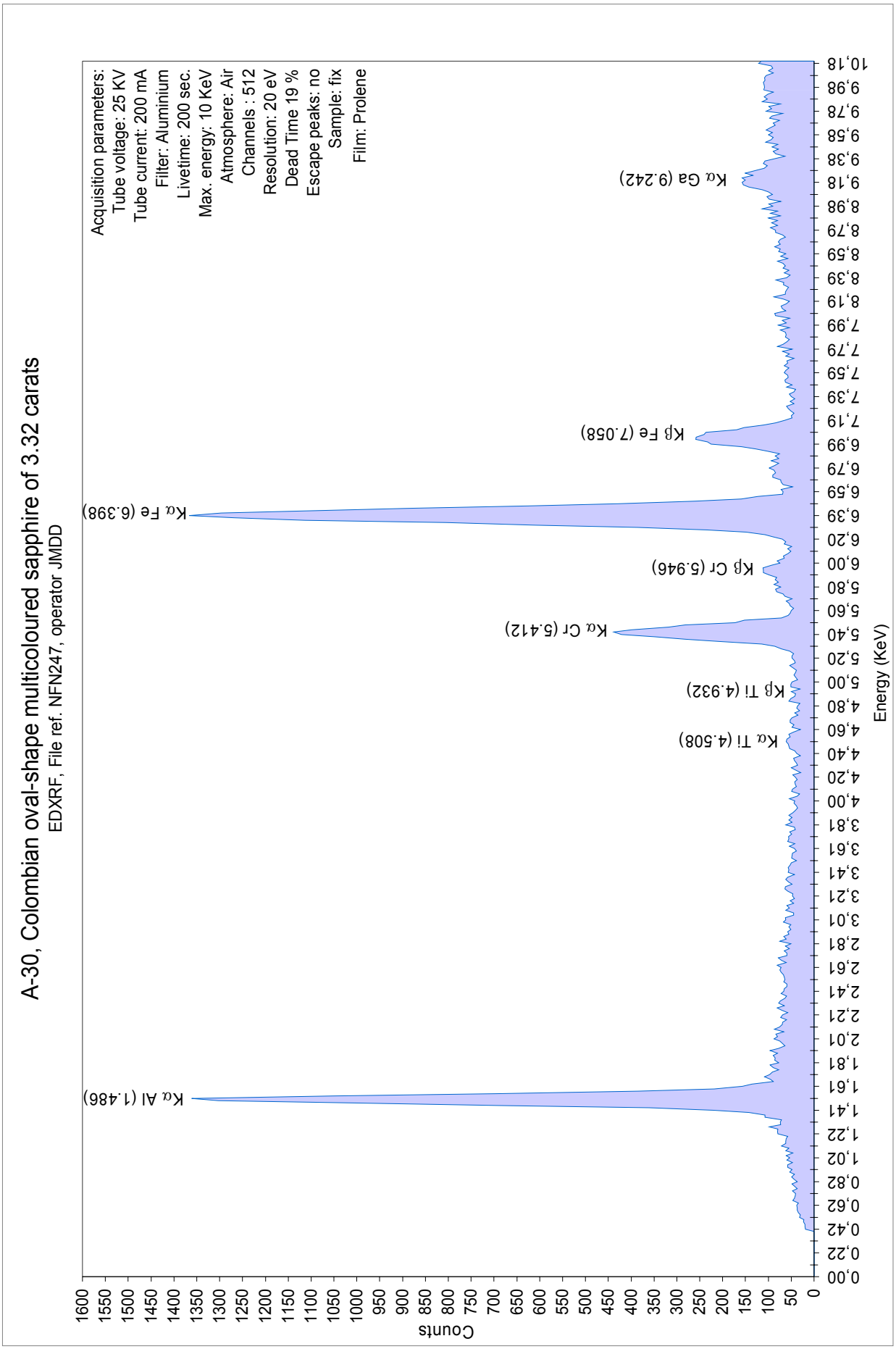
A-30, Colombian oval-shape multicoloured sapphire of 3.32 carats
EDXRF, File ref. NFN247, operator JMDD
Acquisition parameters:
Tube voltage: 25 KV
Tube current: 200 mA
Filter: Aluminium
Livetime: 200 sec.
Max. energy: 10 KeV
Atmosphere: Air
Channels : 512
Resolution: 20 eV
Dead Time 19 %
Escape peaks: no
Sample: fix
Film: Prolene
Kα Al (1.486)
Kα Ti (4.508)
Kβ Ti (4.932)
Kα Cr (5.412)
Kβ Cr (5.946)
Kα Fe (6.398)
Kβ Fe (7.058)
Kα Ga (9.242)
Counts
Energy (KeV)

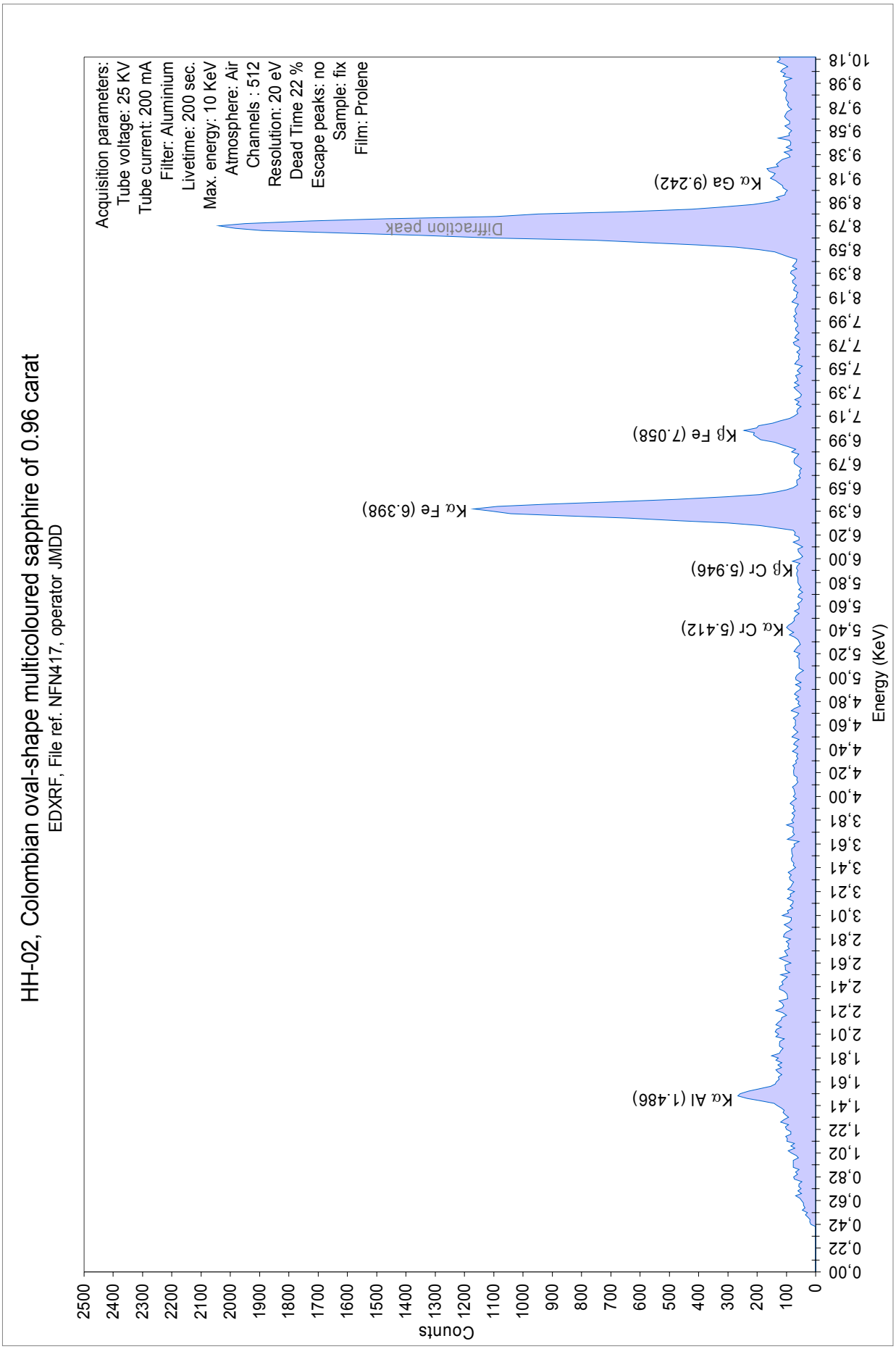
HH-02, Colombian oval-shape multicoloured sapphire of 0.96 carat
EDXRF, File ref. NFN417, operator JMDD
Acquisition parameters:
Tube voltage: 25 KV
Tube current: 200 mA
Filter: Aluminium
Livetime: 200 sec.
Max. energy: 10 KeV
Atmosphere: Air
Channels : 512
Resolution: 20 eV
Dead Time 22 %
Escape peaks: no
Sample: fix
Film: Prolene
Diffraction peak
Kα Al (1.486)
Kα Cr (5.412)
Kβ Cr (5.946)
Kα Fe (6.398)
Kβ Fe (7.058)
Kα Ga (9.242)
Counts
Energy (KeV)

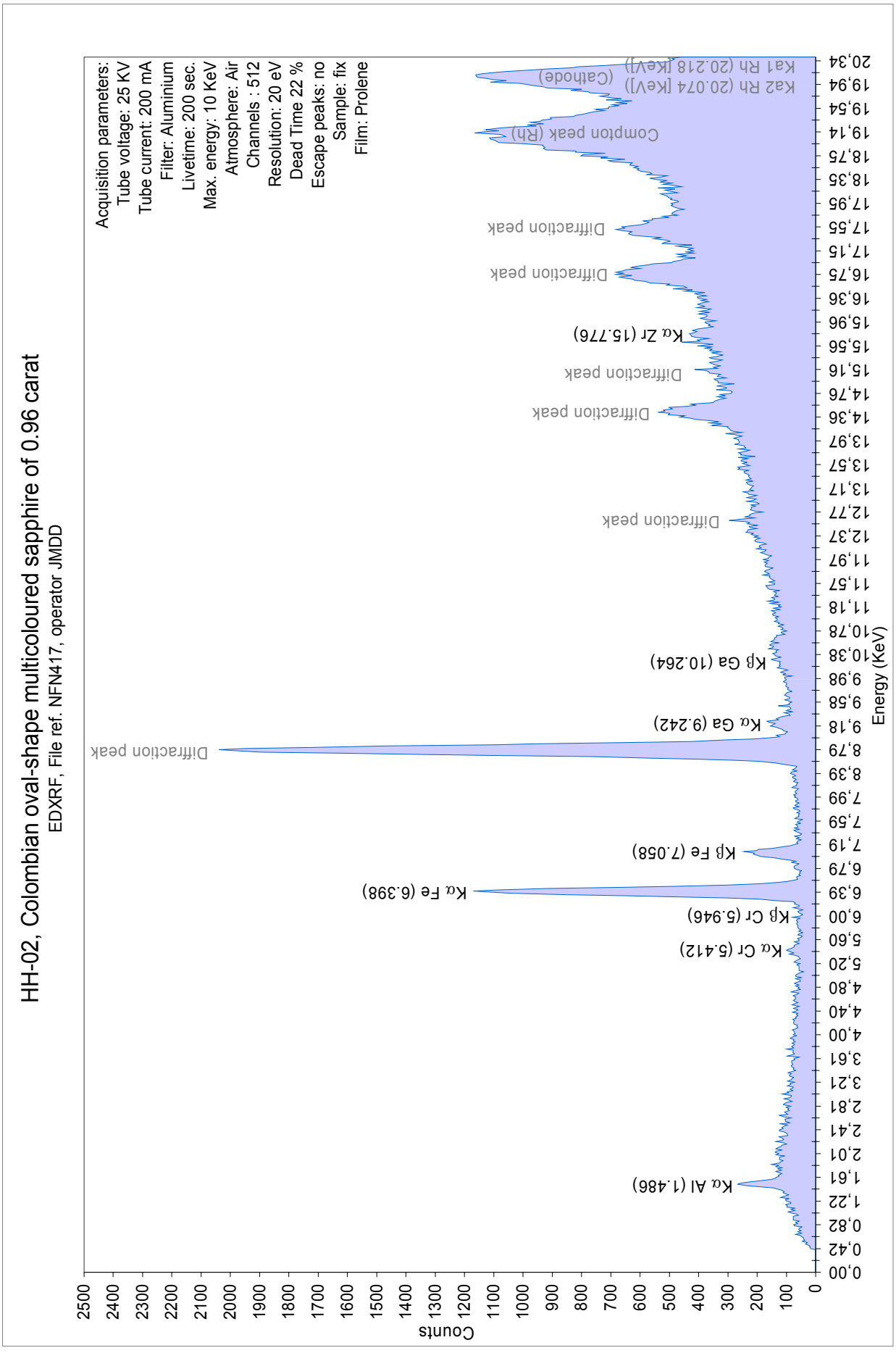
HH-02, Colombian oval-shape multicoloured sapphire of 0.96 carat
EDXRF, File ref. NFN417, operator JMDD
Acquisition parameters:
Tube voltage: 25 KV
Tube current: 200 mA
Filter: Aluminium
Livetime: 200 sec.
Max. energy: 10 KeV
Atmosphere: Air
Channels : 512
Resolution: 20 eV
Dead Time 22 %
Escape peaks: no
Sample: fix
Film: Prolene
Counts
Energy (KeV)
Kα Al (1.486)
Kα Cr (5.412)
Kβ Cr (5.946)
Kα Fe (6.398)
Kβ Fe (7.058)
Diffraction peak
Kα Ga (9.242)
Kβ Ga (10.264)
Diffraction peak
Diffraction peak
Diffraction peak
Kα Zr (15.776)
Diffraction peak
Diffraction peak
Compton peak (Rh)
Kα2 Rh (20.074 [KeV])
Kα1 Rh (20.218 [KeV])
(Cathode)

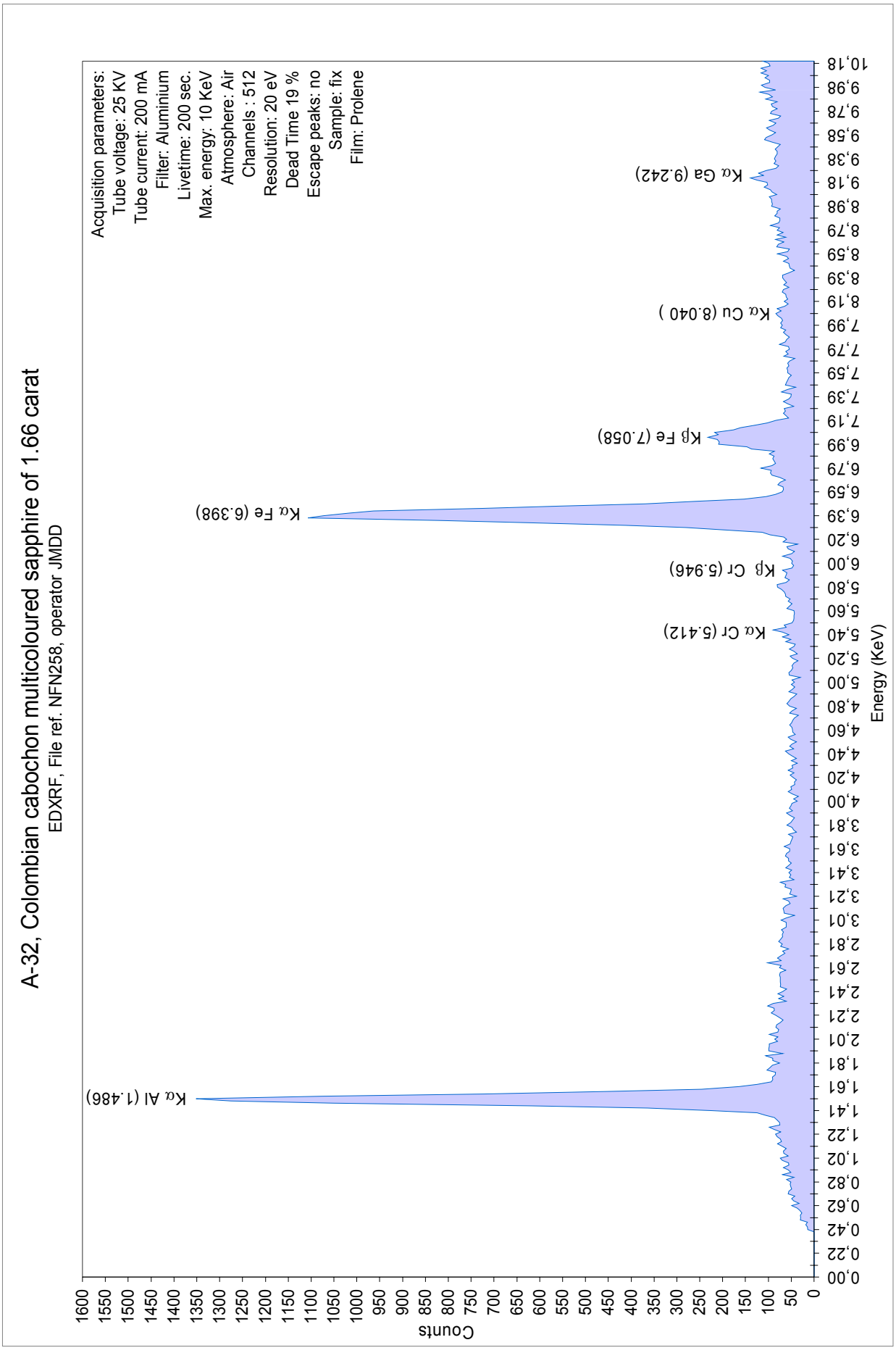
A-32, Colombian cabochon multicoloured sapphire of 1.66 carat
EDXRF, File ref. NFN258, operator JMDD
Acquisition parameters:
Tube voltage: 25 KV
Tube current: 200 mA
Filter: Aluminium
Livetime: 200 sec.
Max. energy: 10 KeV
Atmosphere: Air
Channels : 512
Resolution: 20 eV
Dead Time 19 %
Escape peaks: no
Sample: fix
Film: Prolene
Kα Al (1.486)
Kα Fe (6.398)
Kβ Cr (5.946)
Kα Cr (5.412)
Kβ Fe (7.058)
Kα Cu (8.040)
Kα Ga (9.242)
Counts
Energy (KeV)

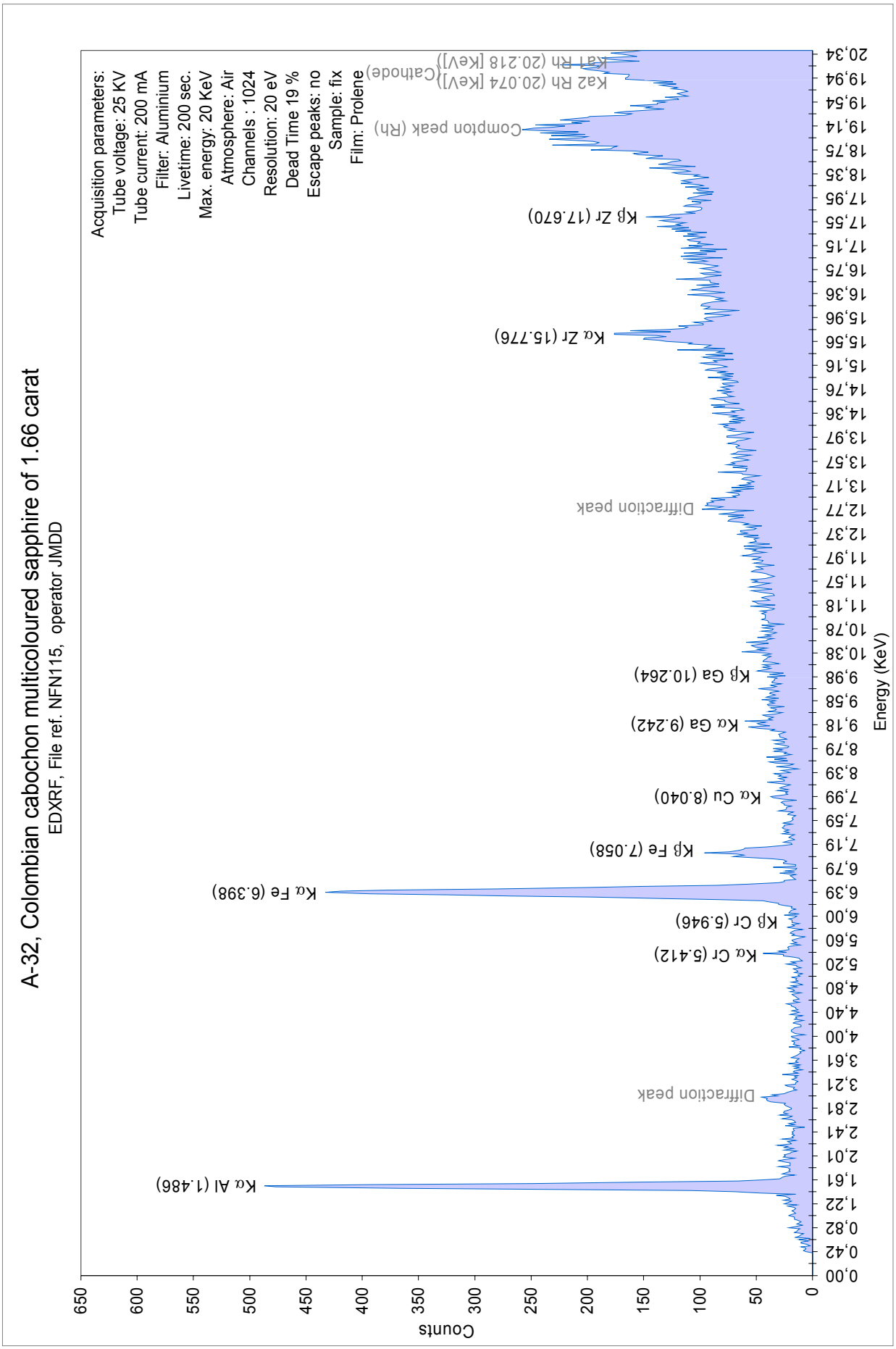
A-32, Colombian cabochon multicoloured sapphire of 1.66 carat
EDXRF, File ref. NFN115, operator JMDD
Acquisition parameters:
Tube voltage: 25 KV
Tube current: 200 mA
Filter: Aluminium
Livetime: 200 sec.
Max. energy: 20 KeV
Atmosphere: Air
Channels : 1024
Resolution: 20 eV
Dead Time 19 %
Escape peaks: no
Sample: fix
Film: Prolene
Kα Al (1.486)
Diffraction peak
Kα Cr (5.412)
Kβ Cr (5.946)
Kα Fe (6.398)
Kβ Fe (7.058)
Kα Cu (8.040)
Kα Ga (9.242)
Kβ Ga (10.264)
Diffraction peak
Kα Zr (15.776)
Kβ Zr (17.670)
Compton peak (Rh)
Kα2 Rh (20.074 [keV])
Kα1 Rh (20.218 [keV])
(Cathode)
Counts
Energy (KeV)

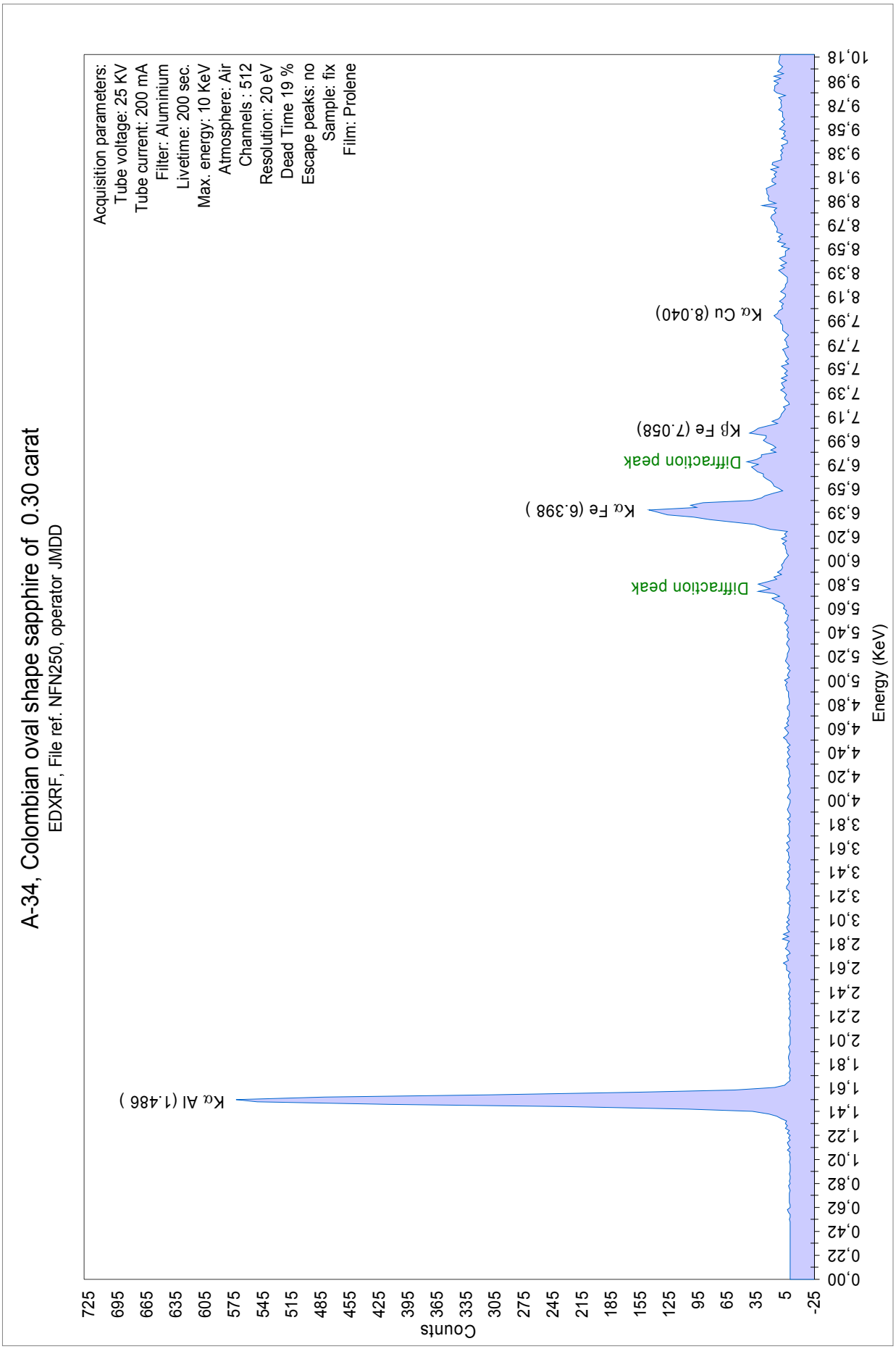
A-34, Colombian oval shape sapphire of 0.30 carat
EDXRF, File ref. NFN250, operator JMDD
Acquisition parameters:
Tube voltage: 25 KV
Tube current: 200 mA
Filter: Aluminium
Livetime: 200 sec.
Max. energy: 10 KeV
Atmosphere: Air
Channels : 512
Resolution: 20 eV
Dead Time 19 %
Escape peaks: no
Sample: fix
Film: Prolene
Counts
Energy (KeV)
Kα Al (1.486)
Kα Fe (6.398)
Diffraction peak
Diffraction peak
Kβ Fe (7.058)
Kα Cu (8.040)

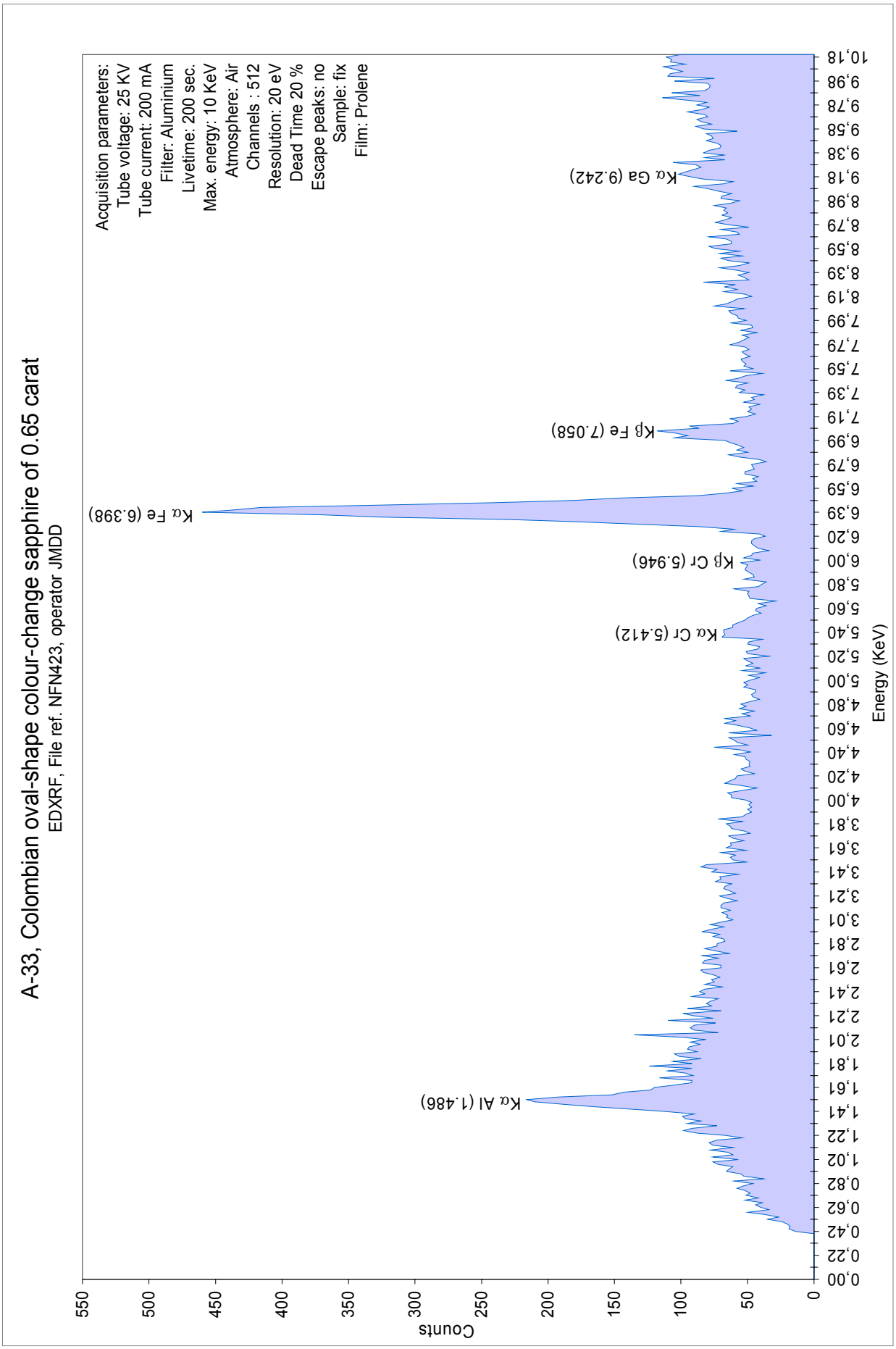
A-33, Colombian oval-shape colour-change sapphire of 0.65 carat
EDXRF, File ref. NFN423, operator JMDD
Acquisition parameters:
Tube voltage: 25 KV
Tube current: 200 mA
Filter: Aluminium
Livetime: 200 sec.
Max. energy: 10 KeV
Atmosphere: Air
Channels : 512
Resolution: 20 eV
Dead Time 20 %
Escape peaks: no
Sample: fix
Film: Prolene
Kα Al (1.486)
Kα Cr (5.412)
Kβ Cr (5.946)
Kα Fe (6.398)
Kβ Fe (7.058)
Kα Ga (9.242)
Counts
Energy (KeV)

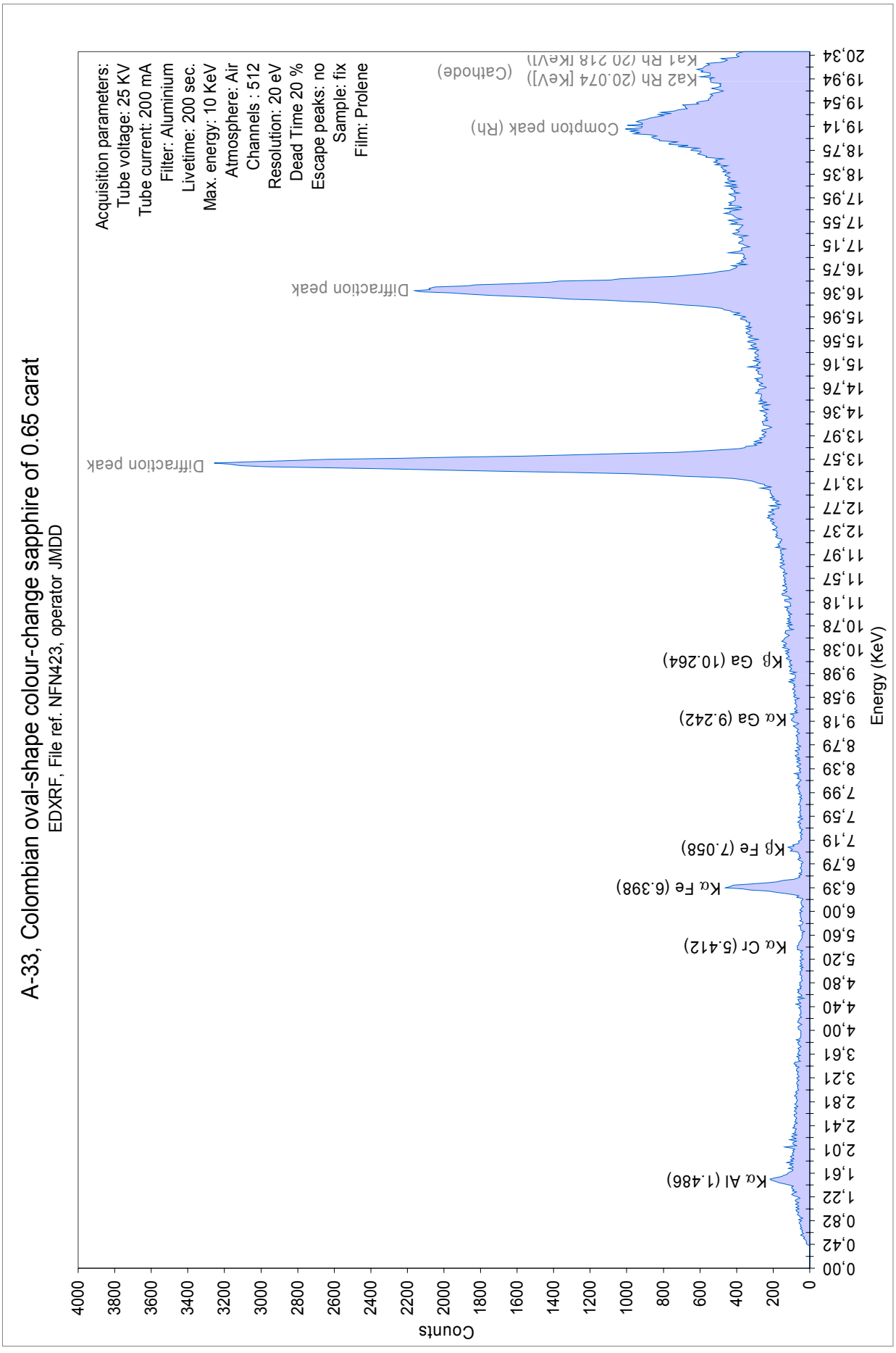
A-33, Colombian oval-shape colour-change sapphire of 0.65 carat
EDXRF, File ref. NFN423, operator JMDD
Acquisition parameters:
Tube voltage: 25 KV
Tube current: 200 mA
Filter: Aluminium
Livetime: 200 sec.
Max. energy: 10 KeV
Atmosphere: Air
Channels : 512
Resolution: 20 eV
Dead Time 20 %
Escape peaks: no
Sample: fix
Film: Prolene
Counts
Energy (KeV)
Kα Al (1.486)
Kα Cr (5.412)
Kα Fe (6.398)
Kβ Fe (7.058)
Kα Ga (9.242)
Kβ Ga (10.264)
Diffraction peak
Diffraction peak
Compton peak (Rh)
Ka2 Rh (20.074 [keV])
Ka1 Rh (20.218 [keV])
(Cathode)

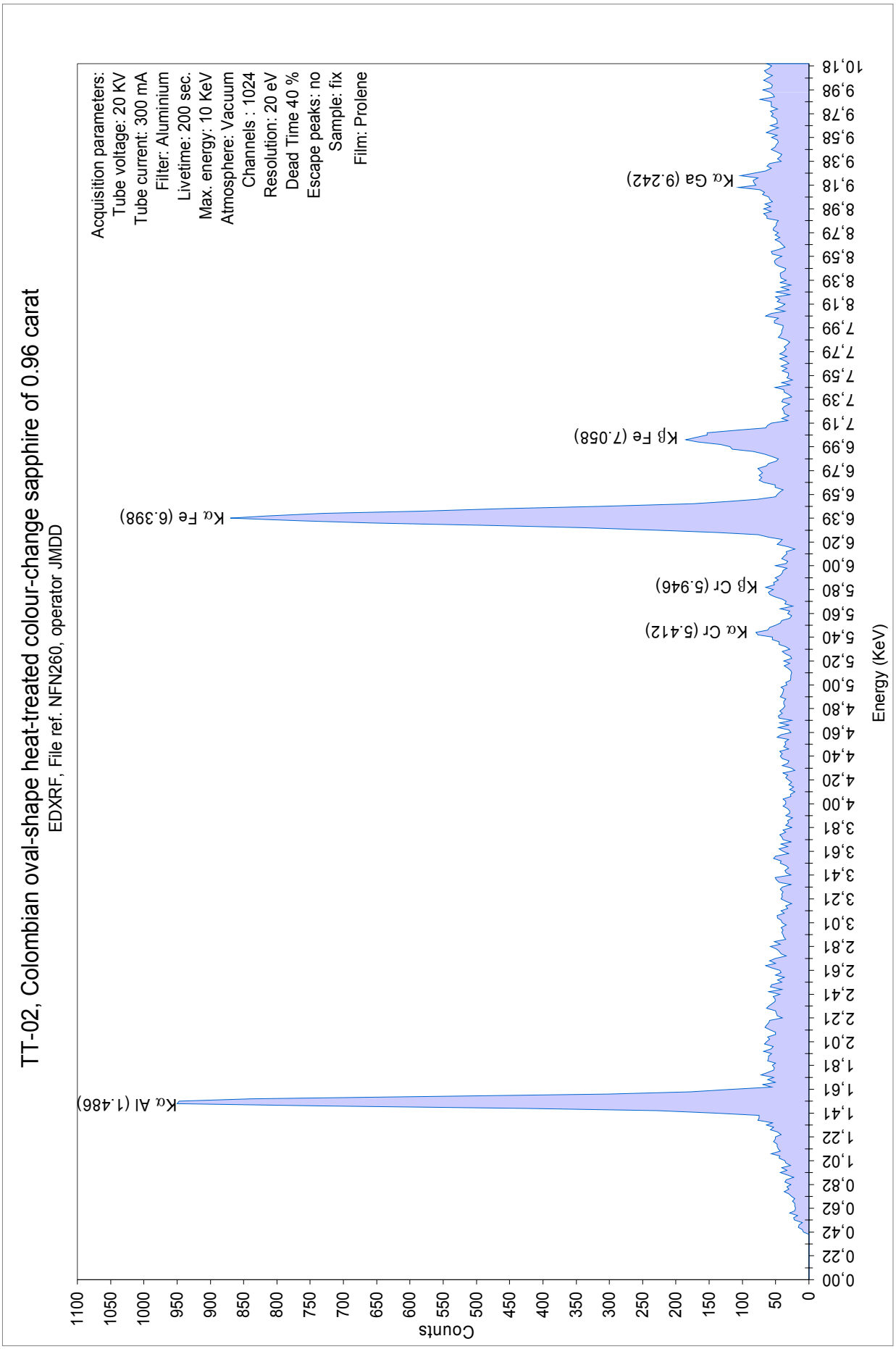
TT-02, Colombian oval-shape heat-treated colour-change sapphire of 0.96 carat
EDXRF, File ref. NFN260, operator JMDD
Acquisition parameters:
Tube voltage: 20 KV
Tube current: 300 mA
Filter: Aluminium
Livetime: 200 sec.
Max. energy: 10 KeV
Atmosphere: Vacuum
Channels : 1024
Resolution: 20 eV
Dead Time 40 %
Escape peaks: no
Sample: fix
Film: Prolene
Kα Al (1.486)
Kα Fe (6.398)
Kβ Fe (7.058)
Kα Ga (9.242)
Kα Cr (5.412)
Kβ Cr (5.946)
Counts
Energy (KeV)

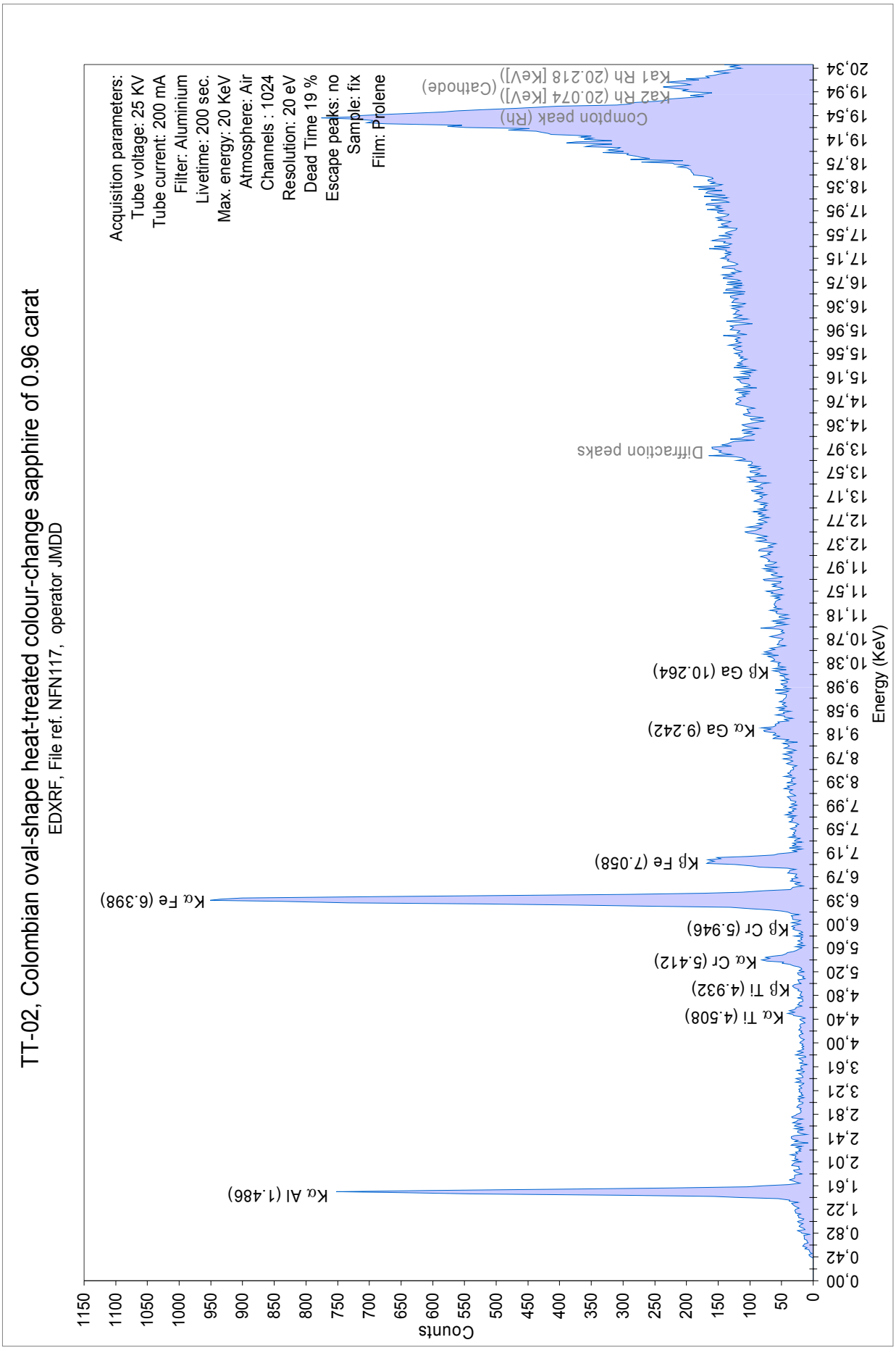
TT-02, Colombian oval-shape heat-treated colour-change sapphire of 0.96 carat
EDXRF, File ref. NFN117, operator JMDD
Acquisition parameters:
Tube voltage: 25 KV
Tube current: 200 mA
Filter: Aluminium
Livetime: 200 sec.
Max. energy: 20 KeV
Atmosphere: Air
Channels : 1024
Resolution: 20 eV
Dead Time 19 %
Escape peaks: no
Sample: fix
Film: Prolene
Kα Al (1.486)
Kα Fe (6.398)
Kβ Fe (7.058)
Kα Ga (9.242)
Kβ Ga (10.264)
Diffraction peaks
Compton peak (Rh)
Kα2 Rh (20.074 [KeV])
Kα1 Rh (20.218 [KeV]) (Cathode)
Kα Ti (4.508)
Kβ Ti (4.932)
Kα Cr (5.412)
Kβ Cr (5.946)
Counts
Energy (KeV)

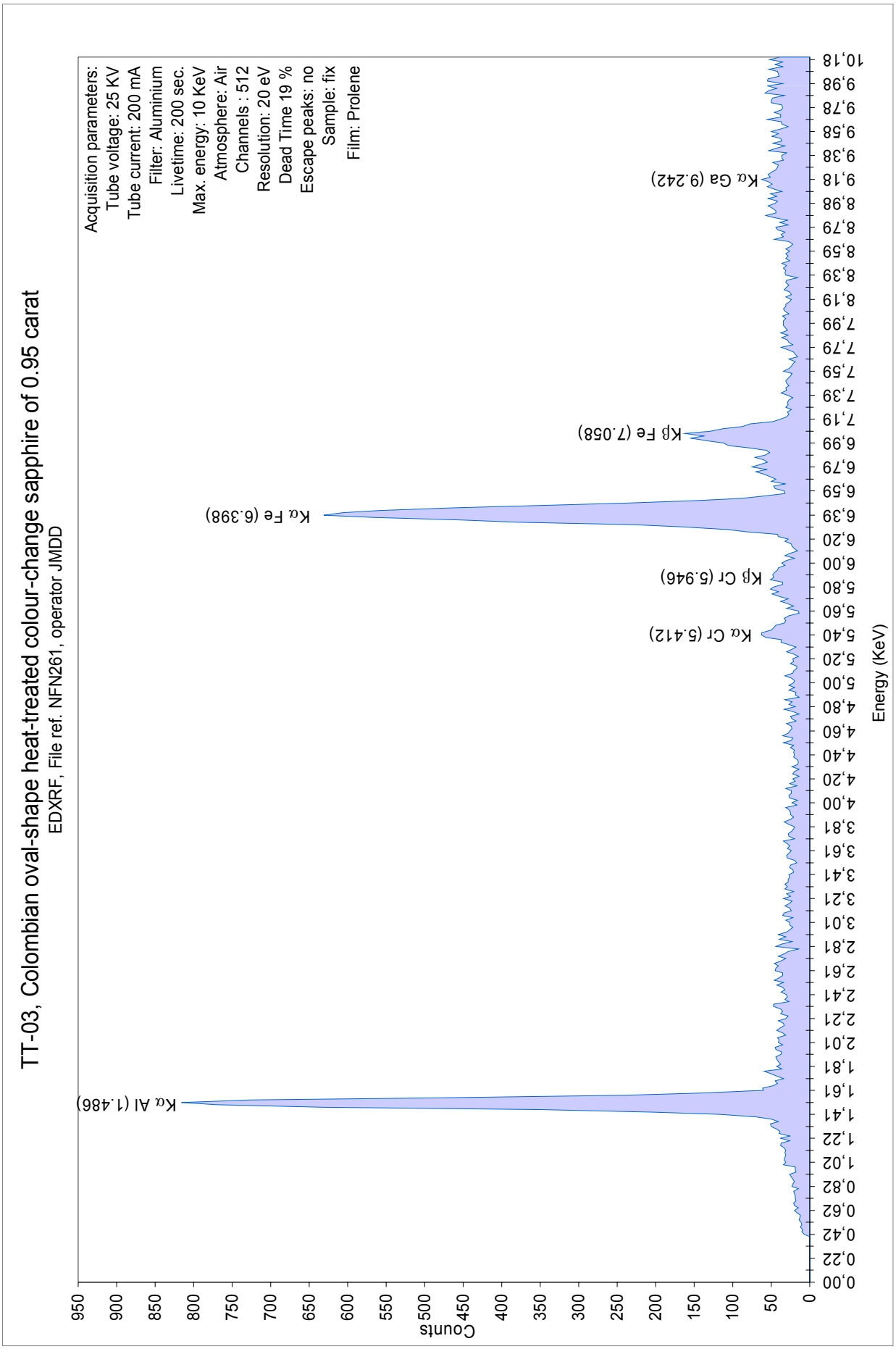
TT-03, Colombian oval-shape heat-treated colour-change sapphire of 0.95 carat
EDXRF, File ref. NFN261, operator JMDD
Acquisition parameters:
Tube voltage: 25 KV
Tube current: 200 mA
Filter: Aluminium
Livetime: 200 sec.
Max. energy: 10 KeV
Atmosphere: Air
Channels : 512
Resolution: 20 eV
Dead Time 19 %
Escape peaks: no
Sample: fix
Film: Prolene
Kα Al (1.486)
Kα Fe (6.398)
Kβ Fe (7.058)
Kα Ga (9.242)
Kα Cr (5.412)
Kβ Cr (5.946)
Counts
Energy (KeV)

ULTRA-VIOLET SPECTROPHOTOMETRY (UV-VIS)

All spectra were obtained on a Hitachi U-3000 UV-VIS spectrometer. This is a double-beam, ratio-recording instrument containing a grating monochromator, coated optical parts, automatic lamp and filter changes, end-on detector, GemTechLab polarizing plate, wavelength programmer unit, automatic gain control and built-in recorder. The instrument scans from 930 to 290 nm. The detector is less sensitive at both ends of the spectral range.
The instrumental working conditions were as follows: spectral bandwidth 1.0 nm, wavelength range 800 to 300 nm, scan speed 300 nm/sec.

Corundum, an allochromatic (literally: *other coloured*) mineral, owes its colour to trace elements not present in its chemical composition. When in its pure state Al_2O_3, corundum is colourless. The colour of sapphires and rubies is the result of various chromophoric elements (Fe, Ti, Cr,…) in the form of *impurities* present in the corundum host, in various amounts, ratios and configurations. These colour-bearing elements have been activated naturally during the growth process of the crystal, producing the colour we perceive.
Rarely are the chromophoric impurities present in the corundum host in ideal proportion and homogeneously distributed throughout the host to produce the beautiful colours of fine quality rubies and sapphires. An unbalanced configuration of the chromophoric elements results in less desirable coloration. For example, excessive amounts of iron/titanium in the blue sapphire produce a dark appearance, and an insufficient amount of these chromophoric elements produce pastel colour.
Sometimes, chromophores acting as colour-modifiers may be present in the corundum, producing an undesirable overcasted secondary colouring (brownish-blue, purplish-red, bluish-red,…), and occasionally appear as colour-patches (colour streaks or stripes, colour zoning, core-colour,…). There are other instances in which chromophoric elements present in the host corundum, have the capacity to produce a potential colour, but have not been activated during the growth process of the corundum (example: *geuda* corundum). These under proper treatment parameters, are heated to produce (or intensify) reduce (or eliminate) colour. To finally obtain the best improvement possible (Themelis, 1992).
Since colour when present, the best (more intense) is in almost all cases vehicled by the ordinary ray (ω), for comparable survey diagrams, all the samples to be tested (either rough or faceted) had their crystal faces oriented prior to scanning, and absorption spectra parallel and perpendicular to the C-axis were obtained separately.

Twenty-five of the rough sapphires (windowed) and twenty-three faceted stones were subjected to UV-VIS spectroscopic examination. The absorption spectrum obtained for these corundums can be viewed in the following pages

<u>The twenty five rough crystals</u>

As mentioned earlier (see chapter appearance), and as can be seen on the recorded spectra, pure colours were virtually not encountered. Most of these rough corundum crystals display an overcasted secondary colour, generally described as brownish, greenish, greyish, or pinkish.
Nearly all the UV-visible spectra obtained for these corundums show a more developped ω-ray than the ε-ray. This confirms that the more intense colour is mainly vehicled by the ω-ray.

Spectroscopic analysis of these rough crystals

The rough corundum crystals reveal two main types of spectrum:

- Those that show only the absorption bands of iron: display sharp bands at 377 nm (Fe^{3+}/Fe^{3+}), and 388 nm (Fe^{2+}), a medium to strong band at 450 nm (Fe^{3+}/Fe^{3+}), and a very broad band at 565 nm (IVCT $Fe^{2+} \rightarrow Ti^{4+}$).
  Their relative intensities however varies substantially from one specimen to another, and these variations are responsible for the different hues recorded (the least iron doped sapphire displays the least developped iron spectrum, and therefore the weakest colour in the blue, green, or yellow hues).

- Those that show the Fe absorption bands already mentioned, plus chromium absorption bands.
  The chromium rich sapphires (example GT-R1, a pinkish-brown sapphire), display a sharp band at 693 nm (Cr^{3+}), a broad band at 554 nm (Cr^{3+}), sharp bands at 475-477 nm (Cr^{3+}), and 468 nm (Cr^{3+}), and a broad band at 405-410 nm (Cr^{3+}). Usually, these absorptions are of rather low intensities, and correspond to the intensity of the red hue observed in these rough corundums.

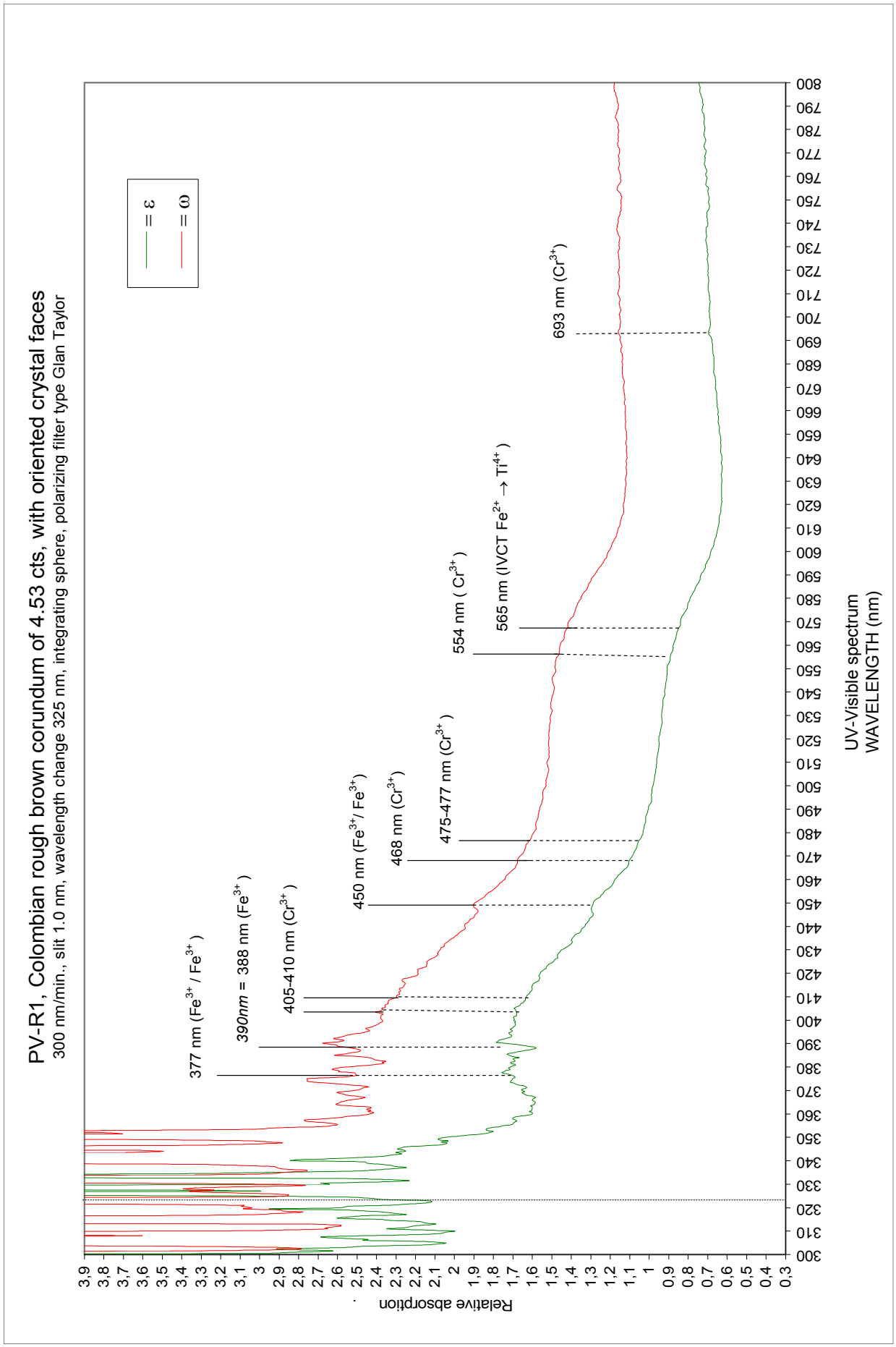
PV-R1, Colombian rough brown corundum of 4.53 cts, with oriented crystal faces
300 nm/min., slit 1.0 nm, wavelength change 325 nm, integrating sphere, polarizing filter type Glan Taylor
ε
ω
377 nm (Fe3+ / Fe3+)
390nm = 388 nm (Fe3+)
405-410 nm (Cr3+)
450 nm (Fe3+/ Fe3+)
468 nm (Cr3+)
475-477 nm (Cr3+)
554 nm (Cr3+)
565 nm (IVCT Fe2+ → Ti4+)
693 nm (Cr3+)
Relative absorption
UV-Visible spectrum
WAVELENGTH (nm)

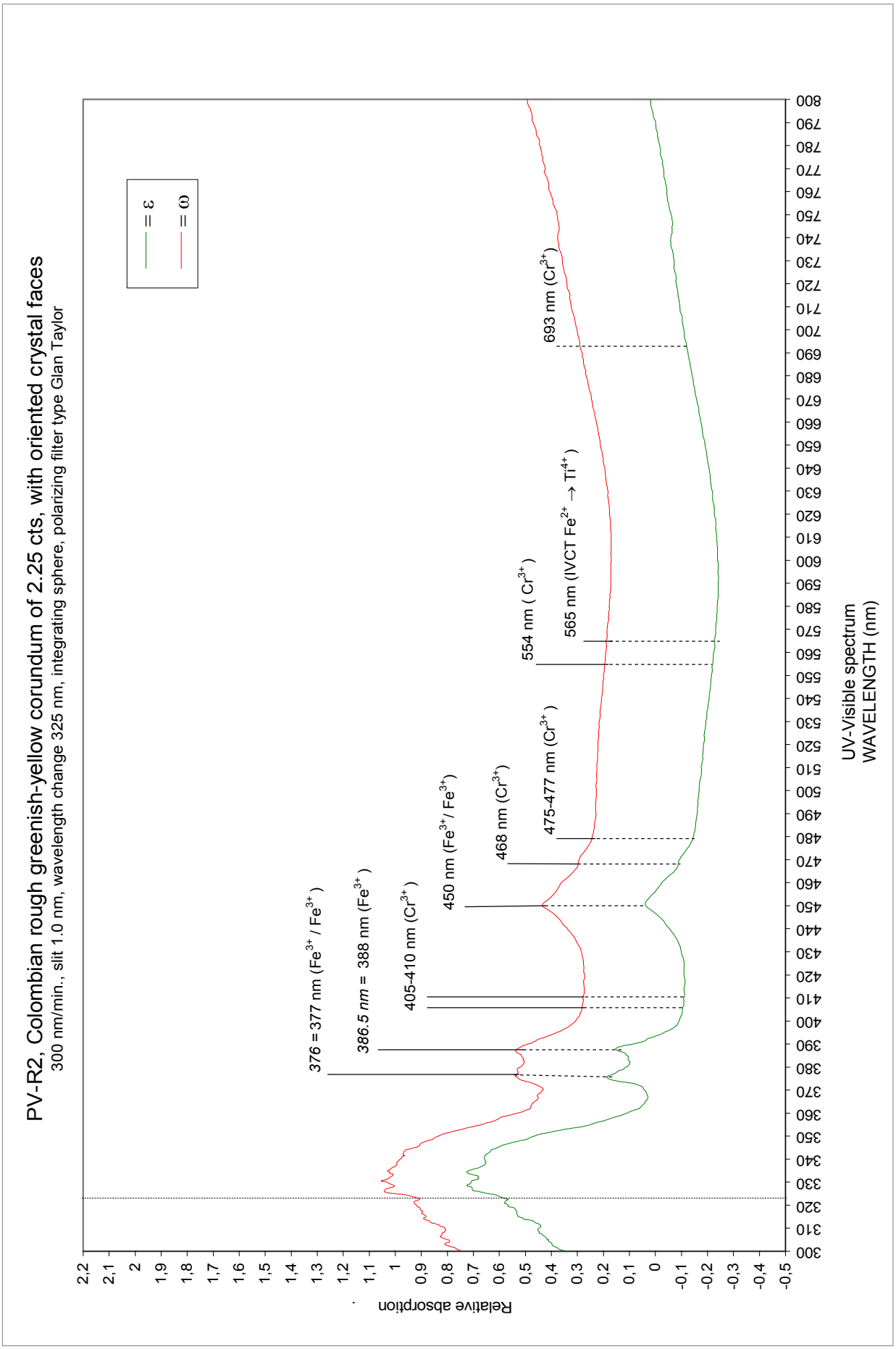
PV-R2, Colombian rough greenish-yellow corundum of 2.25 cts, with oriented crystal faces
300 nm/min., slit 1.0 nm, wavelength change 325 nm, integrating sphere, polarizing filter type Glan Taylor
ε
ω
376 = 377 nm (Fe3+ / Fe3+)
386.5 nm = 388 nm (Fe3+)
405-410 nm (Cr3+)
450 nm (Fe3+/ Fe3+)
468 nm (Cr3+)
475-477 nm (Cr3+)
554 nm (Cr3+)
565 nm (IVCT Fe2+ → Ti4+)
693 nm (Cr3+)
Relative absorption
UV-Visible spectrum
WAVELENGTH (nm)

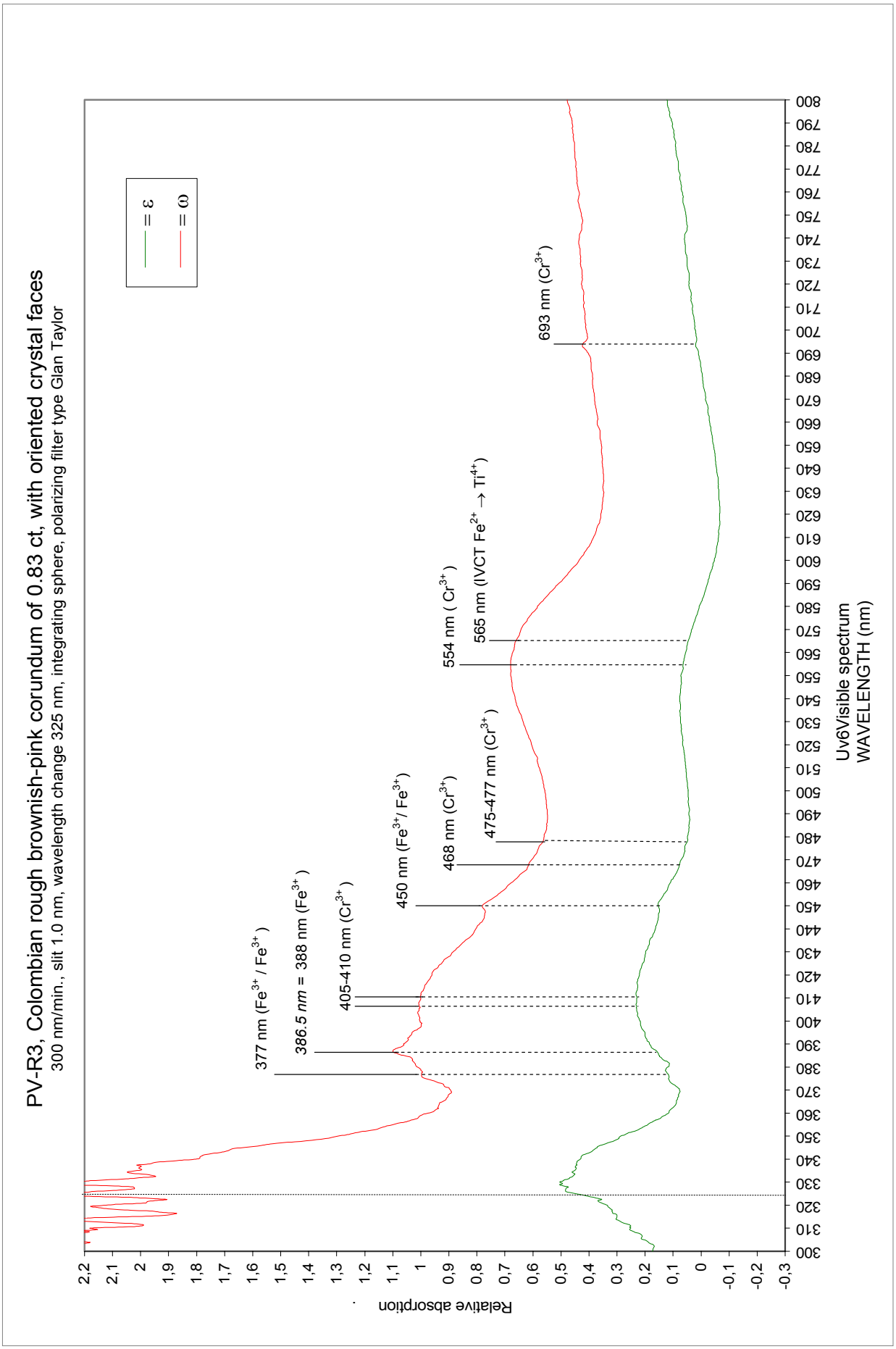
PV-R3, Colombian rough brownish-pink corundum of 0.83 ct, with oriented crystal faces
300 nm/min., slit 1.0 nm, wavelength change 325 nm, integrating sphere, polarizing filter type Glan Taylor
ε
ω
377 nm (Fe3+ / Fe3+)
386.5 nm = 388 nm (Fe3+)
405-410 nm (Cr3+)
450 nm (Fe3+/ Fe3+)
468 nm (Cr3+)
475-477 nm (Cr3+)
554 nm (Cr3+)
565 nm (IVCT Fe2+ → Ti4+)
693 nm (Cr3+)
Relative absorption
Uv6Visible spectrum
WAVELENGTH (nm)

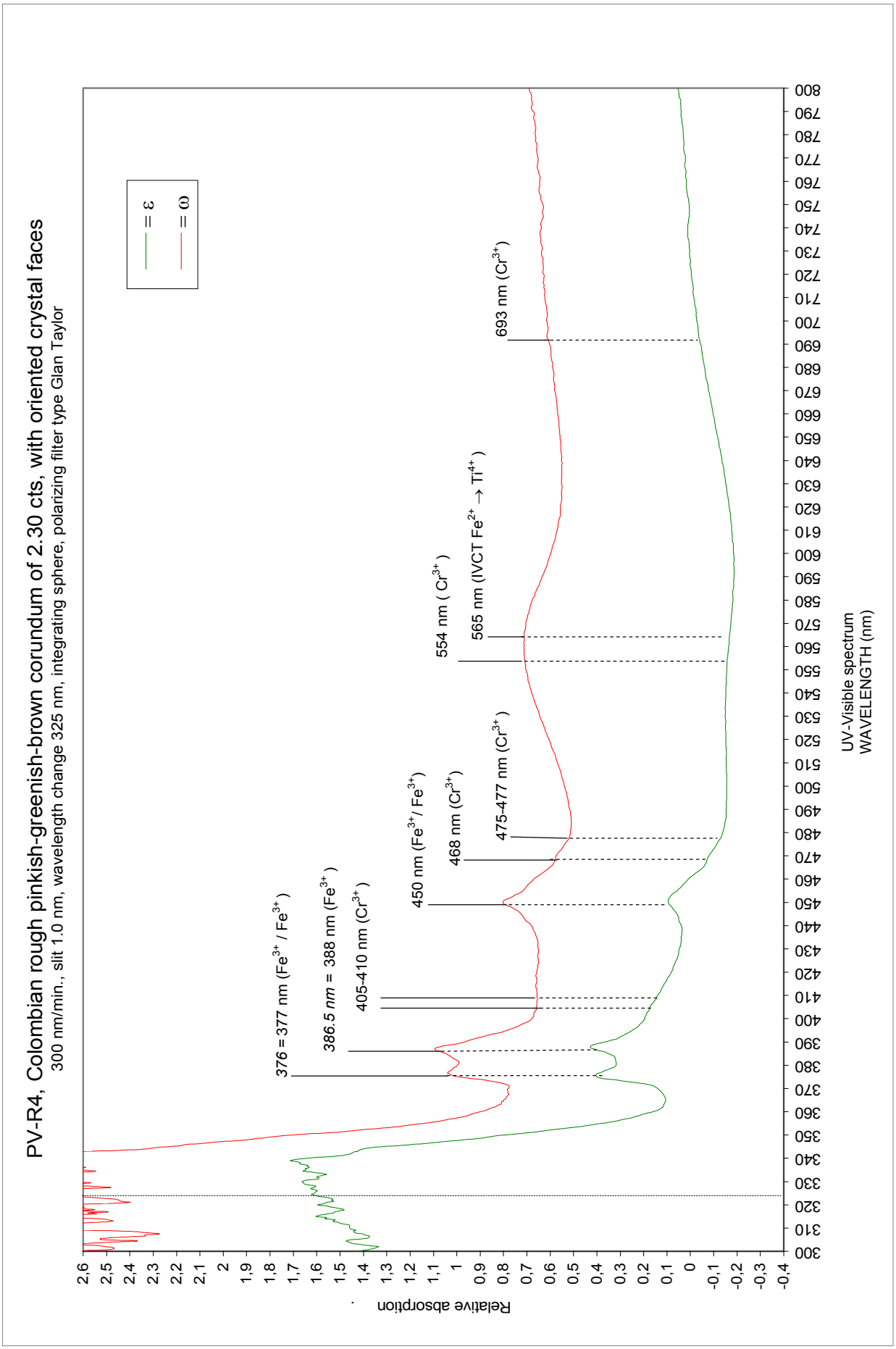
PV-R4, Colombian rough pinkish-greenish-brown corundum of 2.30 cts, with oriented crystal faces
300 nm/min., slit 1.0 nm, wavelength change 325 nm, integrating sphere, polarizing filter type Glan Taylor
ε =
ω =
376 = 377 nm (Fe3+ / Fe3+)
386.5 nm = 388 nm (Fe3+)
405-410 nm (Cr3+)
450 nm (Fe3+/ Fe3+)
468 nm (Cr3+)
475-477 nm (Cr3+)
554 nm (Cr3+)
565 nm (IVCT Fe2+ → Ti4+)
693 nm (Cr3+)
Relative absorption
UV-Visible spectrum
WAVELENGTH (nm)

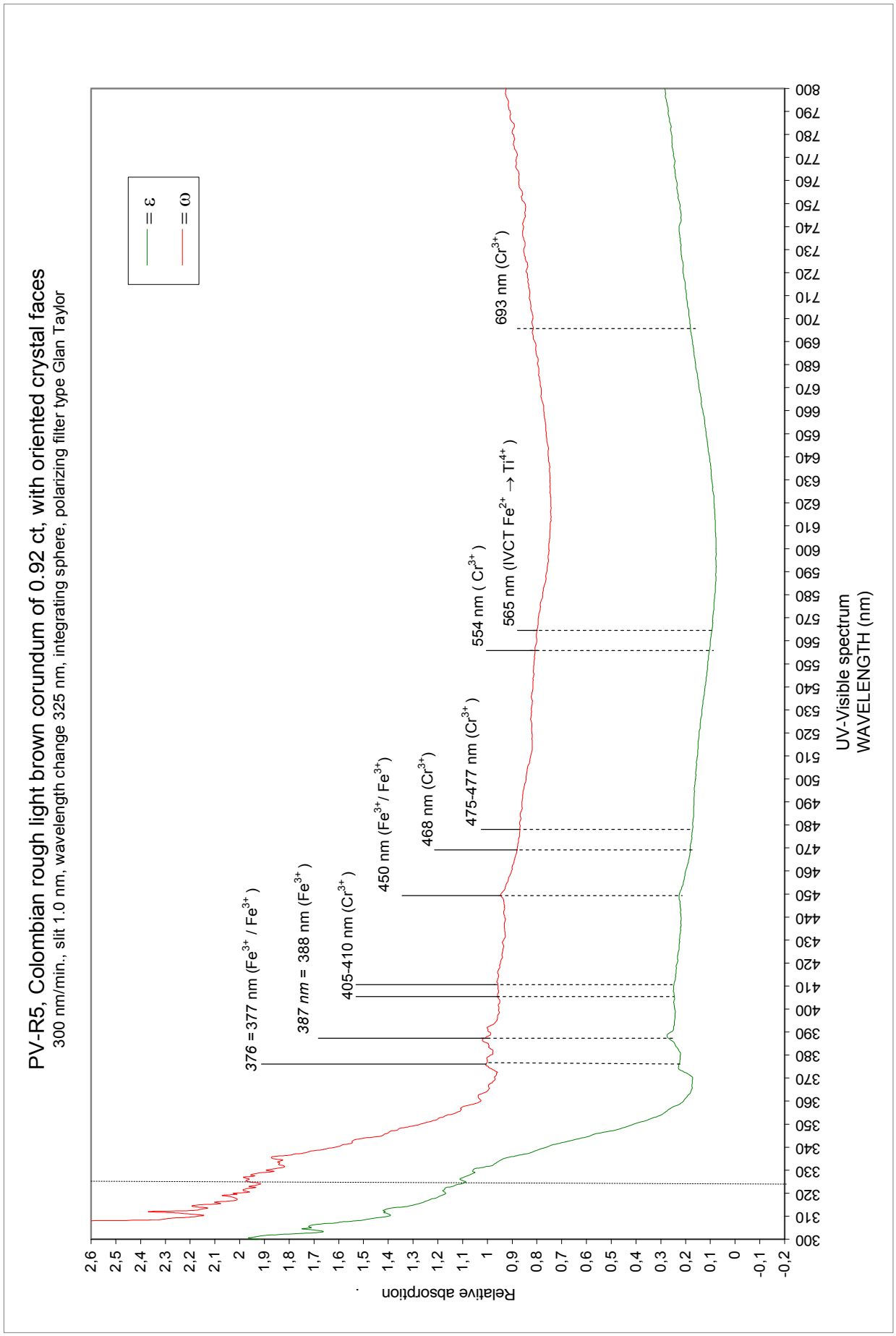
PV-R5, Colombian rough light brown corundum of 0.92 ct, with oriented crystal faces
300 nm/min., slit 1.0 nm, wavelength change 325 nm, integrating sphere, polarizing filter type Glan Taylor
ε
ω
376 = 377 nm (Fe3+ / Fe3+)
387 nm = 388 nm (Fe3+)
405-410 nm (Cr3+)
450 nm (Fe3+/ Fe3+)
468 nm (Cr3+)
475-477 nm (Cr3+)
554 nm (Cr3+)
565 nm (IVCT Fe2+ → Ti4+)
693 nm (Cr3+)
Relative absorption
UV-Visible spectrum
WAVELENGTH (nm)

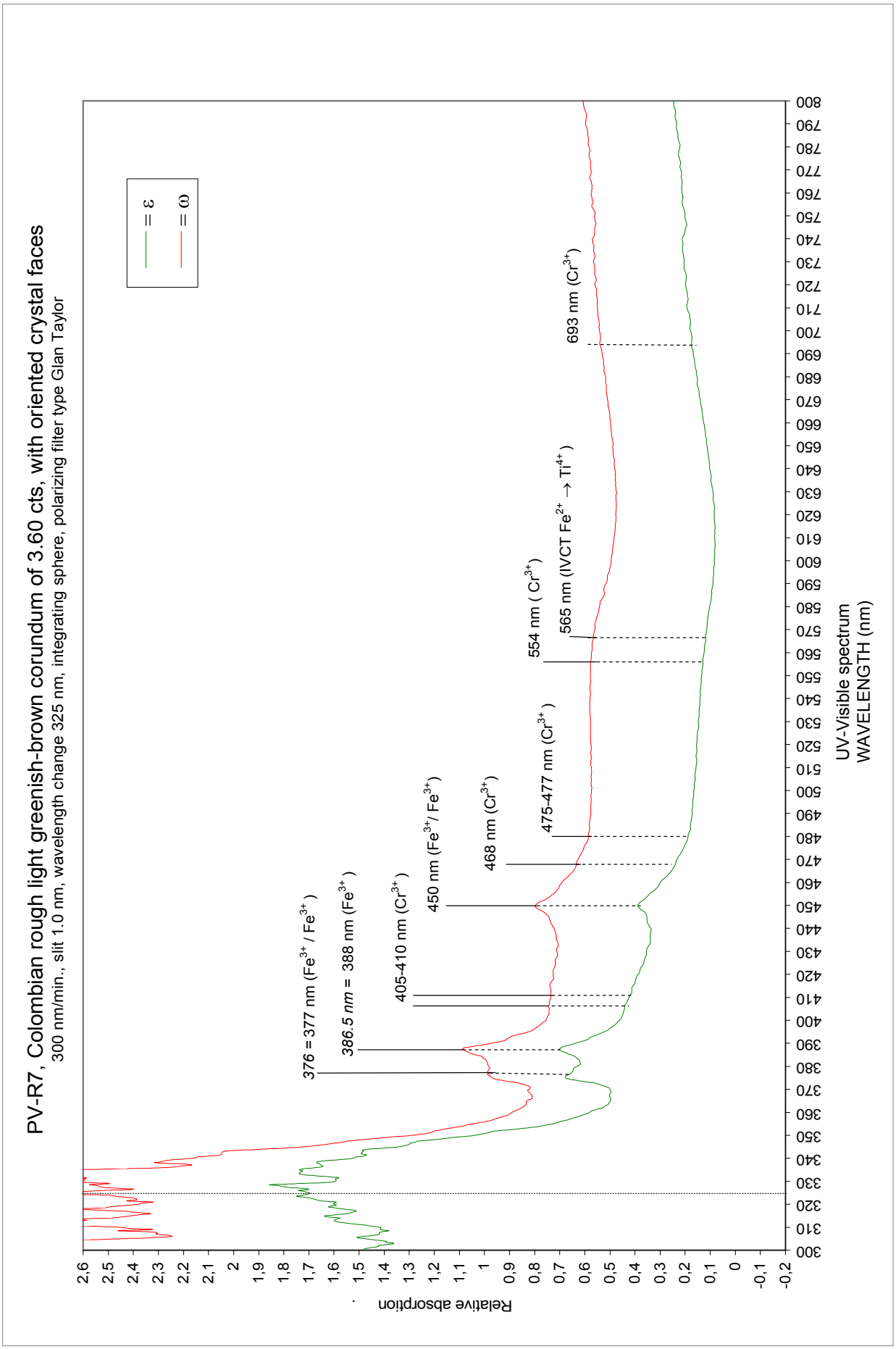
PV-R7, Colombian rough light greenish-brown corundum of 3.60 cts, with oriented crystal faces
300 nm/min., slit 1.0 nm, wavelength change 325 nm, integrating sphere, polarizing filter type Glan Taylor
ε =
ω =
376 = 377 nm (Fe3+ / Fe3+)
386.5 nm = 388 nm (Fe3+)
405-410 nm (Cr3+)
450 nm (Fe3+/ Fe3+)
468 nm (Cr3+)
475-477 nm (Cr3+)
554 nm (Cr3+)
565 nm (IVCT Fe2+ → Ti4+)
693 nm (Cr3+)
Relative absorption
UV-Visible spectrum
WAVELENGTH (nm)

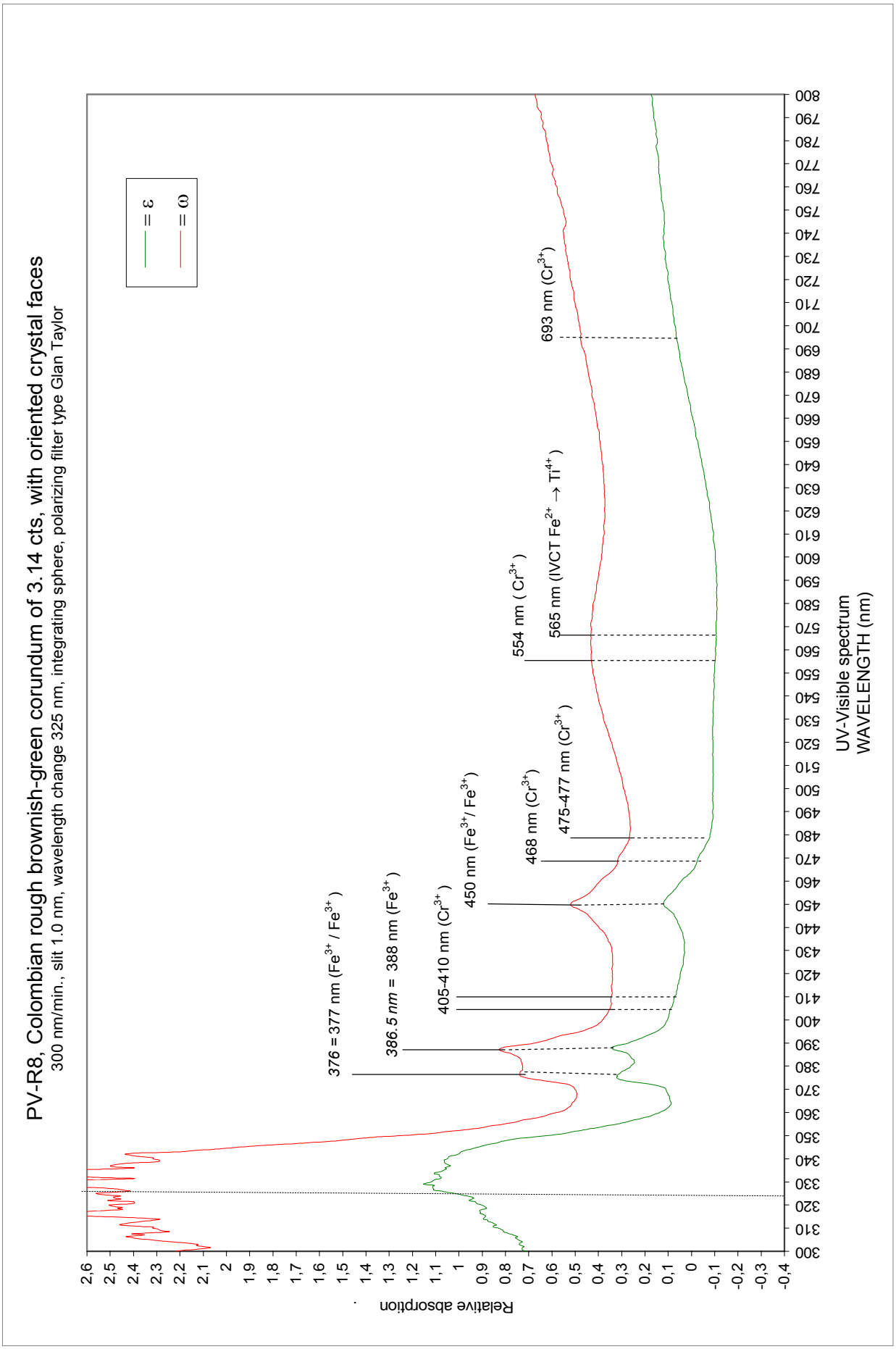
PV-R8, Colombian rough brownish-green corundum of 3.14 cts, with oriented crystal faces
300 nm/min., slit 1.0 nm, wavelength change 325 nm, integrating sphere, polarizing filter type Glan Taylor
ε =
ω =
376 = 377 nm (Fe3+ / Fe3+)
386.5 nm = 388 nm (Fe3+)
405-410 nm (Cr3+)
450 nm (Fe3+/ Fe3+)
468 nm (Cr3+)
475-477 nm (Cr3+)
554 nm (Cr3+)
565 nm (IVCT Fe2+ → Ti4+)
693 nm (Cr3+)
Relative absorption
UV-Visible spectrum
WAVELENGTH (nm)

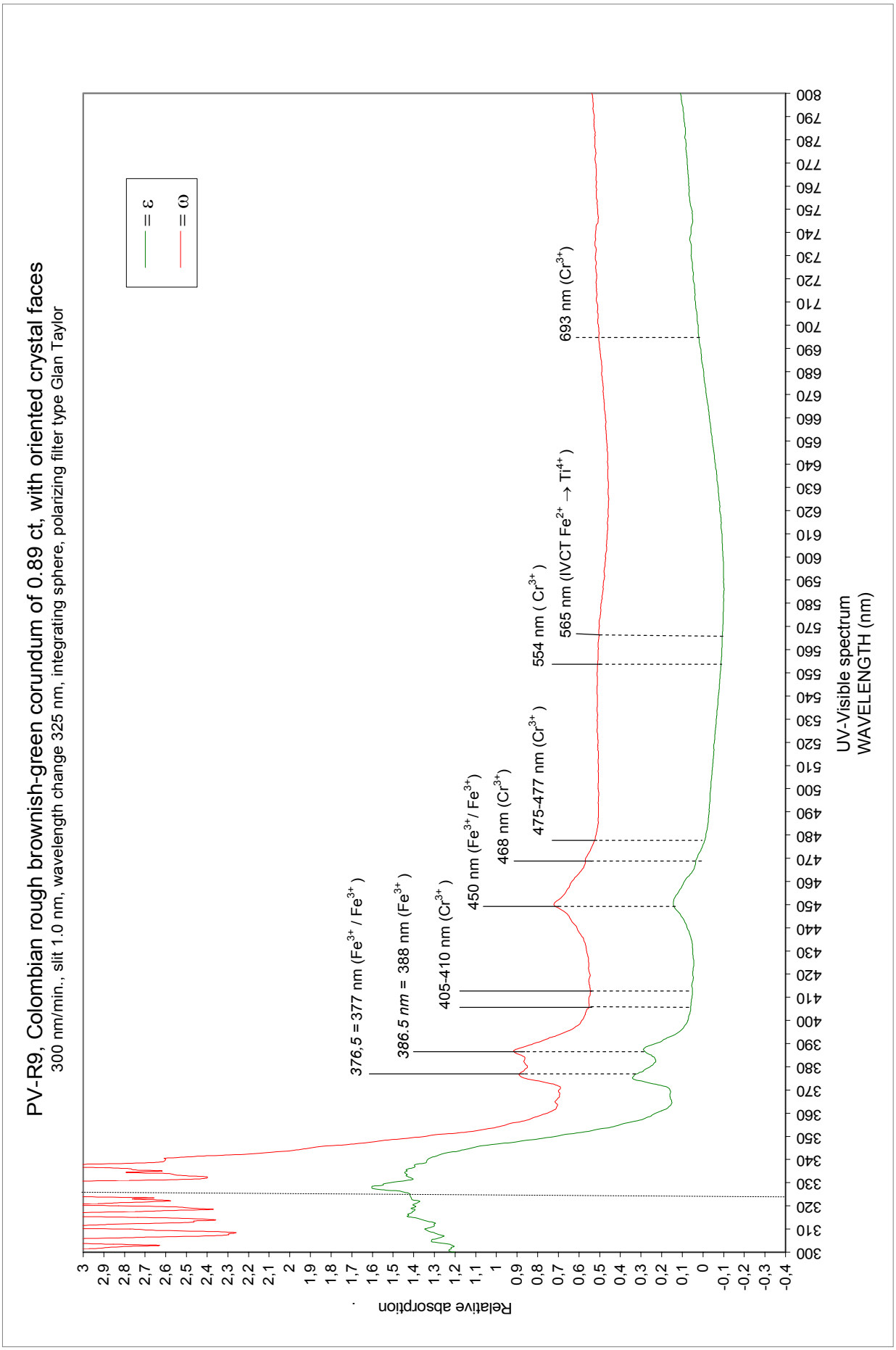
PV-R9, Colombian rough brownish-green corundum of 0.89 ct, with oriented crystal faces
300 nm/min., slit 1.0 nm, wavelength change 325 nm, integrating sphere, polarizing filter type Glan Taylor
ε =
ω =
376,5 = 377 nm (Fe3+ / Fe3+)
386.5 nm = 388 nm (Fe3+)
405-410 nm (Cr3+)
450 nm (Fe3+ / Fe3+)
468 nm (Cr3+)
475-477 nm (Cr3+)
554 nm (Cr3+)
565 nm (IVCT Fe2+ → Ti4+)
693 nm (Cr3+)
Relative absorption
UV-Visible spectrum
WAVELENGTH (nm)

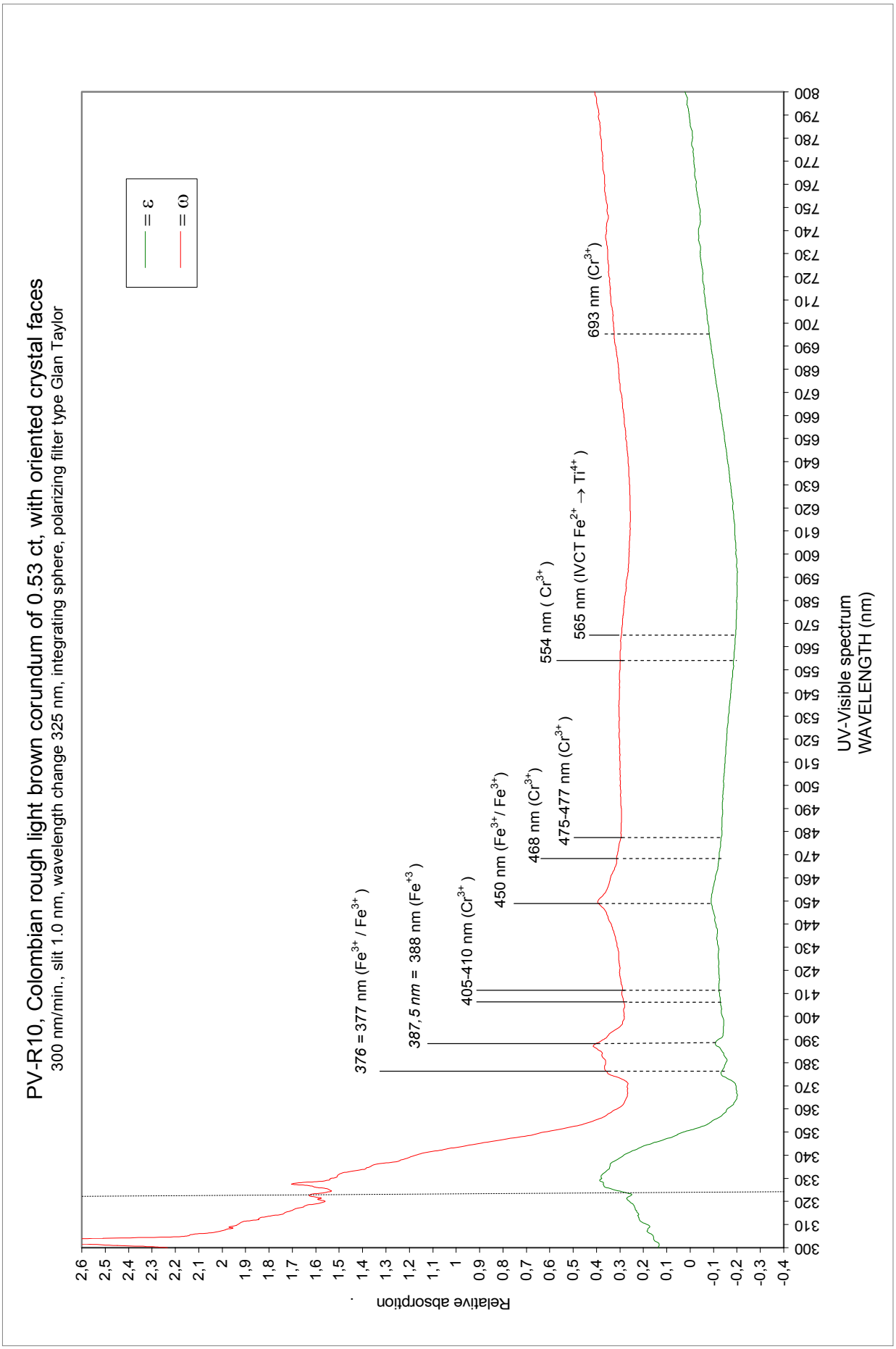
PV-R10, Colombian rough light brown corundum of 0.53 ct, with oriented crystal faces
300 nm/min., slit 1.0 nm, wavelength change 325 nm, integrating sphere, polarizing filter type Glan Taylor
ε =
ω =
376 = 377 nm (Fe3+ / Fe3+)
387,5 nm = 388 nm (Fe+3)
405-410 nm (Cr3+)
450 nm (Fe3+/ Fe3+)
468 nm (Cr3+)
475-477 nm (Cr3+)
554 nm (Cr3+)
565 nm (IVCT Fe2+ → Ti4+)
693 nm (Cr3+)
Relative absorption
UV-Visible spectrum
WAVELENGTH (nm)

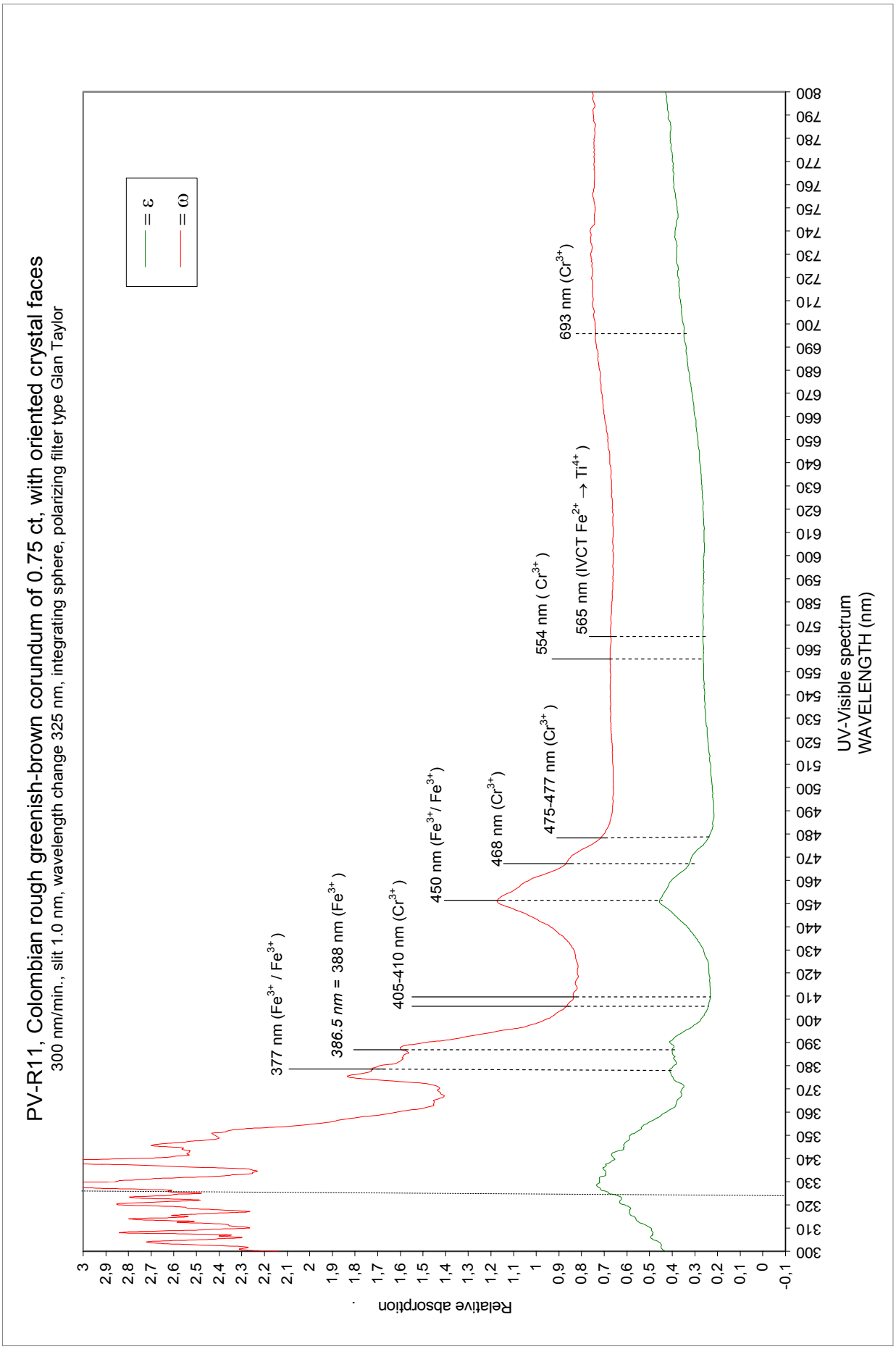
PV-R11, Colombian rough greenish-brown corundum of 0.75 ct, with oriented crystal faces
300 nm/min., slit 1.0 nm, wavelength change 325 nm, integrating sphere, polarizing filter type Glan Taylor
= ε
= ω
377 nm (Fe3+ / Fe3+)
386.5 nm = 388 nm (Fe3+)
405-410 nm (Cr3+)
450 nm (Fe3+/ Fe3+)
468 nm (Cr3+)
475-477 nm (Cr3+)
554 nm (Cr3+)
565 nm (IVCT Fe2+ → Ti4+)
693 nm (Cr3+)
Relative absorption
UV-Visible spectrum
WAVELENGTH (nm)

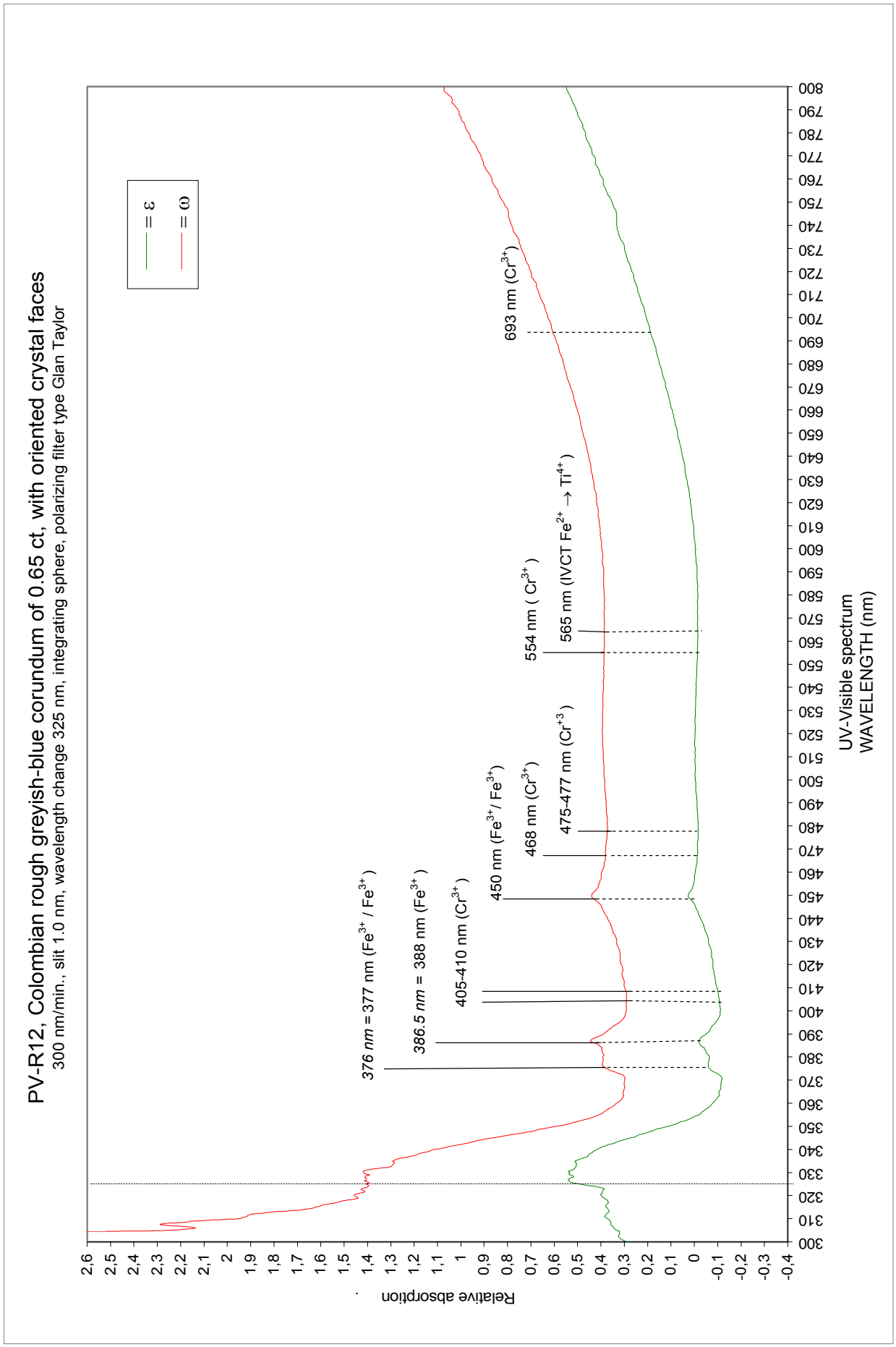
PV-R12, Colombian rough greyish-blue corundum of 0.65 ct, with oriented crystal faces
300 nm/min., slit 1.0 nm, wavelength change 325 nm, integrating sphere, polarizing filter type Glan Taylor
= ε
= ω
376 nm = 377 nm (Fe3+ / Fe3+)
386.5 nm = 388 nm (Fe3+)
405-410 nm (Cr3+)
450 nm (Fe3+/ Fe3+)
468 nm (Cr3+)
475-477 nm (Cr+3)
554 nm (Cr3+)
565 nm (IVCT Fe2+ → Ti4+)
693 nm (Cr3+)
Relative absorption
UV-Visible spectrum
WAVELENGTH (nm)

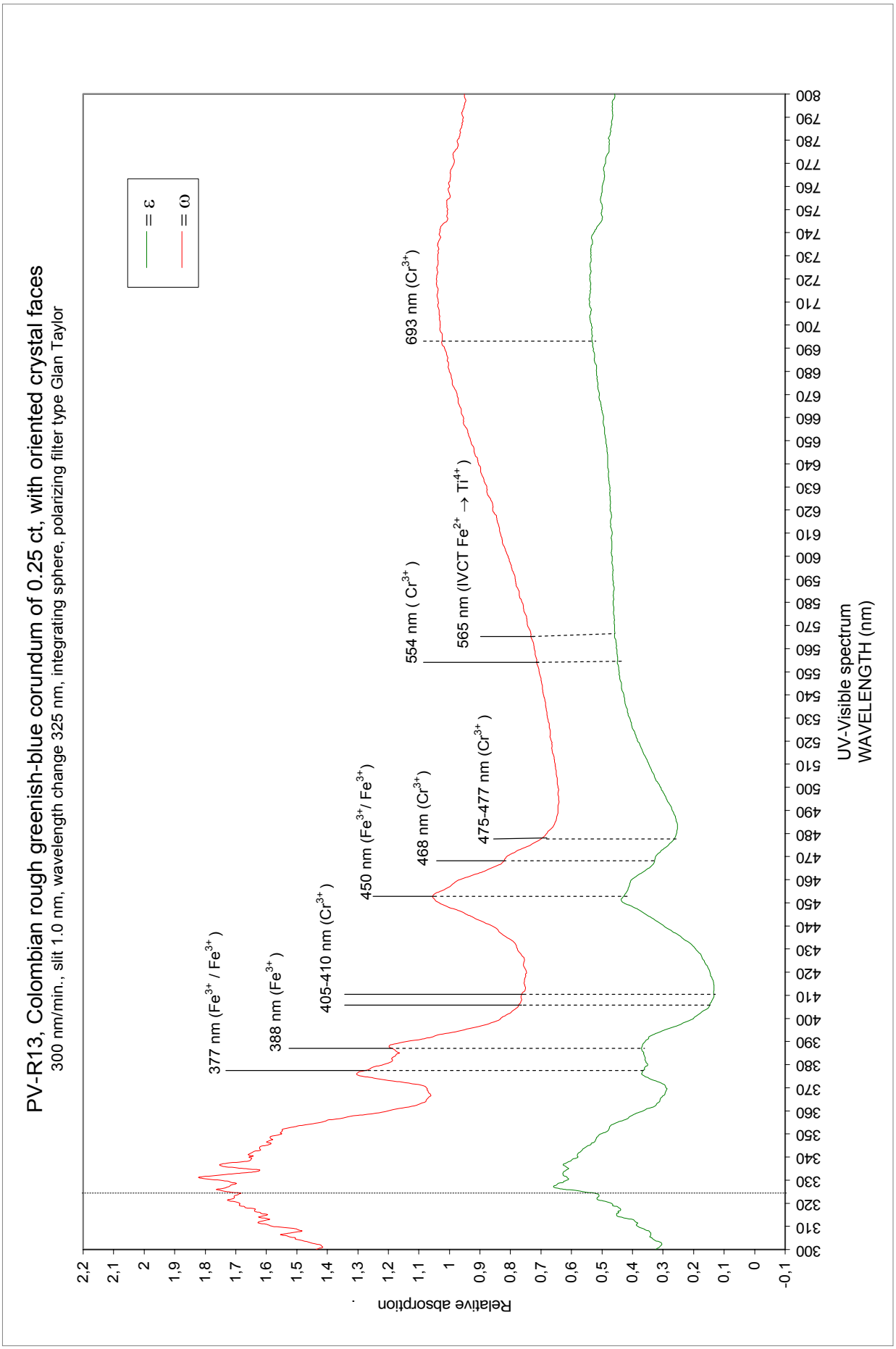
PV-R13, Colombian rough greenish-blue corundum of 0.25 ct, with oriented crystal faces
300 nm/min., slit 1.0 nm, wavelength change 325 nm, integrating sphere, polarizing filter type Glan Taylor
ε =
ω =
377 nm (Fe3+ / Fe3+)
388 nm (Fe3+)
405-410 nm (Cr3+)
450 nm (Fe3+/ Fe3+)
468 nm (Cr3+)
475-477 nm (Cr3+)
554 nm (Cr3+)
565 nm (IVCT Fe2+ → Ti4+)
693 nm (Cr3+)
Relative absorption
UV-Visible spectrum
WAVELENGTH (nm)

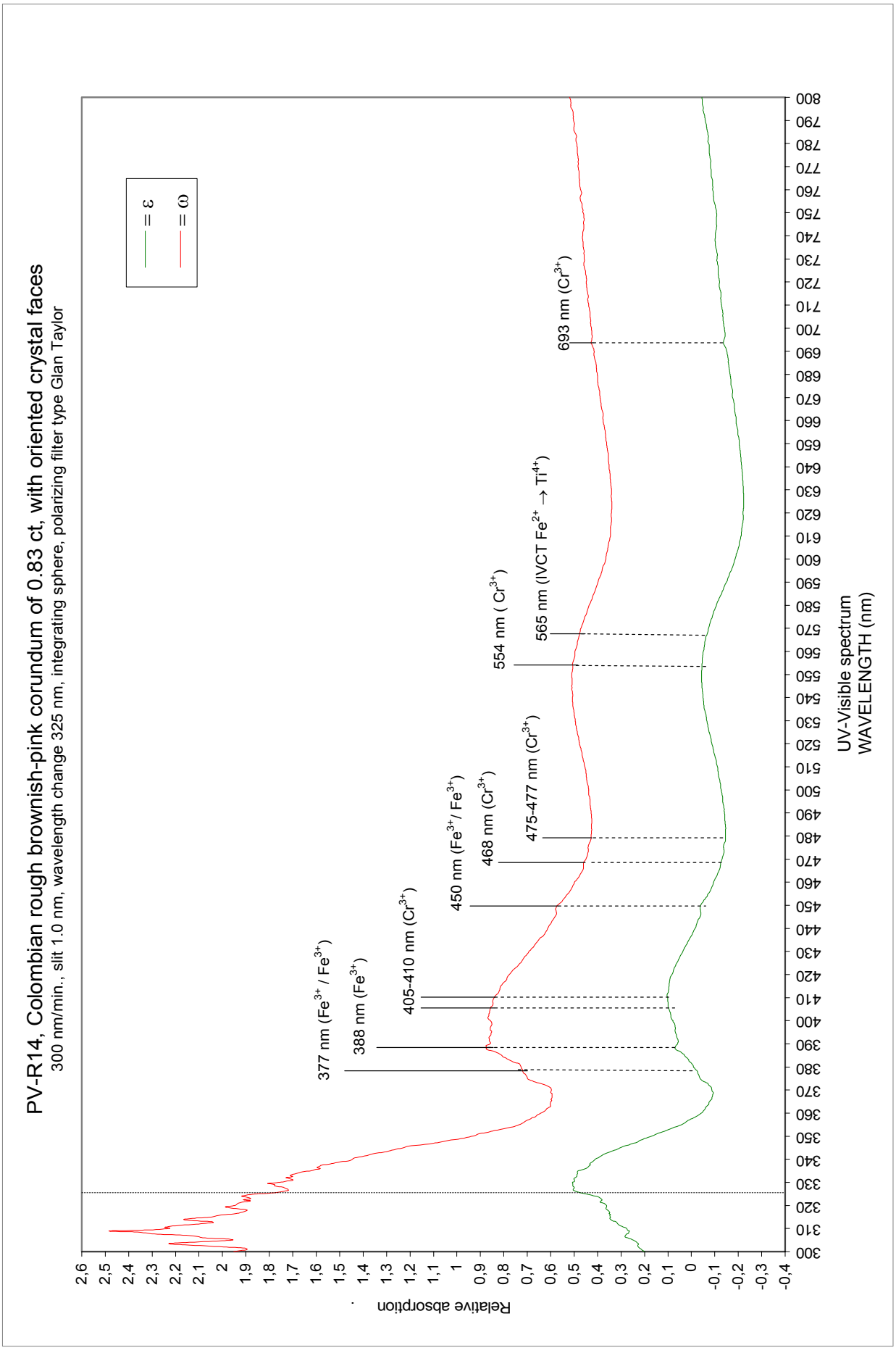
PV-R14, Colombian rough brownish-pink corundum of 0.83 ct, with oriented crystal faces
300 nm/min., slit 1.0 nm, wavelength change 325 nm, integrating sphere, polarizing filter type Glan Taylor
ε
ω
377 nm (Fe3+ / Fe3+)
388 nm (Fe3+)
405-410 nm (Cr3+)
450 nm (Fe3+ / Fe3+)
468 nm (Cr3+)
475-477 nm (Cr3+)
554 nm (Cr3+)
565 nm (IVCT Fe2+ → Ti4+)
693 nm (Cr3+)
Relative absorption
UV-Visible spectrum
WAVELENGTH (nm)

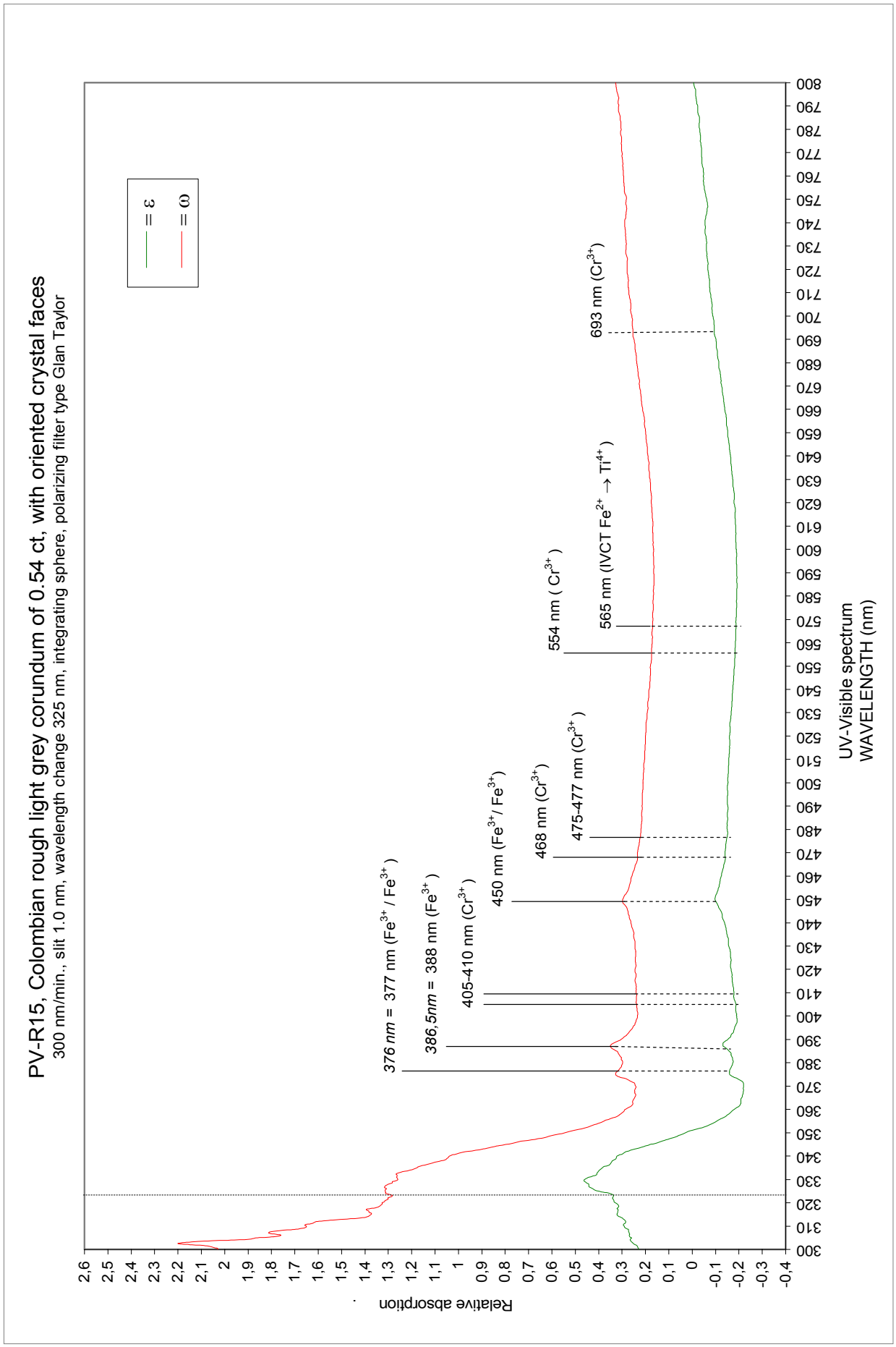
PV-R15, Colombian rough light grey corundum of 0.54 ct, with oriented crystal faces
300 nm/min., slit 1.0 nm, wavelength change 325 nm, integrating sphere, polarizing filter type Glan Taylor
= ε
= ω
376 nm = 377 nm (Fe3+ / Fe3+)
386,5nm = 388 nm (Fe3+)
405-410 nm (Cr3+)
450 nm (Fe3+/ Fe3+)
468 nm (Cr3+)
475-477 nm (Cr3+)
554 nm (Cr3+)
565 nm (IVCT Fe2+ → Ti4+)
693 nm (Cr3+)
Relative absorption
UV-Visible spectrum
WAVELENGTH (nm)

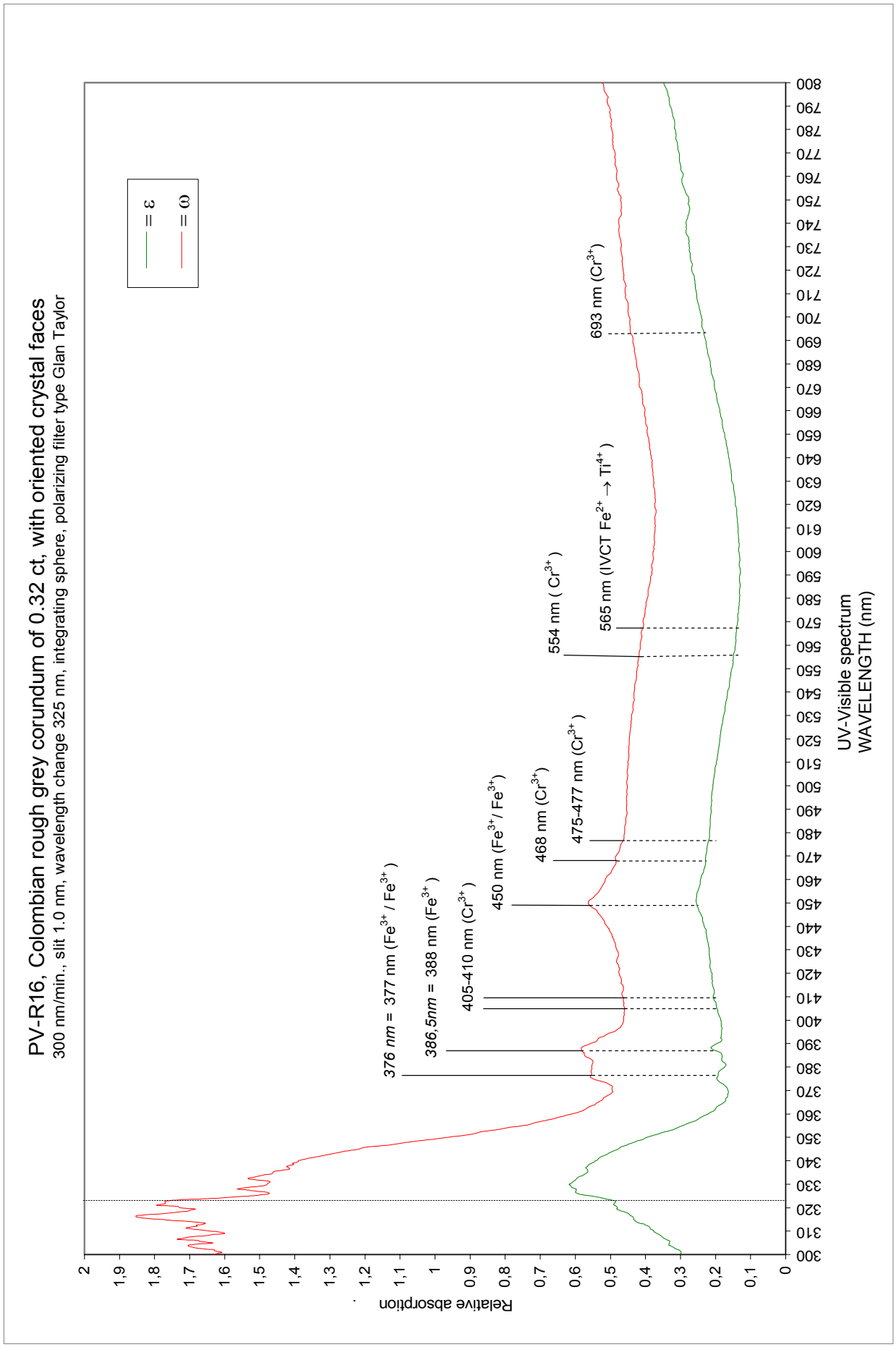
PV-R16, Colombian rough grey corundum of 0.32 ct, with oriented crystal faces
300 nm/min., slit 1.0 nm, wavelength change 325 nm, integrating sphere, polarizing filter type Glan Taylor
= ε
= ω
376 nm = 377 nm (Fe3+ / Fe3+)
386,5nm = 388 nm (Fe3+)
405-410 nm (Cr3+)
450 nm (Fe3+ / Fe3+)
468 nm (Cr3+)
475-477 nm (Cr3+)
554 nm (Cr3+)
565 nm (IVCT Fe2+ → Ti4+)
693 nm (Cr3+)
Relative absorption
UV-Visible spectrum
WAVELENGTH (nm)

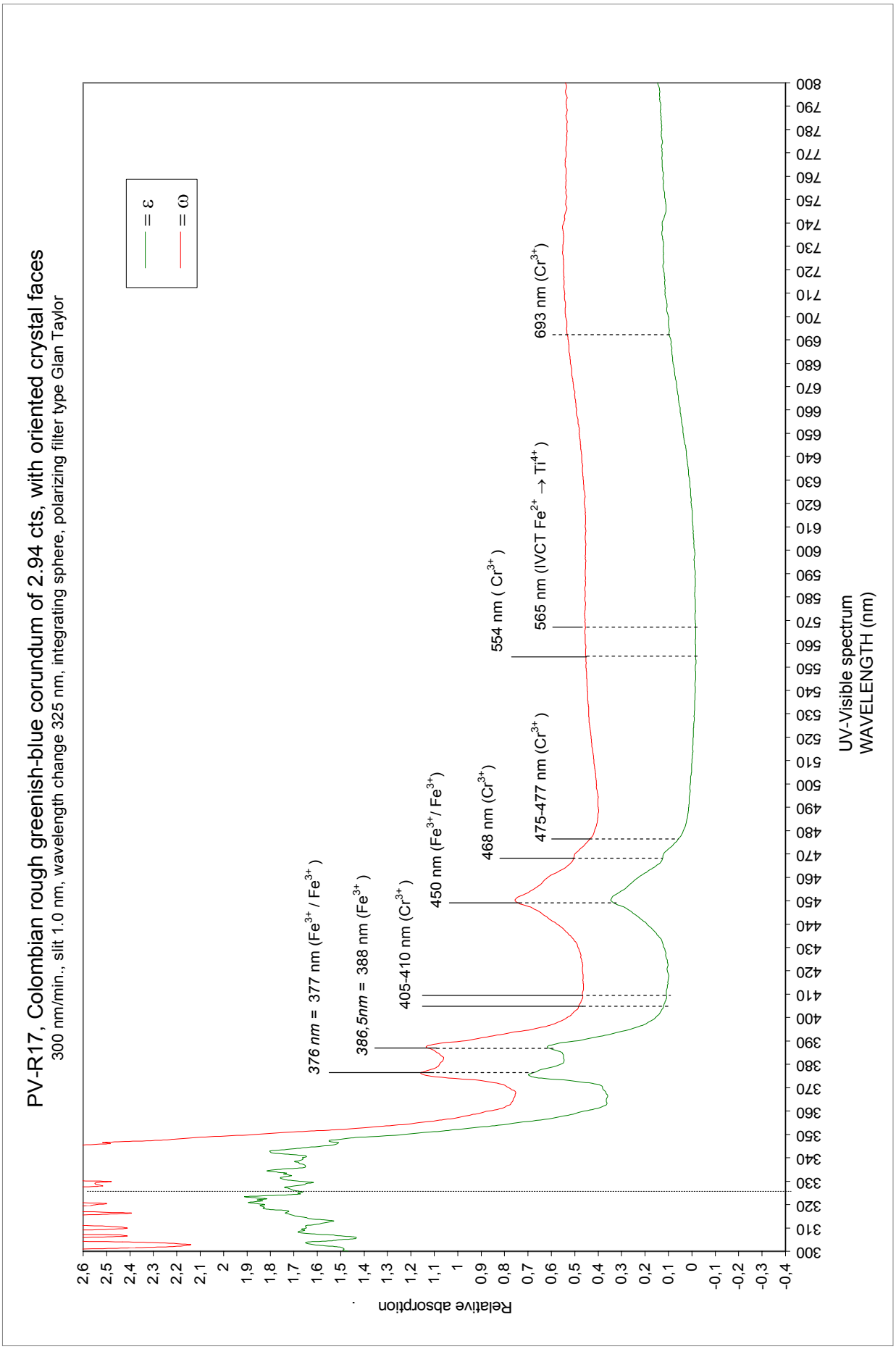
PV-R17, Colombian rough greenish-blue corundum of 2.94 cts, with oriented crystal faces
300 nm/min., slit 1.0 nm, wavelength change 325 nm, integrating sphere, polarizing filter type Glan Taylor
= ε
= ω
376 nm = 377 nm (Fe3+ / Fe3+)
386,5nm = 388 nm (Fe3+)
405-410 nm (Cr3+)
450 nm (Fe3+/ Fe3+)
468 nm (Cr3+)
475-477 nm (Cr3+)
554 nm (Cr3+)
565 nm (IVCT Fe2+ → Ti4+)
693 nm (Cr3+)
Relative absorption
UV-Visible spectrum
WAVELENGTH (nm)

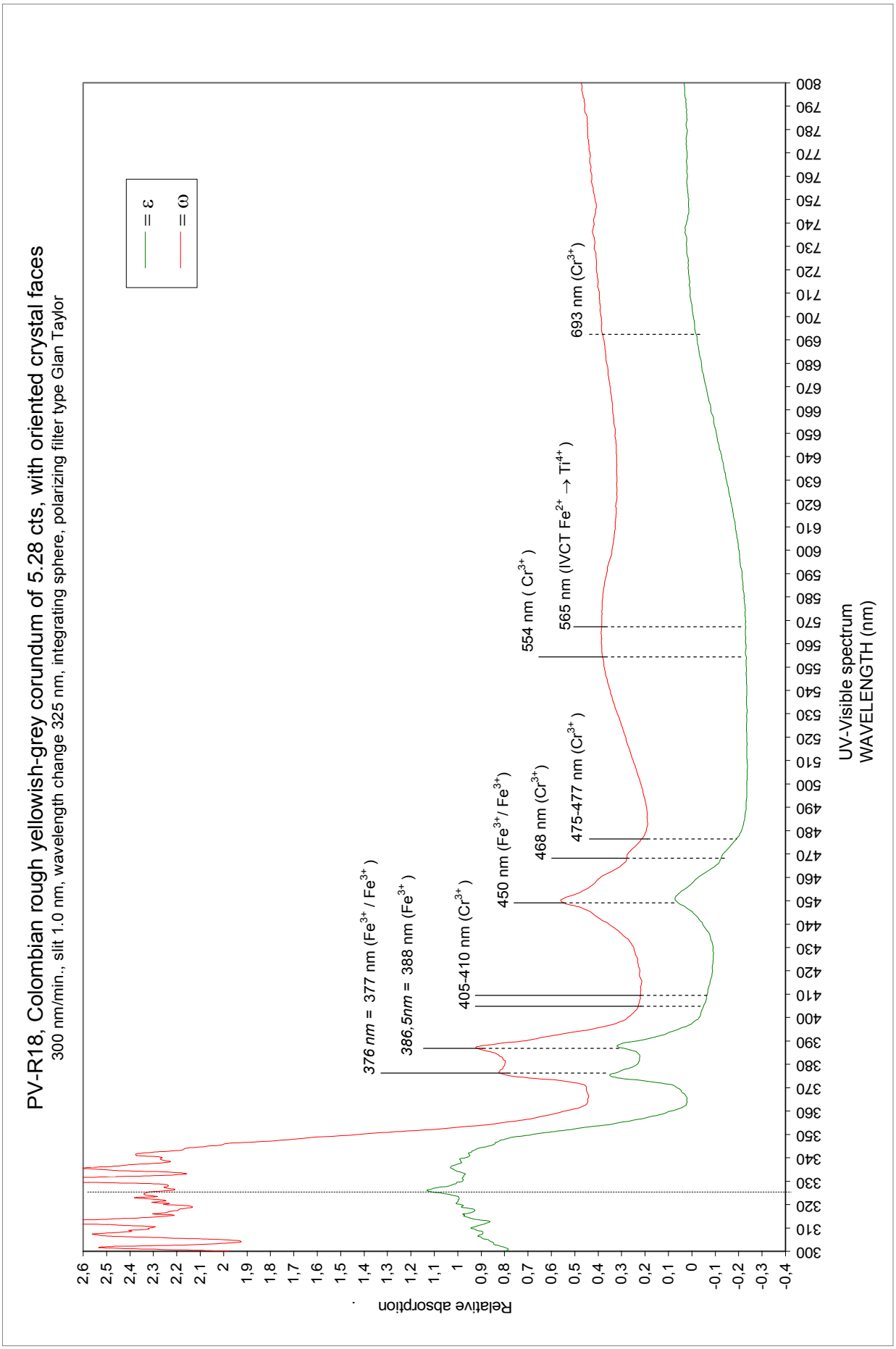
PV-R18, Colombian rough yellowish-grey corundum of 5.28 cts, with oriented crystal faces
300 nm/min., slit 1.0 nm, wavelength change 325 nm, integrating sphere, polarizing filter type Glan Taylor
= ε
= ω
376 nm = 377 nm (Fe3+ / Fe3+)
386,5nm = 388 nm (Fe3+)
405-410 nm (Cr3+)
450 nm (Fe3+/ Fe3+)
468 nm (Cr3+)
475-477 nm (Cr3+)
554 nm (Cr3+)
565 nm (IVCT Fe2+ → Ti4+)
693 nm (Cr3+)
Relative absorption
UV-Visible spectrum
WAVELENGTH (nm)

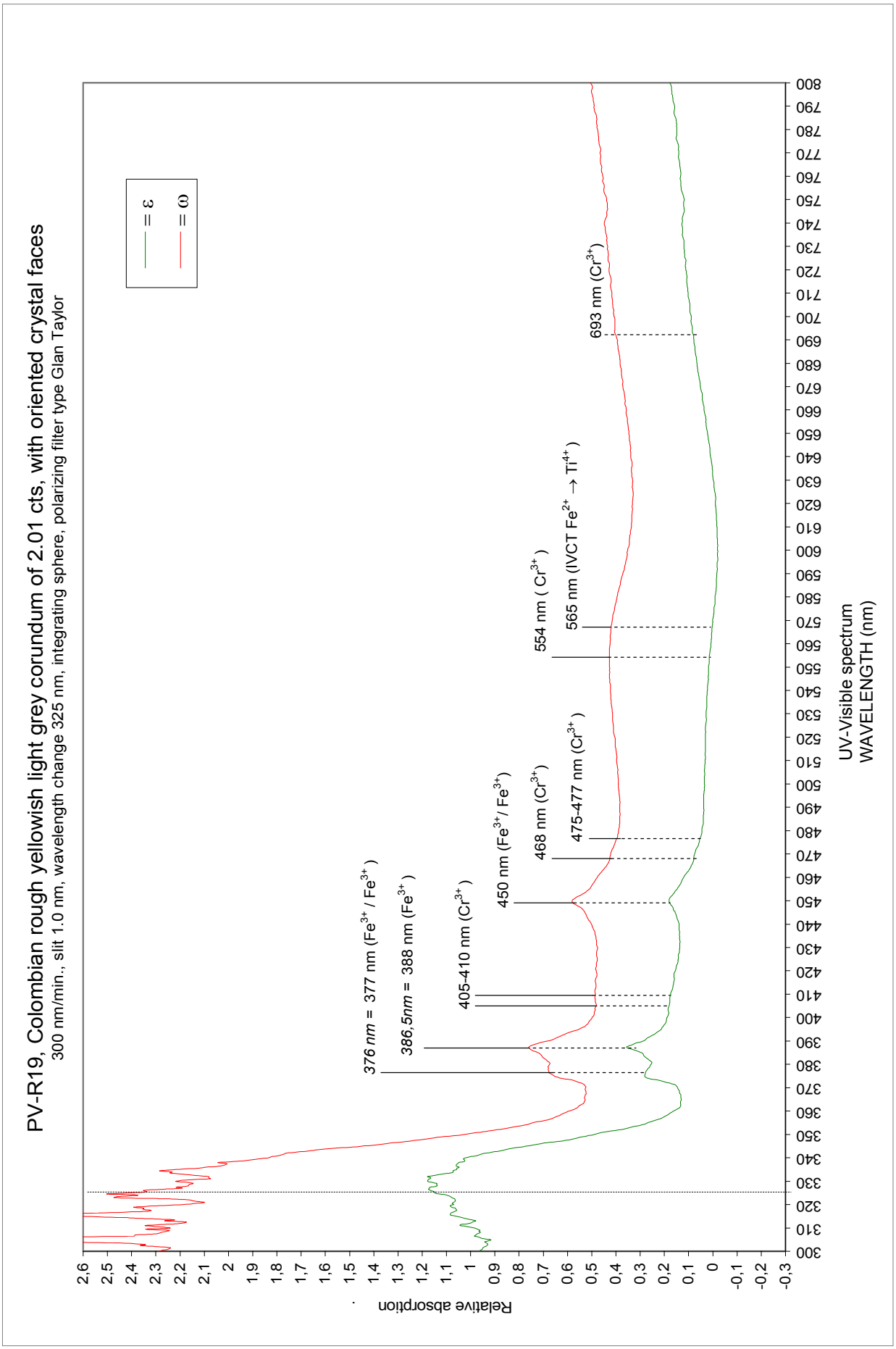
PV-R19, Colombian rough yellowish light grey corundum of 2.01 cts, with oriented crystal faces
300 nm/min., slit 1.0 nm, wavelength change 325 nm, integrating sphere, polarizing filter type Glan Taylor
= ε
= ω
376 nm = 377 nm (Fe3+ / Fe3+)
386,5nm = 388 nm (Fe3+)
405-410 nm (Cr3+)
450 nm (Fe3+/ Fe3+)
468 nm (Cr3+)
475-477 nm (Cr3+)
554 nm (Cr3+)
565 nm (IVCT Fe2+ → Ti4+)
693 nm (Cr3+)
Relative absorption
UV-Visible spectrum
WAVELENGTH (nm)

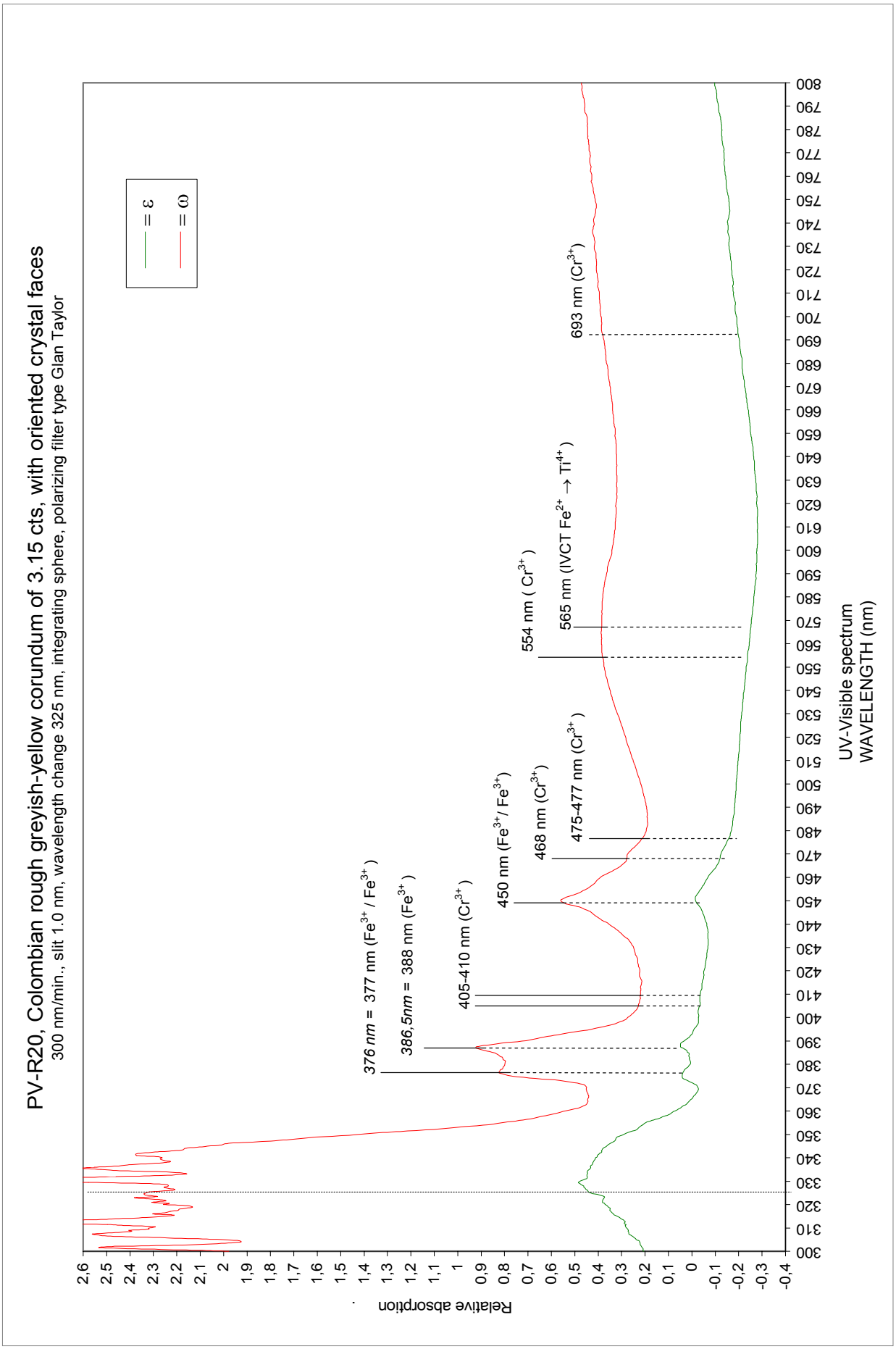
PV-R20, Colombian rough greyish-yellow corundum of 3.15 cts, with oriented crystal faces
300 nm/min., slit 1.0 nm, wavelength change 325 nm, integrating sphere, polarizing filter type Glan Taylor
= ε
= ω
376 nm = 377 nm (Fe3+ / Fe3+)
386,5nm = 388 nm (Fe3+)
405-410 nm (Cr3+)
450 nm (Fe3+/ Fe3+)
468 nm (Cr3+)
475-477 nm (Cr3+)
554 nm (Cr3+)
565 nm (IVCT Fe2+ → Ti4+)
693 nm (Cr3+)
Relative absorption
UV-Visible spectrum
WAVELENGTH (nm)

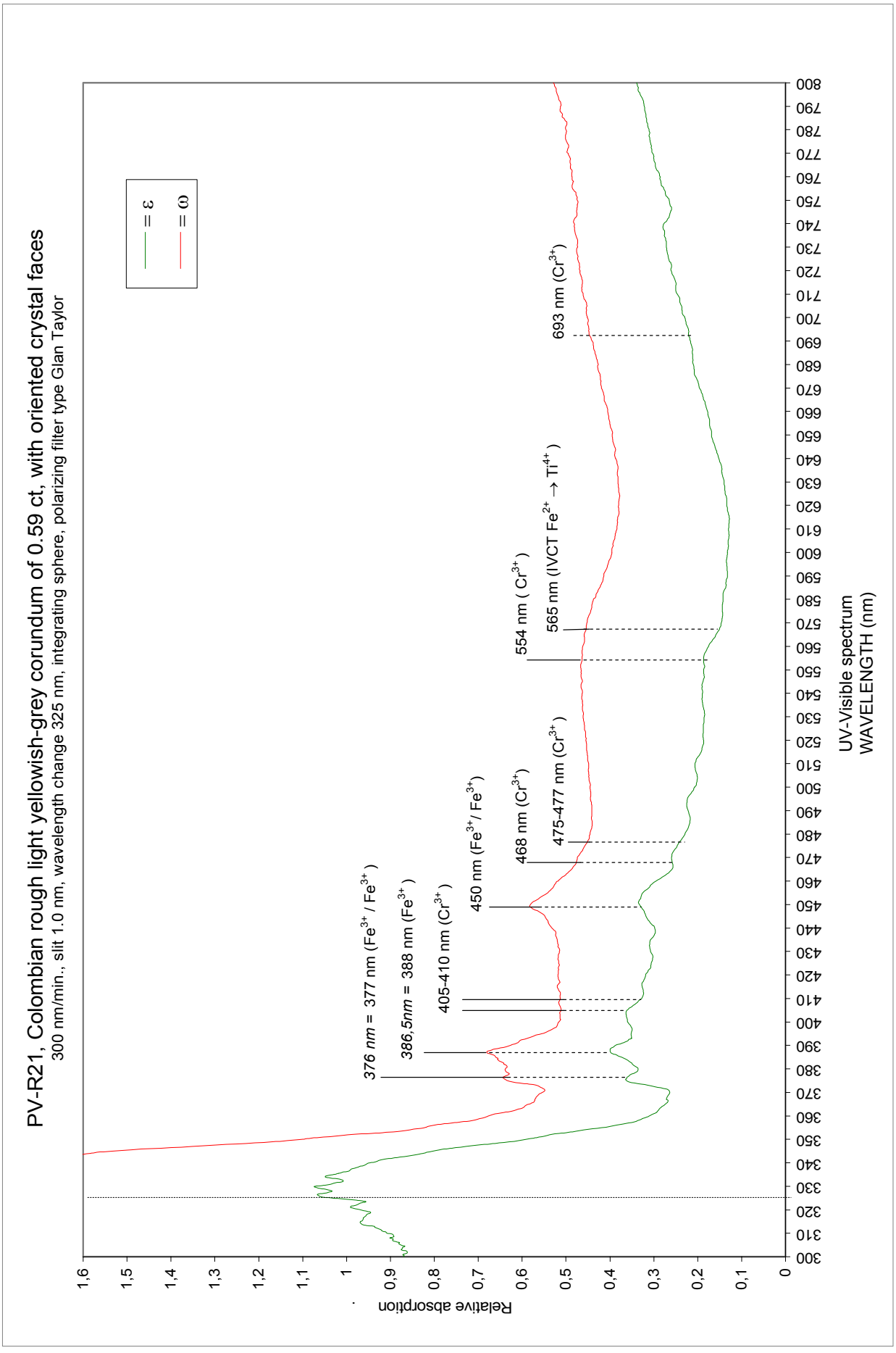
PV-R21, Colombian rough light yellowish-grey corundum of 0.59 ct, with oriented crystal faces
300 nm/min., slit 1.0 nm, wavelength change 325 nm, integrating sphere, polarizing filter type Glan Taylor
ε
ω
376 nm = 377 nm (Fe3+ / Fe3+)
386,5nm = 388 nm (Fe3+)
405-410 nm (Cr3+)
450 nm (Fe3+ / Fe3+)
468 nm (Cr3+)
475-477 nm (Cr3+)
554 nm (Cr3+)
565 nm (IVCT Fe2+ → Ti4+)
693 nm (Cr3+)
Relative absorption
UV-Visible spectrum
WAVELENGTH (nm)

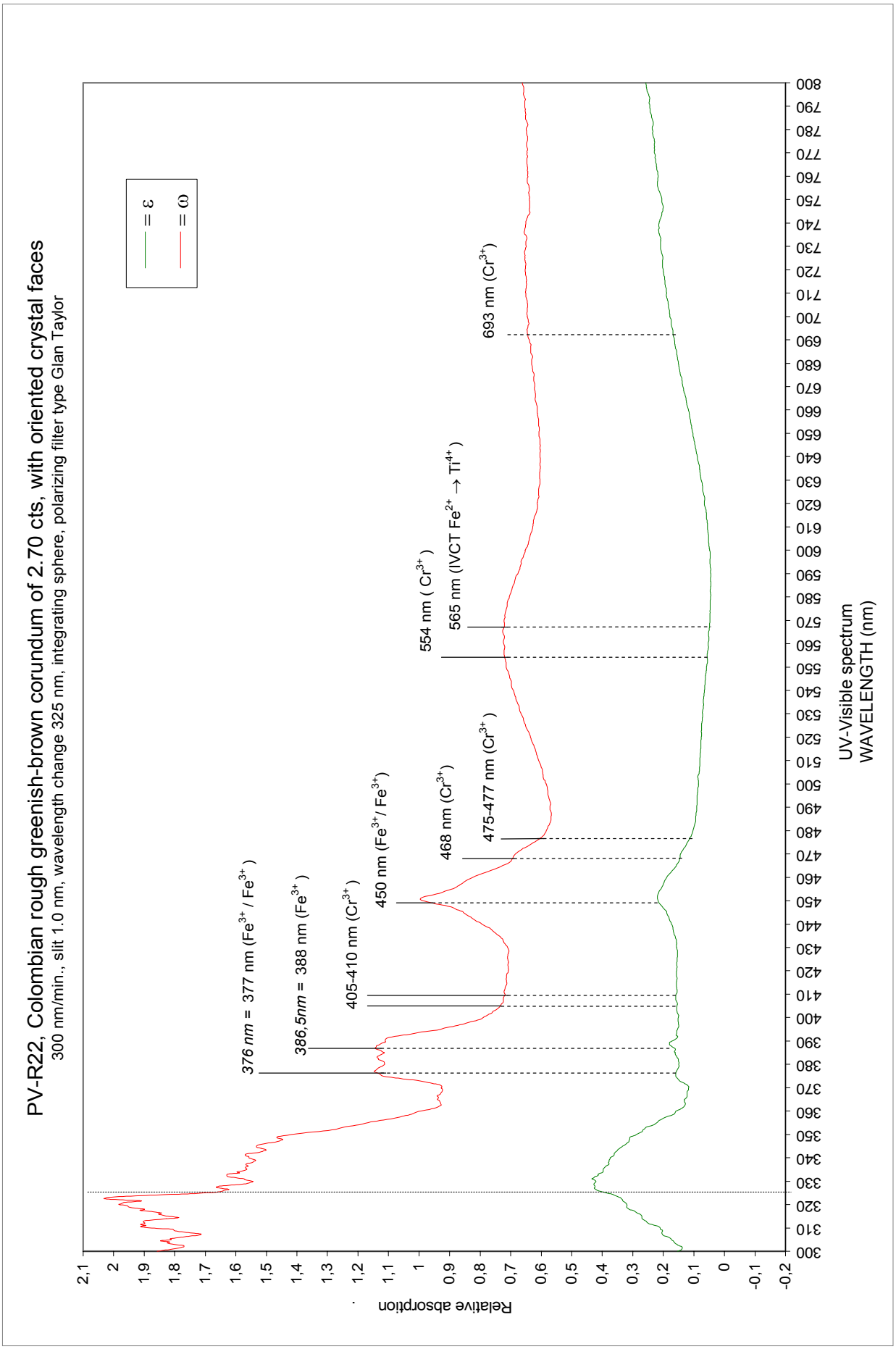
PV-R22, Colombian rough greenish-brown corundum of 2.70 cts, with oriented crystal faces
300 nm/min., slit 1.0 nm, wavelength change 325 nm, integrating sphere, polarizing filter type Glan Taylor
= ε
= ω
376 nm = 377 nm (Fe3+ / Fe3+)
386,5nm = 388 nm (Fe3+)
405-410 nm (Cr3+)
450 nm (Fe3+/ Fe3+)
468 nm (Cr3+)
475-477 nm (Cr3+)
554 nm (Cr3+)
565 nm (IVCT Fe2+ → Ti4+)
693 nm (Cr3+)
Relative absorption
UV-Visible spectrum
WAVELENGTH (nm)

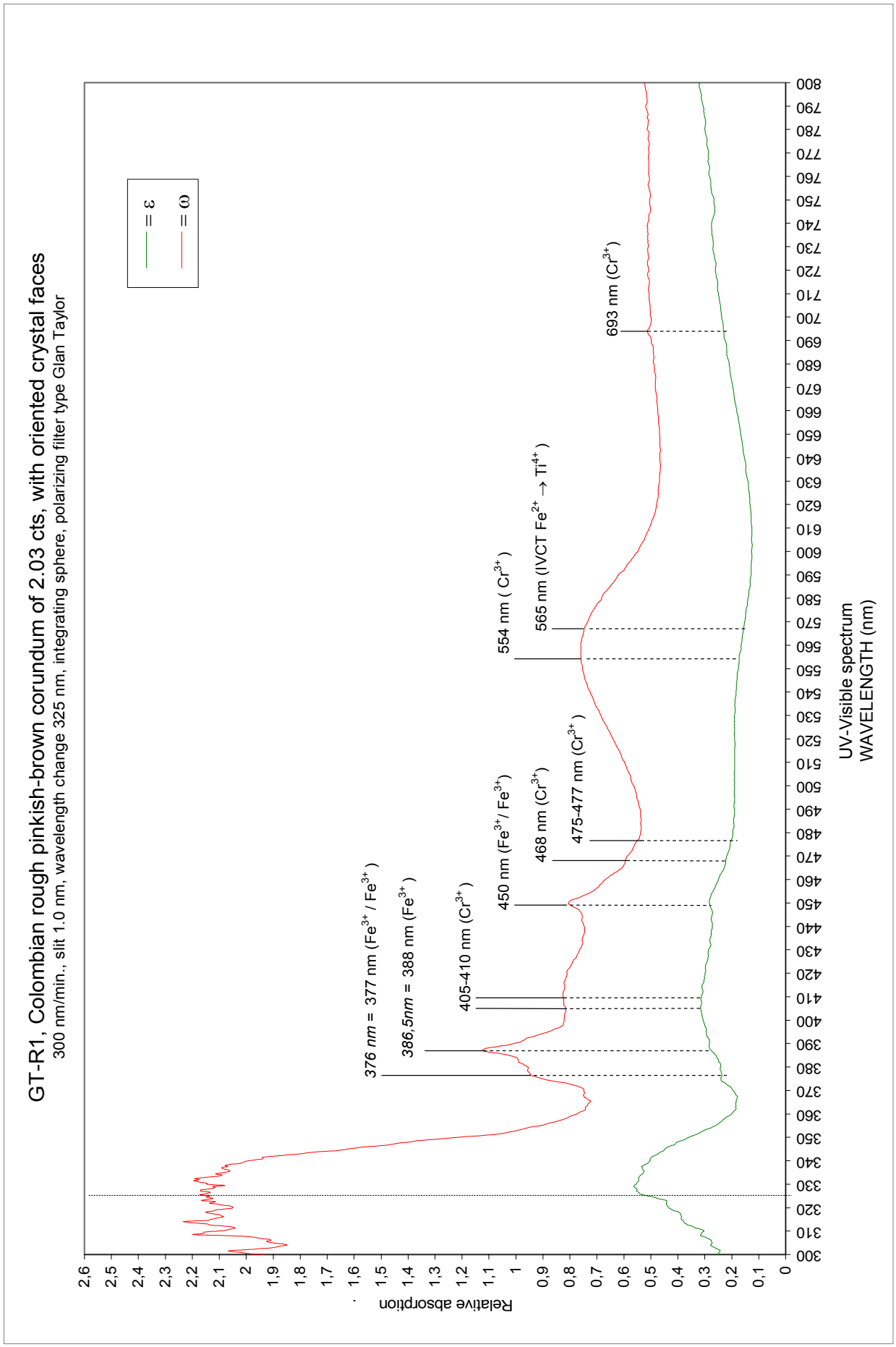
GT-R1, Colombian rough pinkish-brown corundum of 2.03 cts, with oriented crystal faces
300 nm/min., slit 1.0 nm, wavelength change 325 nm, integrating sphere, polarizing filter type Glan Taylor
ε
ω
376 nm = 377 nm (Fe3+ / Fe3+)
386,5nm = 388 nm (Fe3+)
405-410 nm (Cr3+)
450 nm (Fe3+ / Fe3+)
468 nm (Cr3+)
475-477 nm (Cr3+)
554 nm (Cr3+)
565 nm (IVCT Fe2+ → Ti4+)
693 nm (Cr3+)
Relative absorption
UV-Visible spectrum
WAVELENGTH (nm)

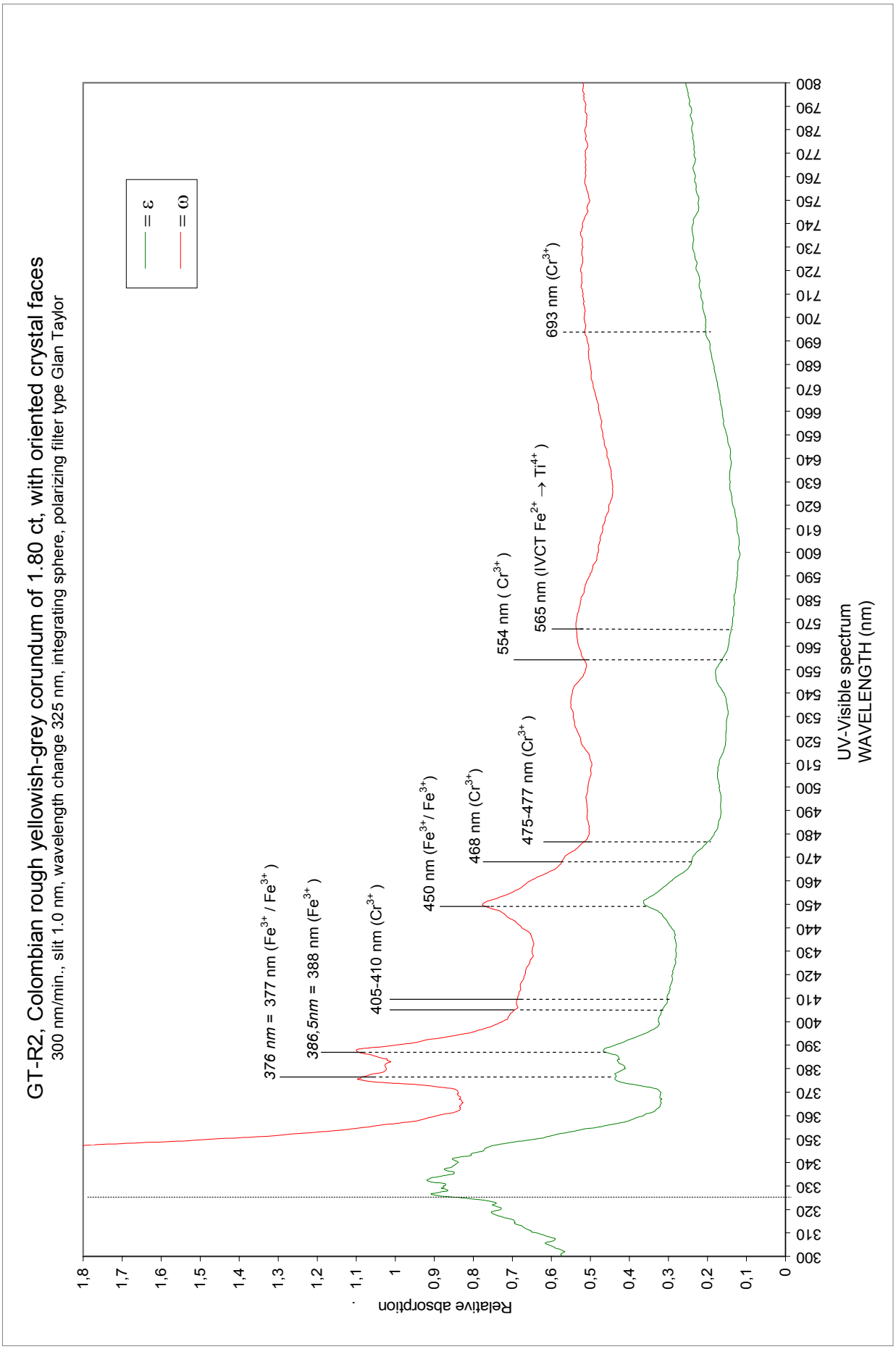
GT-R2, Colombian rough yellowish-grey corundum of 1.80 ct, with oriented crystal faces
300 nm/min., slit 1.0 nm, wavelength change 325 nm, integrating sphere, polarizing filter type Glan Taylor
ε
ω
376 nm = 377 nm (Fe3+ / Fe3+)
386,5nm = 388 nm (Fe3+)
405-410 nm (Cr3+)
450 nm (Fe3+ / Fe3+)
468 nm (Cr3+)
475-477 nm (Cr3+)
554 nm (Cr3+)
565 nm (IVCT Fe2+ → Ti4+)
693 nm (Cr3+)
Relative absorption
UV-Visible spectrum
WAVELENGTH (nm)

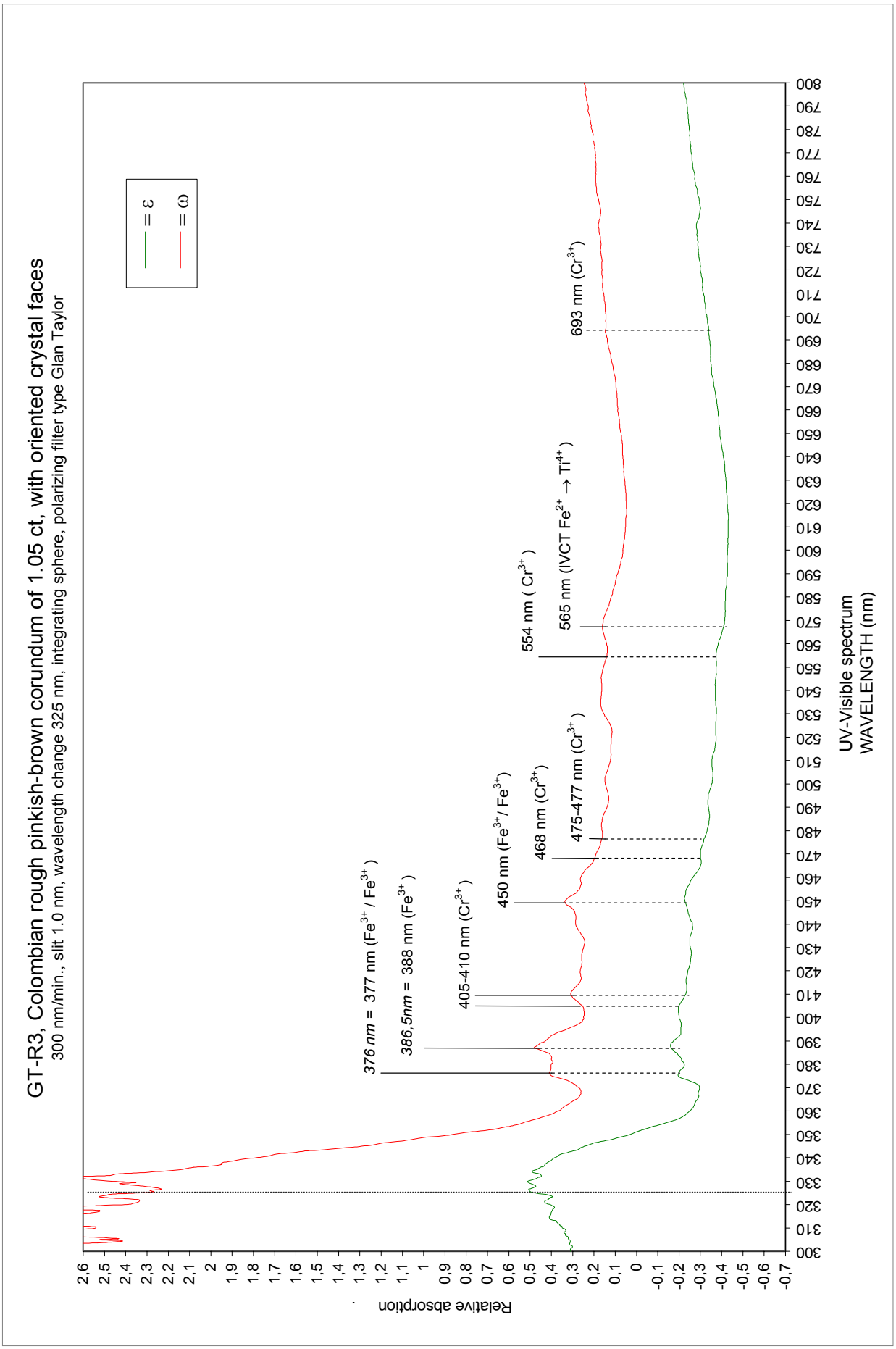
GT-R3, Colombian rough pinkish-brown corundum of 1.05 ct, with oriented crystal faces
300 nm/min., slit 1.0 nm, wavelength change 325 nm, integrating sphere, polarizing filter type Glan Taylor
ε
ω
376 nm = 377 nm (Fe3+ / Fe3+)
386,5nm = 388 nm (Fe3+)
405-410 nm (Cr3+)
450 nm (Fe3+/ Fe3+)
468 nm (Cr3+)
475-477 nm (Cr3+)
554 nm (Cr3+)
565 nm (IVCT Fe2+ → Ti4+)
693 nm (Cr3+)
Relative absorption
UV-Visible spectrum
WAVELENGTH (nm)

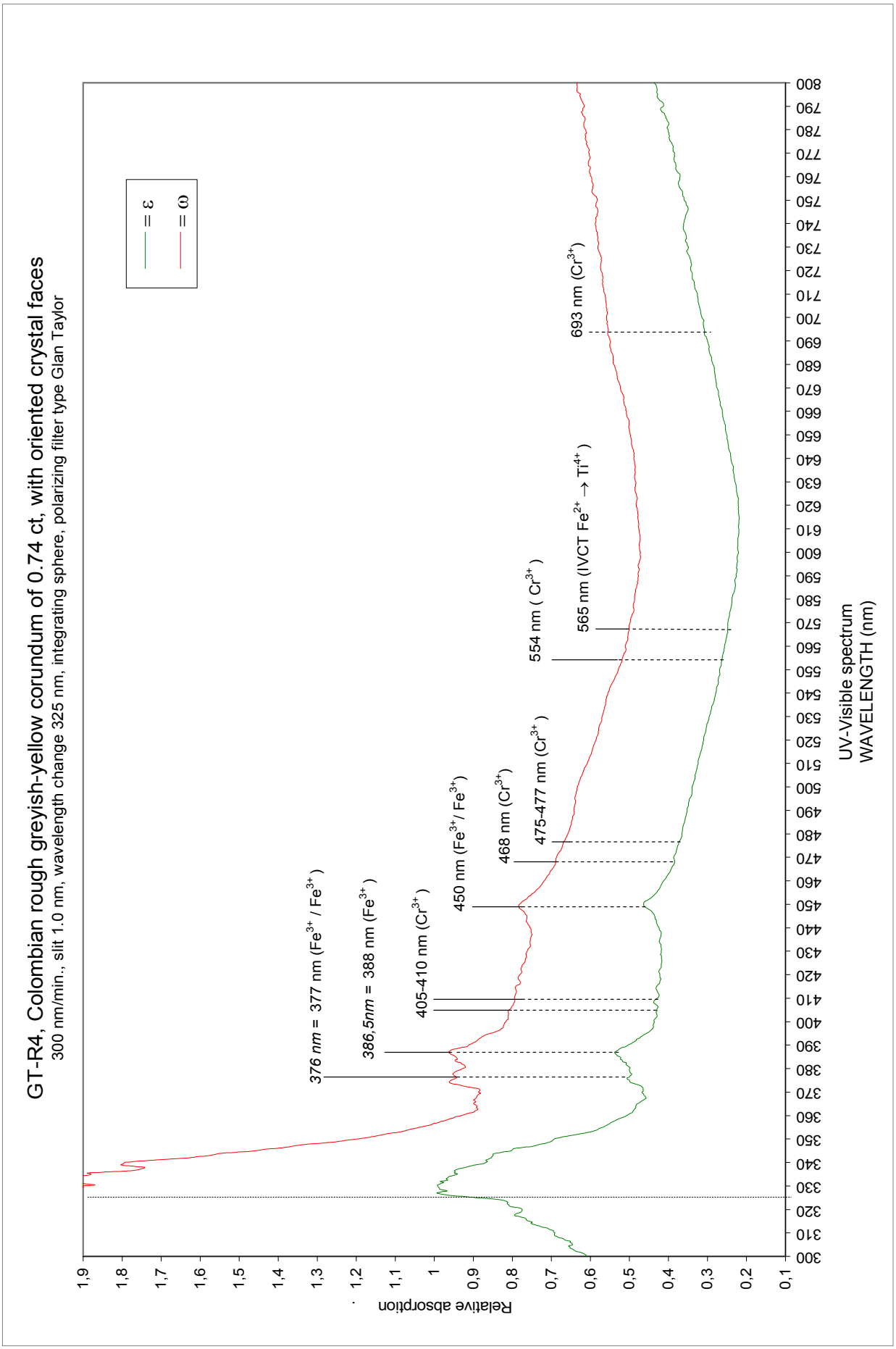
GT-R4, Colombian rough greyish-yellow corundum of 0.74 ct, with oriented crystal faces
300 nm/min., slit 1.0 nm, wavelength change 325 nm, integrating sphere, polarizing filter type Glan Taylor
ε
ω
376 nm = 377 nm (Fe3+ / Fe3+)
386,5nm = 388 nm (Fe3+)
405-410 nm (Cr3+)
450 nm (Fe3+/ Fe3+)
468 nm (Cr3+)
475-477 nm (Cr3+)
554 nm (Cr3+)
565 nm (IVCT Fe2+ → Ti4+)
693 nm (Cr3+)
Relative absorption
UV-Visible spectrum
WAVELENGTH (nm)

The five faceted rubies

			Dichroïm intensity	ω-ray colour	ε-ray colour
• Ref. A-01	Pear-shape	1.86 carat	Strong	Purplish-red	Orangy-red
• Ref. A-05	Cabochon	1.66 carat	Strong	Purplish-red	Orangy-red
• Ref. A-06	Cabochon	6.24 carats	Strong	Purplish-red	Orangy-red
• Ref. GT-01	Oval-shape	0.33 carat	Distinct	Purplish-red	Orangy-red
• Ref. GT-02	Pear-shape	0.19 carat	Distinct	Purplish-red	Orangy-red

Spectroscopic analysis of these rubies

The spectra show a more prominent ω-ray than the ε-ray.
The absorption spectrum is dominated by Cr^3 absorption.
All the rubies display a sharp band at 693 nm (Cr^{3+}), a broad band at 554 nm (Cr^{3+}), sharp bands at 475-477 nm (Cr^{3+}), and 468 nm (Cr^{3+}), and a broad band at 405-410 nm (Cr^{3+}). All (except A-05, a cobochon ruby of 1.66 ct) show a weak band at 450 nm (Fe^{3+}/Fe^{3+}), which means that these rubies are not free of colour modifiers, even if a bluish tint was not perceived, some iron is present in the host rubies, which is typical of basaltic type rubies (Bosshart, 1982).
Probably due to experimental problems, two specimens (A-01, a deep pinkish-red ruby, and less so A-05, a pinkish-red ruby) exhibit a flat ε-ray. Reasonably this should point towards a colourless ε-ray, which is the case for neither ε-ray that are described as orangy-red in both stones.

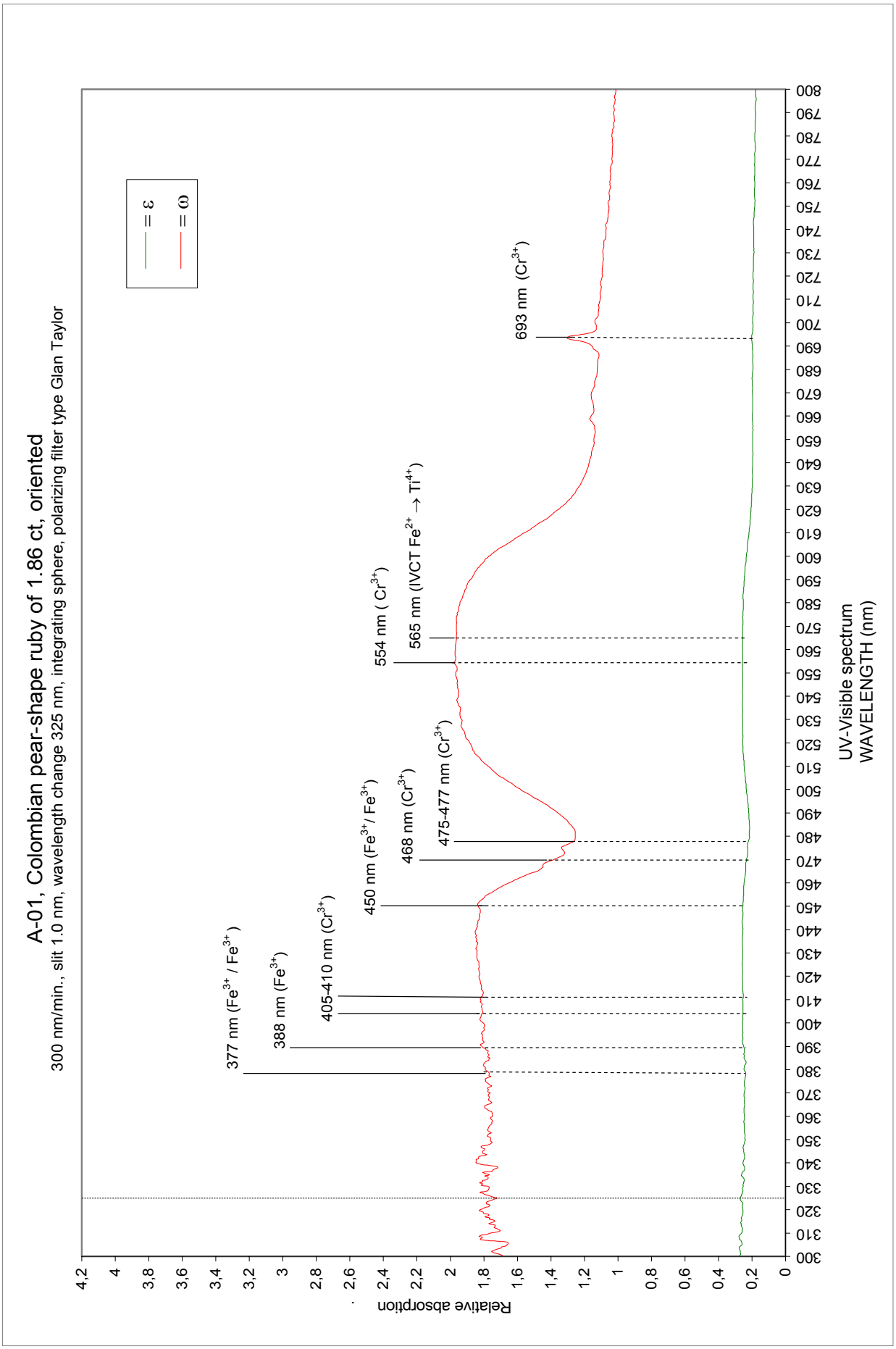
A-01, Colombian pear-shape ruby of 1.86 ct, oriented
300 nm/min., slit 1.0 nm, wavelength change 325 nm, integrating sphere, polarizing filter type Glan Taylor
ε
ω
377 nm (Fe3+ / Fe3+)
388 nm (Fe3+)
405-410 nm (Cr3+)
450 nm (Fe3+/ Fe3+)
468 nm (Cr3+)
475-477 nm (Cr3+)
554 nm (Cr3+)
565 nm (IVCT Fe2+ → Ti4+)
693 nm (Cr3+)
Relative absorption
UV-Visible spectrum
WAVELENGTH (nm)

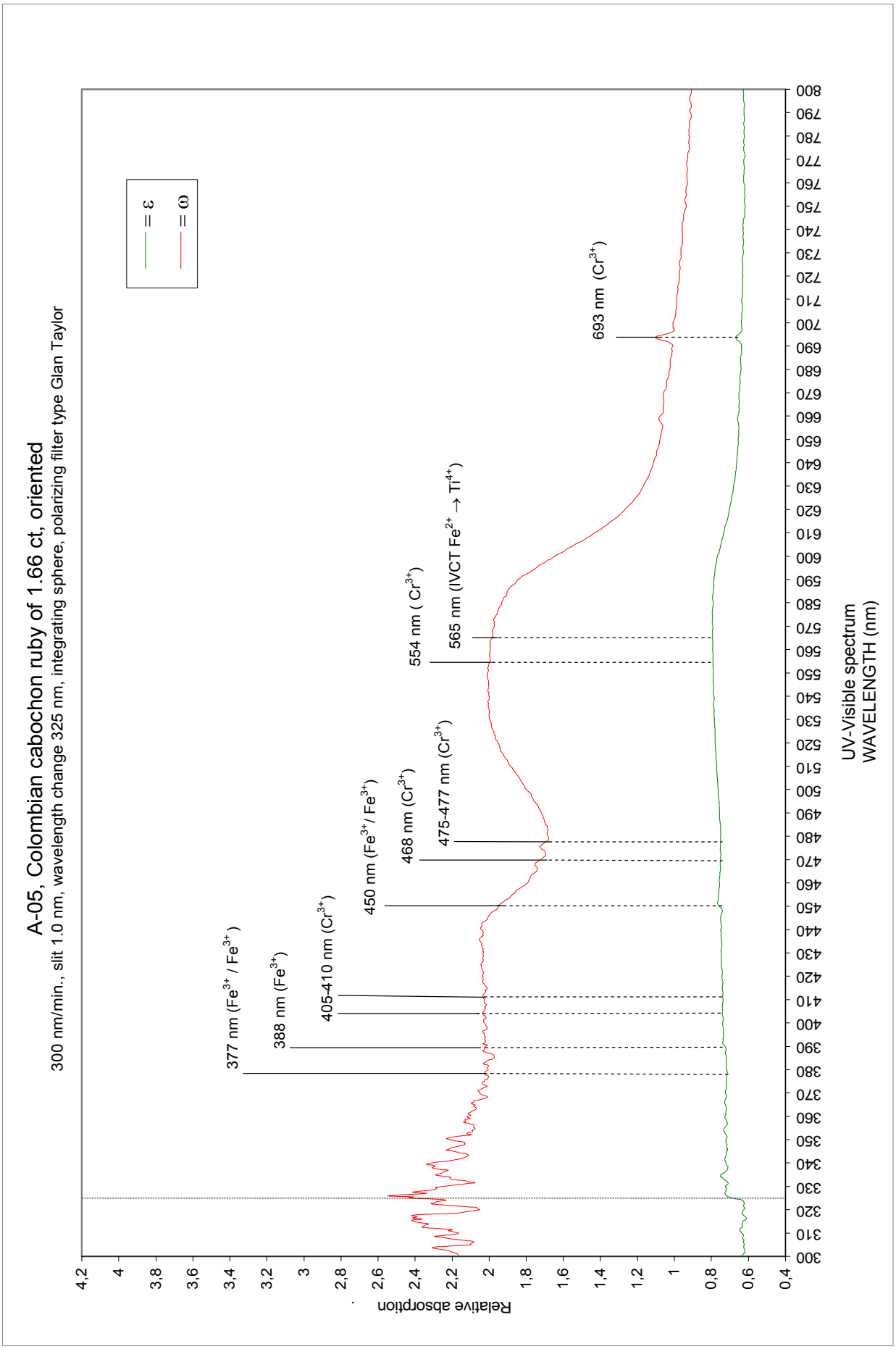
A-05, Colombian cabochon ruby of 1.66 ct, oriented
300 nm/min., slit 1.0 nm, wavelength change 325 nm, integrating sphere, polarizing filter type Glan Taylor
ε
ω
377 nm (Fe3+ / Fe3+)
388 nm (Fe3+)
405-410 nm (Cr3+)
450 nm (Fe3+/ Fe3+)
468 nm (Cr3+)
475-477 nm (Cr3+)
554 nm (Cr3+)
565 nm (IVCT Fe2+ → Ti4+)
693 nm (Cr3+)
Relative absorption
UV-Visible spectrum
WAVELENGTH (nm)

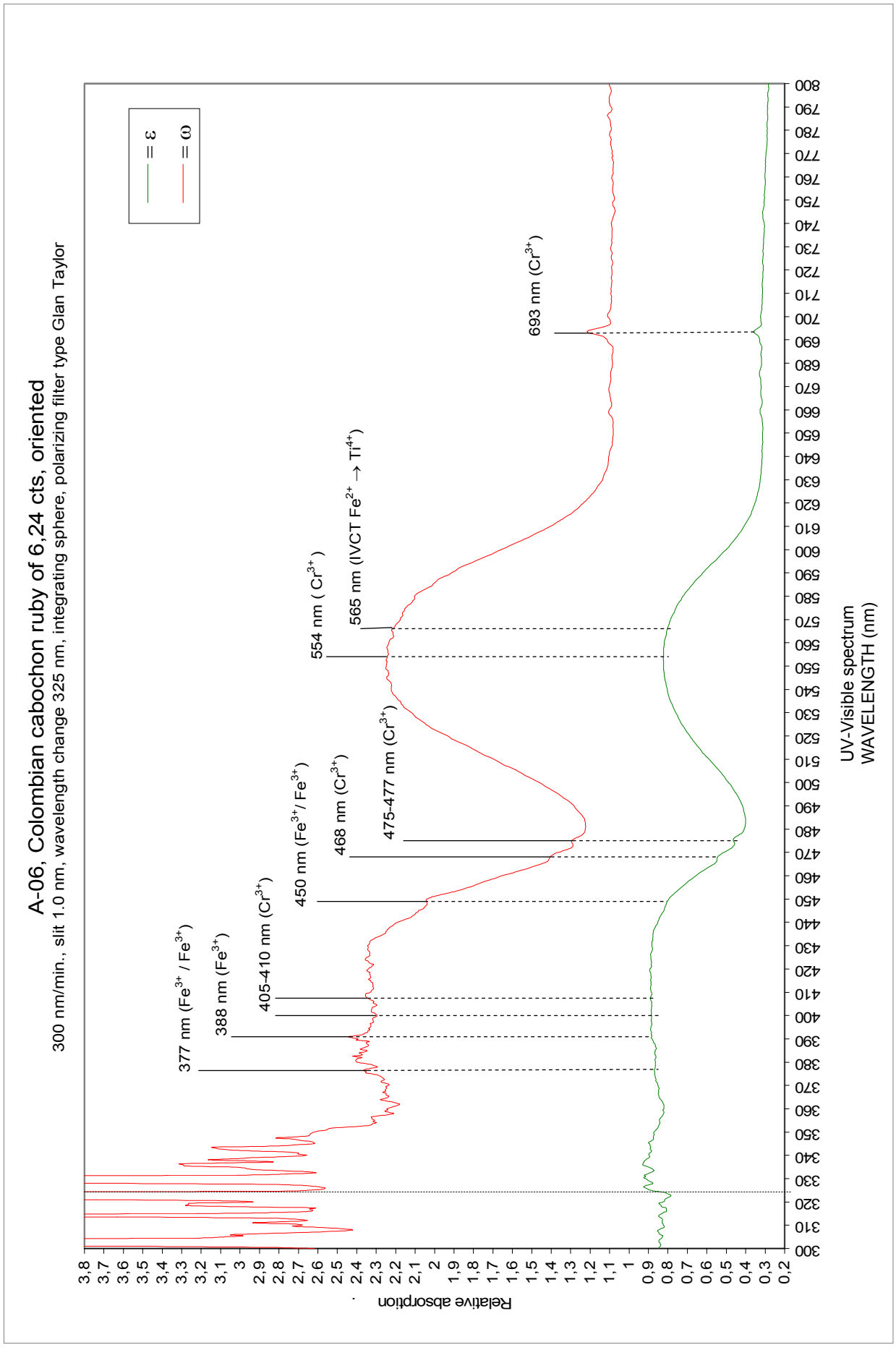
A-06, Colombian cabochon ruby of 6,24 cts, oriented
300 nm/min., slit 1.0 nm, wavelength change 325 nm, integrating sphere, polarizing filter type Glan Taylor
ε =
ω =
377 nm (Fe3+ / Fe3+)
388 nm (Fe3+)
405-410 nm (Cr3+)
450 nm (Fe3+ / Fe3+)
468 nm (Cr3+)
475-477 nm (Cr3+)
554 nm (Cr3+)
565 nm (IVCT Fe2+ → Ti4+)
693 nm (Cr3+)
Relative absorption
UV-Visible spectrum
WAVELENGTH (nm)

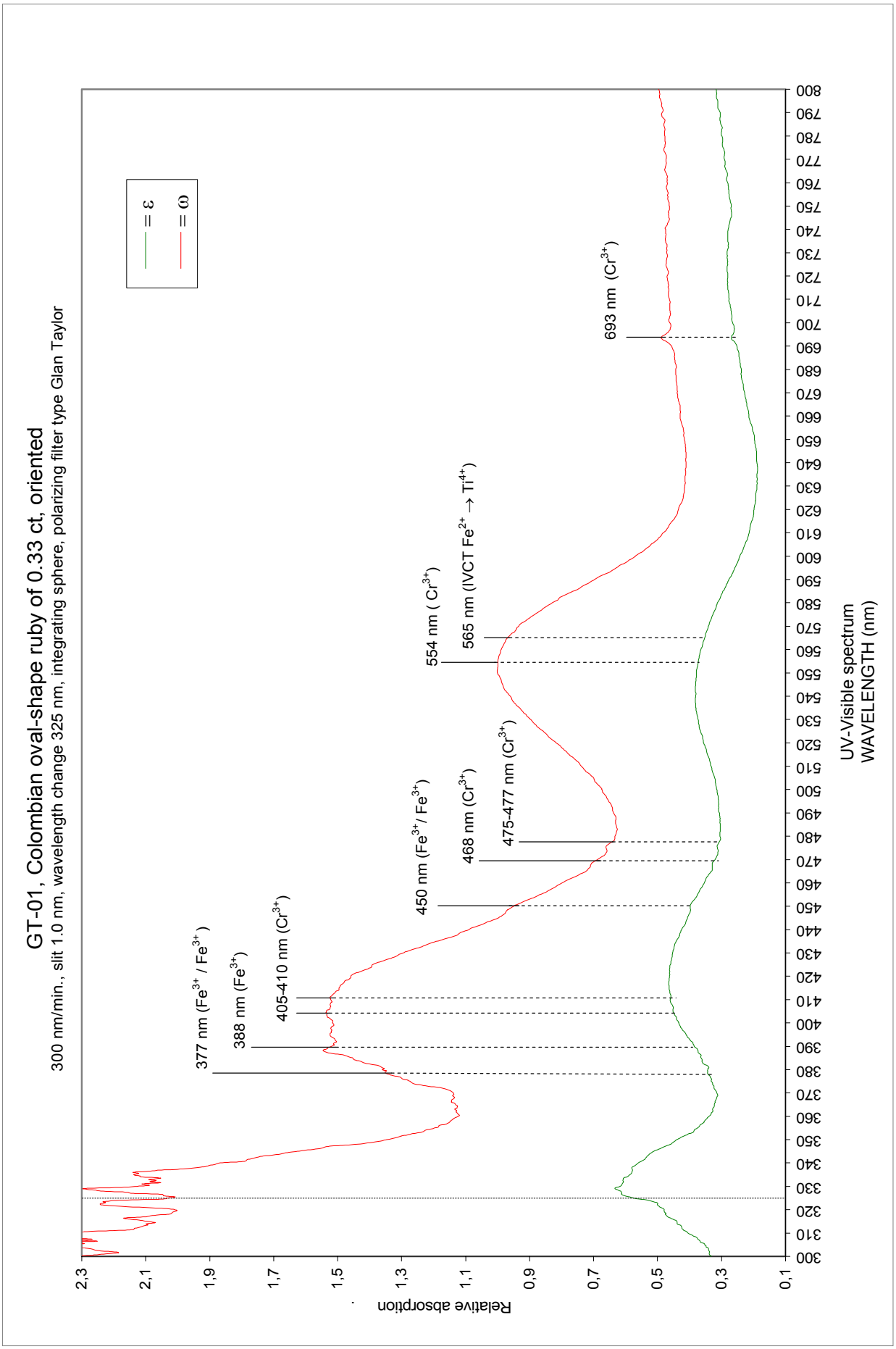
GT-01, Colombian oval-shape ruby of 0.33 ct, oriented
300 nm/min., slit 1.0 nm, wavelength change 325 nm, integrating sphere, polarizing filter type Glan Taylor
ε
ω
377 nm (Fe3+ / Fe3+)
388 nm (Fe3+)
405-410 nm (Cr3+)
450 nm (Fe3+/ Fe3+)
468 nm (Cr3+)
475-477 nm (Cr3+)
554 nm (Cr3+)
565 nm (IVCT Fe2+ → Ti4+)
693 nm (Cr3+)
Relative absorption
UV-Visible spectrum
WAVELENGTH (nm)

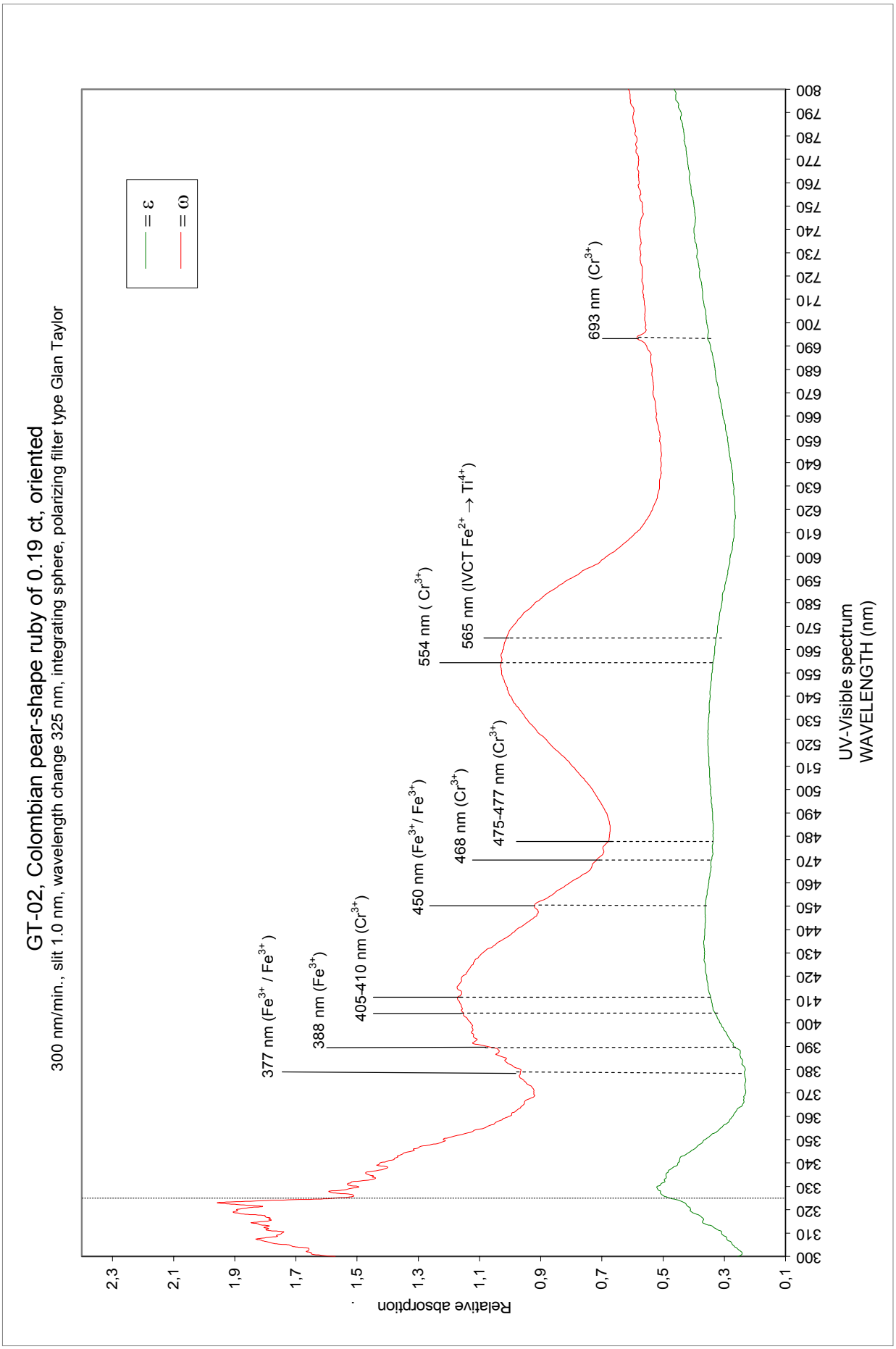
GT-02, Colombian pear-shape ruby of 0.19 ct, oriented
300 nm/min., slit 1.0 nm, wavelength change 325 nm, integrating sphere, polarizing filter type Glan Taylor
ε
ω
377 nm (Fe3+ / Fe3+)
388 nm (Fe3+)
405-410 nm (Cr3+)
450 nm (Fe3+/ Fe3+)
468 nm (Cr3+)
475-477 nm (Cr3+)
554 nm (Cr3+)
565 nm (IVCT Fe2+ → Ti4+)
693 nm (Cr3+)
Relative absorption
UV-Visible spectrum
WAVELENGTH (nm)

The eight faceted sapphires

			Dichroïm intensity	ω-ray colour	ε-ray colour
• Ref. A-07	Cabochon	3.01 carats	Strong	Greyish-blue	Bluish-green
• Ref. A-08	Cabochon	2.66 carats	Strong	Greyish-blue	Bluish-green
• Ref. A-11	Marquise	2.19 carats	Strong	Greyish-blue	Greyish-green
• Ref. A-13	Oval-shape	3.42 carats	Distinct	Greenish-blue	Pale greyish-green
• Ref. A-14	Oval-shape	3.55 carats	Distinct	Greenish-blue	Pale violetish-blue
• Ref. A-17	Oval-shape	1.65 carat	Distinct	Pale greyish-blue	Pale greyish-green
• Ref. HH-01	Oval-shape	4.81 carats	Distinct	Greyish-blue	Pinkish-blue
• Ref. A-31	Cabochon	0.71 carat	Very weak	Pale bluish-grey	Pale pinkish-grey

Spectroscopic analysis of these sapphires

The ω-ray is more developped than the ε-ray.
All show mainly the absorption bands of iron: sharp bands at 377 nm (Fe^{3+}/Fe^{3+}), and 388 nm (Fe^{2+}), a strong band at 450 nm (Fe^{3+}/Fe^{3+}), and a very broad band at 565 nm (IVCT $Fe^{2+} \rightarrow Ti^{4+}$). Their relative intensities however varies substantially from one specimen to another, and these variations are responsible for the different hues recorded (the least iron doped sapphire displays the least developped iron spectrum, and therefore the weakest colour in the blue, green, or yellow hues).
All seem to contain a little chromium. Although the main band 953 nm (Cr^{3+}) is missing, they all show the bands 468 nm (Cr^{3+}), and 475-477 nm (Cr^{3+}).
As already described for the rubies, and most probably due to experimental problems, two of the sapphires show a flat ε-ray (A-11, a greyish-blue sapphire, and A-31, a bluish-grey sapphire), yet none of the ε-ray is colourless. The ε-ray colour is: greyish-green for A-11, and pale pinkish-grey for A-31.

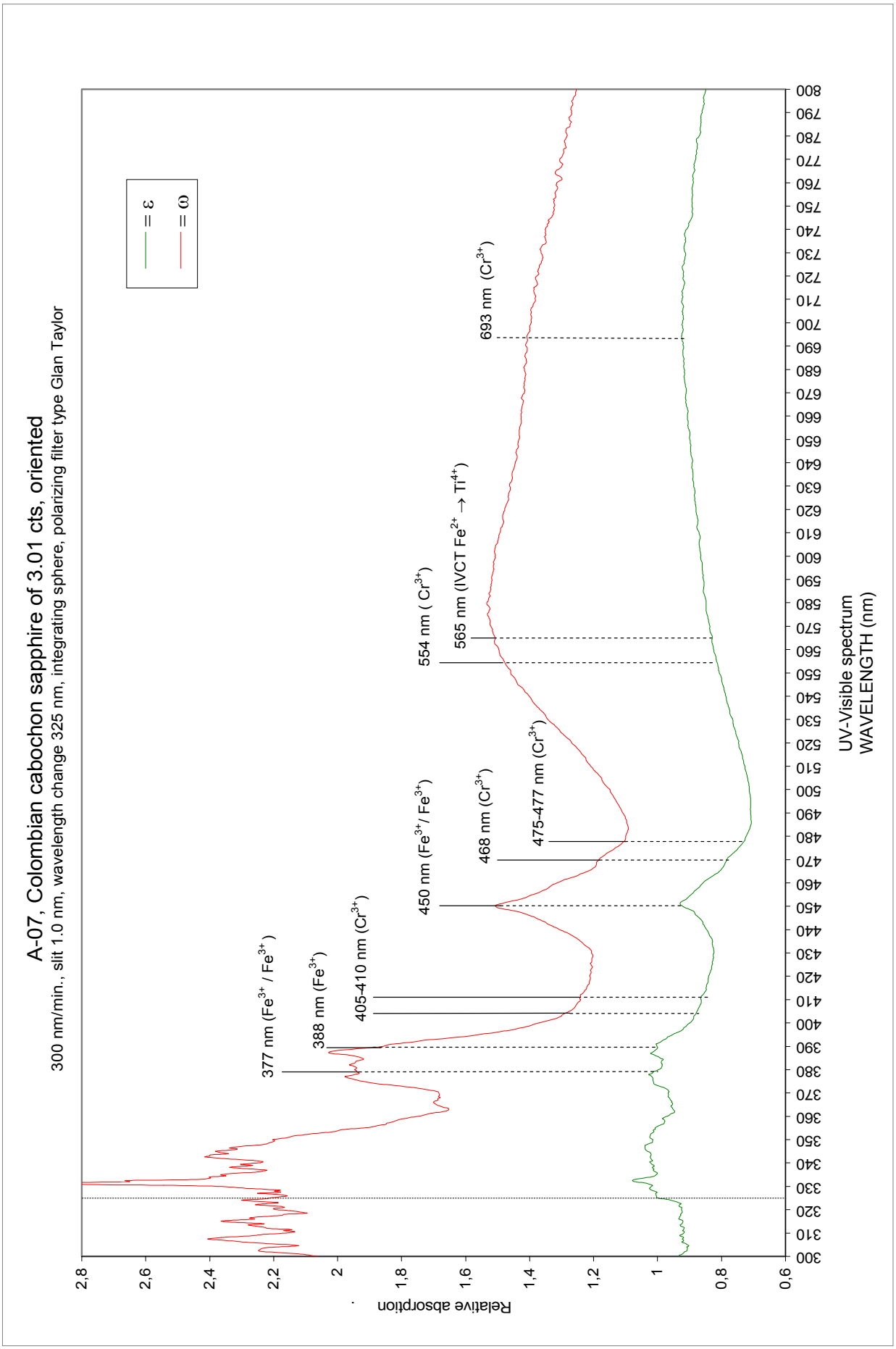
A-07, Colombian cabochon sapphire of 3.01 cts, oriented
300 nm/min., slit 1.0 nm, wavelength change 325 nm, integrating sphere, polarizing filter type Glan Taylor
= ε
= ω
377 nm (Fe3+ / Fe3+)
388 nm (Fe3+)
405-410 nm (Cr3+)
450 nm (Fe3+/ Fe3+)
468 nm (Cr3+)
475-477 nm (Cr3+)
554 nm (Cr3+)
565 nm (IVCT Fe2+ → Ti4+)
693 nm (Cr3+)
Relative absorption
UV-Visible spectrum
WAVELENGTH (nm)

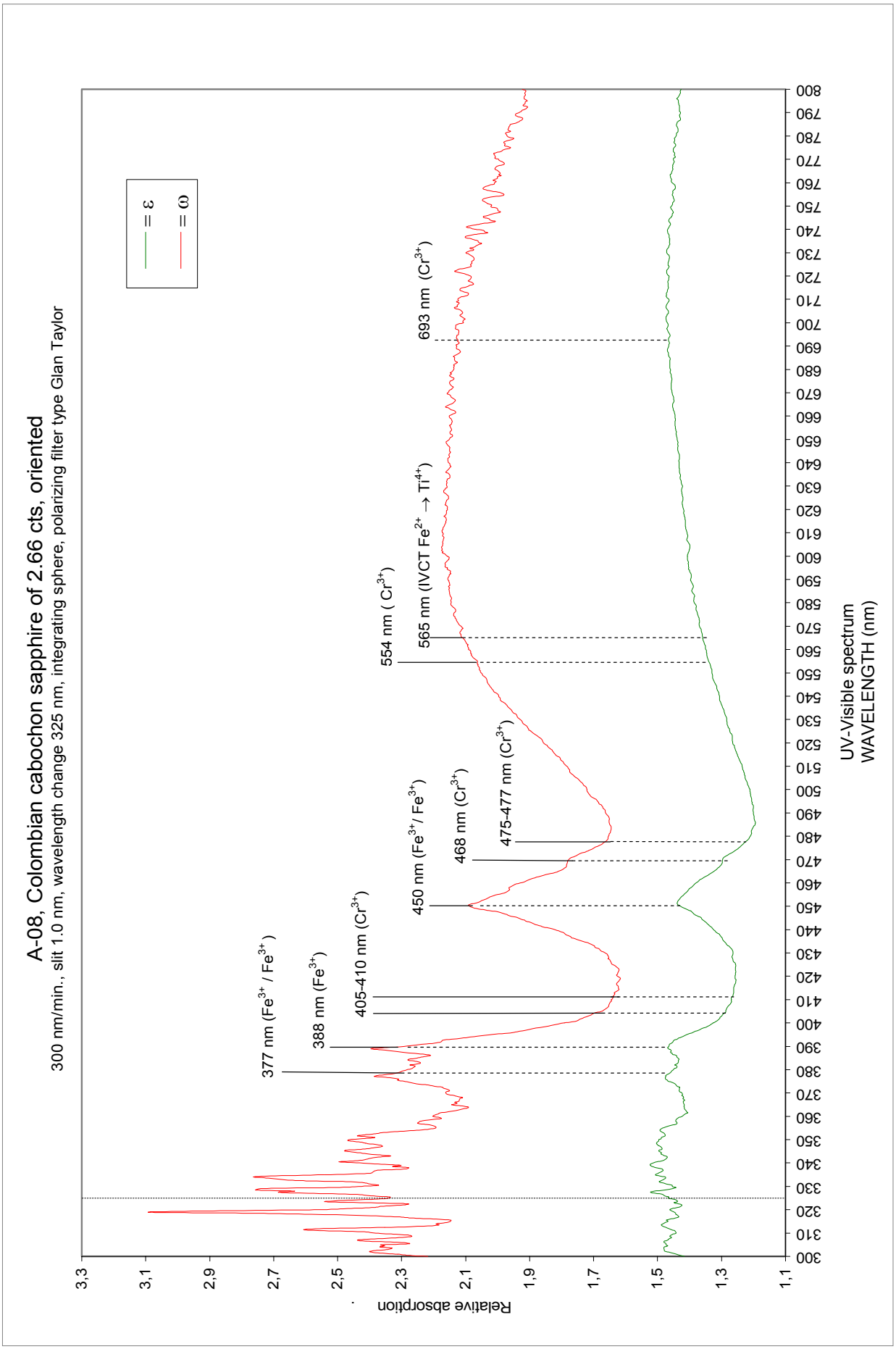
A-08, Colombian cabochon sapphire of 2.66 cts, oriented
300 nm/min., slit 1.0 nm, wavelength change 325 nm, integrating sphere, polarizing filter type Glan Taylor
ε
ω
377 nm (Fe3+ / Fe3+)
388 nm (Fe3+)
405-410 nm (Cr3+)
450 nm (Fe3+/ Fe3+)
468 nm (Cr3+)
475-477 nm (Cr3+)
554 nm (Cr3+)
565 nm (IVCT Fe2+ → Ti4+)
693 nm (Cr3+)
Relative absorption
UV-Visible spectrum
WAVELENGTH (nm)

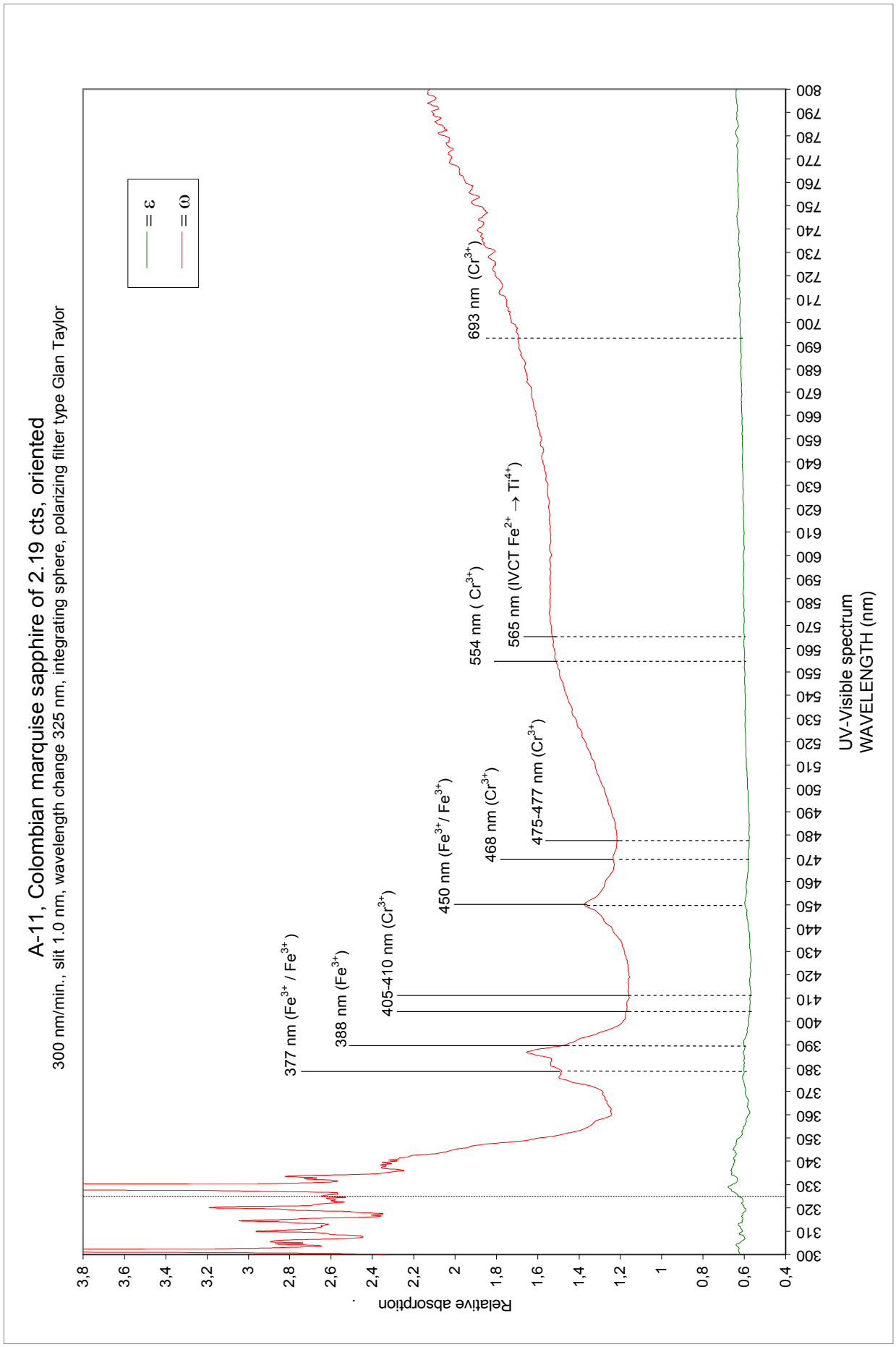
A-11, Colombian marquise sapphire of 2.19 cts, oriented
300 nm/min., slit 1.0 nm, wavelength change 325 nm, integrating sphere, polarizing filter type Glan Taylor
ε =
ω =
377 nm (Fe3+ / Fe3+)
388 nm (Fe3+)
405-410 nm (Cr3+)
450 nm (Fe3+/ Fe3+)
468 nm (Cr3+)
475-477 nm (Cr3+)
554 nm (Cr3+)
565 nm (IVCT Fe2+ → Ti4+)
693 nm (Cr3+)
Relative absorption
UV-Visible spectrum
WAVELENGTH (nm)

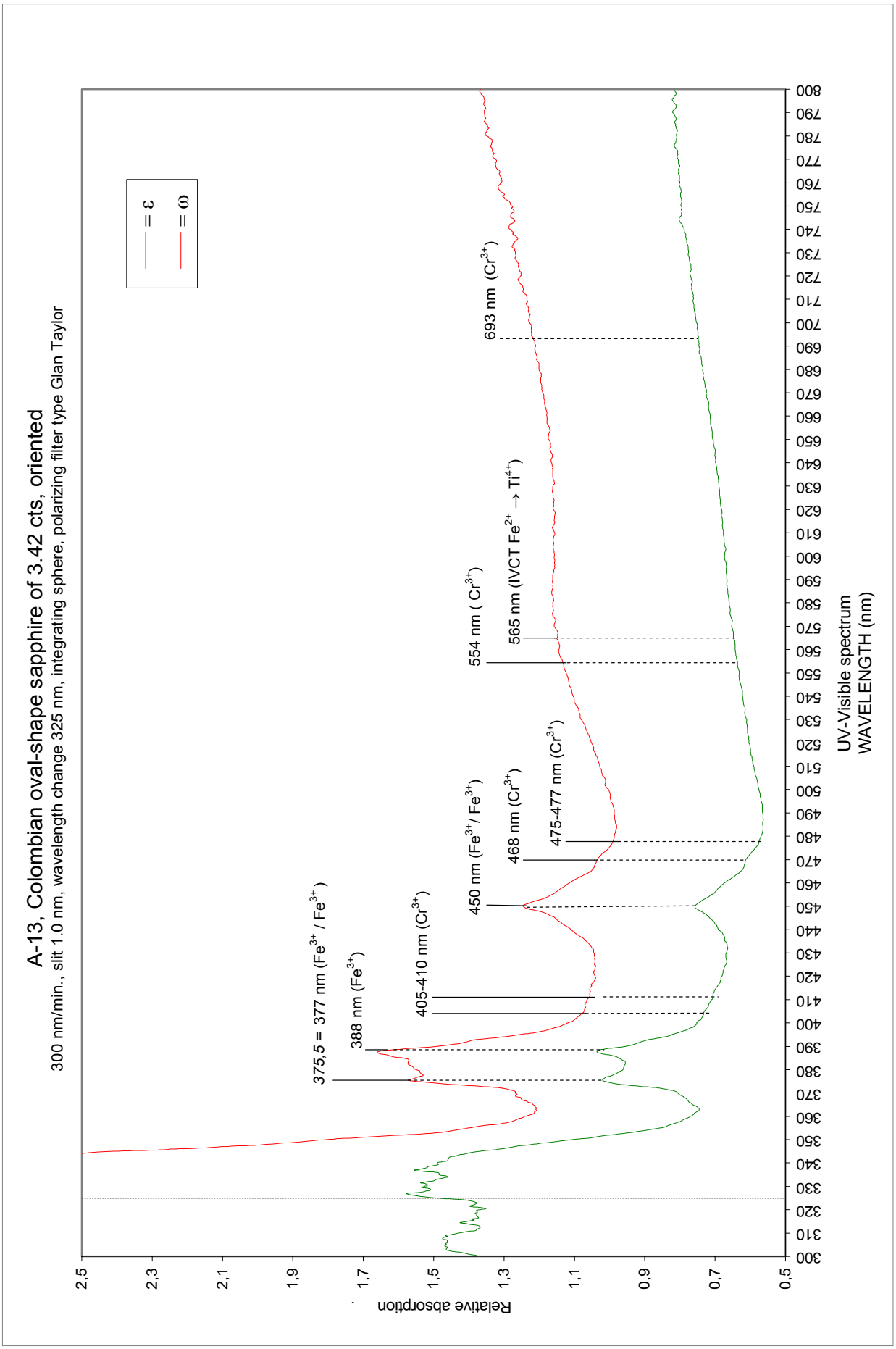
A-13, Colombian oval-shape sapphire of 3.42 cts, oriented
300 nm/min., slit 1.0 nm, wavelength change 325 nm, integrating sphere, polarizing filter type Glan Taylor
= ε
= ω
693 nm (Cr3+)
565 nm (IVCT Fe2+ → Ti4+)
554 nm (Cr3+)
475-477 nm (Cr3+)
468 nm (Cr3+)
450 nm (Fe3+/ Fe3+)
405-410 nm (Cr3+)
388 nm (Fe3+)
375,5 = 377 nm (Fe3+ / Fe3+)
Relative absorption
UV-Visible spectrum
WAVELENGTH (nm)

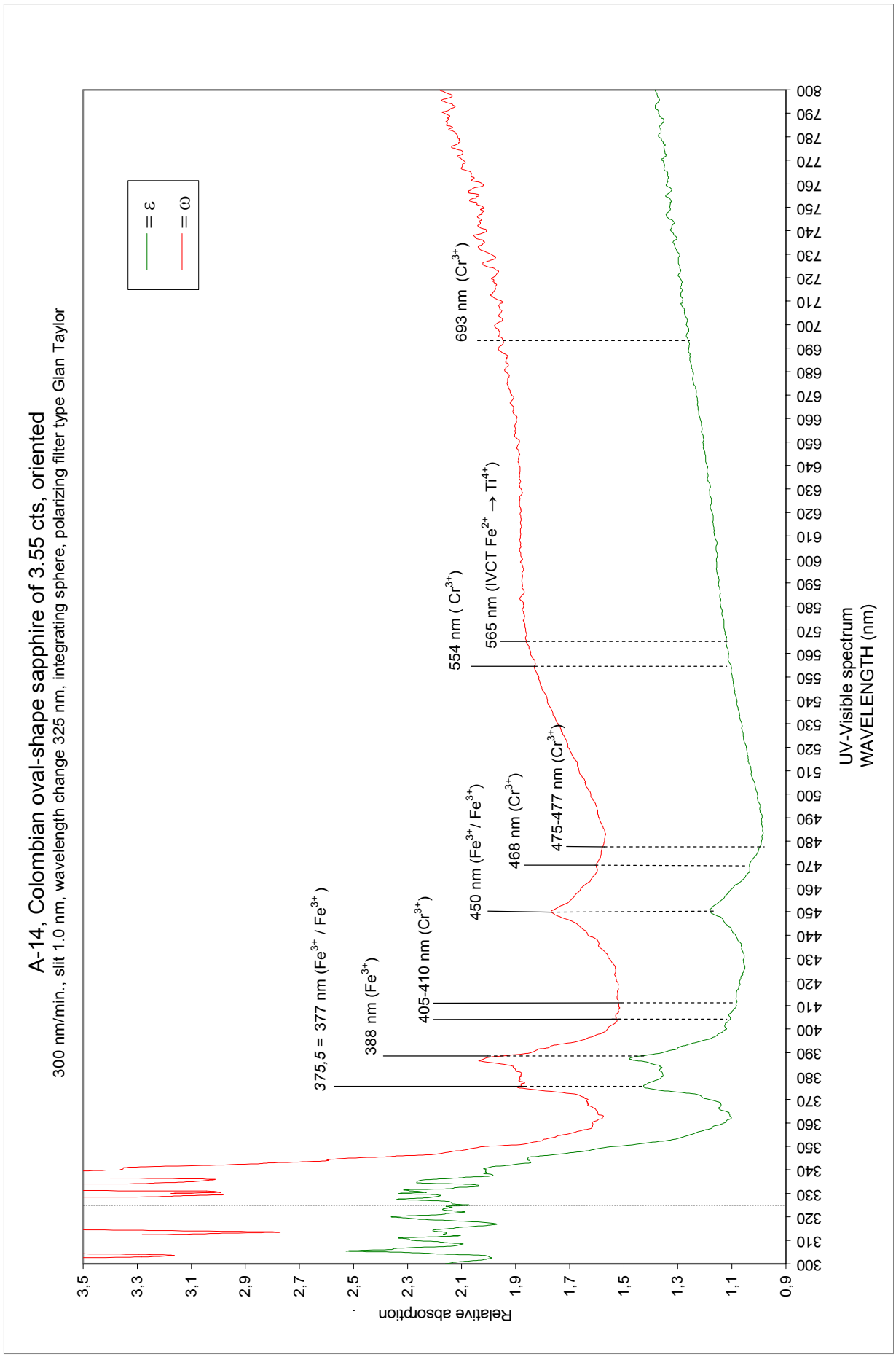
A-14, Colombian oval-shape sapphire of 3.55 cts, oriented
300 nm/min., slit 1.0 nm, wavelength change 325 nm, integrating sphere, polarizing filter type Glan Taylor
= ε
= ω
375,5 = 377 nm (Fe3+ / Fe3+)
388 nm (Fe3+)
405-410 nm (Cr3+)
450 nm (Fe3+/ Fe3+)
468 nm (Cr3+)
475-477 nm (Cr3+)
554 nm (Cr3+)
565 nm (IVCT Fe2+ → Ti4+)
693 nm (Cr3+)
Relative absorption
UV-Visible spectrum
WAVELENGTH (nm)

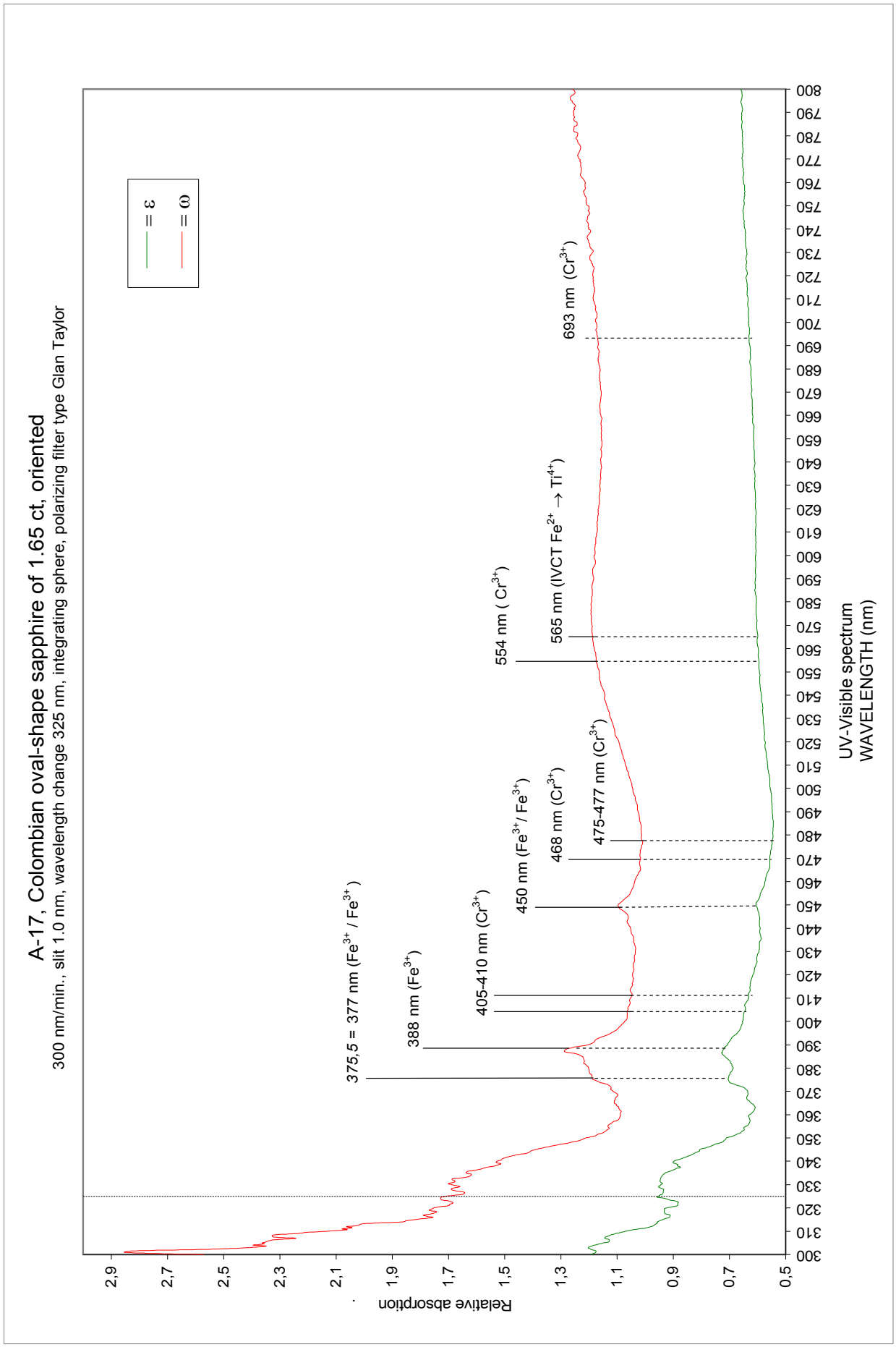
A-17, Colombian oval-shape sapphire of 1.65 ct, oriented
300 nm/min., slit 1.0 nm, wavelength change 325 nm, integrating sphere, polarizing filter type Glan Taylor
ω =
ε =
375,5 = 377 nm (Fe3+ / Fe3+)
388 nm (Fe3+)
405-410 nm (Cr3+)
450 nm (Fe3+/ Fe3+)
468 nm (Cr3+)
475-477 nm (Cr3+)
554 nm (Cr3+)
565 nm (IVCT Fe2+ → Ti4+)
693 nm (Cr3+)
Relative absorption
UV-Visible spectrum
WAVELENGTH (nm)

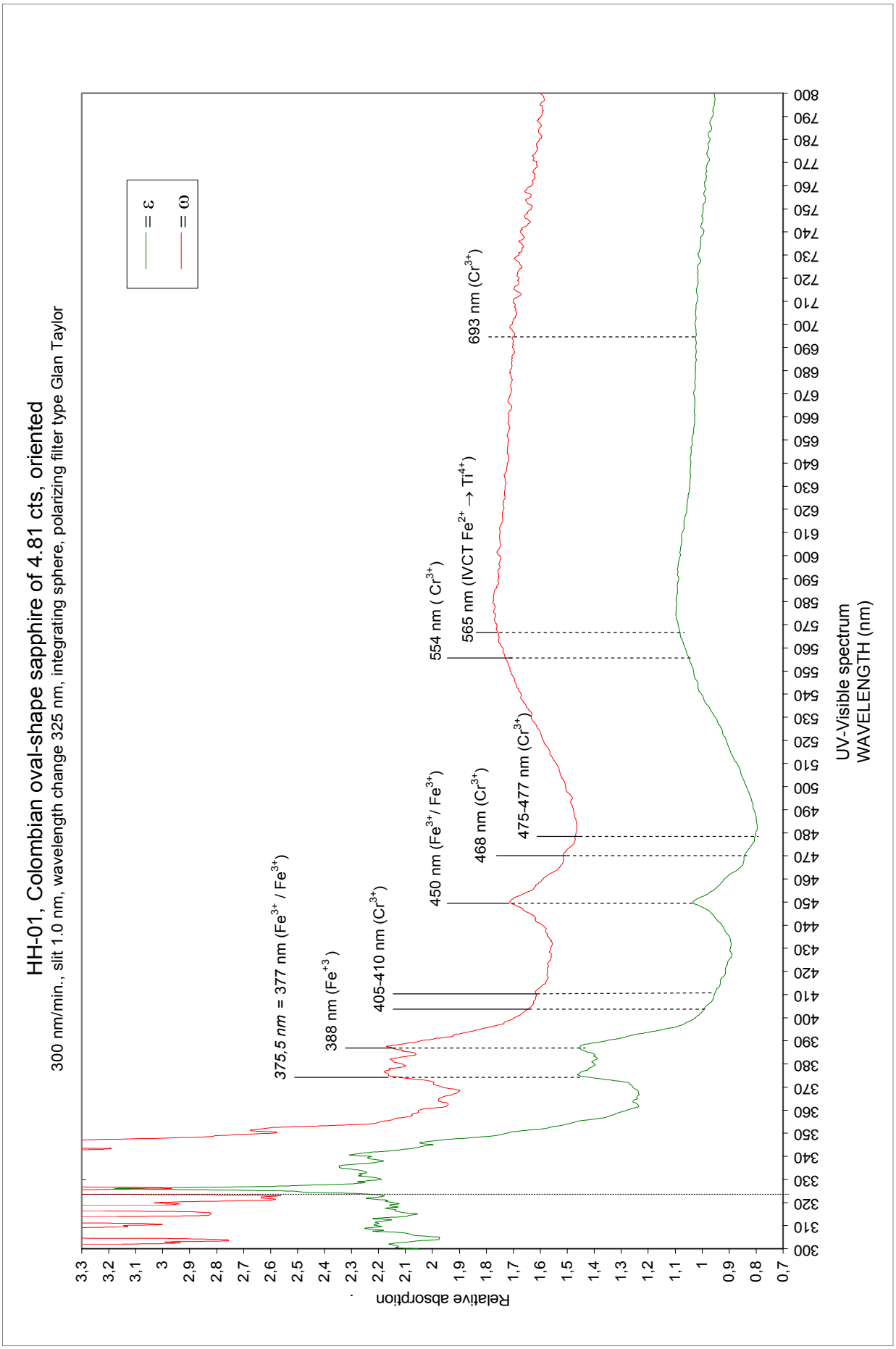
HH-01, Colombian oval-shape sapphire of 4.81 cts, oriented
300 nm/min., slit 1.0 nm, wavelength change 325 nm, integrating sphere, polarizing filter type Glan Taylor
ω =
ε =
375,5 nm = 377 nm (Fe3+ / Fe3+)
388 nm (Fe+3)
405-410 nm (Cr3+)
450 nm (Fe3+/ Fe3+)
468 nm (Cr3+)
475-477 nm (Cr3+)
554 nm (Cr3+)
565 nm (IVCT Fe2+ → Ti4+)
693 nm (Cr3+)
Relative absorption
UV-Visible spectrum
WAVELENGTH (nm)

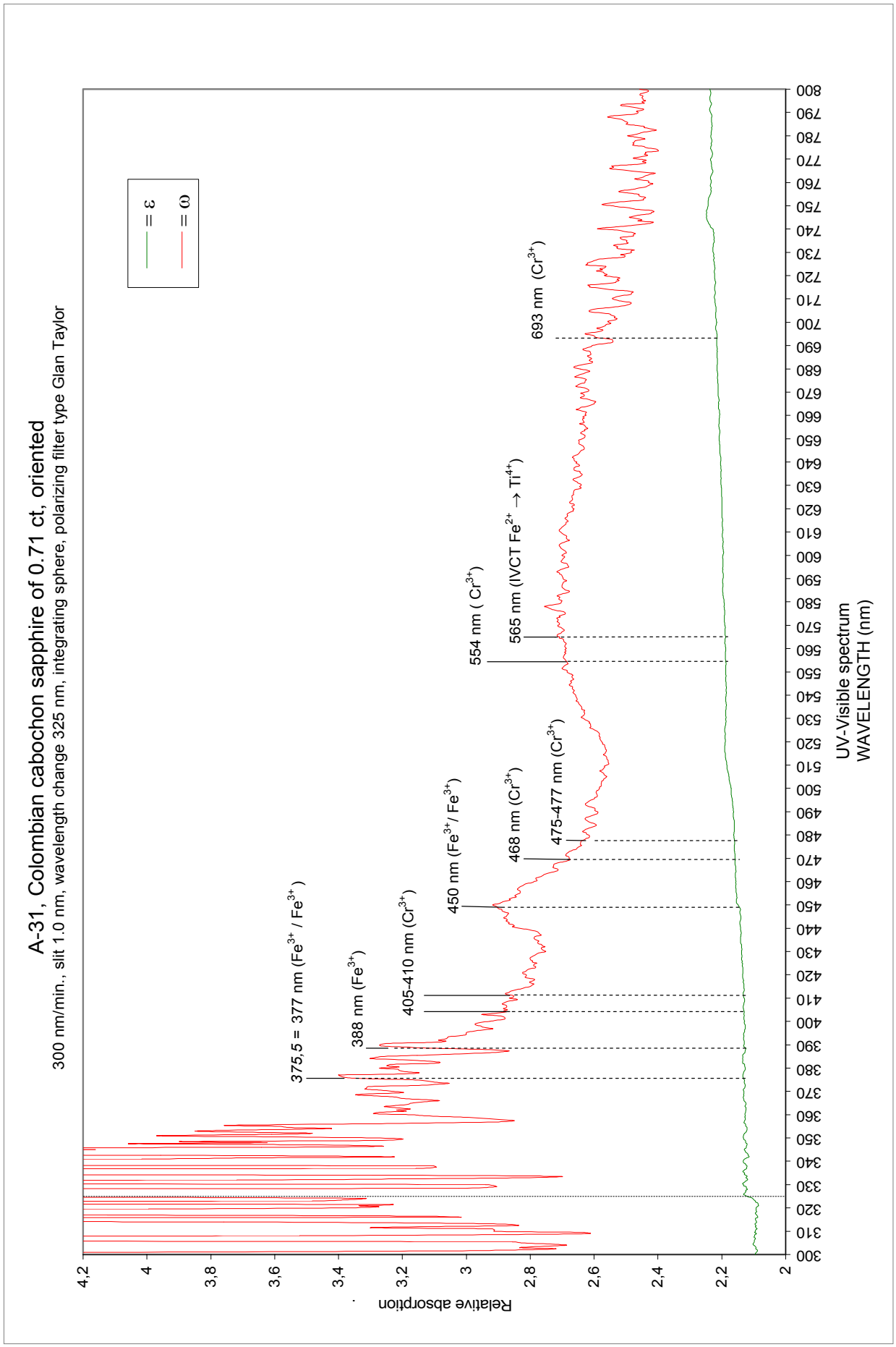
A-31, Colombian cabochon sapphire of 0.71 ct, oriented
300 nm/min., slit 1.0 nm, wavelength change 325 nm, integrating sphere, polarizing filter type Glan Taylor
ε =
ω =
375,5 = 377 nm (Fe3+ / Fe3+)
388 nm (Fe3+)
405-410 nm (Cr3+)
450 nm (Fe3+ / Fe3+)
468 nm (Cr3+)
475-477 nm (Cr3+)
554 nm (Cr3+)
565 nm (IVCT Fe2+ → Ti4+)
693 nm (Cr3+)
Relative absorption
UV-Visible spectrum
WAVELENGTH (nm)

The heat-treated sapphire

			Dichroïm intensity	ω-ray colour	ε-ray colour
• Ref. TT-01	Oval-shape	2.14 carats	Strong	Dark blue	Greenish-blue

Spectroscopic analysis of this sapphire

The ω-ray is more developped than the ε-ray.
The same spectrum as the one described for sapphires is observed. The heat-treatment this stone received is imperceptible on the UV-VIS spectrum.

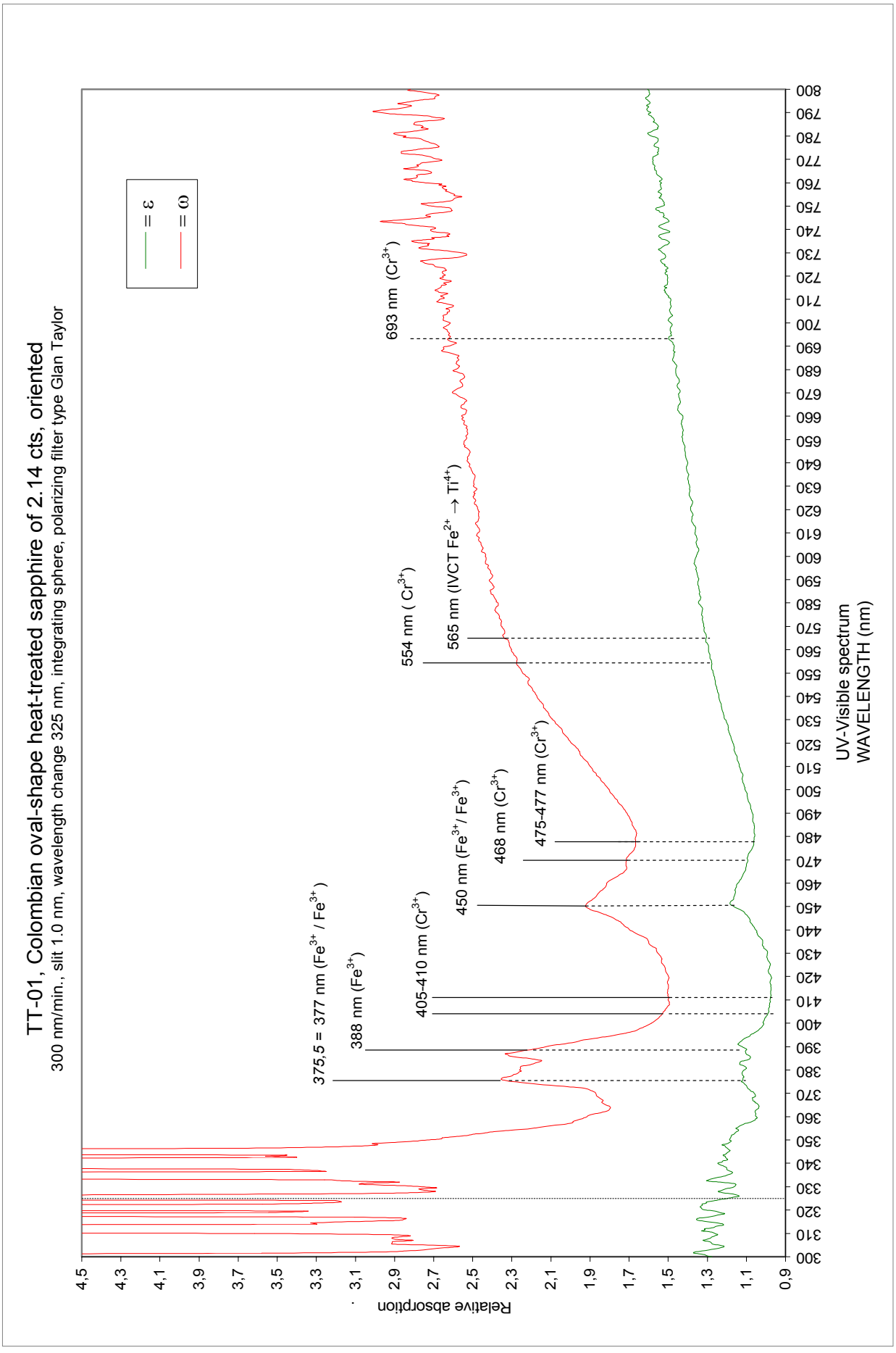
TT-01, Colombian oval-shape heat-treated sapphire of 2.14 cts, oriented
300 nm/min., slit 1.0 nm, wavelength change 325 nm, integrating sphere, polarizing filter type Glan Taylor
ε =
ω =
693 nm (Cr3+)
554 nm (Cr3+)
565 nm (IVCT Fe2+ → Ti4+)
475-477 nm (Cr3+)
468 nm (Cr3+)
450 nm (Fe3+/ Fe3+)
405-410 nm (Cr3+)
388 nm (Fe3+)
375,5 = 377 nm (Fe3+ / Fe3+)
Relative absorption
UV-Visible spectrum
WAVELENGTH (nm)

The six multicoloured faceted sapphires

			Dichroïm intensity	ω-ray colour	ε-ray colour
• Ref. A-25	Oval-shape	2.58 carats	Strong	Pink	Pale yellow-green
• Ref. A-28	Oval-shape	1.53 carat	Strong	Violetish-pink	Greenish-yellow
• Ref. A-30	Oval-shape	3.32 carats	Strong	Violetish-pink	Pink
• Ref. HH-02	Oval-shape	0.96 carat	Strong	Violetish-red	Greyish-red
• Ref. A-32	Cabochon	1.66 carat	Strong	Pinkish-blue	Yellowish-grey
• Ref. A-34	Oval-shape	0.30 carat	Strong	Light blue	Yellowish-green

Spectroscopic analysis of these multicoloured sapphires

The ω-ray is more developped than the ε-ray.
The multicoloured sapphires reveal two main types of spectrum:

- Most show the iron absorption bands, plus the chromium absorption bands.
  The iron bands:
  Sharp bands at 377 nm (Fe^{3+}/Fe^{3+}), and 388 nm (Fe^{2+}), a medium to strong band at 450 nm (Fe^{3+}/Fe^{3+}), and a very broad band at 565 nm (IVCT $Fe^{2+} \rightarrow Ti^{4+}$). Their relative intensities varies according to the iron present in the host corundum
  The chromium bands:
  A sharp band at 693 nm (Cr^{3+}, most often seen but occasionally missing), a broad band at 554 nm (Cr^{3+}), sharp bands at 475-477 nm (Cr^{3+}),and 468 nm (Cr^{3+}), and a broad band at 405-410 nm (Cr^{3+}). Their relative intensities varies according to the chromium ratio, which governs the depth of the red hue observed in these corundums.

- Those that show only the absorption bands of iron: sharp bands at 377 nm (Fe^{3+}/Fe^{3+}), and 388 nm (Fe^{2+}), a medium to strong band at 450 nm (Fe^{3+}/Fe^{3+}), and a very broad band at 565 nm (IVCT $Fe^{2+} \rightarrow Ti^{4+}$).
  Their relative intensities however varies substantially from one specimen to another, and these variations are responsible for the different hues recorded (the least iron doped sapphire displays the least developped iron spectrum, and therefore the weakest colour in the blue, green, or yellow hues).
  As already described for the rubies and sapphires, here a multicoloured sapphires shows a flat ε-ray (A-34, a dark blue, orangy-pink corundum), yet the ε-ray is not colourless. The ε-ray colour is: yellowish.

Note

For all these multicoloured sapphires, the spectrum can vary drastically according to which area of the stone is analysed. To illustrate this, no better example than stone A-32 a blue, yellow, pink corundum, which shows two different spectrums. One seems to make it correspond to the first group (iron + chromium), while the second one with solely iron bands points towards the second group (iron).

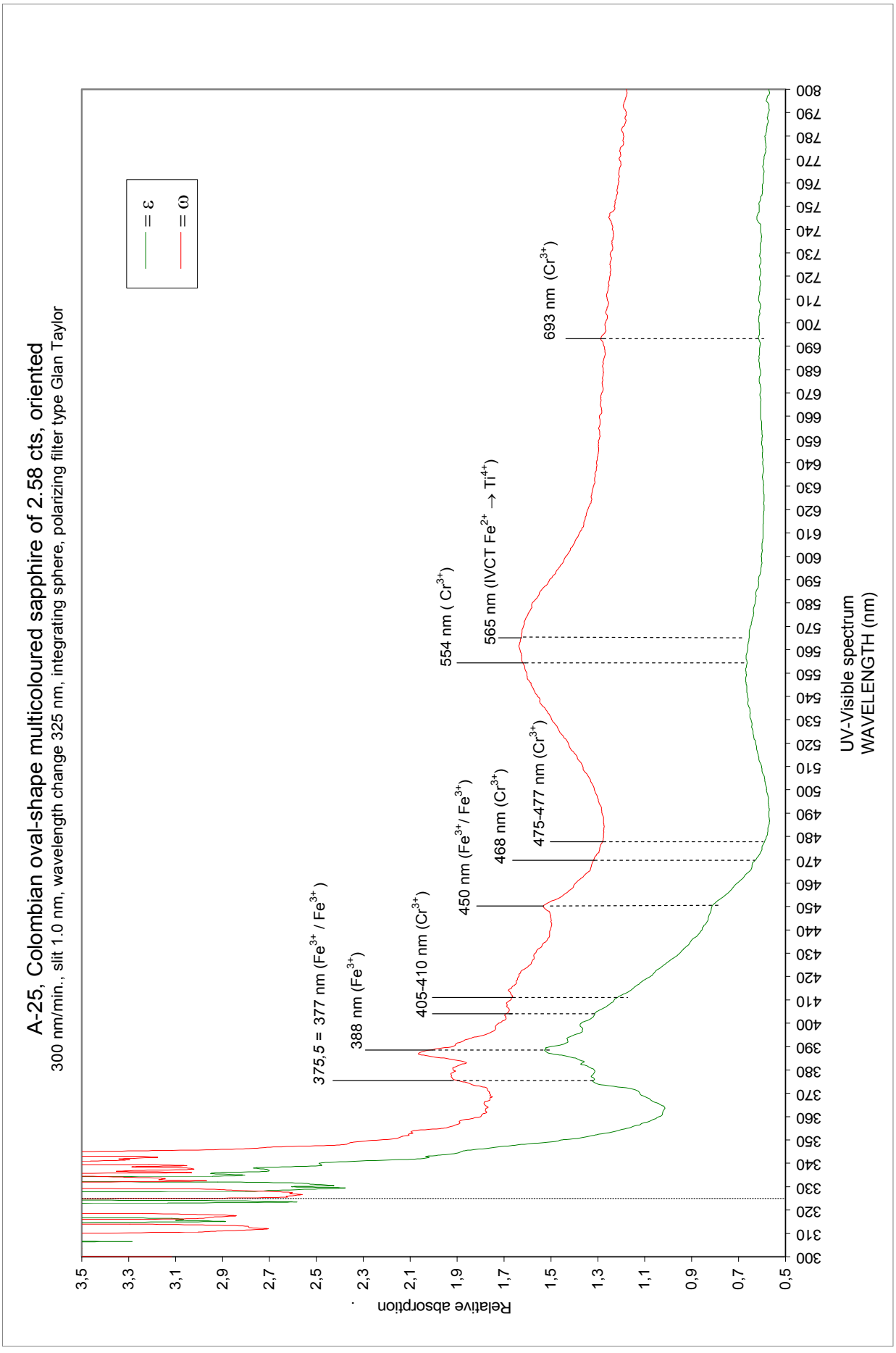
A-25, Colombian oval-shape multicoloured sapphire of 2.58 cts, oriented
300 nm/min., slit 1.0 nm, wavelength change 325 nm, integrating sphere, polarizing filter type Glan Taylor
= ε
= ω
375,5 = 377 nm (Fe3+ / Fe3+)
388 nm (Fe3+)
405-410 nm (Cr3+)
450 nm (Fe3+/ Fe3+)
468 nm (Cr3+)
475-477 nm (Cr3+)
554 nm (Cr3+)
565 nm (IVCT Fe2+ → Ti4+)
693 nm (Cr3+)
Relative absorption
UV-Visible spectrum
WAVELENGTH (nm)

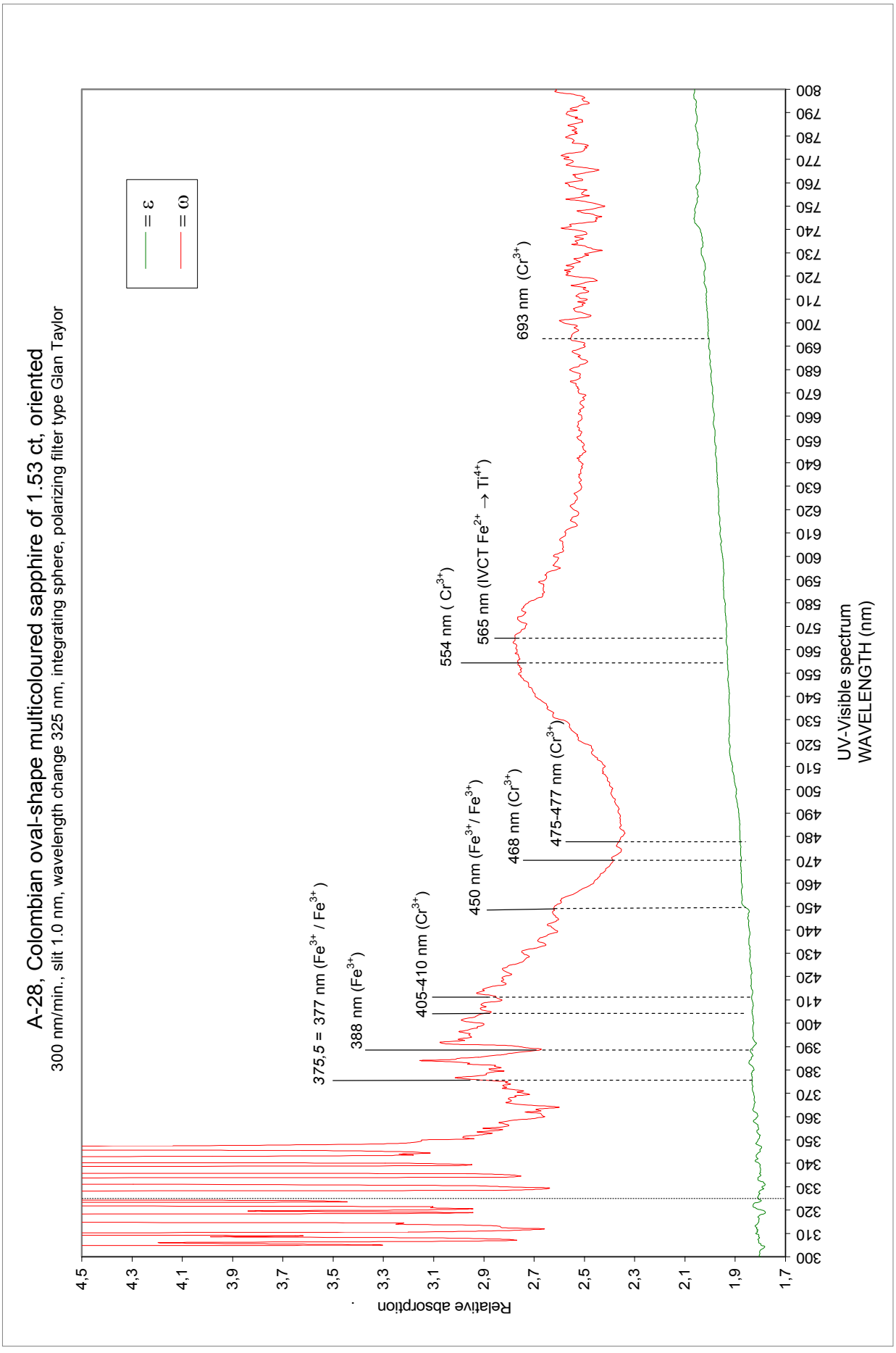
A-28, Colombian oval-shape multicoloured sapphire of 1.53 ct, oriented
300 nm/min., slit 1.0 nm, wavelength change 325 nm, integrating sphere, polarizing filter type Glan Taylor
ε =
ω =
375,5 = 377 nm (Fe3+ / Fe3+)
388 nm (Fe3+)
405-410 nm (Cr3+)
450 nm (Fe3+ / Fe3+)
468 nm (Cr3+)
475-477 nm (Cr3+)
554 nm (Cr3+)
565 nm (IVCT Fe2+ → Ti4+)
693 nm (Cr3+)
Relative absorption
UV-Visible spectrum
WAVELENGTH (nm)

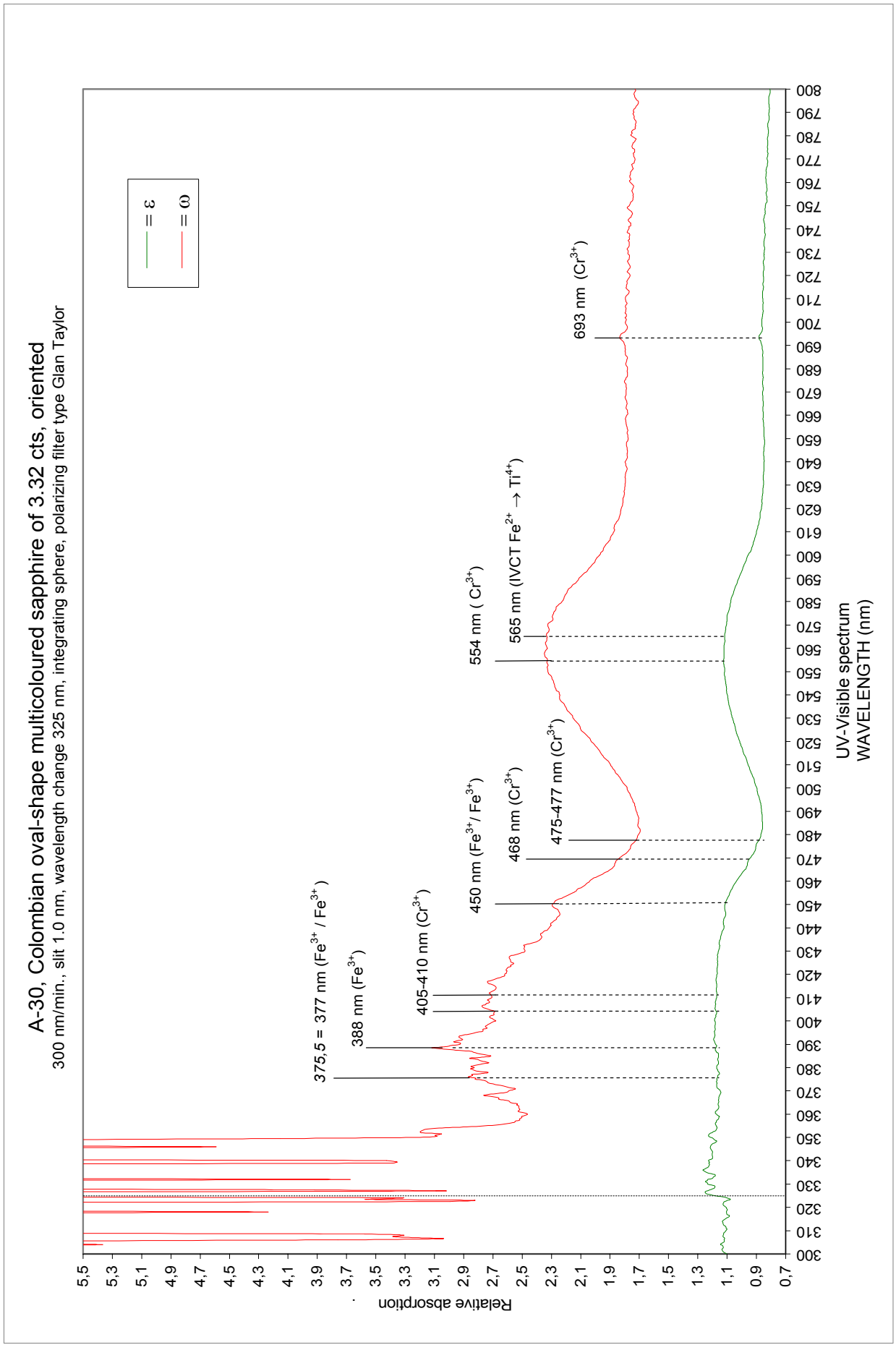
A-30, Colombian oval-shape multicoloured sapphire of 3.32 cts, oriented
300 nm/min., slit 1.0 nm, wavelength change 325 nm, integrating sphere, polarizing filter type Glan Taylor
= ε
= ω
375,5 = 377 nm (Fe3+ / Fe3+)
388 nm (Fe3+)
405-410 nm (Cr3+)
450 nm (Fe3+/ Fe3+)
468 nm (Cr3+)
475-477 nm (Cr3+)
554 nm (Cr3+)
565 nm (IVCT Fe2+ → Ti4+)
693 nm (Cr3+)
Relative absorption
UV-Visible spectrum
WAVELENGTH (nm)

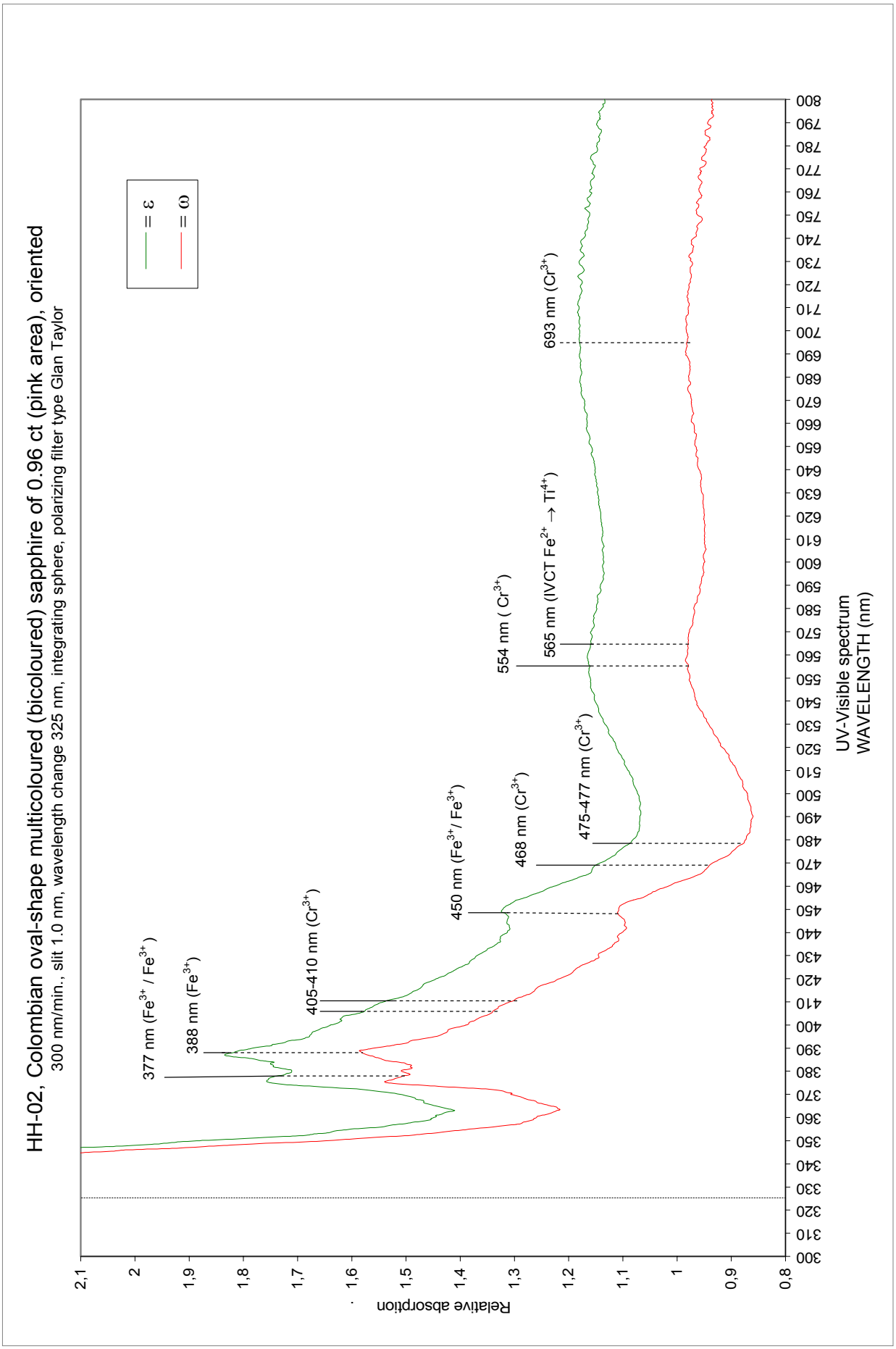
HH-02, Colombian oval-shape multicoloured (bicoloured) sapphire of 0.96 ct (pink area), oriented
300 nm/min., slit 1.0 nm, wavelength change 325 nm, integrating sphere, polarizing filter type Glan Taylor
= ε
= ω
377 nm (Fe3+ / Fe3+)
388 nm (Fe3+)
405-410 nm (Cr3+)
450 nm (Fe3+ / Fe3+)
468 nm (Cr3+)
475-477 nm (Cr3+)
554 nm (Cr3+)
565 nm (IVCT Fe2+ → Ti4+)
693 nm (Cr3+)
Relative absorption
UV-Visible spectrum
WAVELENGTH (nm)

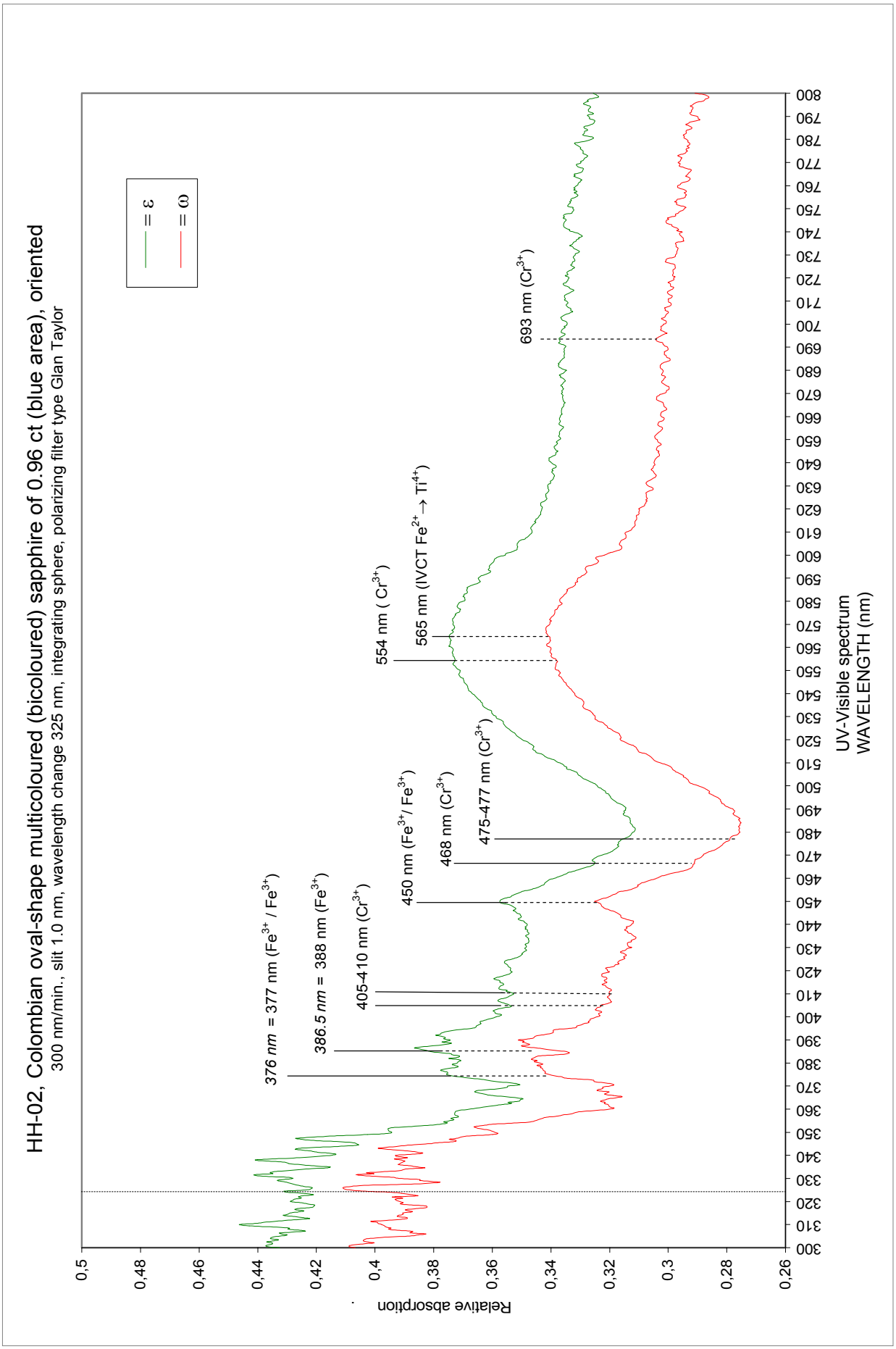
HH-02, Colombian oval-shape multicoloured (bicoloured) sapphire of 0.96 ct (blue area), oriented
300 nm/min., slit 1.0 nm, wavelength change 325 nm, integrating sphere, polarizing filter type Glan Taylor
ε =
ω =
376 nm = 377 nm (Fe3+ / Fe3+)
386.5 nm = 388 nm (Fe3+)
405-410 nm (Cr3+)
450 nm (Fe3+/ Fe3+)
468 nm (Cr3+)
475-477 nm (Cr3+)
554 nm (Cr3+)
565 nm (IVCT Fe2+→ Ti4+)
693 nm (Cr3+)
Relative absorption
UV-Visible spectrum
WAVELENGTH (nm)

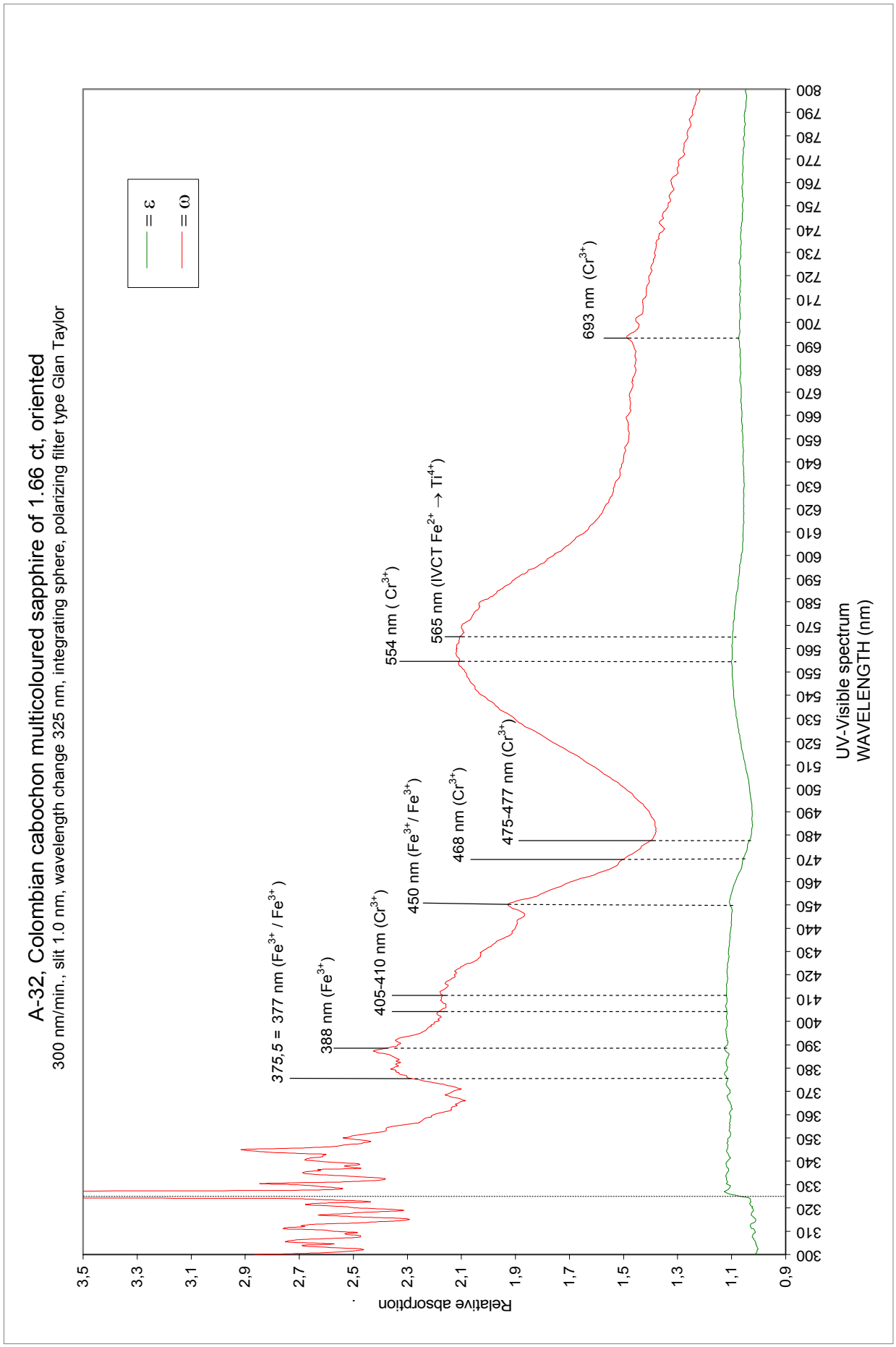
A-32, Colombian cabochon multicoloured sapphire of 1.66 ct, oriented
300 nm/min., slit 1.0 nm, wavelength change 325 nm, integrating sphere, polarizing filter type Glan Taylor
ε =
ω =
375,5 = 377 nm (Fe3+ / Fe3+)
388 nm (Fe3+)
405-410 nm (Cr3+)
450 nm (Fe3+/ Fe3+)
468 nm (Cr3+)
475-477 nm (Cr3+)
554 nm (Cr3+)
565 nm (IVCT Fe2+ → Ti4+)
693 nm (Cr3+)
Relative absorption
UV-Visible spectrum
WAVELENGTH (nm)

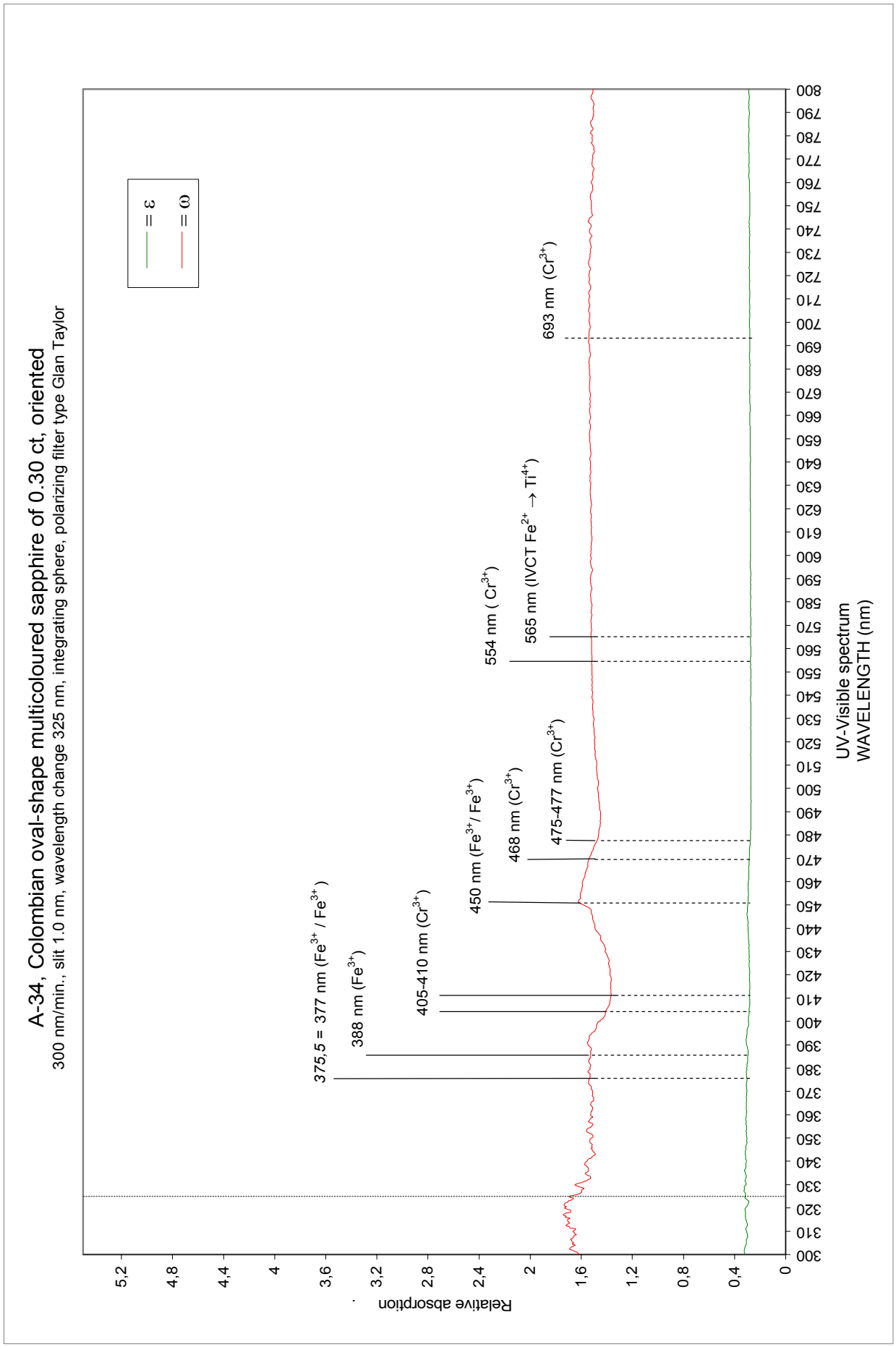
A-34, Colombian oval-shape multicoloured sapphire of 0.30 ct, oriented
300 nm/min., slit 1.0 nm, wavelength change 325 nm, integrating sphere, polarizing filter type Glan Taylor
ε =
ω =
375,5 = 377 nm (Fe3+ / Fe3+)
388 nm (Fe3+)
405-410 nm (Cr3+)
450 nm (Fe3+/ Fe3+)
468 nm (Cr3+)
475-477 nm (Cr3+)
554 nm (Cr3+)
565 nm (IVCT Fe2+ → Ti4+)
693 nm (Cr3+)
Relative absorption
UV-Visible spectrum
WAVELENGTH (nm)

The colour-change sapphire

			Dichroïm intensity	ω-ray colour	ε-ray colour
• Ref. A-33	Oval-shape	0.65 carat	Strong	Purple	Yellowish-grey

Spectroscopic analysis of this colour-change sapphire

The ω-ray is more developped than the ε-ray.
The same spectrum as the one described for multicoloured sapphires that show iron and chromium absorption bands is observed.

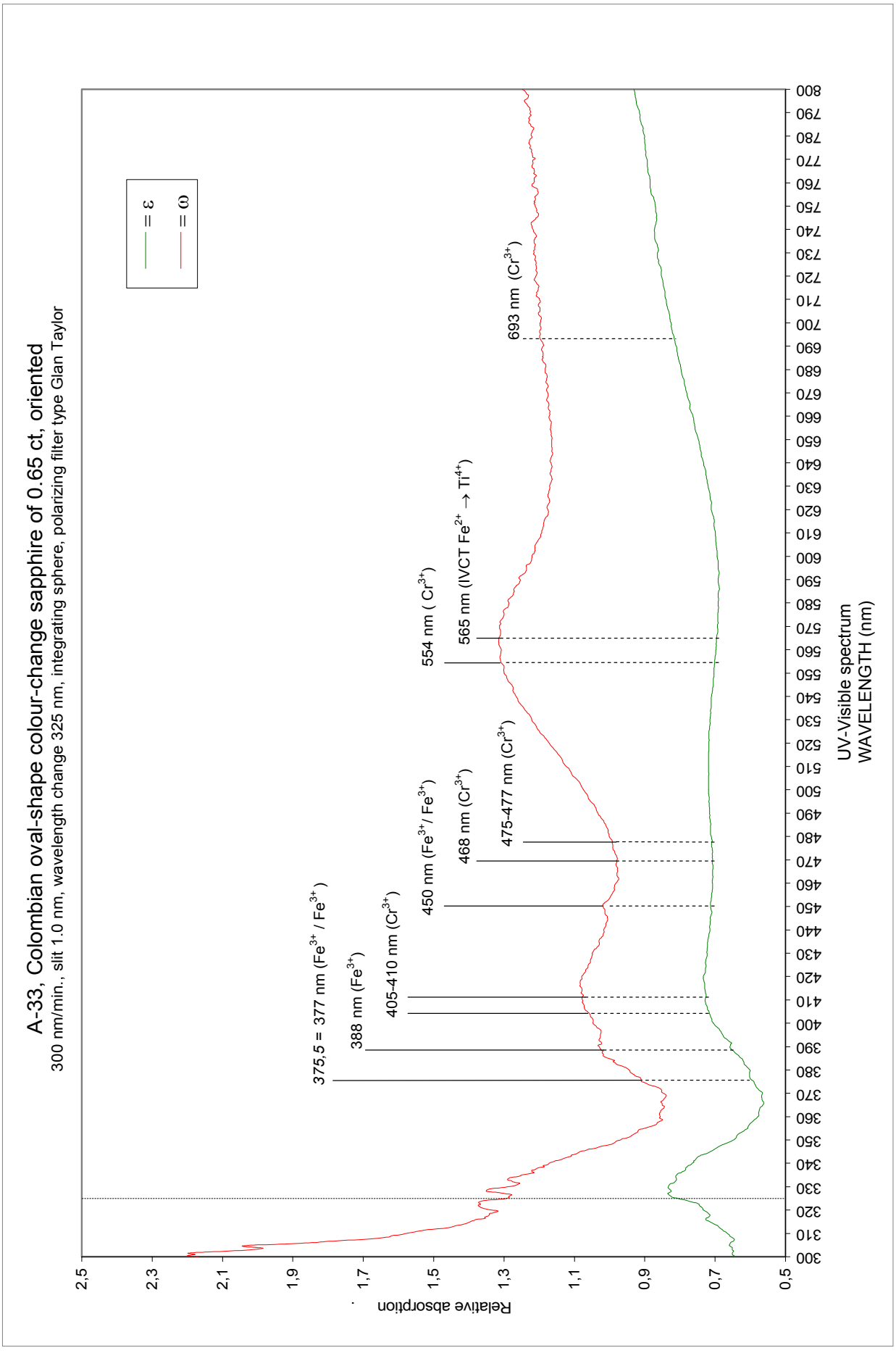
A-33, Colombian oval-shape colour-change sapphire of 0.65 ct, oriented
300 nm/min., slit 1.0 nm, wavelength change 325 nm, integrating sphere, polarizing filter type Glan Taylor
ε
ω
375,5 = 377 nm (Fe3+ / Fe3+)
388 nm (Fe3+)
405-410 nm (Cr3+)
450 nm (Fe3+/ Fe3+)
468 nm (Cr3+)
475-477 nm (Cr3+)
554 nm (Cr3+)
565 nm (IVCT Fe2+ → Ti4+)
693 nm (Cr3+)
Relative absorption
UV-Visible spectrum
WAVELENGTH (nm)

The two heat-treated colour-change sapphires

			Dichroïm intensity	ω-ray colour	ε-ray colour
• Ref. TT-02	Oval-shape	0.96 carat	Strong	Purple	Yellowish-grey
• Ref. TT-03	Oval-shape	0.95 carat	Strong	Purple	Greenish-yellow

Spectroscopic analysis of these heat-treated colour-change sapphires

The ω-ray is more developped than the ε-ray.
Similar spectrum as the one described for multicoloured sapphires that shows a good balance between iron and chromium absorption bands, with well defined absorption bands 693 nm (Cr^{3+}), and 450 nm (Fe^{3+}/Fe^{3+}), with other bands at 377 nm (Fe^{3+}/Fe^{3+}), and 388 nm (Fe^{3+}). The fact that these sapphires were heat-treated, leave no such indication on their UV-VIS spectrum, which prove identical to those recorded for the other Colombian sapphires.

Discussion

It is a well established fact that the blue colour of most sapphires, results from a combination of titanium and iron elements that have replaced some of the aluminium in the corundum structure Al_2O_3. If sapphires of all sources show IVCT $Fe^{2+} \rightarrow Ti^{4+}$ (very broad absorption at 565 nm), those of non basaltic origin (see table 8) owe their colour essentially to this mechanism, and therefore most often show only a weak to diffuse absorption band at 540 nm due to Fe^{3+}/Fe^{3+}.
Sapphires of basaltic origin, on the contrary, owe their colour mainly to Fe^{3+}/Fe^{3+}, and display medium to strong absorptions bands in the region of 377 nm, and 450 nm, and also due to Fe^{3+}, a sharp absorption band at 388 nm.
The UV-visible spectrum recorded for all the different sapphires (including those heat-treated) from Colombia, are typical of sapphires from basaltic sources (again see table 8). They are dominated by three essential absorption mechanisms (Smith *et al.* 1985):

Fe^{3+}	absorption band 388 nm (not developped for metamorphic sapphires).
Fe^{3+}/Fe^{3+}	absorption bands 377 nm, and 450 nm (much less developped in metamorphic sapphires).
IVCT $Fe^{2+} \rightarrow Ti^{4+}$	absorption band 565 nm (present in sapphires of all origins).

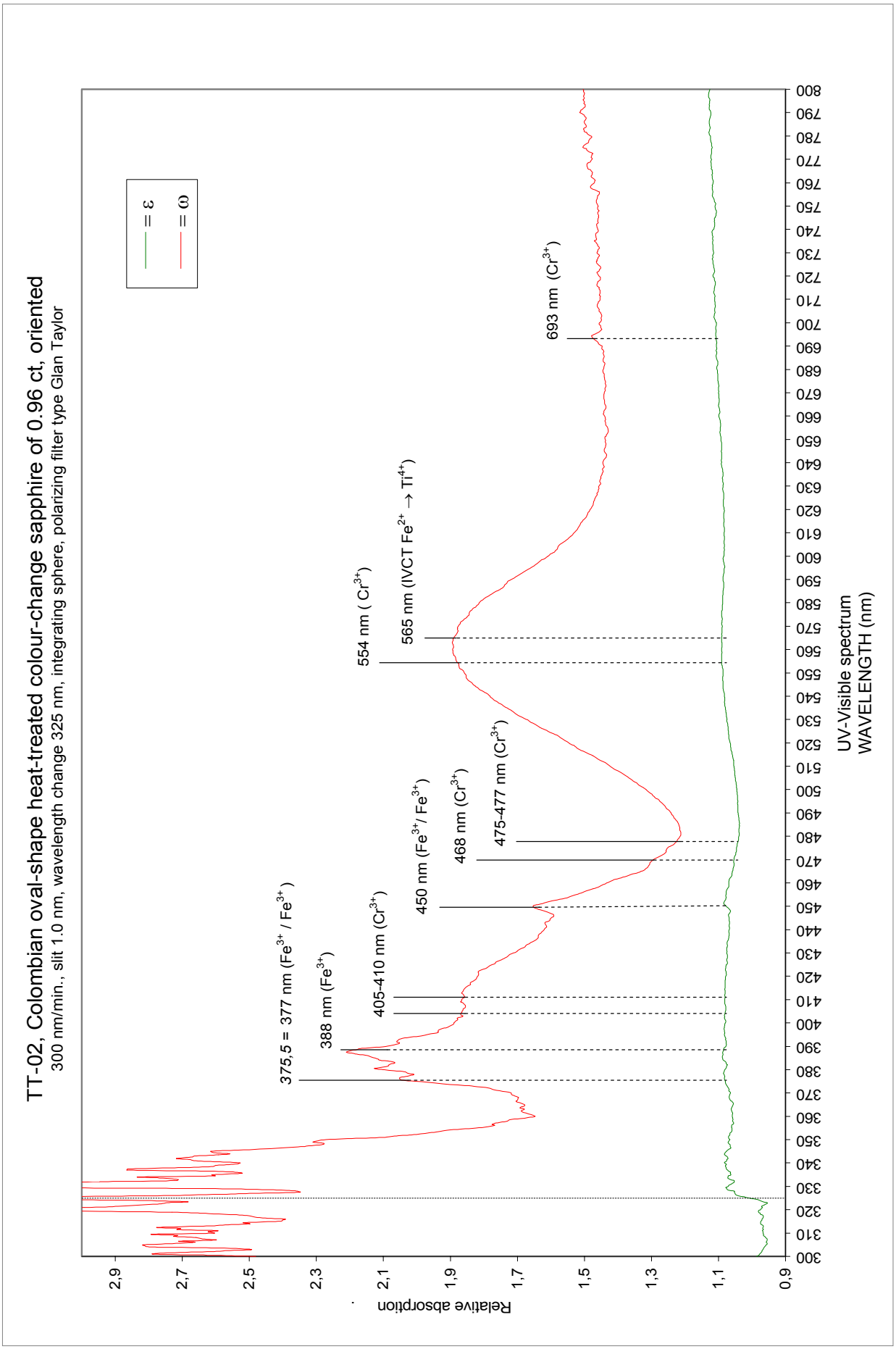
TT-02, Colombian oval-shape heat-treated colour-change sapphire of 0.96 ct, oriented
300 nm/min., slit 1.0 nm, wavelength change 325 nm, integrating sphere, polarizing filter type Glan Taylor
ω
ε
375,5 = 377 nm (Fe3+ / Fe3+)
388 nm (Fe3+)
405-410 nm (Cr3+)
450 nm (Fe3+/ Fe3+)
468 nm (Cr3+)
475-477 nm (Cr3+)
554 nm (Cr3+)
565 nm (IVCT Fe2+ → Ti4+)
693 nm (Cr3+)
Relative absorption
UV-Visible spectrum
WAVELENGTH (nm)

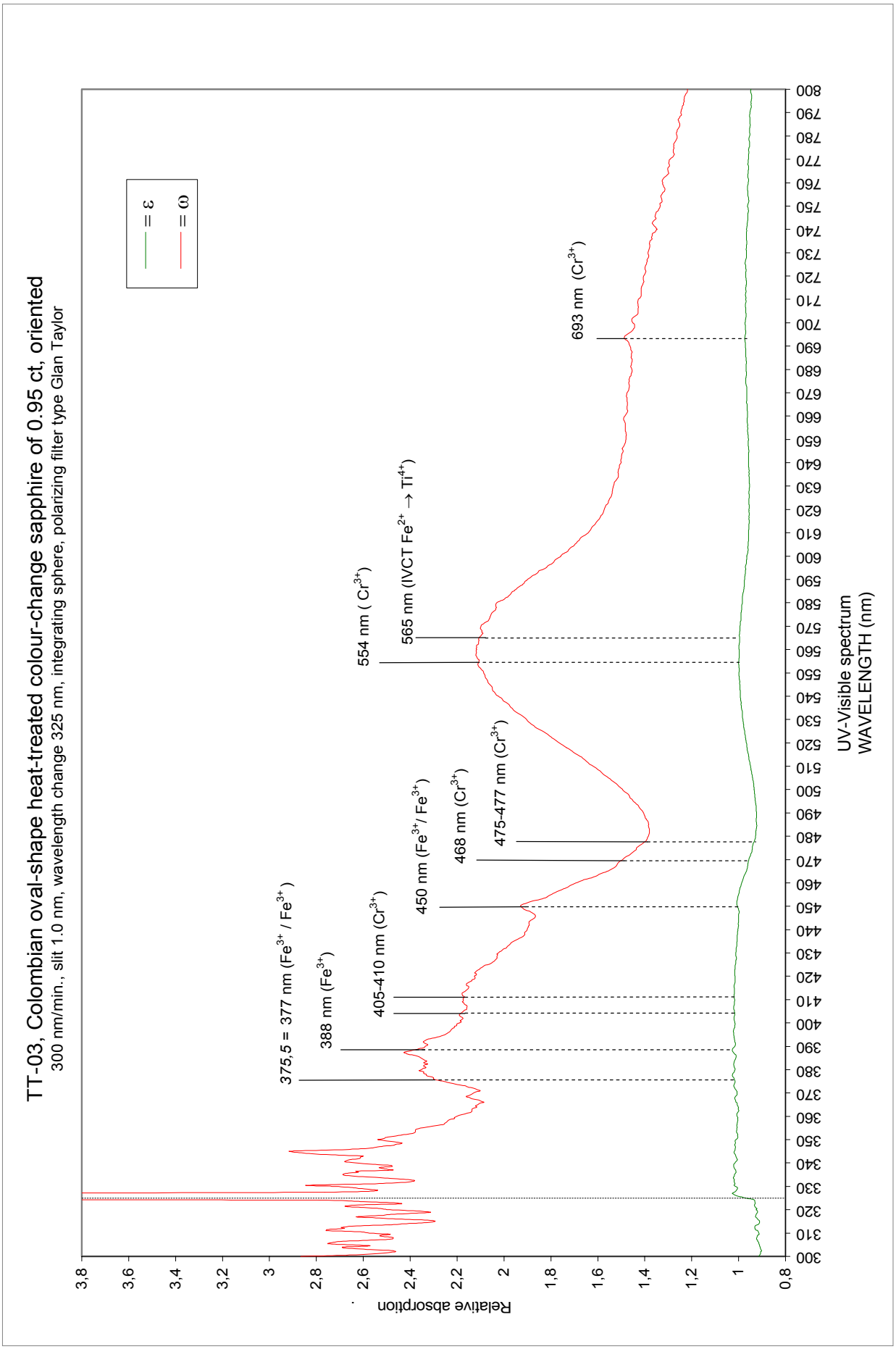
TT-03, Colombian oval-shape heat-treated colour-change sapphire of 0.95 ct, oriented
300 nm/min., slit 1.0 nm, wavelength change 325 nm, integrating sphere, polarizing filter type Glan Taylor
= ω
= ε
375,5 = 377 nm (Fe3+ / Fe3+)
388 nm (Fe3+)
405-410 nm (Cr3+)
450 nm (Fe3+/ Fe3+)
468 nm (Cr3+)
475-477 nm (Cr3+)
554 nm (Cr3+)
565 nm (IVCT Fe2+ → Ti4+)
693 nm (Cr3+)
Relative absorption
UV-Visible spectrum
WAVELENGTH (nm)

INFRA-RED SPECTROPHOTOMETRY (FT-IR)

All spectra were obtained on a Nicolet Magna-IR E.S.P. System 560 spectrometer. This is a double-beam regulation instrument, with KBr beamsplitter, and a series of mirrors, to the DTGS KBr detector, with fully automated record of the absorption spectra.
The instrument scans from 7400 cm^{-1} to 350 cm^{-1} with a resolution of up to 0,125 cm^{-1}, and a speed of 35 scans by second.
The instrumental working conditions were as follows: wavelength range 4000-2000 cm^{-1}, with a resolution of 4 cm^{-1}, number of scans between 100 and 200 proved sufficient.
The specimen being tested usually does not require any particular orientation, and a reflection or transmission technique is used according to its size. A background spectrum must be obtained with a correction for H_2O and CO_2 which is then deduced from the final result.

Twenty three faceted corundums were studied, and their FT-IR results described below.

Five rubies

- Ref. A-01 Pear-shape 1.86 carat
- Ref. A-05 Cabochon 1.66 carat
- Ref. A-06 Cabochon 6.24 carats
- Ref. GT-01 Oval-shape 0.33 carat
- Ref. GT-02 Pear-shape 0.19 carat

Eight faceted sapphires

- Ref. A-07 Cabochon 3.01 carats
- Ref. A-08 Cabochon 2.66 carats
- Ref. A-11 Marquise 2.19 carats
- Ref. A-13 Oval-shape 3.42 carats
- Ref. A-14 Oval-shape 3.55 carats
- Ref. A-17 Oval-shape 1.65 carat
- Ref. HH-01 Oval-shape 4.81 carats
- Ref. A-31 Cabochon 0.71 carat

A heat-treated sapphire

- Ref. TT-01 Oval-shape 2.14 carats

Six multicoloured faceted sapphires

- Ref. A-25 Oval-shape 2.58 carats
- Ref. A-28 Oval-shape 1.53 carat
- Ref. A-30 Oval-shape 3.32 carats
- Ref. HH-02 Oval-shape 0.96 carat
- Ref. A-32 Cabochon 1.66 carat
- Ref. A-34 Oval-shape 0.30 carat

A colour-change sapphire

- Ref. A-33 Oval-shape 0.65 carat

Two heat-treated colour-change sapphires

- Ref. TT-02 Oval-shape 0.96 carat
- Ref. TT-03 Oval-shape 0.95 carat

Spectroscopic analysis of these Colombian corundums

They frequently display a series of absorption peaks in the 2000-4000 $^{cm-1}$ region.
Two distinctly separate combinations of generally three main peaks each in this latter region are encountered and can be distinguished, with only slight variations occurring from one specimen to another. The reason for these slight variations is probably imparted to certain mineral inclusions.

The main peaks observed for the five rubies:

First set (usually three distinct peaks)

± 2850 $^{cm-1}$ (strong)
± 2921 $^{cm-1}$ (strongest)
± 2950 $^{cm-1}$ (moderately strong)

These peaks are due to grease released by our fingers, or Blu-tack (paste used to hold the samples to be tested), or residues of plastic or resin, and therefore must be considered as an artefact (David *et al.,* 2001*)*.

Second set (from two to four peaks, with sometimes a minute shoulder)

± 3232 $^{cm-1}$ (moderate to weak)
± 3261 $^{cm-1}$ (usually moderate to very weak. Occasionally strong)
± 3295 $^{cm-1}$ (often observed as a minute shoulder)
± 3309 $^{cm-1}$ (strongest when present)
± 3620 $^{cm-1}$ (strong)
± 3649 $^{cm-1}$ (weak)
± 3669 $^{cm-1}$ (weak)
± 3696 $^{cm-1}$ (strong)

The peak at ± 3309 $^{cm-1}$, was observed in all of the Colombian rubies except one (A-05), which was proved to be of a non-basaltic origin.
Two rubies display only two peaks: 3275 $^{cm-1}$, and 3309 $^{cm-1}$ (GT-01). 3228 $^{cm-1}$, and 3308 $^{cm-1}$ (GT-02).
A ruby (A-05) shows a totally different spectrum, with three peaks at ± 3620 $^{cm-1}$, ± 3649 $^{cm-1}$, and ± 3696 $^{cm-1}$ (this last peak is the strongest).

For comparison purposes, Table 9, shows for each ruby examined, the main peaks observed, their intensity, position, and last their frequency expressed in percent.

TABLE 9 Main peaks observed in the five Colombian rubies

Ruby source	Peak intensity and location (cm^{-1})									
	Strong ± 3185	*Shoulder* ± 3209	*Moderate* ± 3232	*Weak* ± 3261	*Shoulder* ± 3295	***Strongest*** ± 3309	*Strong* ± 3620	*Weak* ± 3649	*Weak* ± 3669	*Strong* ± 3696
A-01			3232	3266	3290	**3309**				
A-05							3620	3649	3669	**3696**
A-06			3229	3265	3288	**3309**				
GT-01				3275		**3309**				
GT-02			3228			**3308**				
Syn. Verneuil	3182	3209	**3231**		3292	3309				
Frequency observed	*0%*	*0%*	*60%*	*60%*	*40%*	*80%*	*20%*	*20%*	*20%*	*20%*

Discussion

Amongst the different corundum synthesis (Czochralski, flux-fusion, …), which under infrared spectroscopy, usually (if not further heat treated) show no signal in the mid-infrared range 3000 to 3600 $^{cm-1}$, the Verneuil synthetics (DD-01 synthetic Verneuil ruby of 3.08 cts), like the Colombian rubies, often show the second set of three main peaks (± 3232 $^{cm-1}$, ± 3261 $^{cm-1}$, and ± 3309 $^{cm-1}$), and often a shoulder (± 3295 $^{cm-1}$), in the mid-infrared range 3100 to 3310 $^{cm-1}$.

This second set of three peaks, for the synthetic Verneuil ruby shows similar peak positions, but different intensities compared to those observed for the Colombian rubies: the main peak is at ± 3231 $^{cm-1}$ (± 3309 $^{cm-1}$ for the main peak in Colombian rubies). The next two peaks in intensities are seen at ± 3182 $^{cm-1}$ and ± 3309 $^{cm-1}$ (the next two peaks in intensities ± 3230 $^{cm-1}$ and ± 3260 $^{cm-1}$ for the Colombian rubies).

All the Colombian rubies (except A-05) exhibit the peak at ± 3309 $^{cm-1}$ also observed in the Verneuil synthetics. This peak (as for the peaks at ± 3185 $^{cm-1}$, 3232 $^{cm-1}$, and 3295 $^{cm-1}$) is caused by a OH-dipole linked to a pair of atoms of iron and titanium inside the corundum lattice and if present in all basaltic rubies, it is observed only in the heat-treated non-basaltic rubies (David *et al.,* 2001). Since ruby A-05 was proved non-basaltic, the absence of the peak 3309 $^{cm-1}$ points towards a non heat-treated ruby. It must also be said here that its infra-red spectrum is notably different from those obtained for other non-basaltic corundums, and confirms with PIXE analysis that this ruby could be from Colombia as stated by the provider (source A), which confirms that basaltic and non-basaltic rubies coexist.

Since as demonstrated, the Colombian rubies show similar infra-red spectra to the ones observed for synthetic Verneuil rubies, if devoid of characteristic inclusions, or other parameters that permit a separation, they cannot rely on this method to be distinguished.

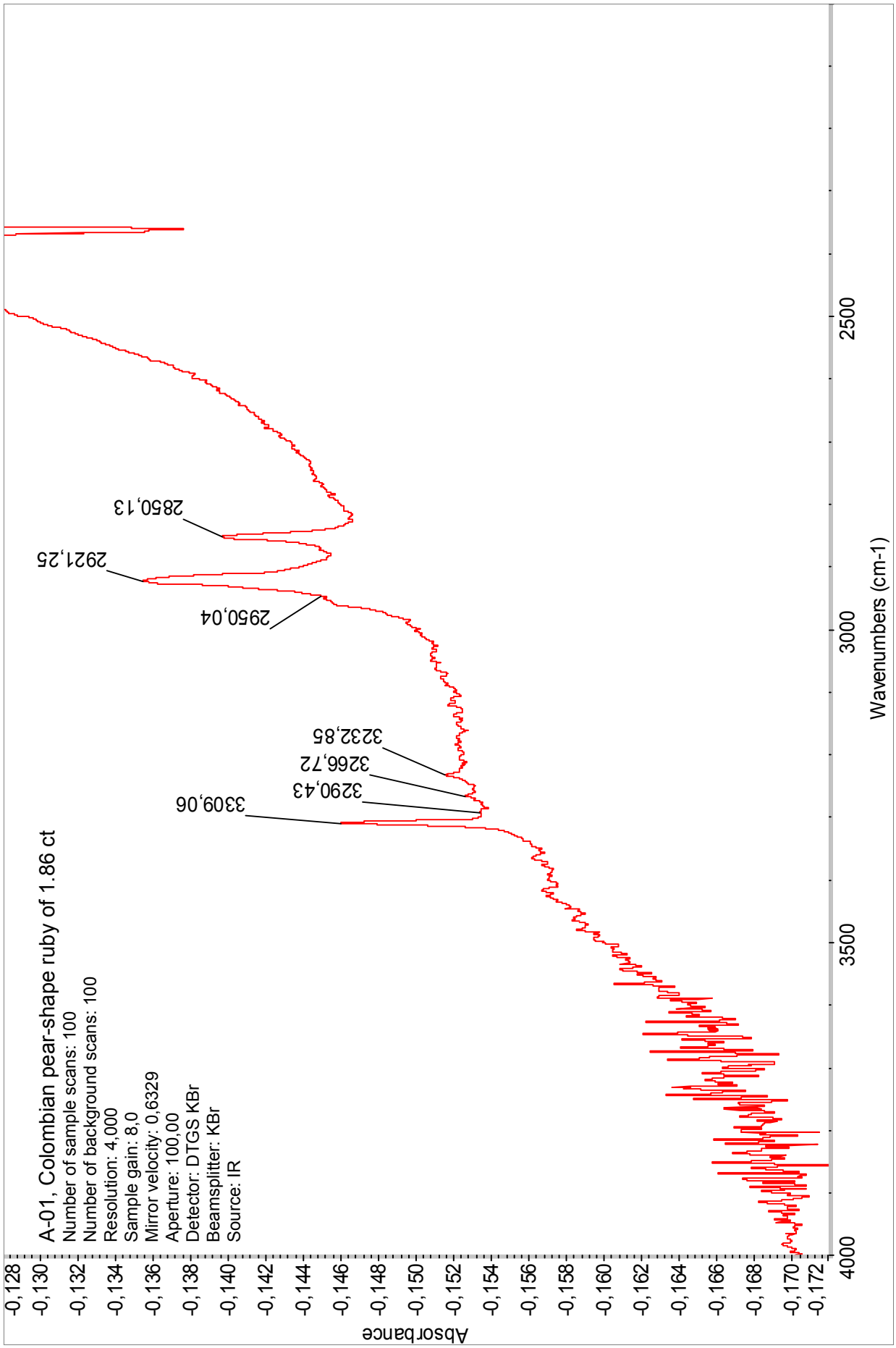
A-01, Colombian pear-shape ruby of 1.86 ct
Number of sample scans: 100
Number of background scans: 100
Resolution: 4,000
Sample gain: 8,0
Mirror velocity: 0,6329
Aperture: 100,00
Detector: DTGS KBr
Beamsplitter: KBr
Source: IR
3309,06
3290,43
3266,72
3232,85
2950,04
2921,25
2850,13
Absorbance
Wavenumbers (cm-1)
4000
3500
3000
2500
-0,128
-0,130
-0,132
-0,134
-0,136
-0,138
-0,140
-0,142
-0,144
-0,146
-0,148
-0,150
-0,152
-0,154
-0,156
-0,158
-0,160
-0,162
-0,164
-0,166
-0,168
-0,170
-0,172

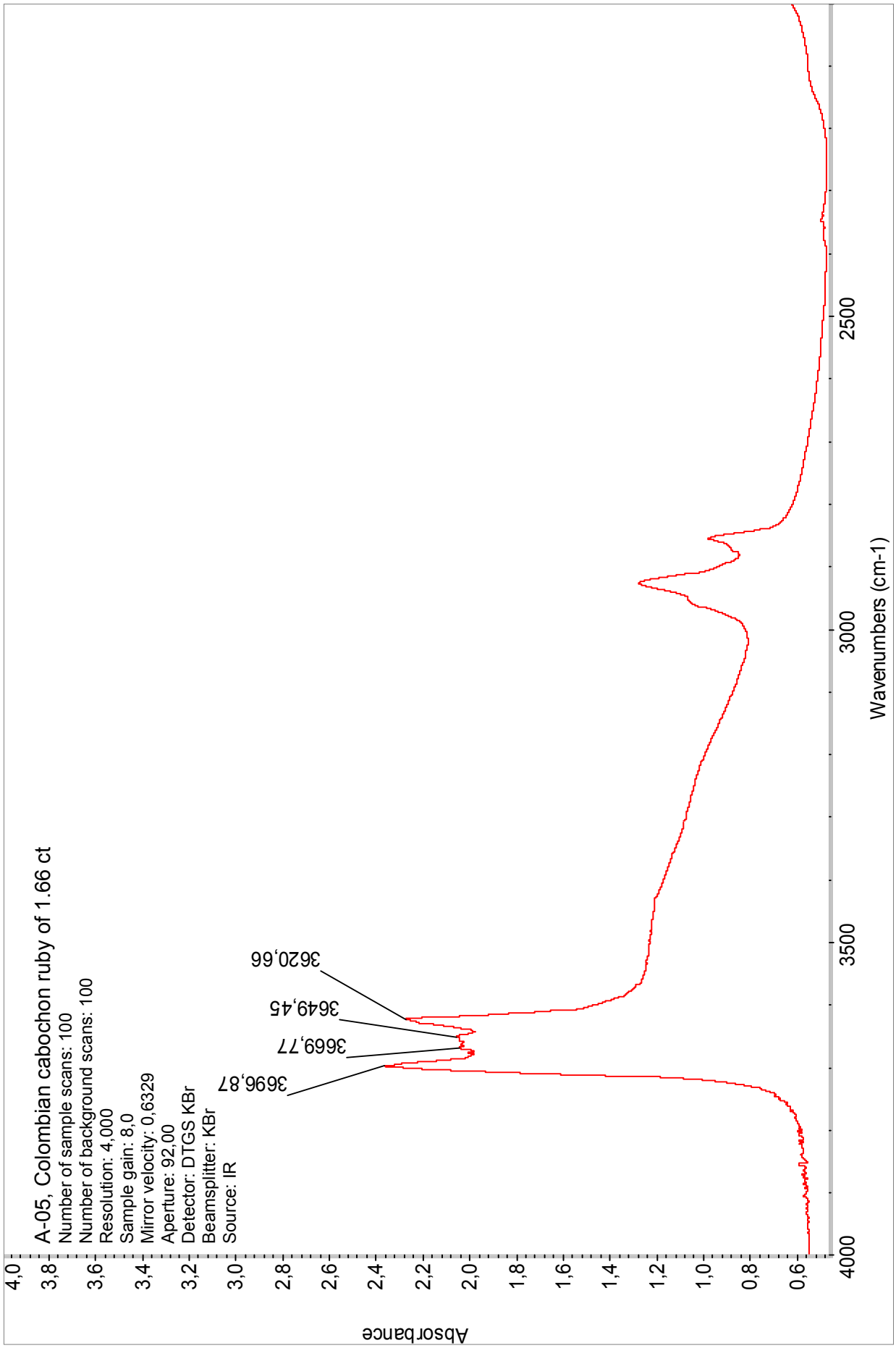
A-05, Colombian cabochon ruby of 1.66 ct
Number of sample scans: 100
Number of background scans: 100
Resolution: 4,000
Sample gain: 8,0
Mirror velocity: 0,6329
Aperture: 92,00
Detector: DTGS KBr
Beamsplitter: KBr
Source: IR
3696,87
3669,77
3649,45
3620,66
Absorbance
Wavenumbers (cm-1)
4000
3500
3000
2500

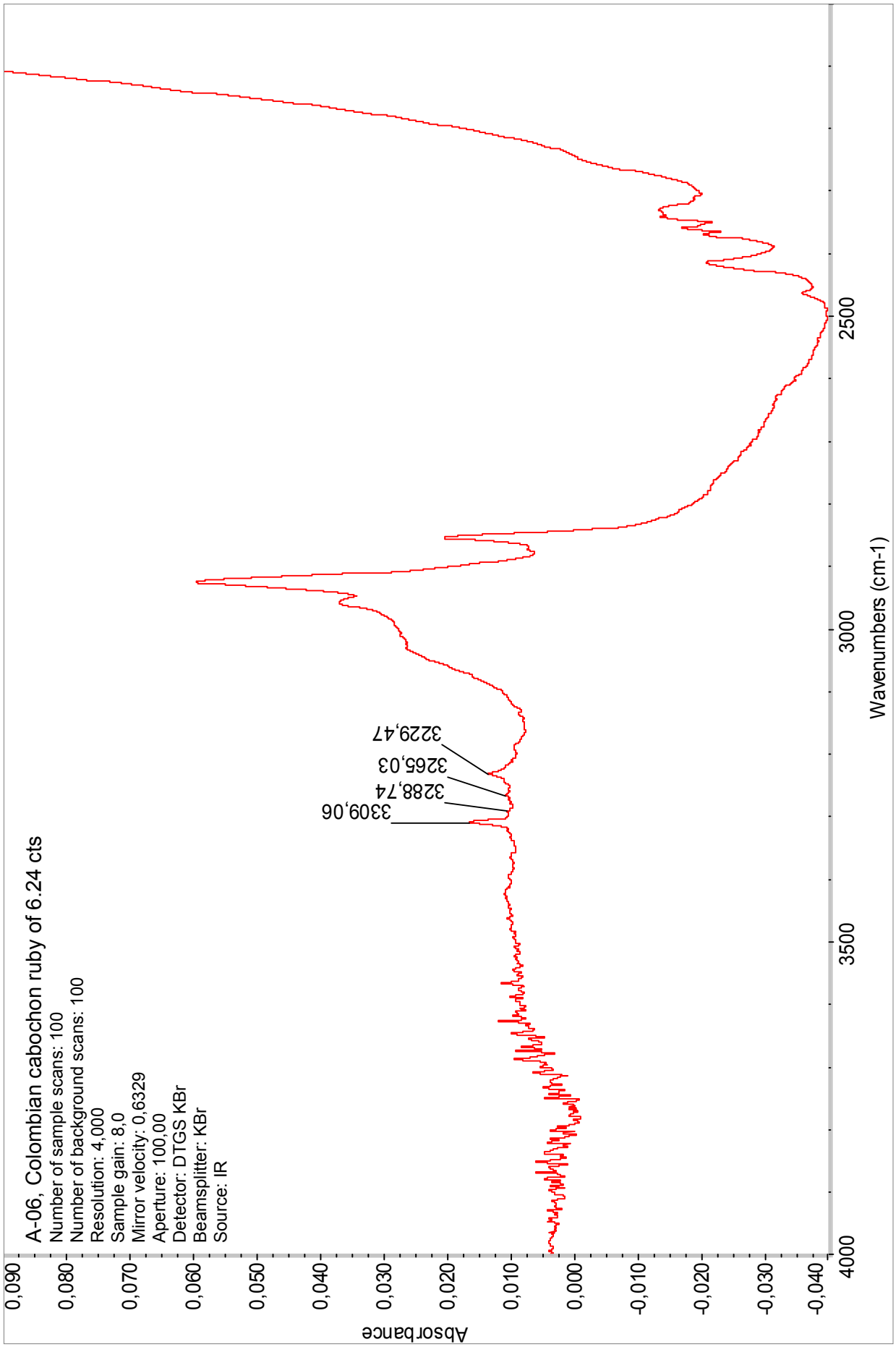
A-06, Colombian cabochon ruby of 6.24 cts
Number of sample scans: 100
Number of background scans: 100
Resolution: 4,000
Sample gain: 8,0
Mirror velocity: 0,6329
Aperture: 100,00
Detector: DTGS KBr
Beamsplitter: KBr
Source: IR
3309,06
3288,74
3265,03
3229,47
Absorbance
Wavenumbers (cm-1)
0,090
0,080
0,070
0,060
0,050
0,040
0,030
0,020
0,010
0,000
-0,010
-0,020
-0,030
-0,040
4000
3500
3000
2500

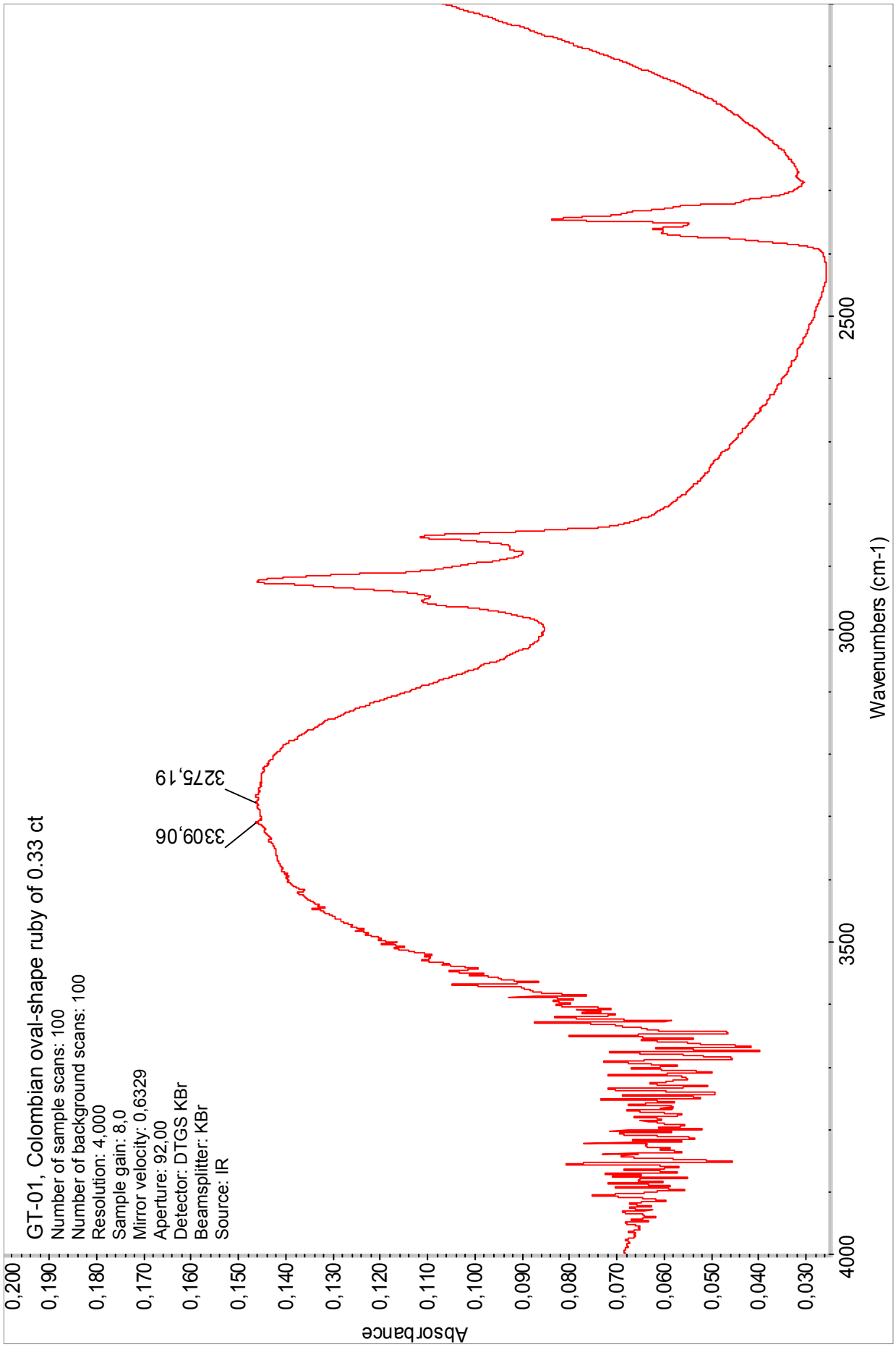
GT-01, Colombian oval-shape ruby of 0.33 ct
Number of sample scans: 100
Number of background scans: 100
Resolution: 4,000
Sample gain: 8,0
Mirror velocity: 0,6329
Aperture: 92,00
Detector: DTGS KBr
Beamsplitter: KBr
Source: IR
3309,06
3275,19
Absorbance
Wavenumbers (cm-1)
0,200
0,190
0,180
0,170
0,160
0,150
0,140
0,130
0,120
0,110
0,100
0,090
0,080
0,070
0,060
0,050
0,040
0,030
4000
3500
3000
2500

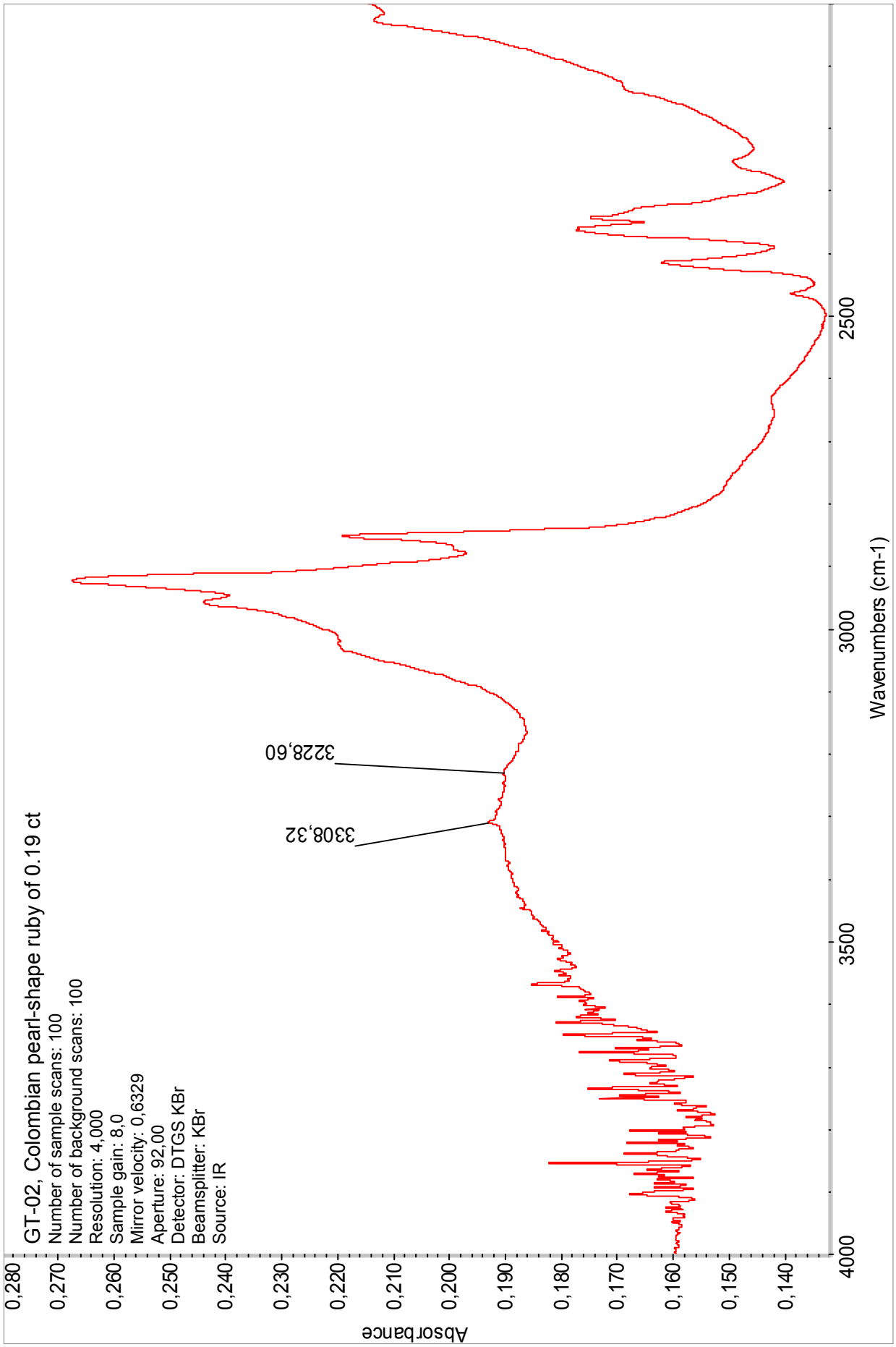
GT-02, Colombian pearl-shape ruby of 0.19 ct
Number of sample scans: 100
Number of background scans: 100
Resolution: 4,000
Sample gain: 8,0
Mirror velocity: 0,6329
Aperture: 92,00
Detector: DTGS KBr
Beamsplitter: KBr
Source: IR
3228,60
3308,32
Absorbance
Wavenumbers (cm-1)
0,280
0,270
0,260
0,250
0,240
0,230
0,220
0,210
0,200
0,190
0,180
0,170
0,160
0,150
0,140
4000
3500
3000
2500

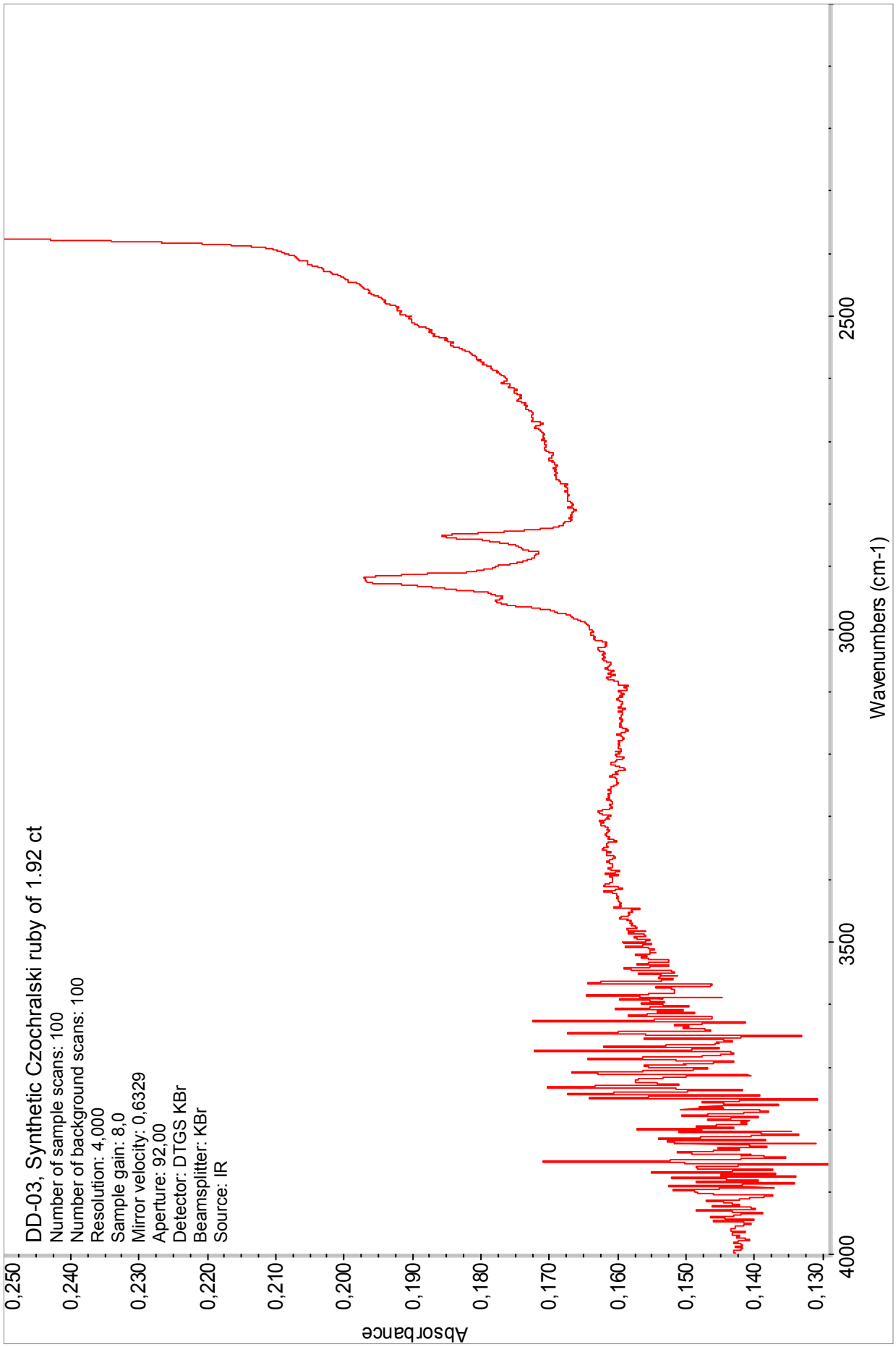
DD-03, Synthetic Czochralski ruby of 1.92 ct
Number of sample scans: 100
Number of background scans: 100
Resolution: 4,000
Sample gain: 8,0
Mirror velocity: 0,6329
Aperture: 92,00
Detector: DTGS KBr
Beamsplitter: KBr
Source: IR
Absorbance
0,250
0,240
0,230
0,220
0,210
0,200
0,190
0,180
0,170
0,160
0,150
0,140
0,130
4000
3500
3000
2500
Wavenumbers (cm-1)

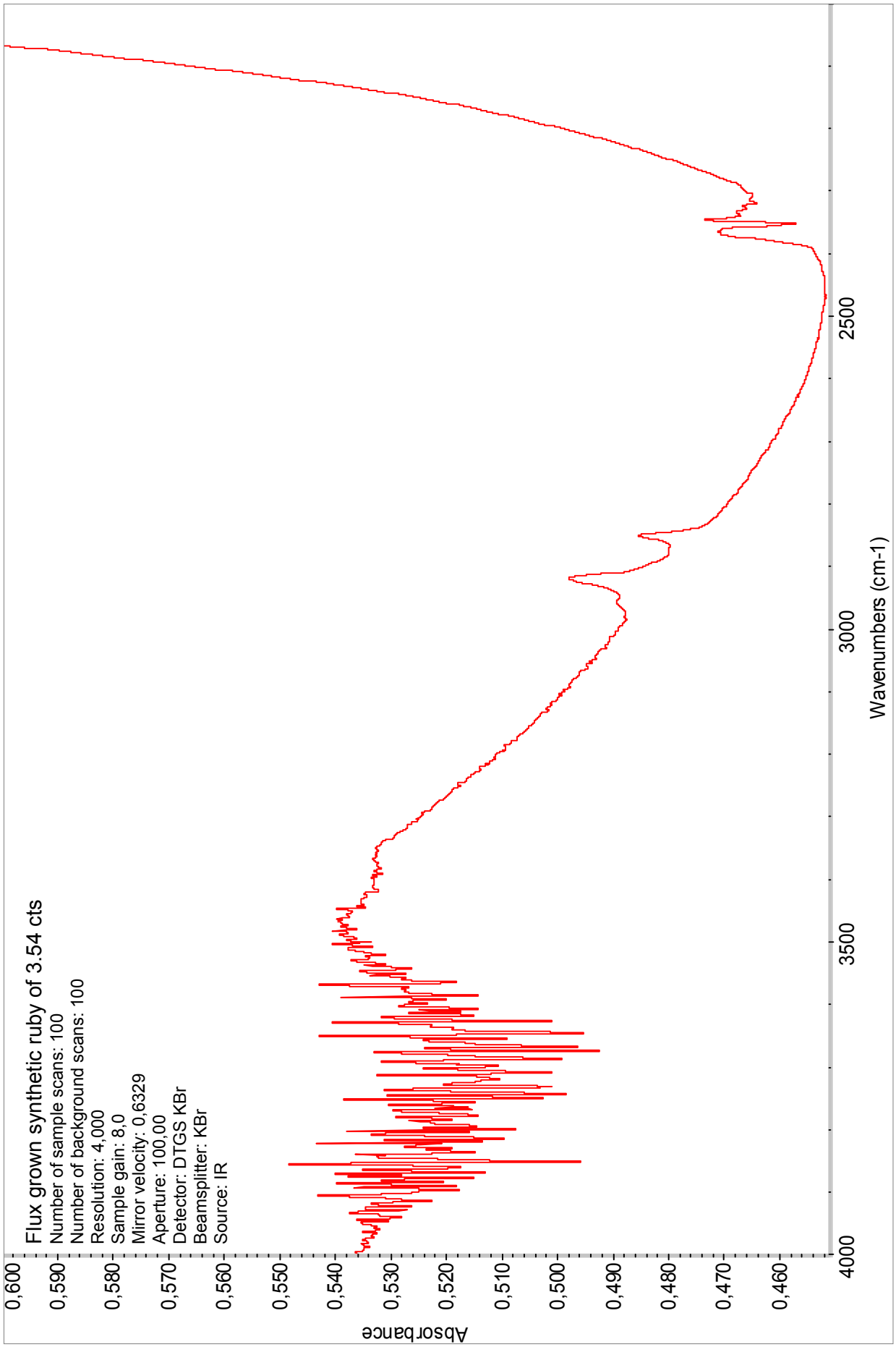
Flux grown synthetic ruby of 3.54 cts
Number of sample scans: 100
Number of background scans: 100
Resolution: 4,000
Sample gain: 8,0
Mirror velocity: 0,6329
Aperture: 100,00
Detector: DTGS KBr
Beamsplitter: KBr
Source: IR
Absorbance
0,600
0,590
0,580
0,570
0,560
0,550
0,540
0,530
0,520
0,510
0,500
0,490
0,480
0,470
0,460
4000
3500
3000
2500
Wavenumbers (cm-1)

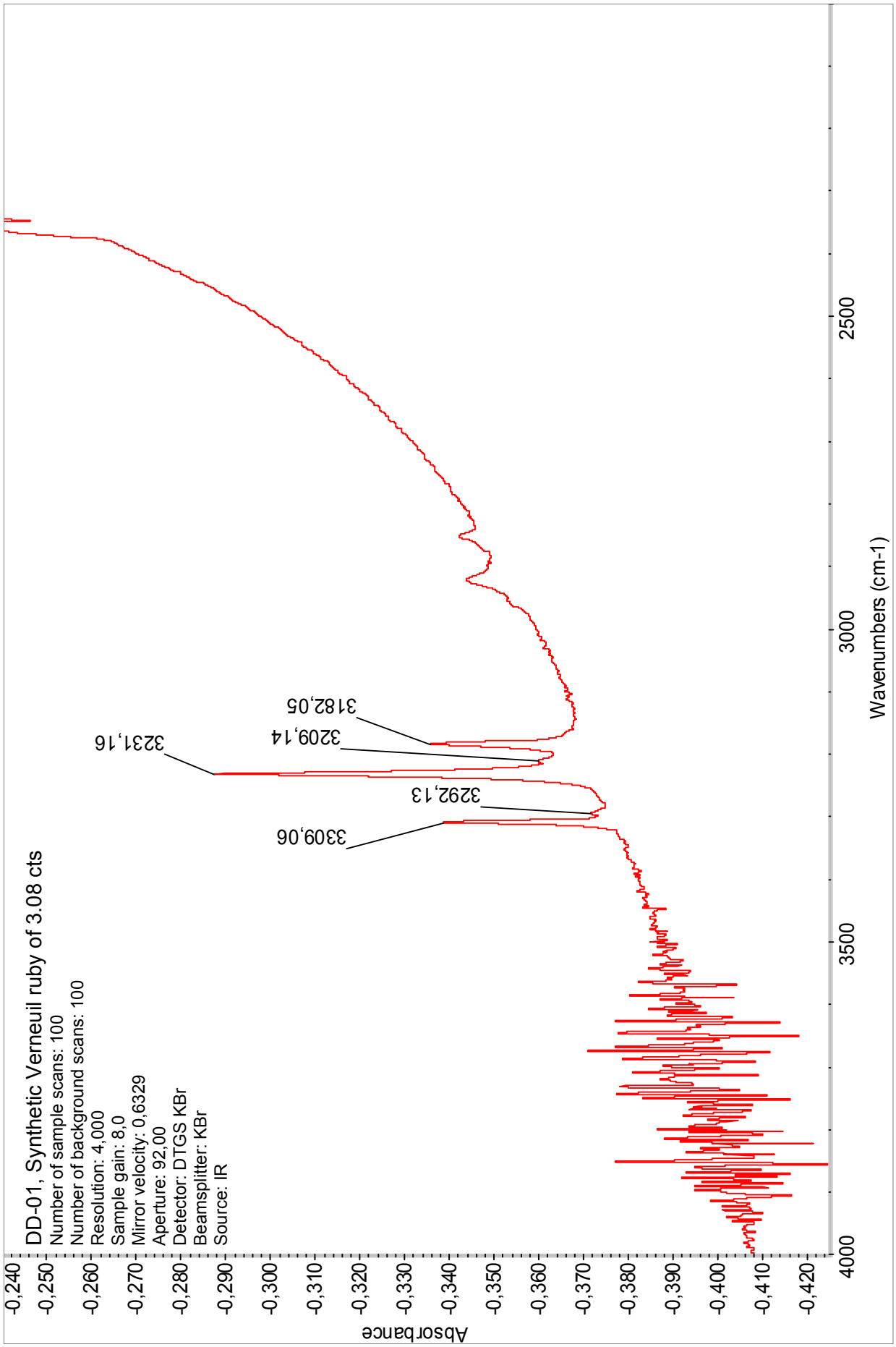
DD-01, Synthetic Verneuil ruby of 3.08 cts
Number of sample scans: 100
Number of background scans: 100
Resolution: 4,000
Sample gain: 8,0
Mirror velocity: 0,6329
Aperture: 92,00
Detector: DTGS KBr
Beamsplitter: KBr
Source: IR
3309,06
3292,13
3231,16
3209,14
3182,05
Absorbance
Wavenumbers (cm-1)

The main peaks observed for the eighteen sapphires:

Most often a group of five peaks, less often two to seven peaks, and occasionally only a single peak, are observed in the mid-infrared range 3100 to 3310 $^{cm-1}$.

± 3185 $^{cm-1}$ (strong to moderate weak)
± 3209 $^{cm-1}$ (shoulder)
± 3232 $^{cm-1}$ (very strong)
± 3261 $^{cm-1}$ (weak)
± 3295 $^{cm-1}$ (weak shoulder)
± 3309 $^{cm-1}$ (generally, the strongest)
± 3366 $^{cm-1}$ (moderate peak)

- Ten sapphires show the peak at ± 3184 $^{cm-1}$ (A-11, A-13, A-14, A-17, HH-01, TT-01, A-28, HH-02, A-32, and A-34).
- Five sapphires show the shoulder at ± 3209 $^{cm-1}$ (A-11, A-13, A-14, A-28, and TT-02).
- Twelve sapphires show the peak at ± 3232 $^{cm-1}$ (A-07, A-11, A-13, A-14, A-17, HH-01, TT-01, A-25, A-28, HH-02, A-32, and A-34).
- Five sapphires show a supplementary fourth peak at ± 3261 $^{cm-1}$ (A-13, A-14, A-17, TT-01, and A-34).
- Twelve sapphires show the shoulder at ± 3295 $^{cm-1}$ (A-11, A-13, A-14, A-17, HH-01, A-28, HH-02, A-32, A-34, A-33, TT-02, and TT-03).
- All the sapphires show the peak at ± 3309 $^{cm-1}$ (three sapphires, A-08, A-31, and A-30, show only this peak). A sapphire TT-02 (a heat-treated colour-change sapphire) shows its strongest peak at ± 3209 $^{cm-1}$.
- Seven sapphires show the peak at ± 3366 $^{cm-1}$ (A-11, A-13, A-14, A-17, HH-01, TT-01, and HH-02).

For comparison purposes, Table 10, shows for every sapphire examined, the main peaks observed, their intensity, position, and last their frequency expressed in percent.

TABLE 10 Main peaks observed in the eighteen Colombian sapphires

Sapphire source	Peak intensity and location (cm^{-1})						
	Strong to weak ± 3185	*Shoulder* ± 3209	*Very strong* ± 3232	*Weak* ± 3261	*Shoulder* ± 3295	***Strongest*** ± 3309	*Moderate* ± 3366
A-07			3229			**3309**	
A-08						**3309**	
A-11	3182	3207	3231		3292	**3309**	3364
A-13	3182	3205	3231	3265	3293	**3309**	3366
A-14	3182	3207	3231	3263	3292	**3309**	3368
A-17	3182		3231	3261	3293	**3309**	3364
HH-01	3182		3231		3292	**3309**	3364
A-31						**3310**	
TT-01	3185		3232	3263		**3309**	3364
A-25			3227			**3309**	
A-28	3186		3233		3294	**3310**	
A-30		3215				**3309**	
HH-02	3183		3231		3290	**3309**	3364
A-32	3183		3231		3292	**3309**	
A-34	3187		3231	3261	3292	**3309**	
A-33					3290	**3309**	
TT-02		**3209**			3292	3309	
TT-03					3290	**3309**	
Synthetic Verneuil	3182		3231	3261	3290	**3309**	3364
Frequency observed	*55.6%*	*27.8%*	*66.7%*	*27.8%*	*66.7%*	*100%*	*38.9%*

It is of interest to note that all these peaks and shoulders are displayed by the synthetic Verneuil sapphire (see table 9).

Discussion

As already said:

- Non basaltic sapphires owe their colour mainly to IVTC $Fe^{2+} \rightarrow Ti^{4+}$, to a lesser degree to Fe^{3+}/Fe^{3+}, and not to Fe^{3+}.
- Basaltic sapphires owe their colour chiefly to Fe^{3+}/Fe^{3+}, Fe^{3+}, and to a lesser degree to IVTC $Fe^{2+} \rightarrow Ti^{4+}$.

One of the characteristics of the basaltic sapphires, is that when the hot lava erupting from fissures or volcanoes on the earth's surface, some of these hot lavas vehicled the corundums that crystallized at great depth to the surface. Such is the case with many alkali-olivine basalts, which may bring sapphire or ruby from a depth of up to 100 km (Keller, 1990). These corundums transported as xenocrystic passengers by the basalt, were enriched with iron and heated by the basalt.

The peak observed at ± 3309 $^{cm-1}$, which is not observed in natural (non-heated) metamorphic sapphires, nor in all (non-heat treated) synthetic sapphires except those issued from the Verneuil flame-fusion syntheses (DD-007, synthetic Verneuil sapphire of 1.28 ct), as already said is due (as for the peaks ± 3295 $^{cm-1}$, ± 3232 $^{cm-1}$, and ± 3185 $^{cm-1}$) to a OH-dipole linked to atoms of iron and titanium inside the corundum lattice. The peak ± 3366 $^{cm-1}$, it is due to OH clusters linked to a titanium atom.

A comparison between the infrared spectra recorded for the Colombian sapphires and the infrared spectra obtained for the synthetic Verneuil sapphire, shows that there is a total similitude both in peak positions and intensities. Therefore, the Colombian sapphires (if free from inclusions, and other parameters that permit a division) cannot be separated by this method from their Verneuil synthetics.

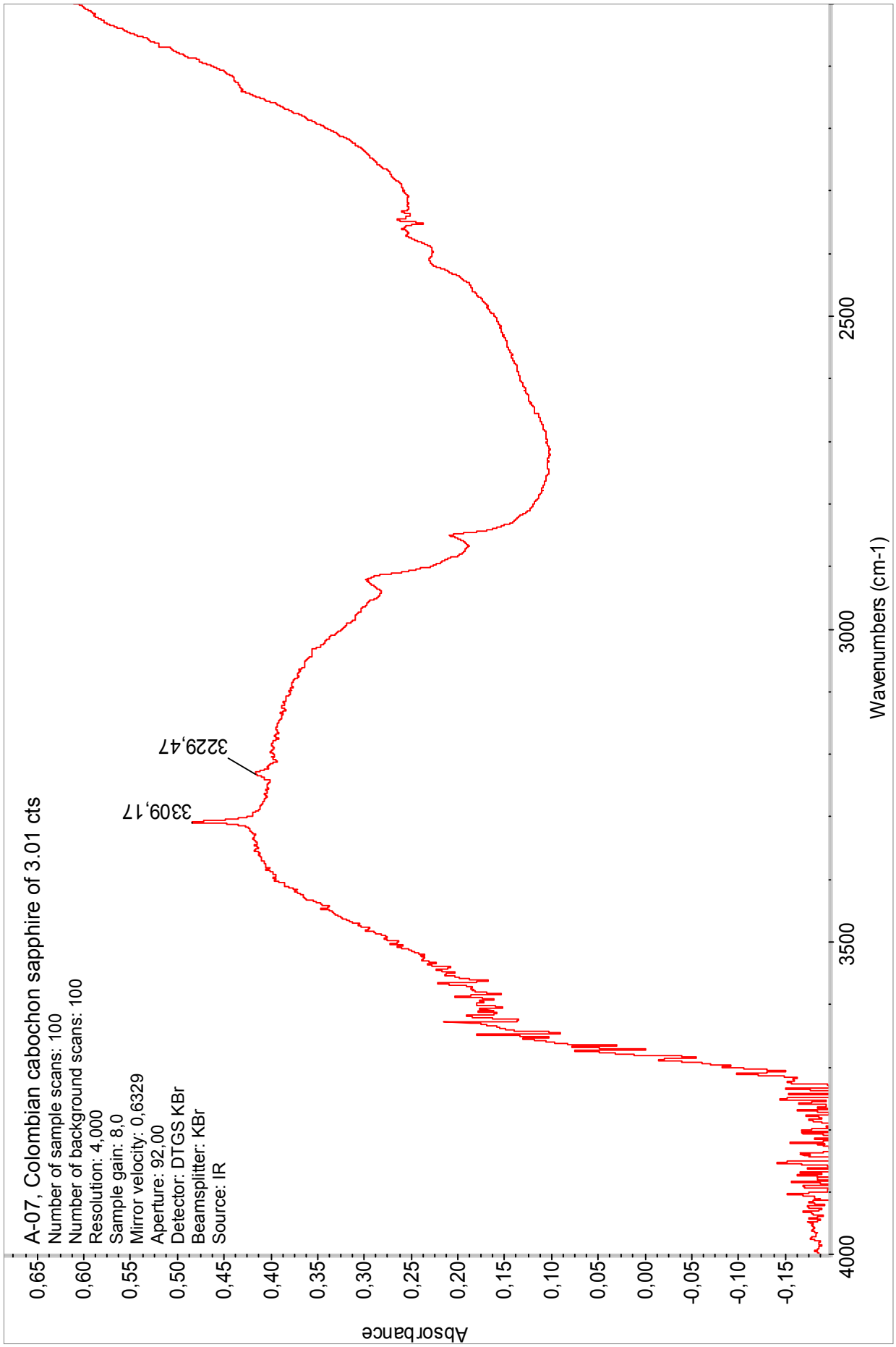
A-07, Colombian cabochon sapphire of 3.01 cts
Number of sample scans: 100
Number of background scans: 100
Resolution: 4,000
Sample gain: 8,0
Mirror velocity: 0,6329
Aperture: 92,00
Detector: DTGS KBr
Beamsplitter: KBr
Source: IR
3309,17
3229,47
Absorbance
Wavenumbers (cm-1)
0,65
0,60
0,55
0,50
0,45
0,40
0,35
0,30
0,25
0,20
0,15
0,10
0,05
0,00
-0,05
-0,10
-0,15
4000
3500
3000
2500

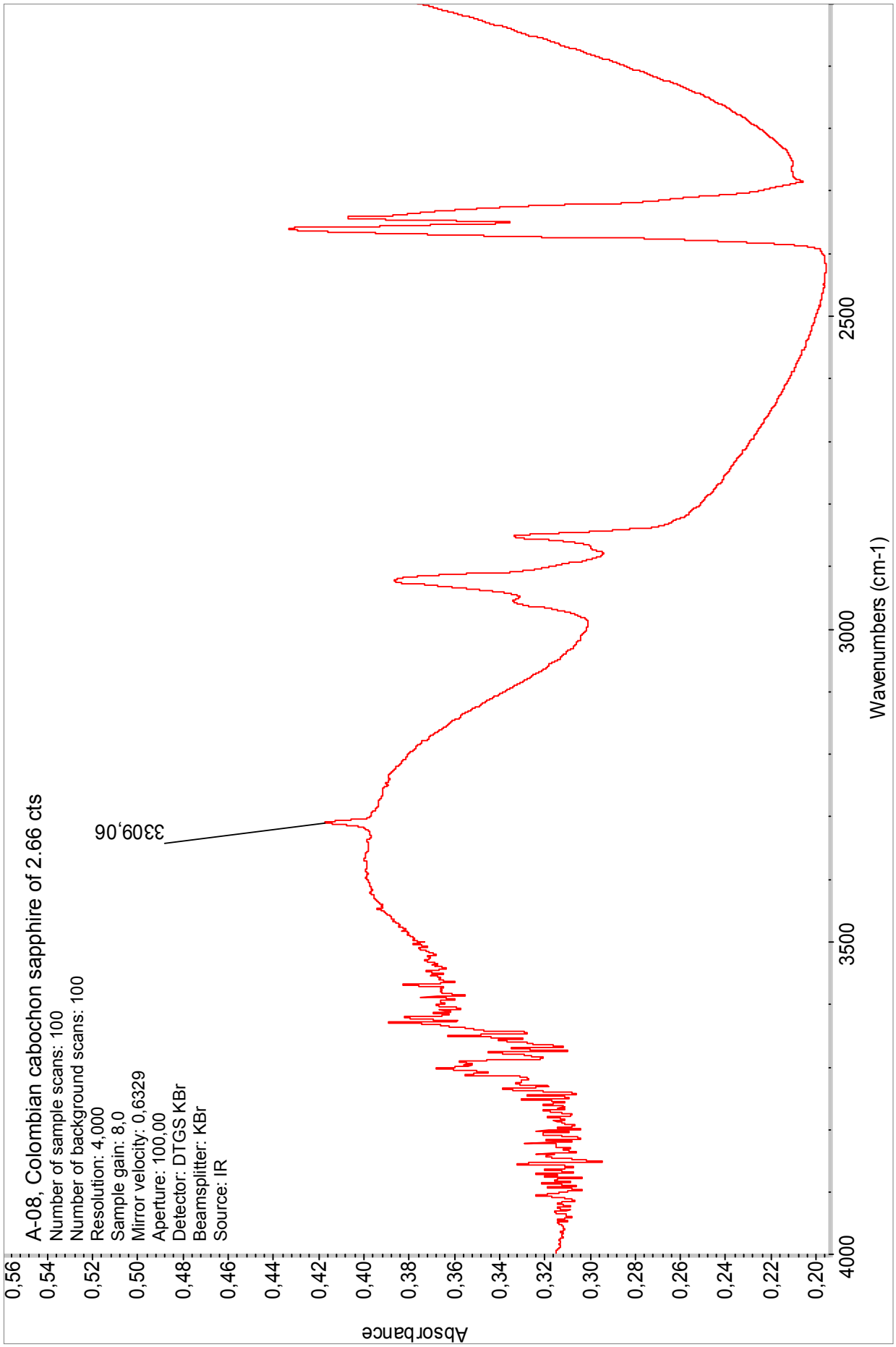
A-08, Colombian cabochon sapphire of 2.66 cts
Number of sample scans: 100
Number of background scans: 100
Resolution: 4,000
Sample gain: 8,0
Mirror velocity: 0,6329
Aperture: 100,00
Detector: DTGS KBr
Beamsplitter: KBr
Source: IR
3309,06
Absorbance
Wavenumbers (cm-1)
0,56
0,54
0,52
0,50
0,48
0,46
0,44
0,42
0,40
0,38
0,36
0,34
0,32
0,30
0,28
0,26
0,24
0,22
0,20
4000
3500
3000
2500

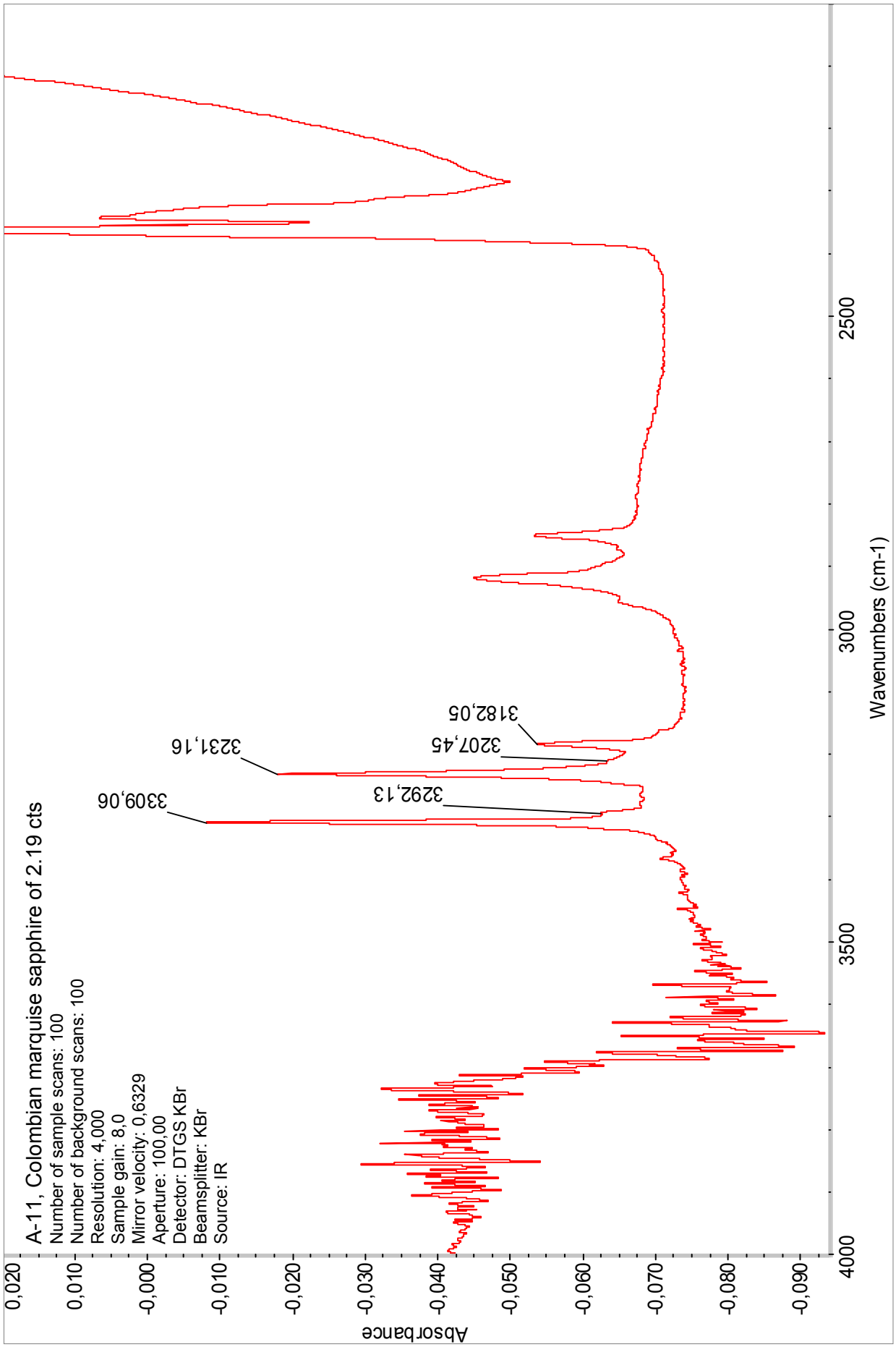
A-11, Colombian marquise sapphire of 2.19 cts
Number of sample scans: 100
Number of background scans: 100
Resolution: 4,000
Sample gain: 8,0
Mirror velocity: 0,6329
Aperture: 100,00
Detector: DTGS KBr
Beamsplitter: KBr
Source: IR
3309,06
3231,16
3292,13
3207,45
3182,05
Absorbance
Wavenumbers (cm-1)
0,020
0,010
-0,000
-0,010
-0,020
-0,030
-0,040
-0,050
-0,060
-0,070
-0,080
-0,090
4000
3500
3000
2500

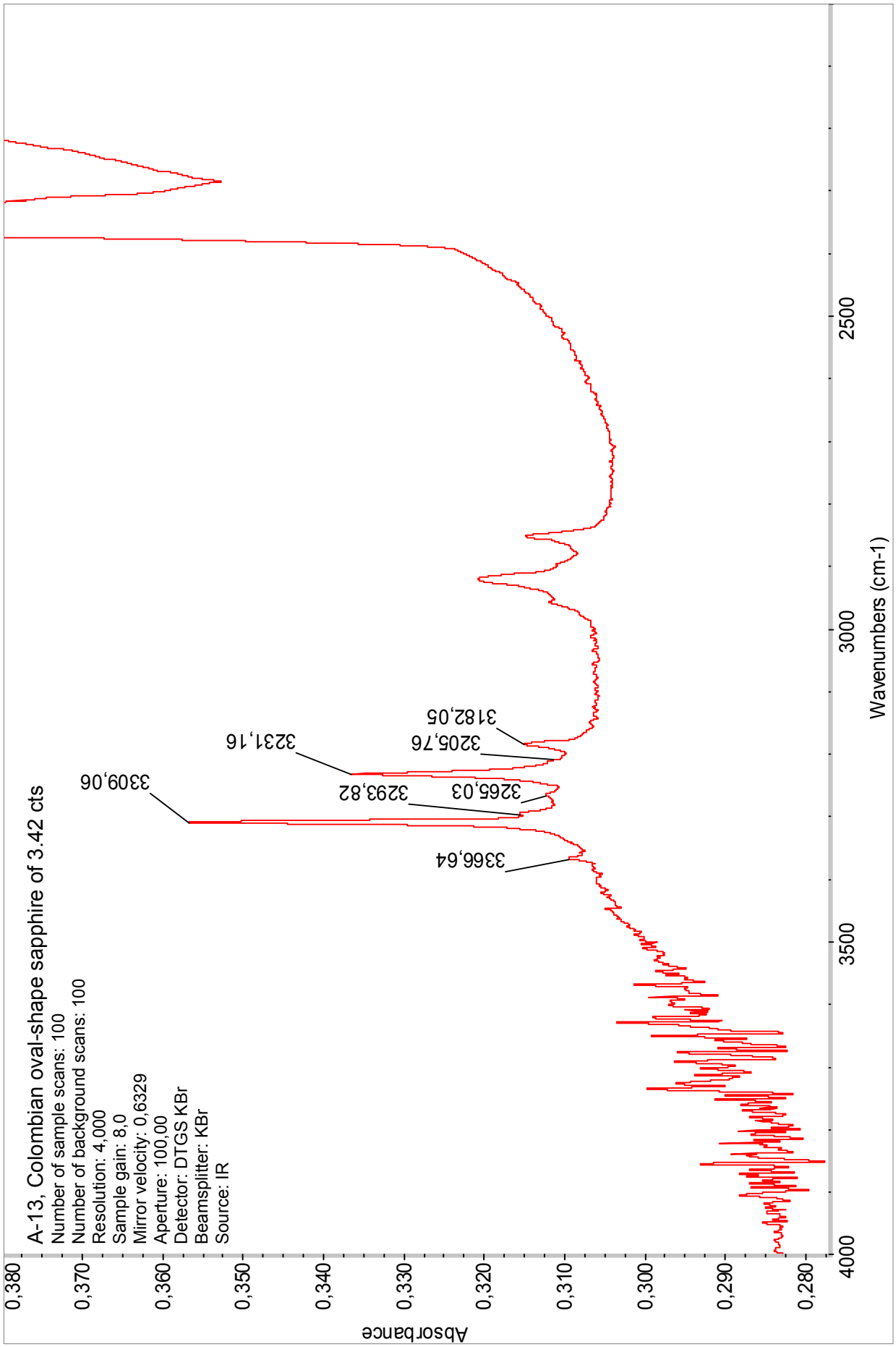
A-13, Colombian oval-shape sapphire of 3.42 cts
Number of sample scans: 100
Number of background scans: 100
Resolution: 4,000
Sample gain: 8,0
Mirror velocity: 0,6329
Aperture: 100,00
Detector: DTGS KBr
Beamsplitter: KBr
Source: IR
3309,06
3366,64
3265,03
3293,82
3231,16
3205,76
3182,05
Absorbance
Wavenumbers (cm-1)
0,380
0,370
0,360
0,350
0,340
0,330
0,320
0,310
0,300
0,290
0,280
4000
3500
3000
2500

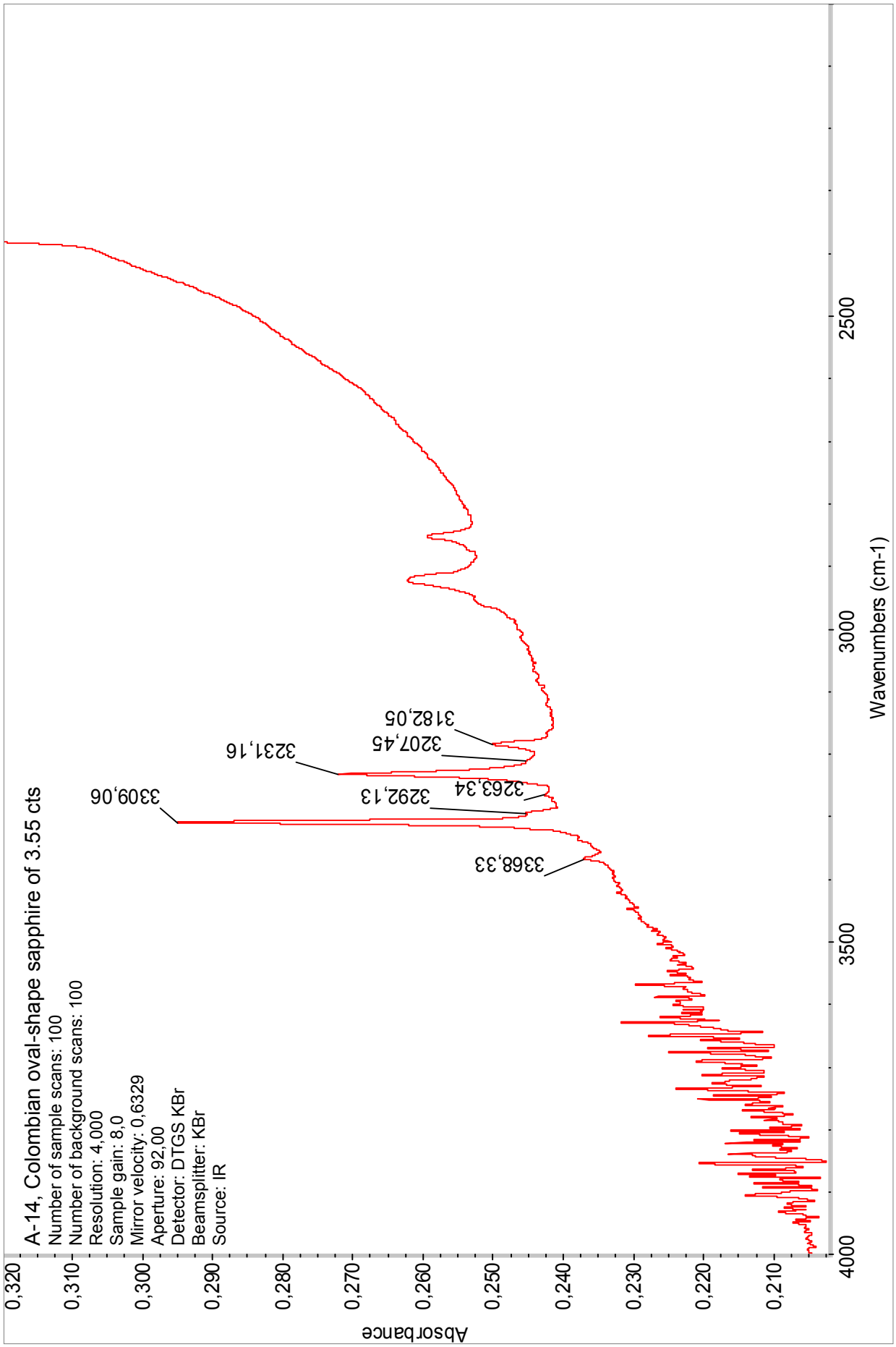
A-14, Colombian oval-shape sapphire of 3.55 cts
Number of sample scans: 100
Number of background scans: 100
Resolution: 4,000
Sample gain: 8,0
Mirror velocity: 0,6329
Aperture: 92,00
Detector: DTGS KBr
Beamsplitter: KBr
Source: IR
3309,06
3368,33
3292,13
3263,34
3231,16
3207,45
3182,05
Absorbance
Wavenumbers (cm-1)
0,320
0,310
0,300
0,290
0,280
0,270
0,260
0,250
0,240
0,230
0,220
0,210
4000
3500
3000
2500

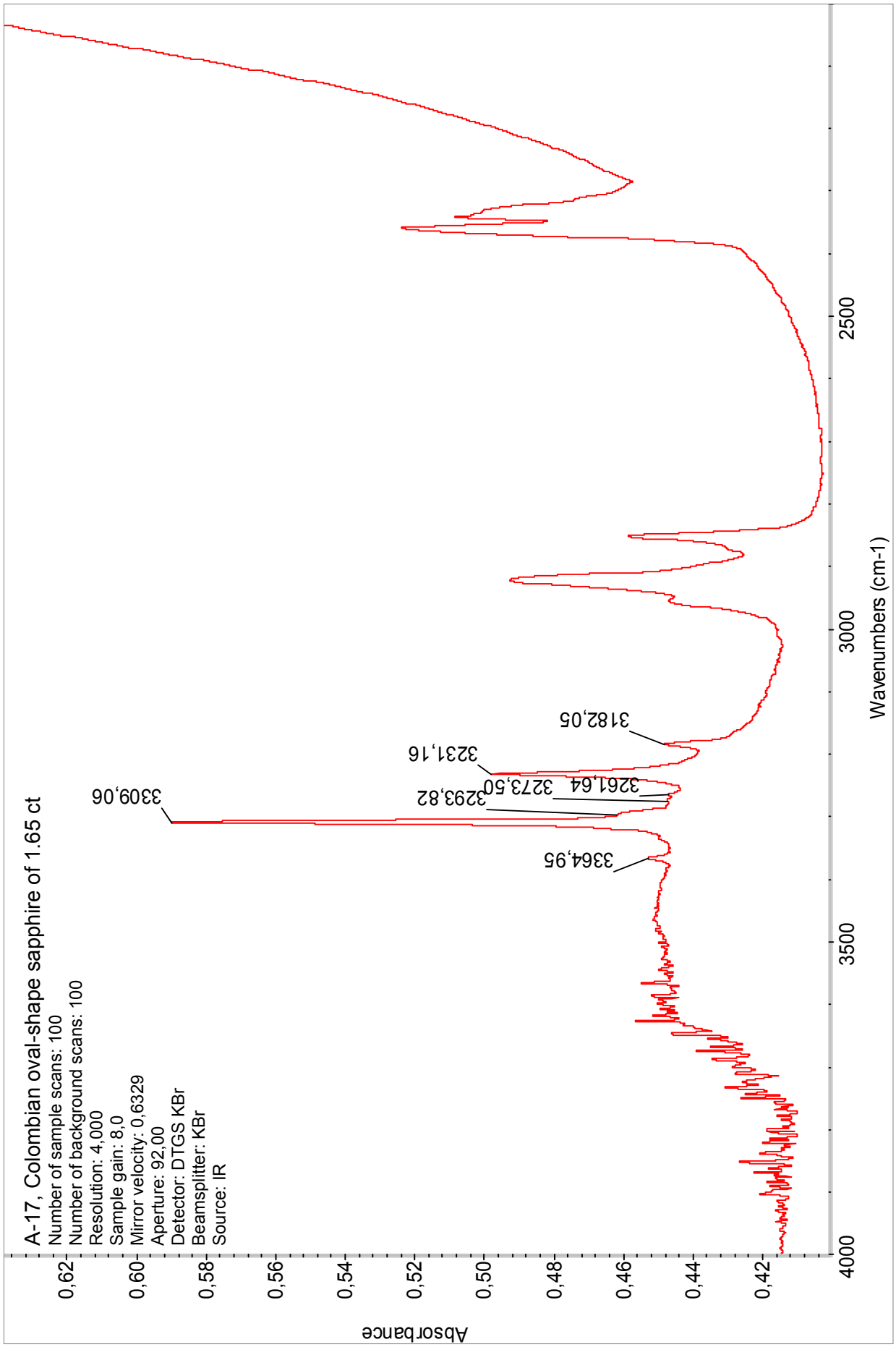
A-17, Colombian oval-shape sapphire of 1.65 ct
Number of sample scans: 100
Number of background scans: 100
Resolution: 4,000
Sample gain: 8,0
Mirror velocity: 0,6329
Aperture: 92,00
Detector: DTGS KBr
Beamsplitter: KBr
Source: IR
Absorbance
Wavenumbers (cm-1)
0,62
0,60
0,58
0,56
0,54
0,52
0,50
0,48
0,46
0,44
0,42
4000
3500
3000
2500
3309,06
3364,95
3293,82
3261,64
3273,50
3231,16
3182,05

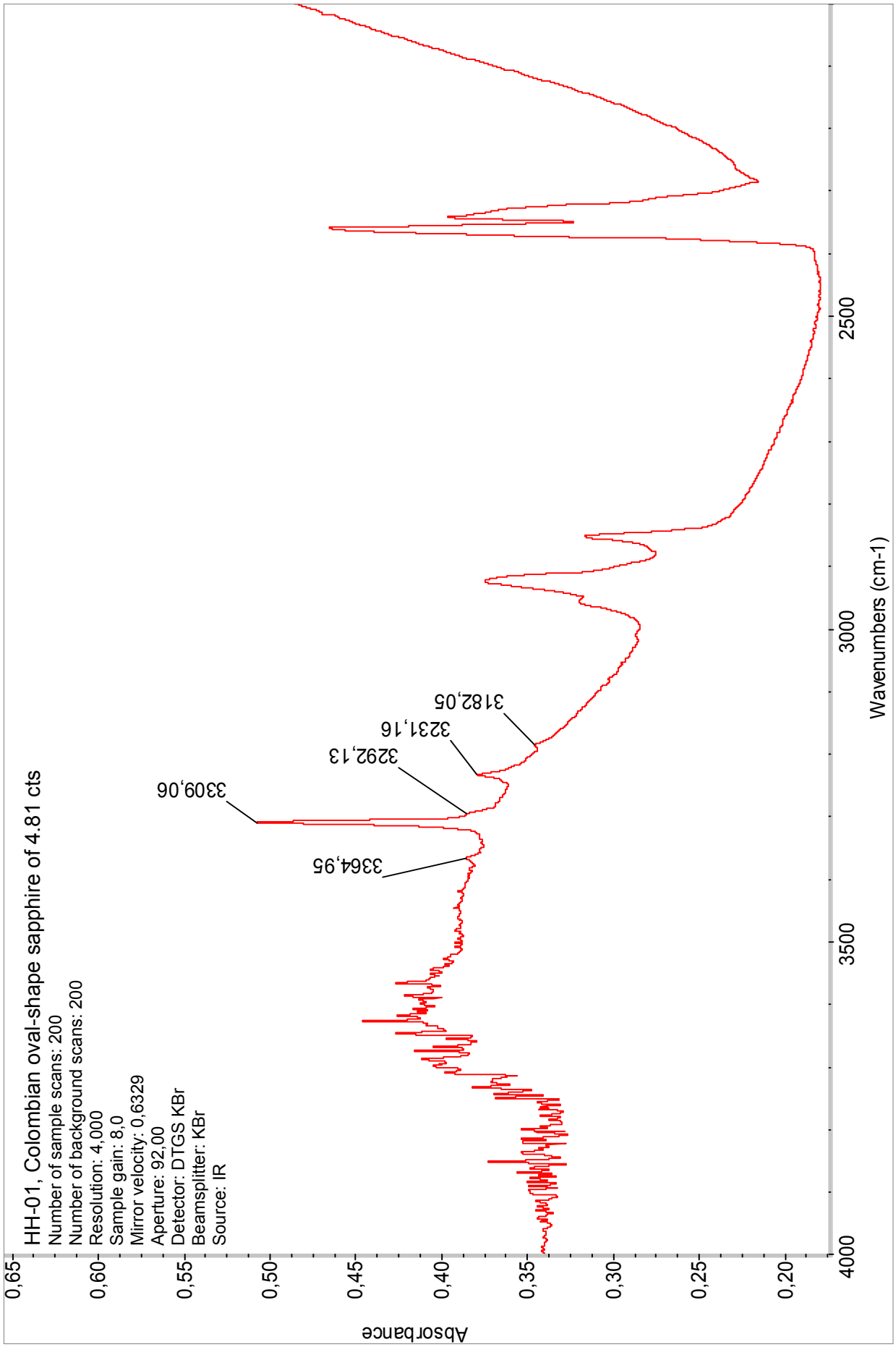
HH-01, Colombian oval-shape sapphire of 4.81 cts
Number of sample scans: 200
Number of background scans: 200
Resolution: 4,000
Sample gain: 8,0
Mirror velocity: 0,6329
Aperture: 92,00
Detector: DTGS KBr
Beamsplitter: KBr
Source: IR
3309,06
3364,95
3292,13
3231,16
3182,05
Absorbance
Wavenumbers (cm-1)
0,65
0,60
0,55
0,50
0,45
0,40
0,35
0,30
0,25
0,20
4000
3500
3000
2500

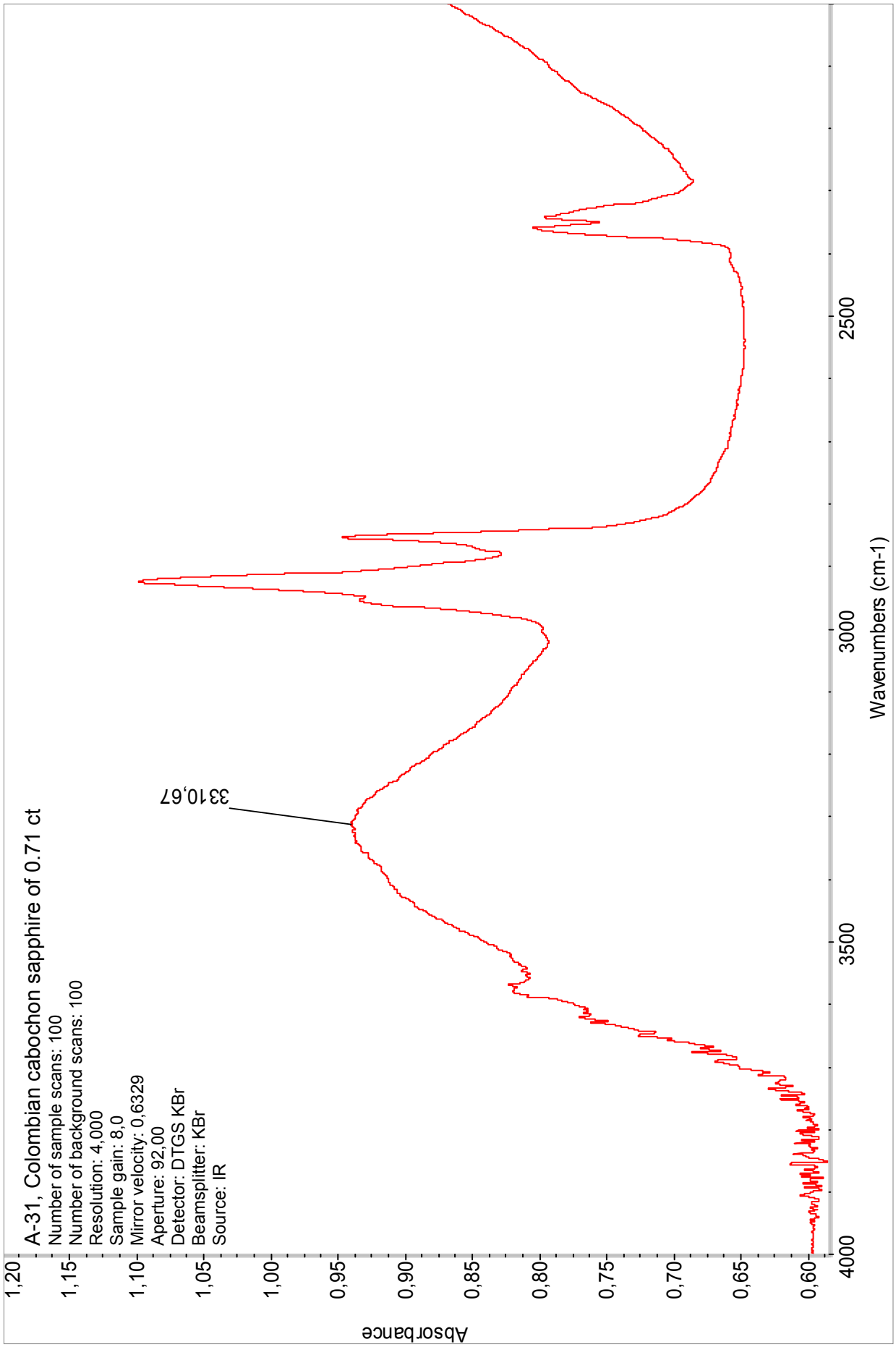
A-31, Colombian cabochon sapphire of 0.71 ct
Number of sample scans: 100
Number of background scans: 100
Resolution: 4,000
Sample gain: 8,0
Mirror velocity: 0,6329
Aperture: 92,00
Detector: DTGS KBr
Beamsplitter: KBr
Source: IR
3310,67
Absorbance
Wavenumbers (cm-1)
1,20
1,15
1,10
1,05
1,00
0,95
0,90
0,85
0,80
0,75
0,70
0,65
0,60
4000
3500
3000
2500

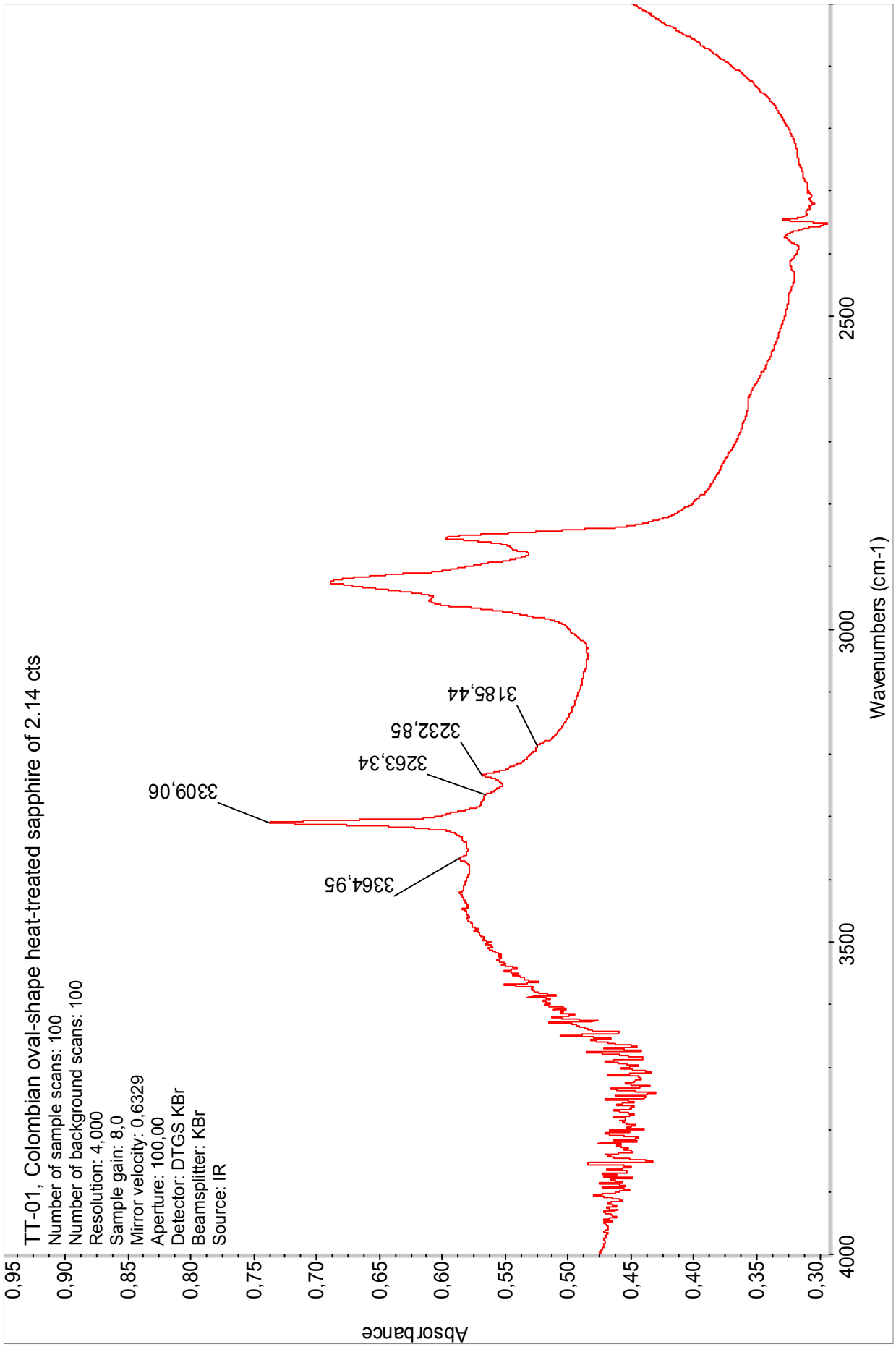
TT-01, Colombian oval-shape heat-treated sapphire of 2.14 cts
Number of sample scans: 100
Number of background scans: 100
Resolution: 4,000
Sample gain: 8,0
Mirror velocity: 0,6329
Aperture: 100,00
Detector: DTGS KBr
Beamsplitter: KBr
Source: IR
3364,95
3309,06
3263,34
3232,85
3185,44
Absorbance
Wavenumbers (cm-1)
0,95
0,90
0,85
0,80
0,75
0,70
0,65
0,60
0,55
0,50
0,45
0,40
0,35
0,30
4000
3500
3000
2500

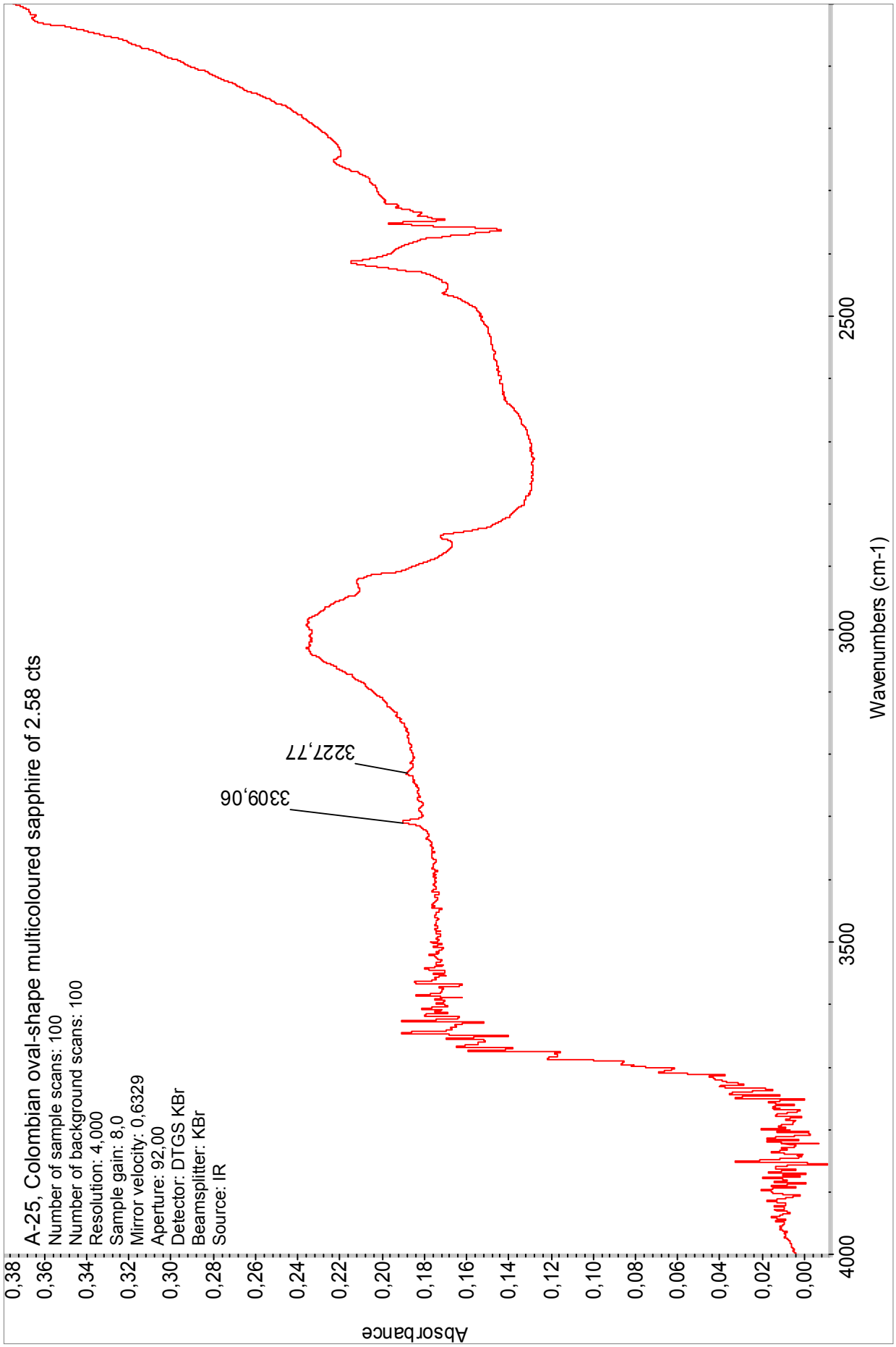
A-25, Colombian oval-shape multicoloured sapphire of 2.58 cts
Number of sample scans: 100
Number of background scans: 100
Resolution: 4,000
Sample gain: 8,0
Mirror velocity: 0,6329
Aperture: 92,00
Detector: DTGS KBr
Beamsplitter: KBr
Source: IR
3309,06
3227,77
Absorbance
Wavenumbers (cm-1)
0,38
0,36
0,34
0,32
0,30
0,28
0,26
0,24
0,22
0,20
0,18
0,16
0,14
0,12
0,10
0,08
0,06
0,04
0,02
0,00
4000
3500
3000
2500

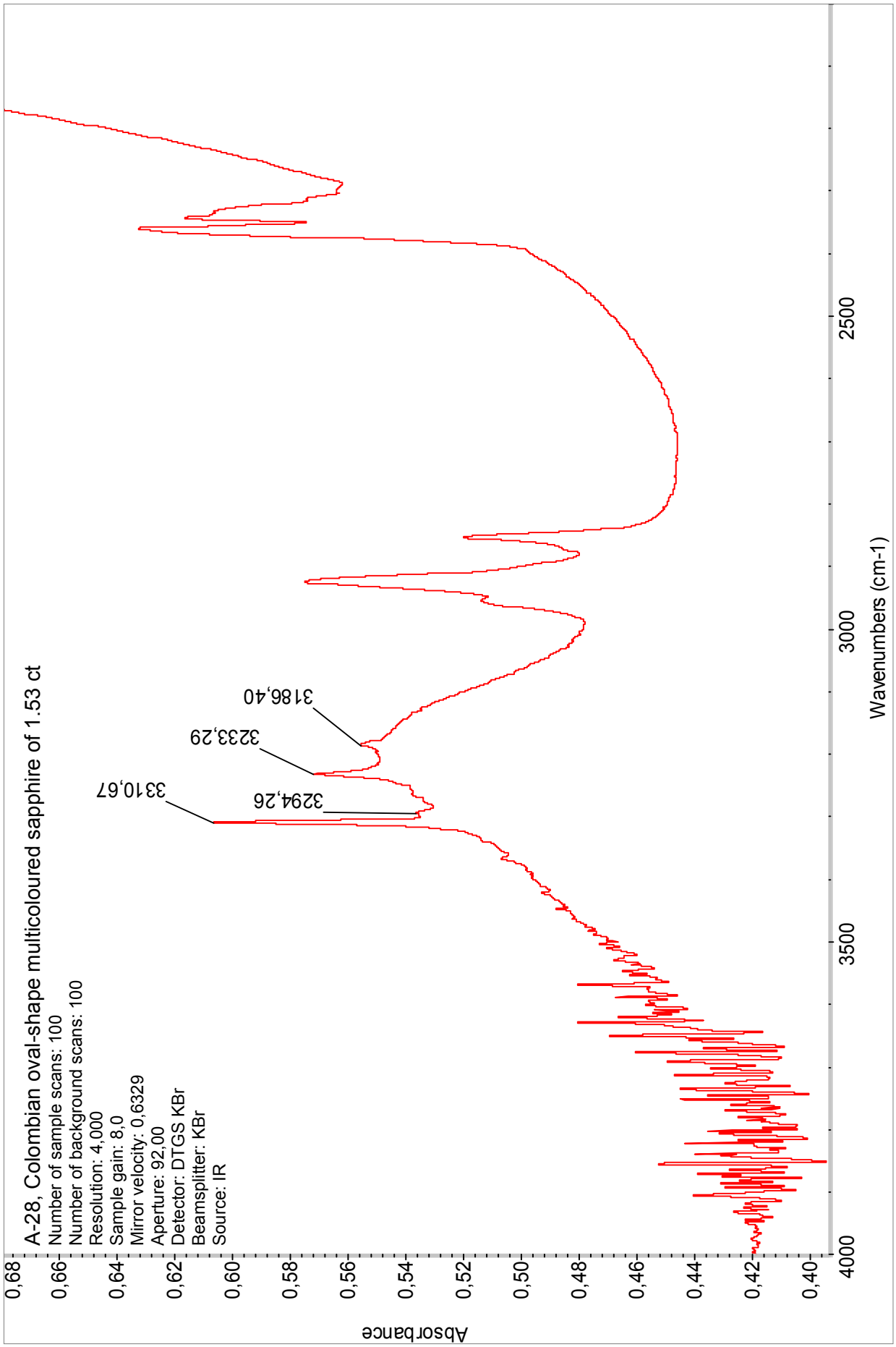
A-28, Colombian oval-shape multicoloured sapphire of 1.53 ct
Number of sample scans: 100
Number of background scans: 100
Resolution: 4,000
Sample gain: 8,0
Mirror velocity: 0,6329
Aperture: 92,00
Detector: DTGS KBr
Beamsplitter: KBr
Source: IR
3310,67
3294,26
3233,29
3186,40
Absorbance
Wavenumbers (cm-1)
0,68
0,66
0,64
0,62
0,60
0,58
0,56
0,54
0,52
0,50
0,48
0,46
0,44
0,42
0,40
4000
3500
3000
2500

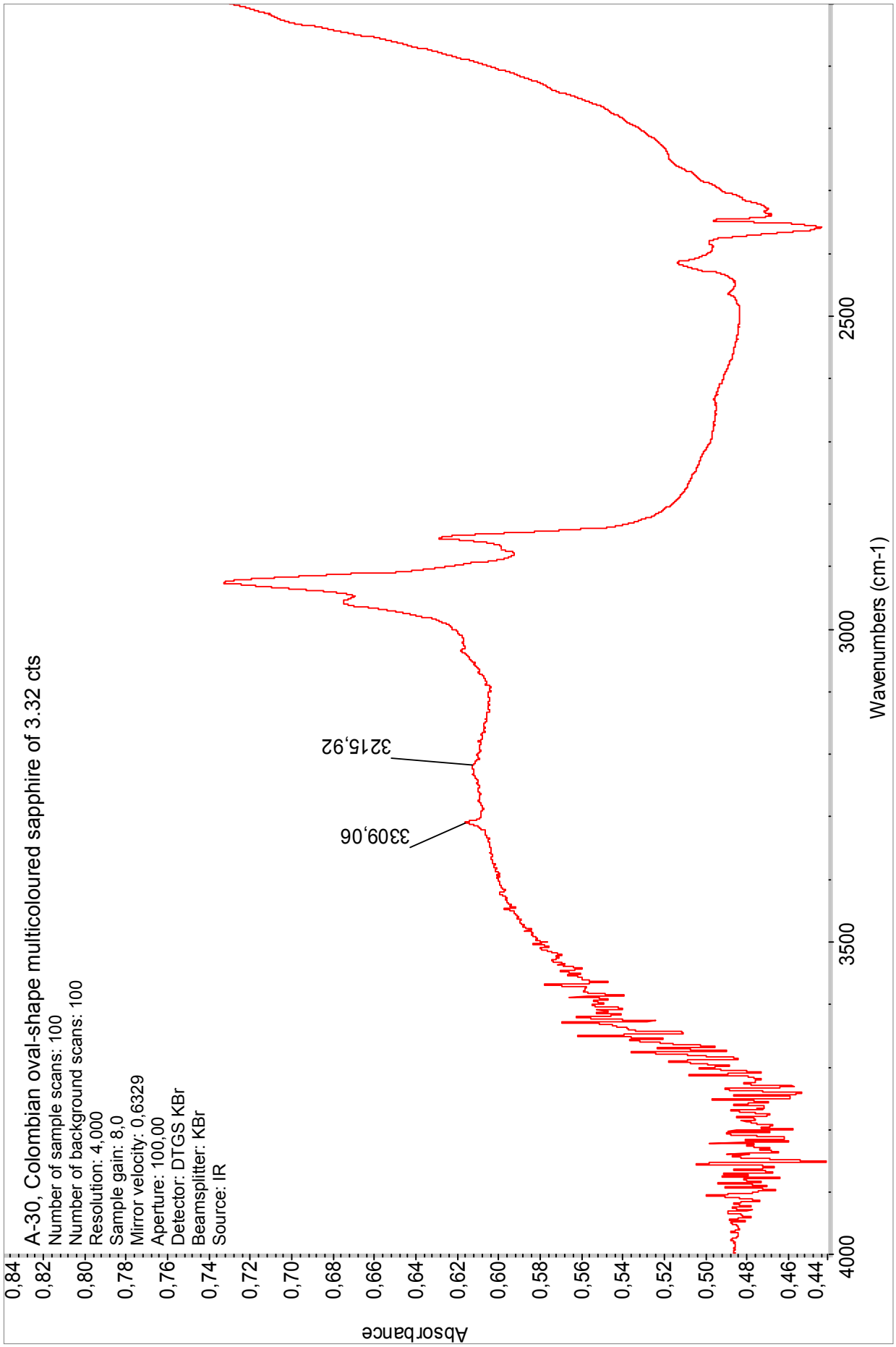
A-30, Colombian oval-shape multicoloured sapphire of 3.32 cts
Number of sample scans: 100
Number of background scans: 100
Resolution: 4,000
Sample gain: 8,0
Mirror velocity: 0,6329
Aperture: 100,00
Detector: DTGS KBr
Beamsplitter: KBr
Source: IR
3309,06
3215,92
Absorbance
Wavenumbers (cm-1)
0,84
0,82
0,80
0,78
0,76
0,74
0,72
0,70
0,68
0,66
0,64
0,62
0,60
0,58
0,56
0,54
0,52
0,50
0,48
0,46
0,44
4000
3500
3000
2500

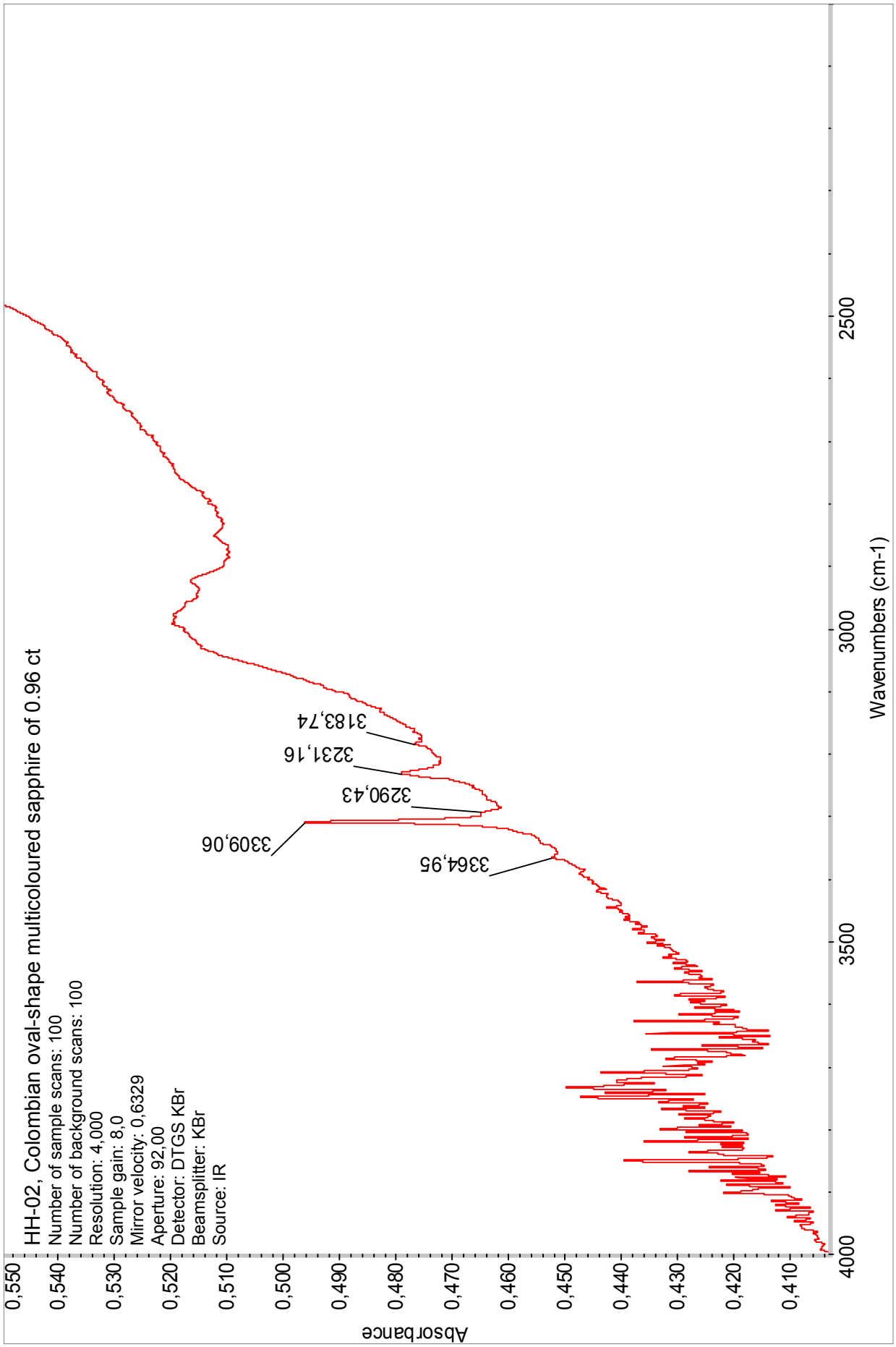
HH-02, Colombian oval-shape multicoloured sapphire of 0.96 ct
Number of sample scans: 100
Number of background scans: 100
Resolution: 4,000
Sample gain: 8,0
Mirror velocity: 0,6329
Aperture: 92,00
Detector: DTGS KBr
Beamsplitter: KBr
Source: IR
3364,95
3309,06
3290,43
3231,16
3183,74
Absorbance
Wavenumbers (cm-1)

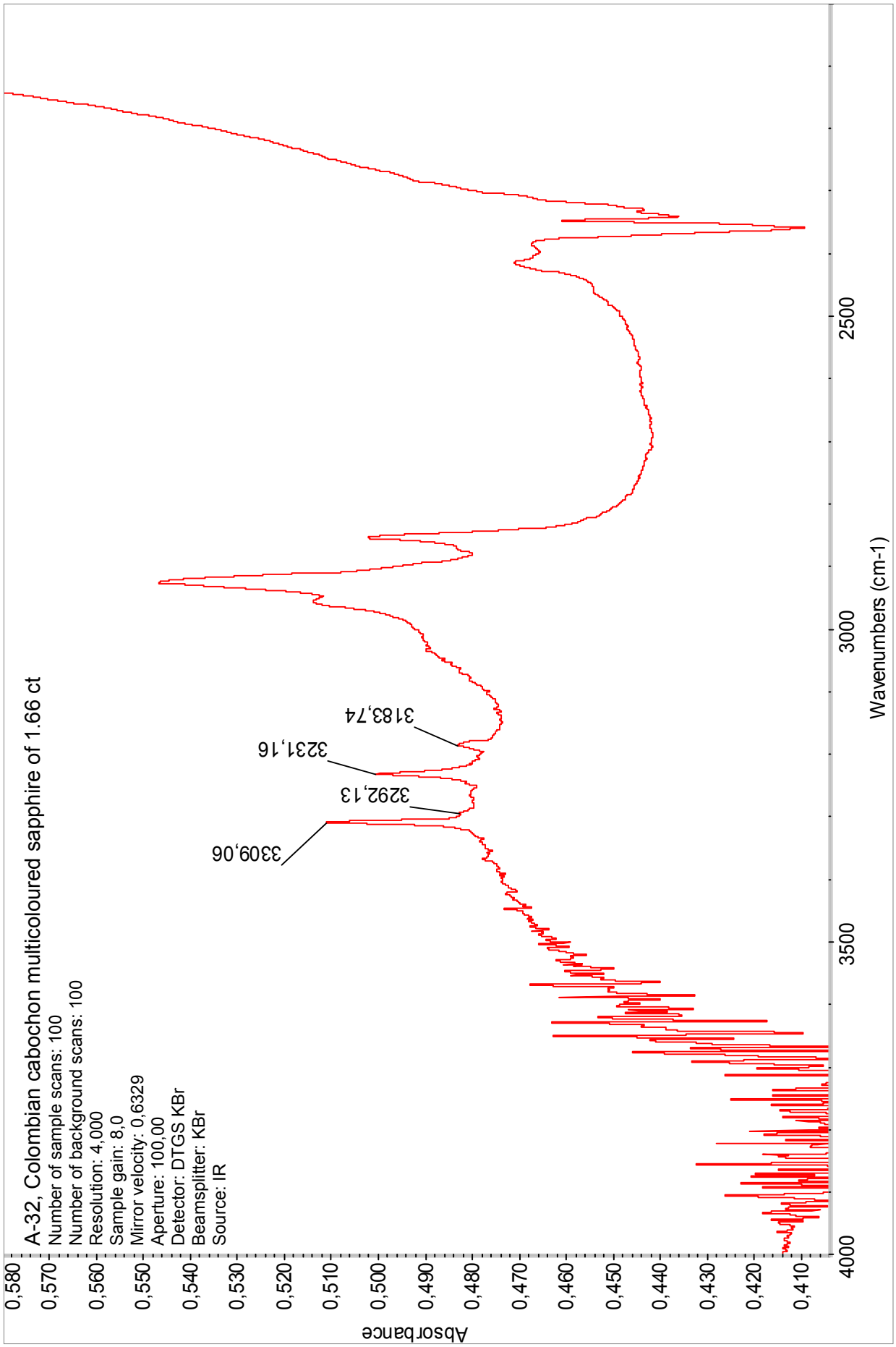
A-32, Colombian cabochon multicoloured sapphire of 1.66 ct
Number of sample scans: 100
Number of background scans: 100
Resolution: 4,000
Sample gain: 8,0
Mirror velocity: 0,6329
Aperture: 100,00
Detector: DTGS KBr
Beamsplitter: KBr
Source: IR
3309,06
3292,13
3231,16
3183,74
Absorbance
Wavenumbers (cm-1)
0,580
0,570
0,560
0,550
0,540
0,530
0,520
0,510
0,500
0,490
0,480
0,470
0,460
0,450
0,440
0,430
0,420
0,410
4000
3500
3000
2500

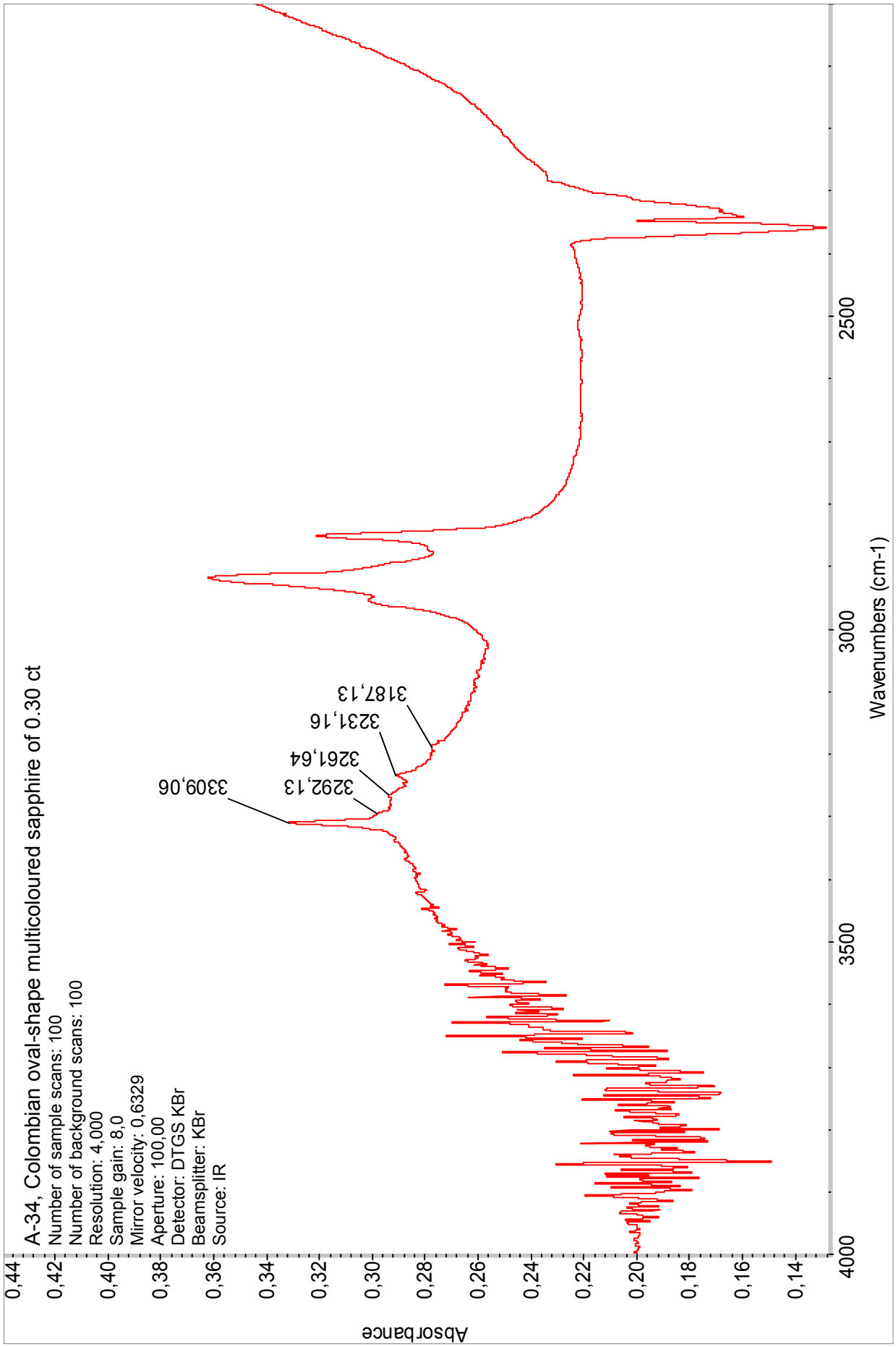
A-34, Colombian oval-shape multicoloured sapphire of 0.30 ct
Number of sample scans: 100
Number of background scans: 100
Resolution: 4,000
Sample gain: 8,0
Mirror velocity: 0,6329
Aperture: 100,00
Detector: DTGS KBr
Beamsplitter: KBr
Source: IR
3309,06
3292,13
3261,64
3231,16
3187,13
Absorbance
Wavenumbers (cm-1)
0,44
0,42
0,40
0,38
0,36
0,34
0,32
0,30
0,28
0,26
0,24
0,22
0,20
0,18
0,16
0,14
4000
3500
3000
2500

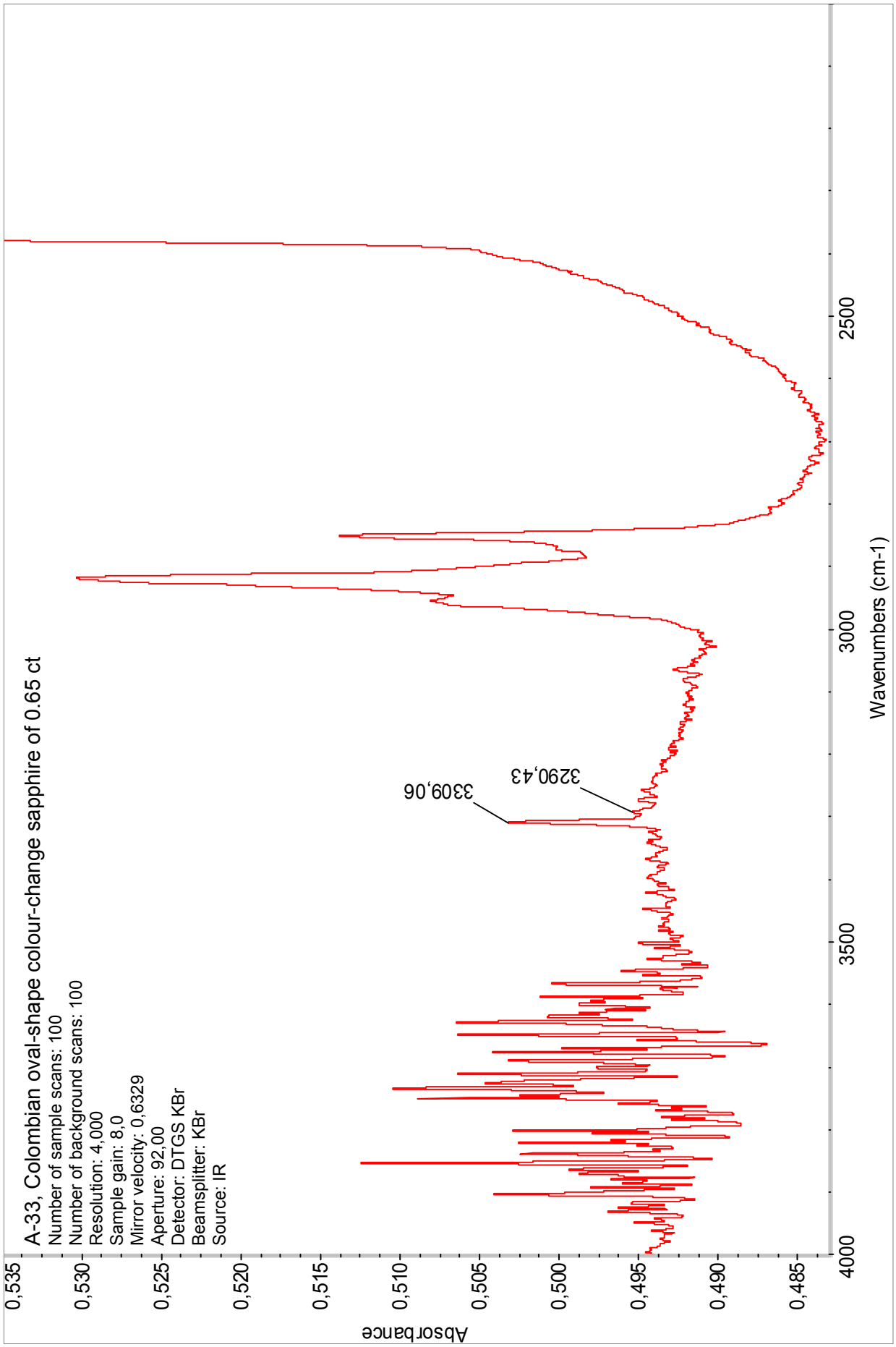
A-33, Colombian oval-shape colour-change sapphire of 0.65 ct
Number of sample scans: 100
Number of background scans: 100
Resolution: 4,000
Sample gain: 8,0
Mirror velocity: 0,6329
Aperture: 92,00
Detector: DTGS KBr
Beamsplitter: KBr
Source: IR
3309,06
3290,43
Absorbance
Wavenumbers (cm-1)
0,535
0,530
0,525
0,520
0,515
0,510
0,505
0,500
0,495
0,490
0,485
4000
3500
3000
2500

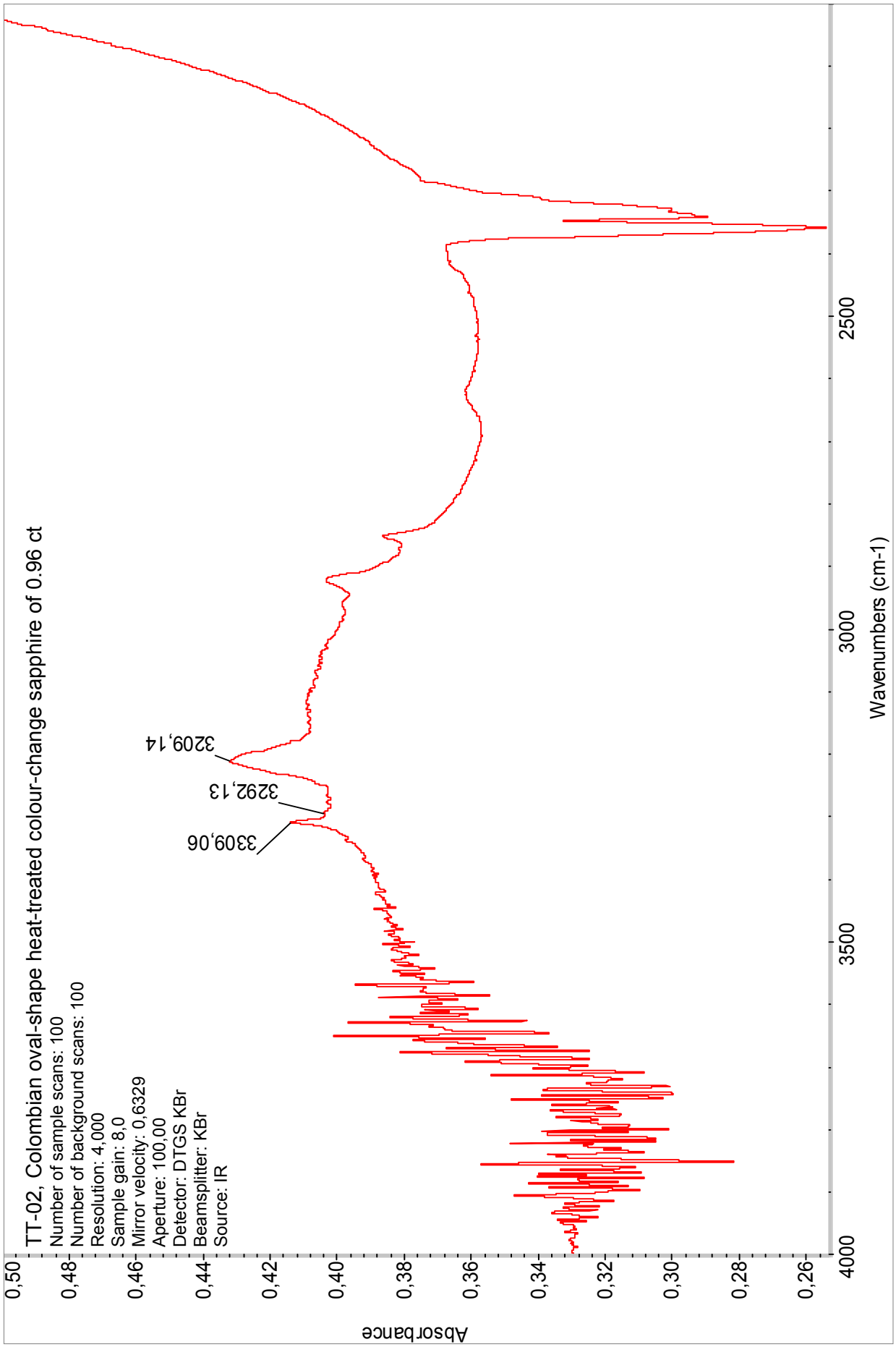
TT-02, Colombian oval-shape heat-treated colour-change sapphire of 0.96 ct
Number of sample scans: 100
Number of background scans: 100
Resolution: 4,000
Sample gain: 8,0
Mirror velocity: 0,6329
Aperture: 100,00
Detector: DTGS KBr
Beamsplitter: KBr
Source: IR
3309,06
3292,13
3209,14
Absorbance
Wavenumbers (cm-1)
0,50
0,48
0,46
0,44
0,42
0,40
0,38
0,36
0,34
0,32
0,30
0,28
0,26
4000
3500
3000
2500

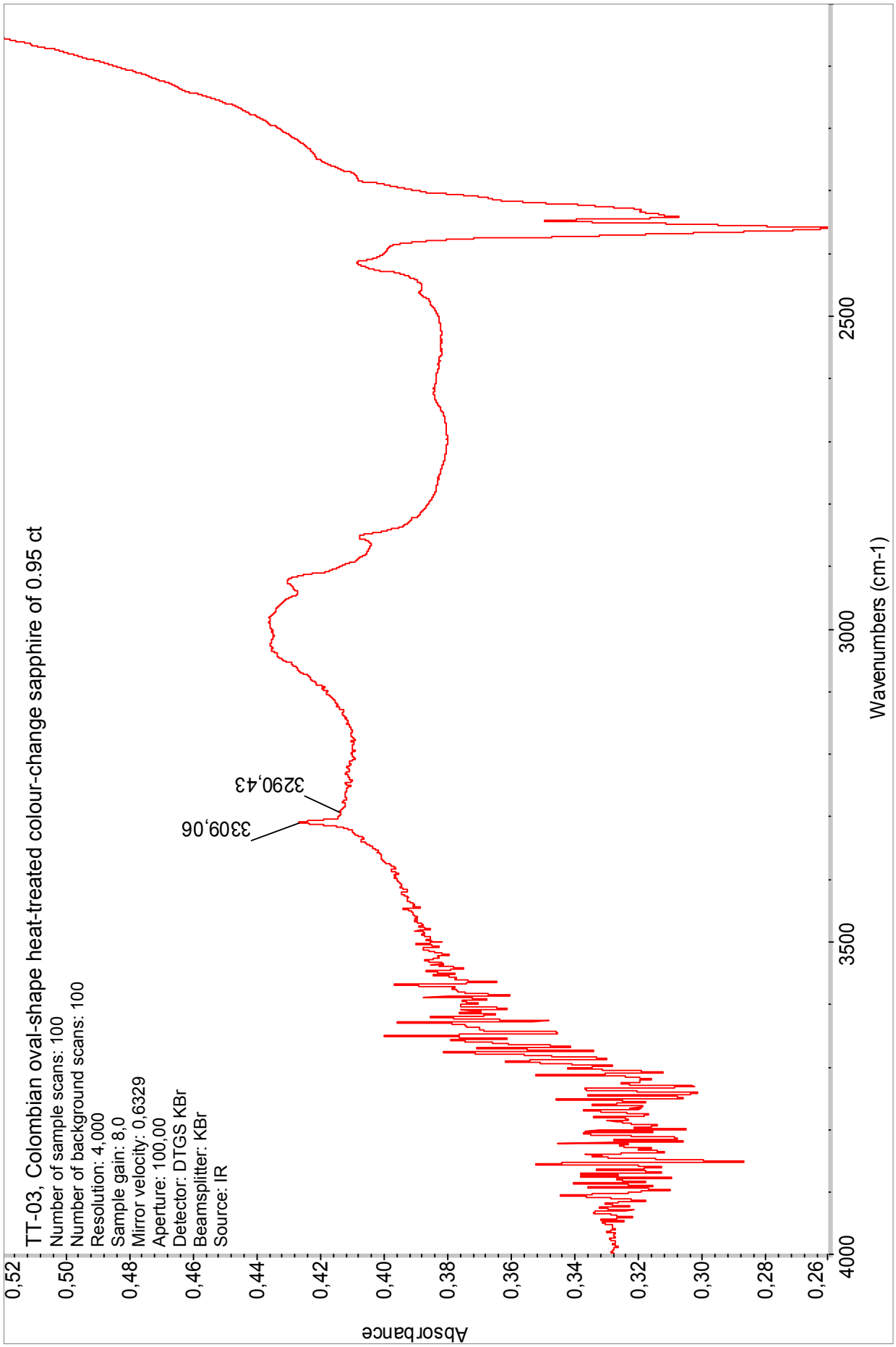
TT-03, Colombian oval-shape heat-treated colour-change sapphire of 0.95 ct
Number of sample scans: 100
Number of background scans: 100
Resolution: 4,000
Sample gain: 8,0
Mirror velocity: 0,6329
Aperture: 100,00
Detector: DTGS KBr
Beamsplitter: KBr
Source: IR
3309,06
3290,43
Absorbance
Wavenumbers (cm-1)
0,52
0,50
0,48
0,46
0,44
0,42
0,40
0,38
0,36
0,34
0,32
0,30
0,28
0,26
4000
3500
3000
2500

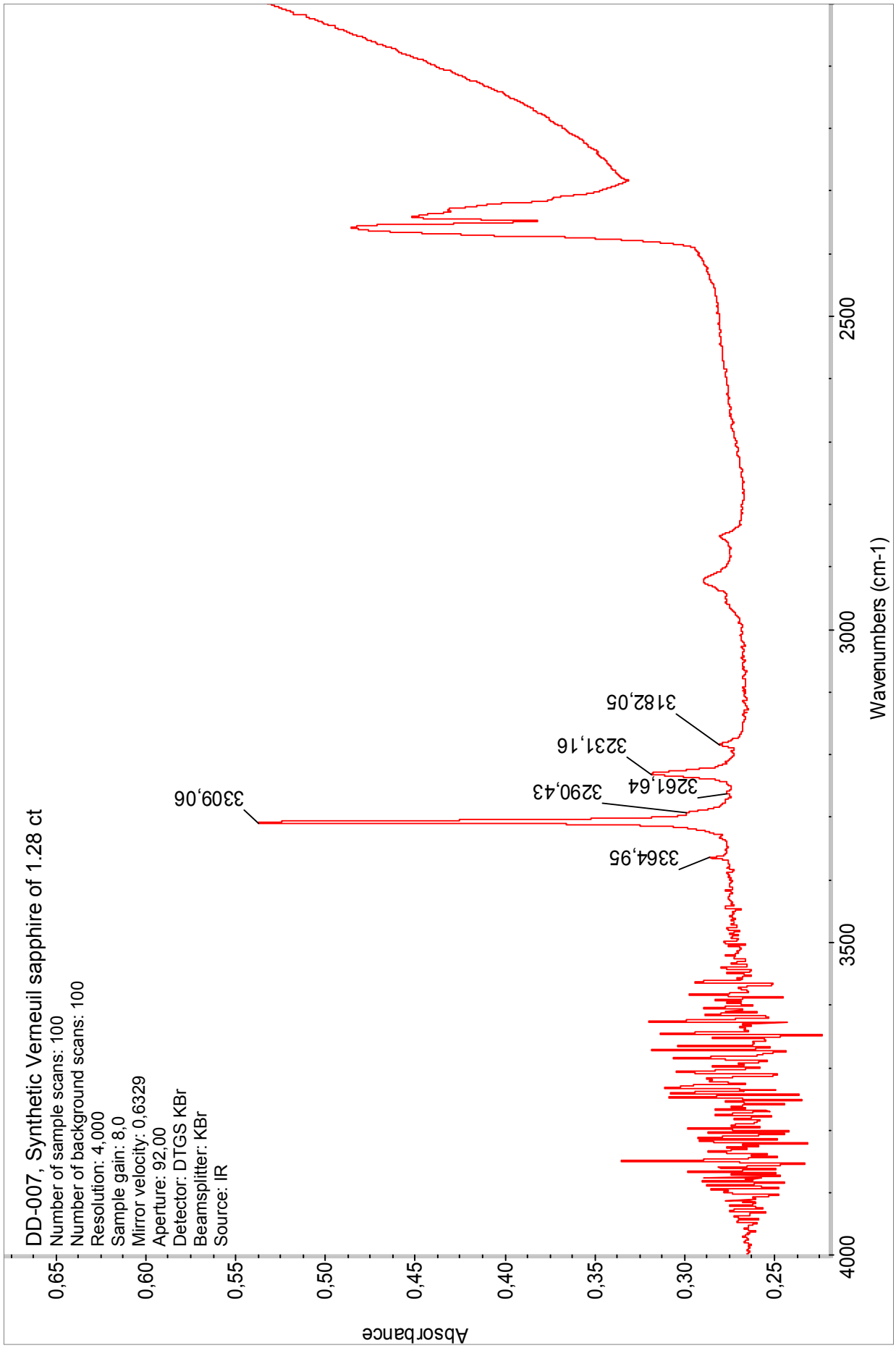
DD-007, Synthetic Verneuil sapphire of 1.28 ct
Number of sample scans: 100
Number of background scans: 100
Resolution: 4,000
Sample gain: 8,0
Mirror velocity: 0,6329
Aperture: 92,00
Detector: DTGS KBr
Beamsplitter: KBr
Source: IR
Absorbance
Wavenumbers (cm-1)
0,65
0,60
0,55
0,50
0,45
0,40
0,35
0,30
0,25
4000
3500
3000
2500
3309,06
3364,95
3290,43
3261,64
3231,16
3182,05

DISCUSSION

PIXE and EDXRF revealed two types of rubies from Colombia:

- Those of non basaltic origin have high amount of chromium (Cr), significant amount of gallium (Ga) with some vanadium (V), but weak amount of iron (Fe): A-05 cabochon ruby of 1.66 ct.
- Those transported by basalts, and referred to as basaltic, have low concentrations of gallium (Ga), with most often no measurable vanadium (V), but high amount of iron (Fe): all the rubies examined except ruby A-05.

- The UV-Visible spectra for the rubies were all dominated by Cr^{3+} absorptions:
  All the rubies displayed the bands 693 nm (Cr^{3+}), 554 nm (Cr^{3+}), 475-477 nm (Cr^{3+}), 468 nm (Cr^{3+}), and the 405-410 nm (Cr^{3+}).
  Again, all except a ruby (A-05 cabochon ruby of 1.66 ct, that corresponds to a non basaltic origin), showed a weak band at 450 nm (Fe^{3+}/Fe^{3+}), which is typical of basaltic origin rubies.
- The infra- red spectra also confirmed the two types of rubies:
  Those devoid of the peak at 3309 $^{cm-1}$: A-05 cabochon ruby of 1.66 ct, corresponds to a non basaltic (unheated) ruby.
  All the other rubies, showing the peak 3309 $^{cm-1}$, and a serial of other peaks in the 2000-4000 $^{cm-1}$, are typical of basaltic rubies.
- The inclusions also confirmed the two origins:
  A small dense nest of very short exsolved rutile needles, similar to those observed in marble-hosted rubies from Myanmar, was encountered in a ruby (A-05 cabochon ruby of 1.66 ct).
  Some other inclusions (e.g. thick boehmite needles, scaffolds of boehmite needles, polysynthetic twinning, …), point towards a basaltic origin, while most crystals included (e.g. zircon, rutile, apatite, plagioclase feldspar, …), or "fingerprints", or growth and colour zones, or healing fractures, are observed in any of the two types of rubies, and solely cannot permit a separation.

- The faceted sapphires examined by PIXE and EDXRF:
  Proved to have a high iron concentration (typical of basaltic sapphires), with gallium (Ga) always present, and titanium (Ti) measured in six sapphires (A-08, A-31, TT-01, A-25, A-30, TT-02). Chromium (Cr) was observed mainly in the multicoloured and heat-treated colour-change sapphires, and zirconium (Zr) observed in six sapphires (A-14 oval-shape sapphire of 3.55 cts, A-17 oval-shape sapphire of 1.65 ct, A-31 cabochon sapphire of 0.17 ct, TT-01 oval-shape heat-treated sapphire of 2.14 cts, HH-02 oval-shape multicoloured sapphire of 0.96 ct, and A-32 cabochon multicoloured sapphire of 1.66 ct).
- The UV-Visible spectra for the rough and faceted sapphires were all dominated by iron absorptions (mainly Fe^{3+}/ Fe^{3+}, characteristic of basaltic sapphires):
  Sharp bands at 377 nm (Fe^{3+}/ Fe^{3+}), and 388 nm (Fe^{3+}), a medium to strong band at 450 nm (Fe^{3+}/ Fe^{3+}), and a very broad band at 565 nm (IVCT $Fe^{2+} \rightarrow Ti^{4+}$).
  The chromium rich multicoloured and heat-treated colour-change sapphires showed the iron bands mentioned above, plus the chromium bands (usually of rather low intensities, that correspond to the intensity of the red hue observed):
  Sharp band at 693 nm (Cr^{3+}), a broad band at 554 nm (Cr^{3+}), sharp bands at 475-477 nm (Cr^{3+}), and 468 nm (Cr^{3+}), and a broad band at 405-410 nm (Cr^{3+}).
  The spectra for the heat-treated sapphires, being similar to those mentioned above, give no indication in regard to their treatment.

- The infra- red spectra also confirmed the basaltic origin of the sapphires:
  Since the sapphires owe their colour chiefly to Fe^{3+}/ Fe^{3+}, Fe^{3+}, and to a lesser degree to IVCT $Fe^{2+} \rightarrow Ti^{4+}$.
- The inclusions encountered in the sapphires being similar to those described for the rubies, and since these are most often observed in non basaltic as well as in basaltic sapphires, taken solely they cannot permit a separation between these two types of sapphires.

From the results of all the tests performed, three facts can be established:

1. The Colombian corundums examined are largely dominated by a basaltic origin.
2. Non basaltic and basaltic Colombian corundums coexist.
3. The data for the Colombian corundums examined are similar to those obtained for other corundums from different sources (see table 7 & 8).

CONCLUSION

Nowadays, corundums are recovered from south-western Colombia, from the Departments of Cauca and Nariño. Although due to political instability (guerilla), the original (in situ) source as well as the parent rock have not yet been determined, since some rough crystals display perfect hexagonal prisms showing sharp edges, proves that these have not suffered from erosion, and indicate that the original source cannot be very far from where these are found.

If Colombia is not one of the most significant corundum sources, it offers an interesting display of sapphires, multicoloured sapphires, colour-change sapphires and rubies.

As for most gemstones, morphological and visual-characteristic studies of the inclusions, proved inadequate to establish their geographic origin (the inclusions of Colombian corundums proved similar to those observed in corundums from other sources), but any of their characteristics described in this work, permits to distinguish a natural ruby or sapphire from its synthetic sisters produced by any of the known manufacturing processes.

Chemically, these rubies and sapphires are also similar to their counterparts from other high-iron basaltic sources (see table 7 & 8). The main difference maybe should be searched in the trace elements which they seem to contain in more abundance than those from other basaltic sources. Those of non-basaltic origin (only a ruby was encountered) can be recognised by a combination of their trace element concentration and by their infra-red spectrum.

UV-VIS spectrometry also confirmed the sapphires and all rubies except one (A-05) to be of basaltic origin. The sapphires in particular proved to be strongly basaltic by their high iron content.

FT-IR spectrometry also confirmed all except one ruby (A-05) to be of basaltic origin. For the sapphires, all except four (A-08, A-31, A-33, and TT-03) were also confirmed as basaltic origin. The four sapphires mentioned only displayed the peak at ± 3309 $^{cm-1}$, which corresponds to the high temperature (1100-1200°) released to them by the basalt when these sapphires were transported as xenocrystals from the depth where they were to the earth crust. These sapphires were all confirmed basaltic by their UV-visible characteristic absorption spectrum.

It was also demonstrated, that the Colombian rubies and sapphires of basaltic origin cannot be distinguished from their synthetic Verneuil sisters, by infra-red spectroscopy, since their spectra are similar.

Finally, although for the moment it is impossible to separate these Colombian corundums from corundums of other geographic origins, it is with morphological and visual-characteristic studies of the inclusions, correlated by the chemistry, UV-VIS spectrometry and FT-IR spectroscopy, that a possible location from which these stones derived can be obtained.

"Qui ne corrige son erreur commet une nouvelle erreur"
K'ong-fou-tseu (Confucius)

REFERENCES

Bosshart G. (1982). *Distinction of natural and synthetic rubies by ultraviolet spectrophotometry.* Journal of Gemmology, Vol. 18, N°2, p. 151.

David C. & Fritsch E. (2001). *Identification du traitement thermique à haute température des corindons par spectrométrie infra-rouge.* Dossier central (suite). Revue de Gemmologie a.f.g., N°141/142, pp. 27-31.

Duroc-Danner J.M. (1992). Radioactive glass imitation emeralds and an unusual Verneuil synthetic ruby. Journal of Gemmology, Vol. 23, N°2, pp. 80-83.

Fritsch E. & Rossman G.R. (1990). *New technologies of the 1980s: Their impact in gemology.* Gems & Gemology, Vol. 26, No 1, p.71.

Hänni H. (1987). *On corundums from Umba Valley, Tanzania.* Journal of Gemmology, Vol. 20, N°5, pp. 278-284.

Hänni H., Kiefert L., and Chalain J.P. (1997). *A Raman microscope in the gemmological laboratory: first experiences of application.* Journal of Gemmology, Vol. 25, N°6, pp. 394-406.

Johansson S.A.E. & Campbell J.L. (1998). *PIXE: A Novel Technique for Elemental Analysis.* John Wiley & Sons, New York. Pp. 1-21, 96-115.

Keller P.C. (1990). *Gemstones and their origins*. Van Nostrand Reinhold, 115 fith Avenue, New York, NY 10003, p. 71.

Leyden D.E. (19??). *Fundamentals of X-ray spectrometry as applied to energy dispersive techniques.* Gloor instruments, Department of Chemistry, Colorado State University. P. 19.

Muhlmeister S., Fritsch E., Shigley J.E., Devouard B., and Laurs B.M. (1998). *Separating natural and synthetic rubies on the basis of trace-element chemistry.* Gems & Gemology, Vol. 34, No 1, pp. 80-101.

Nasdala L., Irmer G., and Wolf D. (1995). *The degree of metamictization in zircon: a Raman spectroscopic study.* Eur. J. Mineral, 7, pp. 471-478.

Nasdala L., Wenzel M., Vavra G., Irmer G., Wenzel T., and Kober B. (2001). *Metamictisation of natural zircon: accumulation versus thermal annealing of radioactivity-induced damage.* Contrib Mineral Petrol, 141, pp. 125-144.

Pinet M., Smith D.C., and Lasnier B. (1992). *La microsonde Raman en Gemmologie. Utilité de la microsonde Raman pour l'identification non-destructive des gemmes.* Numéro hors série de la Revue de Gemmologie, Association Française de Gemmologie, publié avec le concours du Ministèrede la Recherche et de l'Espace. Pp. 11-61.

Schubnel H.J. (1992). *La microsonde Raman en Gemmologie. Une méthode moderne d'identification et d'authentification des gemmes.* Numéro hors série de la Revue de Gemmologie, Association Française de Gemmologie, publié avec le concours du Ministèrede la Recherche et de l'Espace. Pp. 5-10.

Smith C.P., Kammerling R.C., Keller A.S., Peretti A., Scarratt K.V., Khoa N.D., and Repetto S. (1995). *Sapphires from Southern Vietnam*. Gems & Gemology, Vol. 31, No 3, pp. 183-184.

Tang S.M. (1992). *When is a ruby real?* Physics world, Vol. 5, N°10, pp 21-22.

Tang S.M., Tang S.H., Tay T.S., and Retty A.T. (1991a). *Analysis of Burmese and Thai rubies by PIXE.* Gemological Digest, Vol. 3, N°2, pp 57-62.

Tang S.M., Tang S.H., Mok K.F., Retty A.T., and Tay T.S. (1991b). *A study of natural and synthetic rubies by PIXE*. Gemological Digest, Vol. 3, N°2, pp 63-67.

Themelis T. (1992). *The heat treatment of ruby and sapphire*. Gemlab Inc. U.S.A., p. 20.

Wopenka B., Jolliff B.L., Zinner E., and Kremser D.T. (1996). *Trace element zoning and incipient metamictization in a lunar zircon: Application of three microprobe techniques.* American Mineralogist, Vol. 81, pp. 902-912.

Zhang M., Salje E.K.H., Farnan I., Graeme-Barber A., Daniel P., Ewing C. Clark A.M., and Leroux H. (2000). *Metamictization of zircon: Raman spectroscopic study*. J. Phys.: Condens. Matter, 12, pp. 1915-1925.